UNIVERSITY OF CALIFORNIA,
IRVINE

Exploring the relationship of primary cilia and psychiatric disorders to further define the role of ciliary MCHR1 in social & cognitive functions

DISSERTATION

submitted in partial satisfaction of the requirements
for the degree of

DOCTOR OF PHILOSOPHY

in Pharmacological Sciences

by

Wedad S Alhassen

Dissertation Committee:
Professor Amal Alachkar, Chair
Professor Olivier Civelli
Professor Geoffrey Abbott

2023

Dedication

To my dad

Table of Contents

List of Figures

List of Tables

Acknowledgements

I am filled with profound gratitude and utmost appreciation towards Dr. Amal Alachkar. Throughout my journey, her unwavering support, guidance, and encouragement have been invaluable. Her patience, empathy, and critical advice have helped me navigate the challenges of research.

I would also like to acknowledge Dr. Olivier Civelli for his mentorship and the opportunities I had to discuss my research with him alongside the constructive feedback he provided. I extend my thanks to Dr. Geoffrey Abbott, for his valuable time and the feedback specifically His advice helped me overcome wavering fears and anxiety which grew my confidence.

I am thankful to the Alachkar and Civelli lab for their unwavering support and assistance throughout the years. The valuable guidance and patience of Dr. Ryan Yoshimura, whose thought-provoking challenges and questions helped to shape me in the early stages. Additionally, I would like to thank Dr. Surya Nauli for his help and support throughout my fellowship process. I would like to express my appreciation to my friends and family, specifically Lamees and Sammy, who provided me with their support and encouragement that made this accomplishment possible. Without their help, I would not be where I am today.

The text of this dissertation is a reprint of the materials as it appears in,

Wedad Alhassen, Siwei Chen, Marquis Vawter, Brianna Kay Robbins, Henry Nguyen, Thant Nyi Myint, Yumiko Saito, Anton Schulmann, Surya M. Nauli, Olivier Civelli, Pierre Baldi, Amal Alachkar, 2020. Patterns of Cilia Gene Dysregulations in Major Psychiatric Disorders. *Progress in Neuropsychopharmacology & Biological Psychiatry, in press* January 2021

Pierre Baldi, **Wedad Alhassen**, Siwei Chen, Henry Nguyen, Mohammad Khoudari, & Amal Alachkar. (2021). **Large-scale analysis reveals spatiotemporal circadian patterns of cilia transcriptomes in the primate brain**. Journal of Neuroscience Research, 99, 2610–2624. https://doi.org/10.1002/jnr.24919

Wedad Alhassen, Yuki Kobayashi, Jessica Su, Brianna Robbins, Henry Nguyen, Thant Myint, Micah Yu, Surya Nauli, Yumiko Saito, Amal Alachkar. **Regulation of Brain Primary Cilia Length by MCH Signaling: Evidence from Pharmacological, Genetic, Optogenetic, and Chemogenic Manipulations**. Mol Neurobiol. 2022 Jan;59(1):245-265.

Wedad Alhassen, Sammy Alhassen, Jiaqi Chen, Roudabeh Vakil Monfared, Amal Alachkar. **Cilia in the Striatum Mediate Timing-Dependent Functions**. Mol Neurobiol. 2023 Feb;60(2):545-565. doi: 10.1007/s12035-022-03095-9. Epub 2022 Nov 2. PMID: 36322337; PMCID: PMC9849326.

used with permission from Progress in Neuro-Psychopharmacology & Biological Psychiatry,

Journal of Neuroscience Research and Molecular Neurobiology.

Financial support was provided by the National Institute of Mental Health through the F31 Ruth L. Kirschstein National Research Service Award Individual Predoctoral Fellowship, F31MH126565

Vita

Wedad S Alhassen

EDUCATION

University of California, Irvine Fall 2018-2023
Doctor of Philosophy in Pharmacological Sciences GPA: 4.0

Thesis Committee: Amal Alachkar, Olivier Civelli, Geoffrey Abbott

University of California, Riverside Fall 2015-2016
Masters of Science in Bioengineering GPA: 3.54

University of California, Riverside Fall 2013-Spring 2015
Bachelor of Science in Bioengineering GPA: 3.07

AWARDS

F31 Ruth L. Kirschstein National Research Service Award Individual Predoctoral Fellowship- *Ciliary melanin concentrating hormone receptors and the link to cognitive dysfunction in mice* **-**F31MH126565- National Institute Of Mental Health

2023 Chancellor's Graduate Student Award Recipient for Undergraduate Mentorship

PUBLICATIONS

[1] **Alhassen, W**., Alhassen, S., Chen, J. Monfared, R.V, Alachkar, A (November 2022). "Cilia in the Striatum Mediate Timing-Dependent Functions: Implications for Neuro-Psychiatric Disorders." *Molecular Neurobiology*

[2] **Alhassen, W**., Y. Kobayashi, J. Su, B. Robbins, Ngyuen, T. Myint, M. Yu, S. M. Nauli, Y. Saito and A. Alachkar (May 2021). "Regulation of Brain Primary Cilia Length by MCH Signaling: Evidence from Pharmacological, Genetic, Optogenetic and Chemogenic Manipulations." *Molecular Neurobiology*

[3] Monfared, R.V.; **Alhassen, W*.;** Truong, T.M.; Gonzales, M.A.M.; Vachirakorntong, V.; Chen, S.; Baldi, P.; Civelli, O.; Alachkar, A (2021). Transcriptome Profiling of Dysregulated GPCRs Reveals Overlapping Patterns across Psychiatric Disorders and Age-Disease Interactions. Cells 2021, 10, 2967.

[4] Chen S, **Alhassen W***, Monfared R, Vachirakorntong B, Nauli S, Baldi P, Alachkar A (2021). "Dynamic Changes of Brain Cilia Transcriptomes across the Human Lifespan". International Journal of Molecular Sciences

[5] Pierre Baldi, **Wedad Alhassen**, Siwei Chen, Henry Nguyen, Mohammad Khoudari, Amal Alachkar, 2021 High-throughput Profiling of Spatiotemporal Circadian Oscillations of Brain Cilia Genes Reveals Orchestrated Rhythmicity in the Basal Ganglia**,** *Journal of Neuroscience Research*

[6] **Wedad Alhassen**, Siwei Chen, Marquis Vawter, Brianna Kay Robbins, Henry Nguyen, Thant Nyi Myint, Yumiko Saito, Anton Schulmann, Surya M. Nauli, Olivier Civelli, Pierre Baldi, Amal Alachkar, 2020. Patterns of Cilia Gene Dysregulations in Major Psychiatric Disorders. *Progress in Neuropsychopharmacology & Biological Psychiatry, in press* January 2021.

[7] Sanathara, N., Alhassen, L., Marmouzi, I., Khoudari, M., Phan, J., **Alhassen, W**., Civelli, O., Alachkar, A., 2020. Oxytocin-MCH Circuit Regulates Monosynaptic Inputs to MCH Neurons and Modulates Social Recognition Memory.*Neuropharmacology, in press*, November 2020

[8] Chen S, **Alhassen W***, Yoshimura R, De Silva A, Abbott GW, Baldi P, Alachkar A: Metabolomic and transcriptomic signatures of prenatal excessive methionine support nature rather than nurture in schizophrenia pathogenesis. *Communications Biology* 2020, 3(1):409.

[9]J Phan, L. Alhassen, A. Argelagos, **W.Alhassen**, B. Vachirakorntong, Z. Lin, N. Sanathara, A. Alachkar, 2020, Mating and parenting experiences sculpture mood-modulating effects of oxytocin- MCH signaling, In Press*, Scientific Reports*

[10] Vawter M.P., A. Schulmann, L Alhassen, **W Alhassen**, A.R Hamzeh, J Sakr, L Pauluk, R Yoshimura, X Wang, Q Dai, N Sanathara, O Civelli, A Alachkar. (2020), "Melanin Concentrating Hormone Signaling Deficits in Schizophrenia: Association with Memory and Social Impairments and Abnormal Sensorimotor Gating". *The International Journal of Neuropsychopharmacology.* In press

[11] Alhassen, L., A. Phan, **W. Alhassen**, P. Nguyen, A. Lo, H. Shaharuddin, N. Sanathara, O. Civelli and A. Alachkar (2019) The role of Olfaction in MCH-regulated spontaneous maternal responses." Brain Research 1719: 71-76.

Abstract of the Dissertation

Exploring the relationship of primary cilia and psychiatric disorders to further define the role of ciliary MCHR1 in social & cognitive functions

By

Wedad S Alhassen

Doctor of Philosophy in Pharmacological Sciences

University of California, Irvine, 2023

Professor Amal Alachkar, Chair

The melanin-concentrating hormone (MCH) system, composed of the hypothalamic neuropeptide MCH and its receptor MCHR1, is a critical regulator of several functions, including energy homeostasis, food intake, sleep, stress, mood, aggression, reward, and cognition. The MCH system is expressed primarily in the lateral hypothalamus and zona incerta and projects throughout the central nervous system. MCHR1 is widely distributed in several brain regions, particularly in the frontal cortex, amygdala, nucleus accumbens, and hippocampus, suggesting that MCH may modulate social, emotional, and cognitive functions. MCHR1 is a G protein-coupled receptor that is located in the primary neuronal cilia.

Primary cilia are small microtubule backbones, hair-like structures that protrude from the plasma membrane of almost every cell, including neurons. They serve as sensory organelles that detect and transduce extracellular signals, such as mechanical and chemical stimuli, into intracellular signals that regulate cell signaling pathways and gene expression. Ciliopathies are a group of inherited disorders caused by defects in cilia structure or function, and many of the genes implicated in these disorders have been linked to neurological deficits, including cognitive

impairments. Despite the evidence suggesting that cilia dysfunction may play a role in psychiatric disorders, such as schizophrenia, autism spectrum disorder, bipolar disorder, and major depressive disorder, the specific mechanisms underlying this association remain poorly understood. Alongside, almost all brain cells have cilia that are made of microtubules that play critical roles in brain functions. They are essential for brain formation and maturation during neurodevelopmental stages, and in the adult brain, they act as signaling hubs that receive and transduce various signals, regulating cell-to-cell communications. Cilia are intricate and adaptable sub-cellular systems that work in a coordinated way to perform their structural and functional roles. These roles involve sensing environmental stimuli that follow circadian rhythms, which suggests that genes that encode the components of cilia might also have circadian patterns of expression.

G-protein-coupled receptors (GPCRs) are crucial to the neurobiology of psychiatric disorders, as they mediate the effects of most neurotransmitters implicated in these disorders and are the primary targets of psychotropic drugs. However, their precise role in the development and progression of psychiatric disorders remains poorly understood. The MCH system is a critical player in several physiological and behavioral functions, and the MCHR1 receptor's distribution in neuronal primary cilia suggests that MCH may regulate these functions by modulating cellular signaling pathways. Further research is necessary to understand the exact mechanisms by which MCH exerts its action and how modulation of the MCH system could be utilized for therapeutic purposes.

This thesis investigates the dysregulation of cilia genes in psychiatric disorders, with a focus on circadian patterns, age-related changes, and region-dependent functions. Additionally, the thesis examines the involvement of brain primary cilia in MCH signaling and its role in the manifestation of behavioral deficits related to social and cognitive impairments in animal models

with time-dependent ciliary MCHR1 deletion. Finally, we begin to explore the potential of MCH fragment analogues as treatments for ciliopathies or psychiatric disorders.

To begin we identified patterns of cilia gene dysregulation in psychiatric disorders by analyzing differentially expressed genes from publicly available databases. We found that a significant portion of brain-expressed cilia genes were differentially expressed in these disorders, indicating that cilia signaling pathways may be involved in their pathophysiology. Additionally, we revealed that genes encoding proteins of almost all sub-cilia structural and functional compartments were dysregulated in these disorders, suggesting that cilia dysfunctions may be involved in various aspects of disease pathology. We also found that genes encoding for certain cilia proteins were differentially expressed across multiple psychiatric disorders, indicating that cilia signaling may be a common pathway in their pathophysiology. Overall, this study represents the first step towards understanding the role that cilia components play in the pathophysiological processes of major psychiatric disorders. By shedding light on the role of cilia signaling in these disorders, this study may lead to the development of novel therapeutic targets for these disorders.

Disruptions to the cilia-circadian rhythm connection have been linked to various diseases and disorders, such as obesity, diabetes, and sleep disorders, highlighting the crucial role of cilia in maintaining proper circadian rhythm and overall physiological function. By analyzing the gene expression atlas of primates using computational techniques, we found that approximately 73% of cilia transcripts showed circadian rhythmicity in at least one of the 22 brain regions studied. Furthermore, cilia transcriptomes in 12 brain regions were enriched with circadian oscillating transcripts compared to the rest of the transcriptome. Notably, cilia circadian transcripts shared between the basal ganglia nuclei and prefrontal cortex peaked in a sequential pattern similar to the order of activation of the basal ganglia-cortical circuitry, which is essential for movement

coordination. These findings suggest that the spatiotemporal orchestration of cilia genes expression might play a critical role in the normal physiology of the basal ganglia-cortical circuit and motor control.

It is unknown if MCH system activation in vivo causally regulates cilia length, which is highly dynamic in morphology and length. To investigate this, we used different experimental models and methodologies, including organotypic brain slice cultures from rat prefrontal cortex (PFC) and caudate-putamen (CPu), in vivo pharmacological approaches, germline and conditional genetic deletion of MCHR1 and MCH, optogenetic, and chemogenetic methods. Our results revealed that activation of the MCH system through MCHR1 agonism or optogenetic and chemogenetic excitation of MCH-neurons caused cilia shortening, while MCH signaling inactivation via MCHR1 antagonism or genetic manipulation resulted in cilia lengthening. Our findings indicate that the MCH system plays a significant role in ciliary signaling and highlight MCHR1 located at primary cilia as a potential therapeutic target for pathological conditions associated with abnormal primary cilia function and modification of its length.

Next, we wanted to understand cilia's role in higher-order brain functions as it remains largely unknown. Acting as a hub that senses and transduces environmental stimuli to generate appropriate cellular responses, cilia-rich brain structures, such as the striatum, receive and integrate various types of information to drive appropriate motor responses. In this study, we employed loxP/Cre technology to remove cilia from the dorsal striatum of male mice and observed the behavioral outcomes. Our results suggest a critical role for striatal cilia in the acquisition and brief storage of information, specifically in learning new motor skills, but not in the consolidation of long-term information or the maintenance of learned motor skills. Moreover, the deficits observed in the behavior of mice without striatal cilia were clustered around the clinical manifestations of neuro-psychiatric disorders that involve striatal functions and timing

perception. Therefore, striatal cilia may act as regulators of the timing functions of the basal ganglia-cortical circuit by maintaining accurate timing perception.

MCHR1's role in primary cilia is not yet fully understood, but has been implicated in regulating a range of physiological processes, such as appetite and energy balance, as well as behaviors related to reward, motivation, and mood. To better understand the role of ciliary MCHR1 in social and cognitive deficits, we utilized an inducible knockout model. Our results revealed that late deletion of ciliary MCHR1 does not significantly affect sociability but leads to an increase in hyperactivity and deficits in cognition and sensorimotor gating. On the other hand, early deletion of ciliary MCHR1 leads to deficits in both social and cognitive function, as well as sensorimotor gating deficits. Additionally, we quantified the amount of ciliary and non-ciliary MCHR1 that localizes to primary cilia to better understand the role they play in these deficits. Our findings suggest that the MCH system's disruption interferes with neurodevelopmental processes, which could contribute to the pathogenesis of schizophrenia.

Lastly, we began to design MCH analogues with improved binding affinity for MCH receptors to potentially develop new therapies for these conditions. We used various in vitro binding techniques to analyze the affinity of the MCH analogues for MCH receptors. In the in vivo experiments, we injected MCH and MCH analogues intracerebroventricularly in mice to study their effects on feeding behavior, energy homeostasis, and cilia length. We discovered an MCH fragment analogue with a reduced number of amino acids and molecular weight that showed potential to bind in vivo. This MCH fragment analogue had a potency comparable to the full MCH peptide and caused cilia shortening in the adult mouse brain and was reversed when administered with an MCHR1 antagonist. We also found that when administered i.c.v similarly to MCH, the mice gained weight. When given simultaneously with an antagonist, it resulted in weight loss. This suggests that MCH fragment analogues could potentially be used as potential

treatments for conditions associated with abnormal MCH signaling, such as ciliopathies or psychiatric disorders. In conclusion, our study provides new insights into the design of MCH analogues with improved binding affinity for MCH receptors. We believe that these findings will contribute to the development of new therapeutic approaches for conditions associated with MCH signaling abnormalities. By providing new insights into the underlying mechanisms of schizophrenia and other neurological disorders, the studies in this thesis may pave the way for the development of novel therapeutic targets for the treatment of these conditions.

Chapter 1: Introduction

1. Primary Cilia: Their Role, Function, and Ciliogenesis

Primary cilia are microtubule-based organelles that project from the surface of most mammalian cells. They are typically composed of a single axoneme, which is surrounded by a specialized plasma membrane, called the ciliary membrane. Primary cilia play a crucial role in signal transduction pathways, which are critical for cellular communication and homeostasis [1-4]. They contain a wide range of receptors, ion channels, and signaling proteins, which enable them to detect extracellular signals and transduce these signals into intracellular responses [5-11]. Primary cilia are involved in a wide range of cellular processes, including cell signaling, sensory perception, and organelle trafficking [12]. The signaling pathways associated with primary cilia play a critical role in various aspects of development and tissue homeostasis, including organogenesis, tissue repair, and maintenance of stem cell niches [13]. In the brain, primary cilia are found in various cell types, including neurons, astrocytes, and oligodendrocytes, and have been implicated in the regulation of neurotransmitter signaling, axon guidance, and synaptic plasticity [14-20].

Primary cilia contain a wide range of receptors, ion channels, and signaling proteins, which enable them to detect extracellular signals and transduce these signals into intracellular responses [21, 22]. One of the best-studied signaling pathways associated with primary cilia is the Sonic Hedgehog (Shh) pathway, which is critical for embryonic development and tissue homeostasis [23-25]. In the Shh pathway, binding of the Shh ligand to its receptor, Patched, on the ciliary membrane leads to the activation of Smoothened, a G protein-coupled receptor. This, in turn, triggers the activation of downstream transcription factors, which regulate target gene expression and cell fate determination [26].

Ciliogenesis is the process by which primary cilia are formed and maintained. It involves the assembly of the ciliary axoneme, which is composed of nine microtubule doublets and a pair of singlet microtubules [38]. The formation of primary cilia occurs through a highly regulated process that involves several steps. The first step in ciliogenesis is the docking of the basal body, a centrosome-derived structure, to the plasma membrane. The basal body serves as the organizing center for cilia assembly and is composed of a pair of centrioles surrounded by pericentriolar material. The basal body docks to the membrane at a specific location, known as the ciliary pocket or basal body pocket. Once the basal body has docked to the membrane, it begins to extend microtubules, which form the core of the cilia. The microtubules grow from the basal body and extend outward, forming the axoneme, the core structure of the cilia. The axoneme is composed of nine microtubule doublets, arranged in a circular pattern, and is surrounded by the ciliary membrane [39-42].

The assembly of primary cilia is a tightly regulated process, and defects in ciliogenesis can lead to a range of diseases, known as ciliopathies [43]. These diseases are characterized by a range of symptoms, including cognitive deficits, developmental abnormalities, and organ dysfunction [44-46]. Ciliopathies can be caused by mutations in genes that are involved in ciliogenesis, such as genes encoding centrosomal and basal body proteins. Ciliogenesis is also important for the maintenance of primary cilia. Primary cilia are dynamic structures that are constantly being assembled and disassembled, and defects in ciliogenesis can lead to cilia loss or dysfunction[47]. Maintenance of primary cilia requires the activity of several proteins, including intraflagellar transport proteins (IFTs), which transport proteins and other cargo along the axoneme, and centrosomal and basal body proteins, which ensure the stability and integrity of the ciliary apparatus [48-51]. Ciliogenesis is a highly regulated process that is essential for the

formation and maintenance of primary cilia. Defects in ciliogenesis can lead to a range of diseases, highlighting the importance of this process for cellular homeostasis and function [52].

1.1 Primary cilia in psychiatric disorders

Primary cilia are particularly abundant in the central nervous system, where they are found on neurons, astrocytes, and other types of glial cells [53-56]. The role of primary cilia in neuronal function has become an area of intense research interest, with growing evidence suggesting that defects in ciliary signaling may contribute to the pathogenesis of several neurological and psychiatric disorders, including schizophrenia [57].

Primary cilia are increasingly recognized as important regulators of neuronal development and function, with mutations in genes encoding ciliary proteins linked to a growing number of developmental disorders, including ciliopathies, intellectual disabilities, and neuropsychiatric disorders [58]. One of the most intriguing aspects of primary cilia is their association with psychiatric disorders, including schizophrenia, bipolar disorder, and autism spectrum disorders (ASD) [59]. Primary cilia are critical components of the Hedgehog (Hh) signaling pathway, which is involved in the development and function of the central nervous system. The Hh pathway has been implicated in the pathogenesis of psychiatric disorders, and ciliary dysfunction has been linked to aberrant Hh signaling in these disorders [60].

Schizophrenia is a complex psychiatric disorder that affects approximately 1% of the general population worldwide. It is characterized by a range of symptoms, including delusions, hallucinations, disordered thinking, and social withdrawal. While the precise causes of schizophrenia are not fully understood, it is widely believed to result from a combination of genetic and environmental factors. Recent studies have shown that primary cilia may play an important role in the pathogenesis of schizophrenia. For example, several genetic mutations that affect ciliary function have been linked to an increased risk of developing schizophrenia [61, 62].

Furthermore, imaging studies have revealed that patients with schizophrenia have a reduced density of primary cilia in certain regions of the brain, particularly in the prefrontal cortex and hippocampus, which are regions involved in cognitive and emotional processing [63].

Several lines of evidence suggest that primary cilia dysfunction may contribute to the pathogenesis of schizophrenia. For example, a study demonstrated that mutations in a gene encoding a ciliary protein, Tctex-1, were associated with an increased risk of schizophrenia. Tctex-1 is a component of the dynein motor complex, which is required for ciliary function, and mutations in Tctex-1 have been linked to ciliopathies and developmental disorders [64, 65]. Another found that genetic variants in genes encoding ciliary proteins were associated with an increased risk of schizophrenia in a large-scale genome-wide association study [66]. The authors identified several genes involved in ciliary structure and function that were significantly associated with schizophrenia, including genes encoding intraflagellar transport proteins and the basal body protein, CEP290 [67]. Overall, these studies suggest that primary cilia dysfunction may contribute to the pathogenesis of several psychiatric disorders, including schizophrenia, bipolar disorder, and ASD. Further research is needed to fully understand the role of primary cilia in these disorders and to identify potential therapeutic targets for their treatment.

1.2 Primary cilia and age and development

Primary cilia are increasingly recognized as important regulators of cellular signaling pathways critical for development and homeostasis in various organs and tissues, including the brain. Primary cilia are present on many cells, including neurons, and are involved in signal transduction pathways critical for proper neuronal function [69]. Aging has been shown to affect the structure and function of primary cilia in several organs and tissues. In the brain, primary cilia play important roles in neuronal development, synaptic plasticity, and sensory perception. Age-related changes in primary cilia have been observed in the brain and have been linked to cognitive

decline and neurodegenerative diseases such as Alzheimer's and Parkinson's disease [55, 70-75]. Age-related changes in primary cilia have also been implicated in the development of neurodegenerative diseases. For example, primary cilia dysfunction has been observed in animal models of Alzheimer's disease and Parkinson's disease [55, 70-75]. In Alzheimer's disease, primary cilia become shorter and less abundant in the hippocampus and cortex, which are brain regions important for memory and cognition. In Parkinson's disease, primary cilia on dopaminergic neurons in the substantia nigra become shorter and less abundant, which may contribute to the loss of dopaminergic neurons in this region [79]. The relationship between primary cilia and age is complex and multifaceted. Age-related changes in primary cilia have been observed in multiple tissues and have been implicated in age-related diseases and functional decline thus further research is needed to fully understand the mechanisms underlying these changes and to identify potential therapeutic targets for age-related diseases.

1.3 Primary cilia and circadian rhythm

Primary cilia have been implicated in the regulation of circadian rhythms, which are essential for the maintenance of the normal sleep-wake cycle and other physiological processes that follow a daily rhythm[80]. The circadian system is governed by a master clock located in the suprachiasmatic nucleus (SCN) of the hypothalamus, which receives light signals from the retina and synchronizes peripheral clocks throughout the body via various signaling pathways [81-84]. Primary cilia are present in many cells of the body, including the SCN neurons, and have been shown to play a role in the regulation of circadian rhythms.

Studies have suggested that primary cilia play a role in regulating the timing of the circadian clock by modulating the activity of clock genes and proteins. One study found that the primary cilium in SCN neurons modulates the expression of the circadian clock gene Period 2 (Per2) by regulating the activity of the transcription factor CREB (cAMP response element-binding

protein [85]. Another study found that primary cilia in fibroblasts regulate the activity of the circadian clock protein BMAL1 (brain and muscle ARNT-like protein 1) by modulating the activity of the protein kinase A (PKA) signaling pathway [86]. These studies suggest that primary cilia play a crucial role in the regulation of circadian rhythms by modulating the activity of clock genes and proteins. Primary cilia have also been shown to play a role in the synchronization of peripheral clocks with the master clock in the SCN. One study found that primary cilia in fibroblasts play a crucial role in the synchronization of peripheral clocks with the SCN clock by regulating the expression of clock genes and proteins [87, 88]. These studies suggest that primary cilia are involved in the synchronization of peripheral clocks with the master clock in the SCN by regulating the expression of clock genes and proteins. These studies suggest that dysfunction of primary cilia can disrupt the circadian clock and contribute to the development of circadian rhythm disorders.

2. Melanin concentrating hormone: Structure, Function, and implications

Melanin-concentrating hormone (MCH) is a neuropeptide that is widely distributed throughout the central nervous system of vertebrates, including mammals, birds, fish, and amphibians [89]. It was first discovered in 1983 in the pituitary gland of teleost fish, where it was shown to have a role in the regulation of skin coloration by stimulating the dispersion of melanin-containing pigment granules in skin cells [90].

2.1 Structure of MCH

The structure of MCH is highly conserved across species, with a 19-amino acid sequence that is identical in humans, rats, mice, and chickens [91]. MCH is synthesized as a larger precursor protein called prepro-MCH, which is then cleaved into a mature 19-amino acid peptide [92]. The crystal structure of MCH has been determined using X-ray crystallography, revealing a compact fold with an α-helical region and a loop structure that is stabilized by a disulfide bond [93, 94]. The

receptor for MCH is a G protein-coupled receptor called MCHR1. In the brain, MCH is primarily expressed in the lateral hypothalamus, the zona incerta, and the dorsal raphe nucleus [92, 95]. MCH-expressing neurons in the lateral hypothalamus project to a number of brain regions involved in the regulation of feeding behavior and energy metabolism, including the paraventricular nucleus, the arcuate nucleus, and the ventromedial hypothalamus [95, 96].

2.2 Functions of MCH

Feeding behavior: MCH has been shown to have a potent orexigenic (appetite-stimulating) effect in rodents and humans [97], and it is thought to play a key role in the regulation of feeding behavior and energy balance. MCH is produced by neurons in the lateral hypothalamus, an area of the brain that is known to be involved in the control of feeding and energy metabolism [98]. When MCH is injected into the brain of rodents, it stimulates feeding behavior and increases body weight, whereas blocking the activity of MCH or its receptor has been shown to reduce food intake and body weight [99]

Energy metabolism: In addition to its role in regulating feeding behavior, MCH has also been shown to have a direct effect on energy metabolism. MCH has been shown to increase glucose uptake and stimulate lipogenesis (the synthesis of fatty acids) in adipose tissue, suggesting that it may play a role in the regulation of energy storage and utilization [100].

Sleep-wake cycles: MCH has been implicated in the regulation of sleep-wake cycles, with evidence suggesting that it promotes the transition from wakefulness to non-REM sleep. MCH neurons in the lateral hypothalamus show increased activity during non-REM sleep, and injection of MCH into the brain of rats has been shown to increase non-REM sleep and decrease wakefulness [101]. MCH has also been shown to be involved in the regulation of REM sleep, with some evidence suggesting that it may promote REM sleep in certain conditions [102].

Anxiety and mood: MCH has been shown to have a modulatory effect on anxiety and mood, with evidence suggesting that it may have anxiolytic and antidepressant effects. MCH neurons in the lateral hypothalamus have been shown to project to brain regions that are involved in the regulation of anxiety and mood, such as the amygdala and prefrontal cortex [95]. MCH has also been shown to modulate the activity of the hypothalamic-pituitary-adrenal (HPA) axis, which is involved in the response to stress [103].

2.3 The role of MCH in cognitive function and psychiatric disorders

MCH is predominantly expressed in high concentration in the brain thus it suggests that MCH is a vital neurotransmitter with a broad range of functions which has been shown in mediating behaviors involved in arousal, food intake, metabolism, sleep, mood disorders such as depression and anxiety, and most recently learning and memory, cognition, and psychiatric disorders like Alzheimer's and schizophrenia [107-113].

MCH interacts with the GPCR MCHR1 which is highly expressed in several regions of the brain including the hippocampus, nucleus accumbens, basolateral amygdala, hypothalamus, locus coeruleus, which suggests it plays a major role in other functions [114].The MCH system is involved in impairments of glutamatergic transmission as well as long-term plasticity in the CA1 of the hippocampus via MCHR1 KO mice [33]. It has also been shown that disruptions in MCHR1 leads to cognitive deficits and alters the NMDA and AMPA receptors which are major players in both LTP and LDP [5, 33]. There have been many studies that have reported that MCH improves memory by promoting memory retention, however the mechanism as to how has yet to be fully conclusive [1]. Many studies have shown that the activation of MCH producing neurons enhances learning and memory [4]. To evaluate both short term and long term memory, studies give administration of MCH directly into the CA1 of the hippocampus, amygdala and cortex, and followed with a step-down inhibitory avoidance test which showed an increase in the response latency thus inducing an increase in memory retention [32]. The MCH system is involved with

modulating sleep, emotional behaviors, learning and memory, which are prominent deficits seen in psychiatric disorders such as Alzheimer's, schizophrenia, and depression. Thus one may postulate the correlation with the dysfunction in the MCH system with the pathophysiology of many psychiatric disorders [13]. A genome-wide association study showed MCHR1 is located on chr:22q13.2, which has been associated with schizophrenia [7, 9]. There have also been human gene studies that showed 5 SNP in the MCHR1 region were significantly associated with schizophrenia suggesting that MCHR1 may influence susceptibility to schizophrenia [9, 8]. These findings suggest that MCHR1 could be an important candidate for drug targets involved in psychiatric disorders.

MCH has also been investigated as a potential target for the treatment of psychiatric disorders, such as anxiety and depression. Several studies have shown that MCH is involved in the regulation of anxiety-like behavior in rodents. For example, MCH knockout mice display reduced anxiety-like behavior in several behavioral tests, including the elevated plus maze and the light/dark box test [115]. In addition to its role in anxiety, MCH has also been implicated in the pathogenesis of depression. Studies in rodents have shown that chronic stress can increase MCH expression in the lateral hypothalamus and that MCH levels are elevated in the cerebrospinal fluid of depressed patients [115]. Moreover, MCH antagonists have been shown to have antidepressant-like effects in several preclinical models of depression [116].

The potential of MCH as a therapeutic target for psychiatric disorders has led to the development of several MCH receptor antagonists. These compounds have shown promising results in preclinical studies and are currently being investigated in clinical trials for the treatment of depression and anxiety. For example, ATC-1906, an MCH receptor antagonist, has been shown to reduce anxiety-like behavior in rodents and is currently in Phase II clinical trials for the treatment of generalized anxiety disorder [117]. Recent evidence suggests that MCH may also

be involved in the pathophysiology of schizophrenia. Melanin-concentrating hormone (MCH) has also been implicated in the pathogenesis of schizophrenia, a severe and chronic mental disorder characterized by a range of cognitive, behavioral, and emotional symptoms.

Several lines of evidence suggest that MCH may play a role in the pathophysiology of schizophrenia. For example, postmortem studies have shown that MCH levels are significantly elevated in the brains of schizophrenia patients, particularly in the dorsolateral prefrontal cortex and the amygdala [118]. These brain regions are known to be involved in cognitive and emotional processing and are implicated in the pathophysiology of schizophrenia. In addition to these findings, studies in rodents have shown that MCH can modulate the activity of dopamine neurons, a key neurotransmitter system implicated in the pathogenesis of schizophrenia [119]. Dopamine dysregulation is thought to be a key feature of schizophrenia, and several antipsychotic medications target dopamine receptors to alleviate symptoms.

Furthermore, several studies have shown that MCH can affect the activity of gamma-aminobutyric acid (GABA) neurons, another key neurotransmitter system implicated in the pathogenesis of schizophrenia. For example, MCH has been shown to enhance the activity of GABA neurons in the nucleus accumbens, a brain region involved in reward processing and motivation [105]. GABA dysregulation has been implicated in the cognitive and emotional symptoms of schizophrenia.The potential role of MCH in the pathophysiology of schizophrenia has led to the development of MCH receptor antagonists as potential therapeutic agents for the disorder. For example, the MCH receptor antagonist SNAP-7941 has been shown to reduce MCH-induced hyperactivity in rodents and has been proposed as a potential treatment for schizophrenia [115].

Despite these findings, the exact role of MCH in the pathophysiology of schizophrenia is still not fully understood. The development of MCH-based therapies for psychiatric disorders is

still in its early stages, and further research is needed to fully understand the role of MCH in these conditions. The potential side effects of MCH antagonists, such as alterations in feeding behavior and energy metabolism, also need to be carefully evaluated. Nonetheless, the identification of MCH as a potential target for the treatment of psychiatric disorders represents a significant advance in our understanding of the neurobiological mechanisms underlying these conditions and may lead to the development of new and more effective therapies in the future.

3. MCH and Primary Cilia

3.1 MCH-mediated regulation of primary cilia

MCHR1 is selectively expressed on neuronal primary cilia [49]. We know that only a few GPCRS localize to neuronal primary cilium thus may play an important role in regulation of the cilium. Studies have shown that there is a link between cilia length and MCH. In vitro, studies show when hRPE1 cells are transfected with MCHR1 and treated with MCH there is a reduction in cilia length via Gi/o-Akt pathway suggesting that MCH plays a sensory role [37]. Additionally, recent studies show that lack of dopaminergic inputs elongates primary cilia of striatal neurons [79]. Although little is known about the MCH system and cilia, there is potential in this field of research that may reveal important findings that could link ciliary MCHR1 to psychiatric disorders.

MCHR1 is a G-protein coupled receptor that is primarily localized on the cilia membrane [120, 121]. Previously MCH has been shown to shorten the length of cilia [122, 123]. Our preliminary immunohistochemistry data demonstrates that via the antibody staining against the cilia marker ADCY3 in ex vivo culture of mouse striatal neurons with MCH (30nM) caused a decrease in cilia length. We also demonstrated the effects of the activation and inactivation of MCH system on cilia lengths by using different methodologies, including pharmacological (MCHR1 agonist and antagonist GW803430), germline and conditional genetic deletion of MCHR1 and MCH, optogenetic (Channelrhodopsin-2(Ch2R)), and chemogenetic (Designer Receptors Exclusively Activated by Designer Drugs (DREADD)) approaches. We found that

stimulation of the MCH system either directly through MCHR1 activation, or indirectly through optogenetic and chemogenetic-mediated excitation of MCH neurons, causes cilia shortening. Multiple regions of the brain were analyzed including hippocampus, striatum, frontal cortex, and nucleus accumbens.

3.2 Associations between cilia genes and GPCRS

There is increasing evidence for associations between cilia genes and G protein-coupled receptors (GPCRs), which are important targets for drug development in various diseases, including psychiatric disorders. GPCRs are a large family of membrane receptors that play important roles in signal transduction and are involved in various physiological processes, including neurotransmission. Several GPCRs have been shown to localize to primary cilia, and ciliary dysfunction has been implicated in the pathogenesis of GPCR-related disorders, including schizophrenia and bipolar disorder.

For example, the dopamine receptor D2 (DRD2) is a GPCR that is critical for dopamine neurotransmission, and its dysfunction has been implicated in the pathogenesis of schizophrenia. DRD2 has been shown to localize to primary cilia, and mutations in genes involved in ciliary function have been associated with altered DRD2 signaling and an increased risk for schizophrenia [124]. Similarly, the serotonin receptor 5-HT6 (HTR6) is a GPCR that has been implicated in the regulation of mood and cognition and has been shown to localize to primary cilia. Mutations in genes involved in ciliary function have been associated with altered 5-HT6 signaling and an increased risk for bipolar disorder [125].

Taken together, these findings suggest that ciliary dysfunction may play a critical role in the pathogenesis of psychiatric disorders through the regulation of GPCRs and other signaling pathways. Further research is needed to elucidate the precise mechanisms underlying these associations and to identify potential targets for the development of novel therapeutics. Recent

studies have shown that cilia genes and GPCRs are functionally and genetically linked, with ciliary dysfunction implicated in the pathogenesis of GPCR-related disorders such as schizophrenia and bipolar disorder.

Chapter 2: Patterns of cilia gene dysregulations in major psychiatric disorders

Alhassen W, Chen S, Vawter M, Robbins BK, Nguyen H, Myint TN, Saito Y, Schulmann A, Nauli SM, Civelli O, Baldi P, Alachkar A. **Patterns of cilia gene dysregulations in major psychiatric disorders.** Prog Neuropsychopharmacol Biol Psychiatry. 2021 Jul 13;109:110255. doi: 10.1016/j.pnpbp.2021.110255.

Abstract

Primary cilia function as cells' antennas to detect and transduce external stimuli and play crucial roles in cell signaling and communication. The vast majority of cilia genes that are causally linked with ciliopathies are also associated with neurological deficits, such as cognitive impairments. Yet, the roles of cilia dysfunctions in the pathogenesis of psychiatric disorders have not been studied. Our aim is to identify patterns of cilia gene dysregulation in the four major psychiatric disorders: schizophrenia (SCZ), autism spectrum disorder (ASD), bipolar disorder (BP), and major depressive disorder (MDD). For this purpose, we acquired differentially expressed genes (DEGs) from the largest and most recent publicly available databases. We found that 42%, 24%, 17%, and 15% of brain-expressed cilia genes were significantly differentially expressed in SCZ, ASD, BP, and MDD, respectively. Several genes exhibited cross-disorder overlap, suggesting that typical cilia signaling pathways' dysfunctions determine susceptibility to more than one psychiatric disorder or may partially underlie their pathophysiology. Our study revealed that genes encoding proteins of almost all sub-cilia structural and functional compartments were dysregulated in the four psychiatric disorders. Strikingly, the genes of 75% of cilia GPCRs and 50% of the transition zone proteins were differentially expressed in SCZ.

The present study is the first to draw associations between cilia and major psychiatric disorders, and is the first step toward understanding the role that cilia components play in their pathophysiological processes, which may lead to novel therapeutic targets for these disorders.

Introduction

Primary cilia are microtubule-based organelles that protrude from the surface of almost all cell types including neurons [1-3]. Cilia, functioning as cells' antennas, detect and transduce external stimuli, thus playing crucial roles in cell communication and signaling. Cilia are essential sites for the sonic hedgehog (Shh) signaling pathway, and therefore, play a vital role in neurogenesis, cell differentiation, and migration [4, 5].

The sensory functions and signal transduction of primary cilia are achieved through specific receptors and downstream signaling components including receptor tyrosine kinases (RTK), hedgehog, WNT, ion channels, and G-protein-coupled receptors (GPCRs) [6-15]. Examples of neuronal cilia GPCRs are somatostatin receptor 3 (SSTR3), serotonin receptor 6 (5HTR6), melanin-concentrating hormone receptor 1 (MCHR1), melanocortin receptors (MC4R), and dopamine receptors (DRD1, DRD2 and DRD5), GPR88, prolactin-releasing hormone receptor (PRLHR), and neuropeptide FF receptor 1 (NPFFR1) [6][16-20].

Mutations or deletions of primary cilia genes cause disruptions in ciliary structure and functions and result in neurodevelopment defects. Of the 187 cilia genes that were causally associated with ciliopathies, several genes have been associated with neurological deficits such as cognitive deficits [21-23].

Since primary cilia's main function is to receive extracellular signals, cilia dysfunctions can cause defects in cellular response to extracellular cues. On the other hand, neuronal GPCRs play essential roles in regulating emotions, memory, and cognition (see [24-29] for reviews). Therefore, defects in the cilia GPCRs are expected to correlate with psychiatric disorders.

Given the background information, our premises indicate that cilia structure/function has critical roles in brain cognitive functions. Thus, we hypothesize that the dysfunctions of cilia components are associated with psychiatric disorders.

In support of this hypothesis, the causative gene for the ciliopathy Joubert Syndrome AHI1, which is involved in the ciliogenesis [30], and PCM1 and TSGA14, which are necessary for

cilia assembly, have been linked with schizophrenia (SCZ) and autism spectrum disorder (ASD) [31-38]. Olfactory neural progenitor (ONP) cells derived from paranoid SCZ and bipolar disorder (BD) patients display a deficit in cilia assembly and maintenance [39].

However, a comprehensive study on the conclusive role of cilia in psychiatric disorders has never been conducted yet. Therefore, we examined here the changes in gene expression of cilia associated proteins in four psychiatric disorders including SCZ, ASD, BP, and major depressive disorder (MDD). We used publicly available databases of RNA sequencing (RNA-seq) and RNA-microarray in the largest cohorts of cases and controls to acquire differentially expressed genes (DEGs) in the four psychiatric disorders.

Materials and Methods

Compilation of brain cilia genes list

Genes experimentally probed and identified to be involved in cilia structure, ciliogenesis or ciliary function were collected from different studies and databases including Nauli et al.

SysCilia Gold Standard (SCGS) version 1 database [40], CilDB database [41-42] and CiliaCarta [40]. Search criteria included Homo sapiens species cilia genes. CiliaCarta database contains about 1000 putative cilia genes, including genes from Syscilia (302 genes) and Gene Ontology (GO) annotated genes (677), with 232 genes overlapped, as well as bayesian predictions (285 genes). Our initial list included the Sycilia and GO genes but not bayesian predictions. GPCRs (G-protein coupled receptor) localized on cilia were acquired from Schou et al. [43]. Ciliary evidence was then verified using CilDB. It is important to disclose that lists of cilia genes are continuously being updated, and one will never be 'complete' as novel cilia genes might always be identified. Thus, our list is a working list of cilia genes that will be updated as needed.

The 455 candidate ciliary genes in the list were then compiled and further analyzed using Genotype-Tissue Expression (GTEx) https://gtexportal.org/home/. GTEx database was queried for cross tissue comparisons to determine each of the cilia genes' brain location. Cilia genes were located in the following brain regions: amygdala, caudate, cerebral hemisphere, cortex, frontal cortex, hippocampus, hypothalamus, nucleus accumbens, putamen, and substantia nigra and expressed as the median transcripts per million (TPM). Cilia genes not located in the brain were removed from the list. Therefore, the final list of cilia genes totaled 281.

Transcriptomic analysis of cilia genes in SCZ, ASD, BP, and MDD

We screened publically available datasets for gene expression of genes encoding cilia associated proteins. We obtained the gene expression data of prefrontal cortex tissue samples (559 SCZ, 51 ASD, 222 BP, and 936 controls) from the study of Gandal et al. [44], which retrieved RNA-seq data from PsychEncode (PEC, Brain-GVEX study) and CommonMind (CMC) datasets [44-47] The DEGs data of cortical brain tissue samples (87 MDD, and 293 controls) were obtained

from the study of Gandal et al. [48], which performed meta-analyses of microarray data that were obtained from the Gene Expression Omnibus (GEO), ArrayExpress, or from the study authors directly conducted [48-49]. Cilia differentially expressed genes (DEGs) in SCZ, ASD, BP, and MDD ($P < 0.05$) were identified from the transcriptomic data and underwent Fisher exact test to examine the enrichment of differentially expressed cilia genes in SCZ, ASD, BP, and MDD. The overlap of DEGs across the psychiatric disorders was computed using Fisher's exact test. Cilia genes were then categorized based on their localization to the cilium, including basal body, axoneme, intraflagellar transport cargo (IFTA and IFTB), kinesin, dynein, transition zone, bbsome, golgi, nucleus, cytosol and the ciliary membrane. If unknown, the genes were placed in one group designated as other.

Results

Brain cilia list

Using SysCilia, CilDB, and CiliaCarta databases, we identified and verified 455 candidate ciliary genes. Using GTEX, 281 genes out of these cilia genes were confirmed to be expressed in the brain's following regions: amygdala, caudate, cerebral hemisphere, cortex, frontal cortex, hippocampus, hypothalamus, nucleus accumbens, putamen, and substantia nigra. The heatmap shows GTEx expression profiles in median TPMs of the cilia genes (Fig. 2.1). Genes were considered if the median TPM was greater than zero. Although few genes had considerably low median TPMs, they were included in the list, as they are not vastly localized in other non-brain tissues in the body.

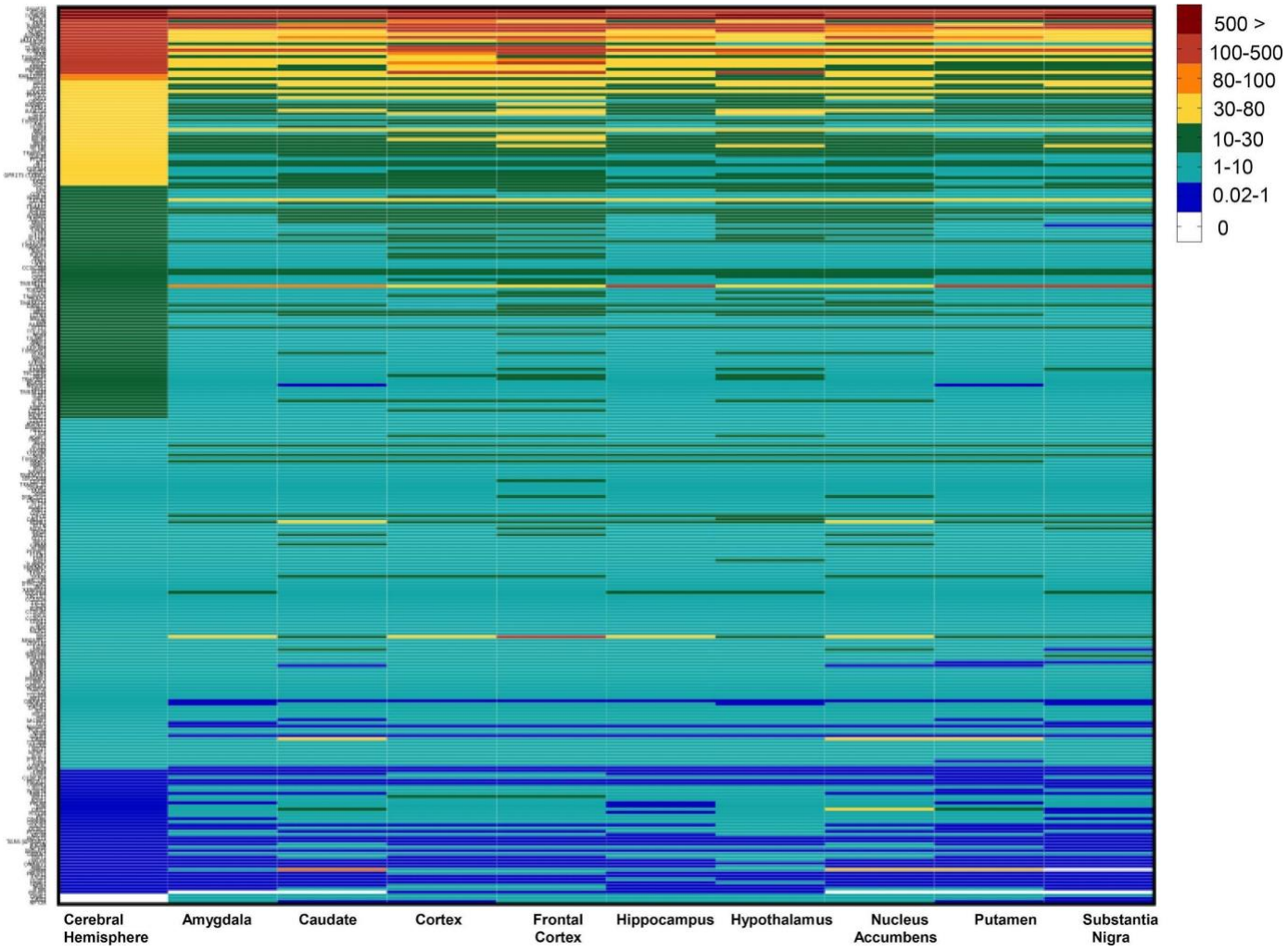

Figure 2.1. Identification of cilia gene expression across specific brain tissues in GTEx. Heatmap of gene expressions of cilia genes in the GTEx brain tissues from the GTEx dataset. Columns denote brain regions and rows represent cilia genes. Genes are shown and categorized in median Transcripts Per Million (TPM).

The expressions of cilia genes are altered in psychiatric disorders

The RNA-Seq data for 268 genes of the 281 cilia genes in our compiled list were extracted from the largest TWAS study of psychiatric disorders [44][48]. Out of the 268 cilia genes, 113 were differentially expressed in SCZ, (48 downregulated and 65 upregulated) compared to 7726

out of 25,502 for non-cilia genes (Fig. 2.2a). Of these genes, 97 genes passed false discovery rate (FDR) < 0.1, and 74 genes passed FDR < 0.05. Exact fisher analysis revealed significant enrichment of differentially expressed cilia genes in SCZ (Odd ratio OR = 1.67, P < 0.0001, Fig. 2.2b). Strikingly, out of the 20 known cilia-associated GPCRs, 15 were differentially expressed in SCZ. Fisher analysis of cilia GPCRs revealed significant enrichment of cilia GPCRs in SCZ (OR: 5.35, P = 0.0003, Fig. 2.2c).

Out of the 268 cilia genes, 63 genes including 3 GPCRs (39 genes downregulated and 24 upregulated), and 46 cilia genes including 7 GPCRs (13 genes downregulated and 33 genes upregulated) were differentially expressed in ASD and BP respectively (Fig. 2.2d,e). Exact fisher test revealed no significant enrichment of the cilia genes as a cluster in ASD (OR = 1.20, P = 0.2) or BP (OR = 0.91, P = 0.6). In MDD, 41 cilia genes including 3 GPCRs were differentially expressed, of which 31 genes were downregulated and only 10 were upregulated (Fig. 2.2f). Exact fisher test revealed no significant enrichment of the cilia genes in MDD (OR = 0.81, P = 0.23).

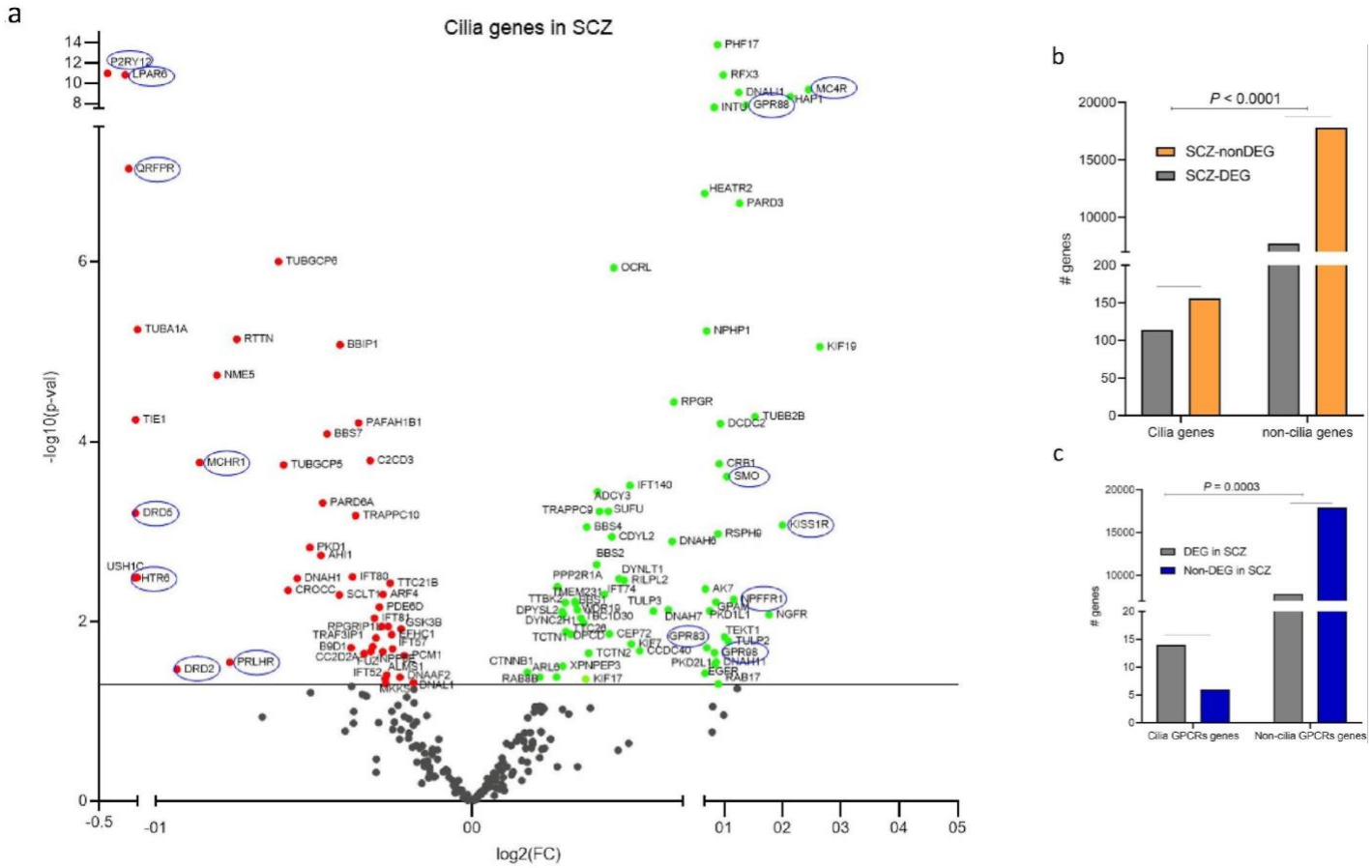
a
Cilia genes in SCZ
-log10(p-val)
log2(FC)
b
P < 0.0001
SCZ-nonDEG
SCZ-DEG
genes
Cilia genes
non-cilia genes
c
P = 0.0003
DEG in SCZ
Non-DEG in SCZ
genes
Cilia GPCRs genes
Non-cilia GPCRs genes

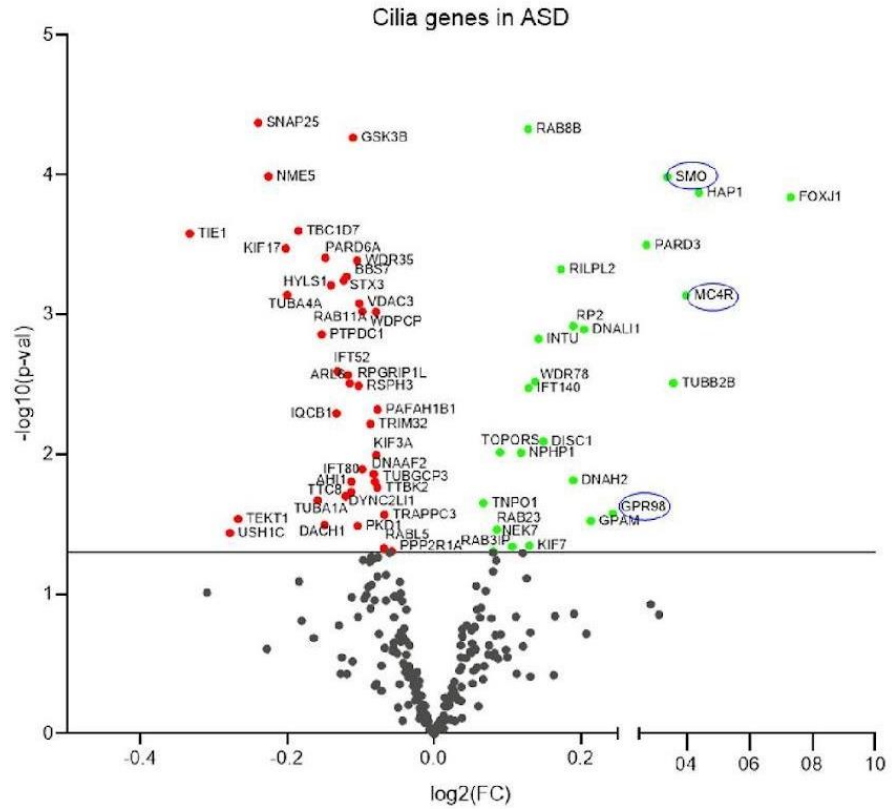
Cilia genes in ASD
-log10(p-val)
log2(FC)
SNAP25
GSK3B
NME5
TIE1
TBC1D7
KIF17
PARD6A
WDR35
BBS7
HYLS1
STX3
TUBA4A
VDAC3
RAB11A
WDPCP
PTPDC1
IFT52
ARL6
RPGRIP1L
RSPH3
IQCB1
PAFAH1B1
TRIM32
KIF3A
DNAAF2
IFT80
TUBGCP3
AHI1
TTBK2
TTC8
DYNC2LI1
TUBA1A
TRAPPC3
TEKT1
USH1C
DACH1
PKD1
RABL5
PPP2R1A
RAB8B
SMO
HAP1
FOXJ1
PARD3
RILPL2
MC4R
RP2
DNALI1
INTU
WDR78
IFT140
TUBB2B
TOPORS
DISC1
NPHP1
DNAH2
TNPO1
GPR98
RAB23
GPAM
NEK7
RAB3IP
KIF7

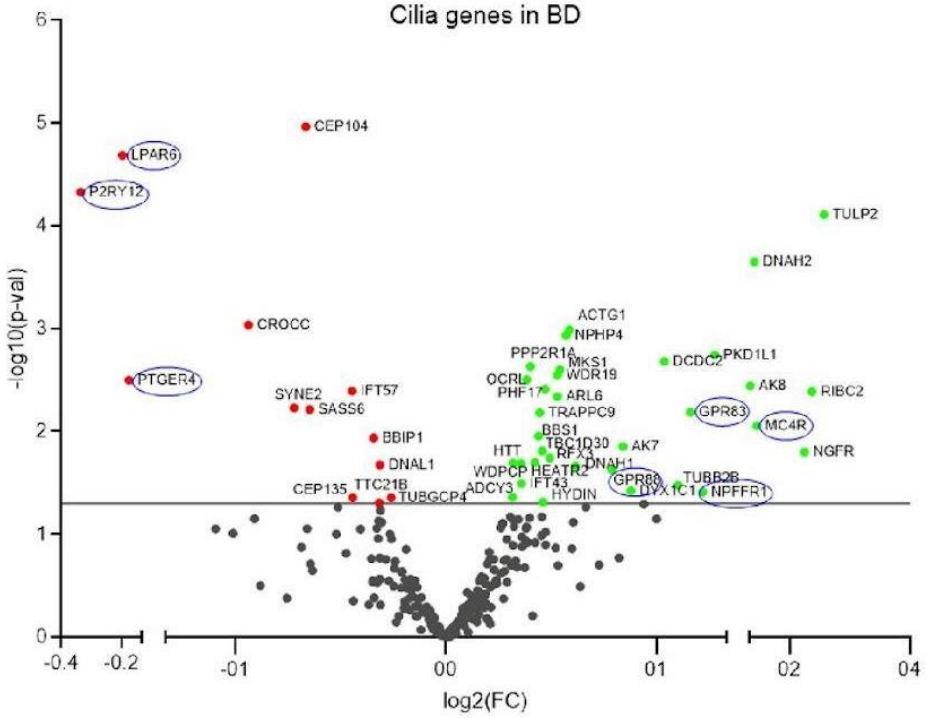
Cilia genes in BD
-log10(p-val)
log2(FC)
CEP104
LPAR6
P2RY12
PTGER4
CROCC
SYNE2
IFT57
SASS6
BBIP1
DNAL1
CEP135
TTC21B
TUBGCP4
ACTG1
NPHP4
PPP2R1A
MKS1
WDR19
OCRL
PHF17
ARL6
TRAPPC9
BBS1
TBC1D30
HTT
RFX3
DNAH1
WDPCP
HEATR2
ADCY3
IFT43
HYDIN
DCDC2
PKD1L1
AK8
RIBC2
GPR83
MC4R
AK7
NGFR
GPR88
TUBB2B
DYX1C1
NPFFR1
TULP2
DNAH2

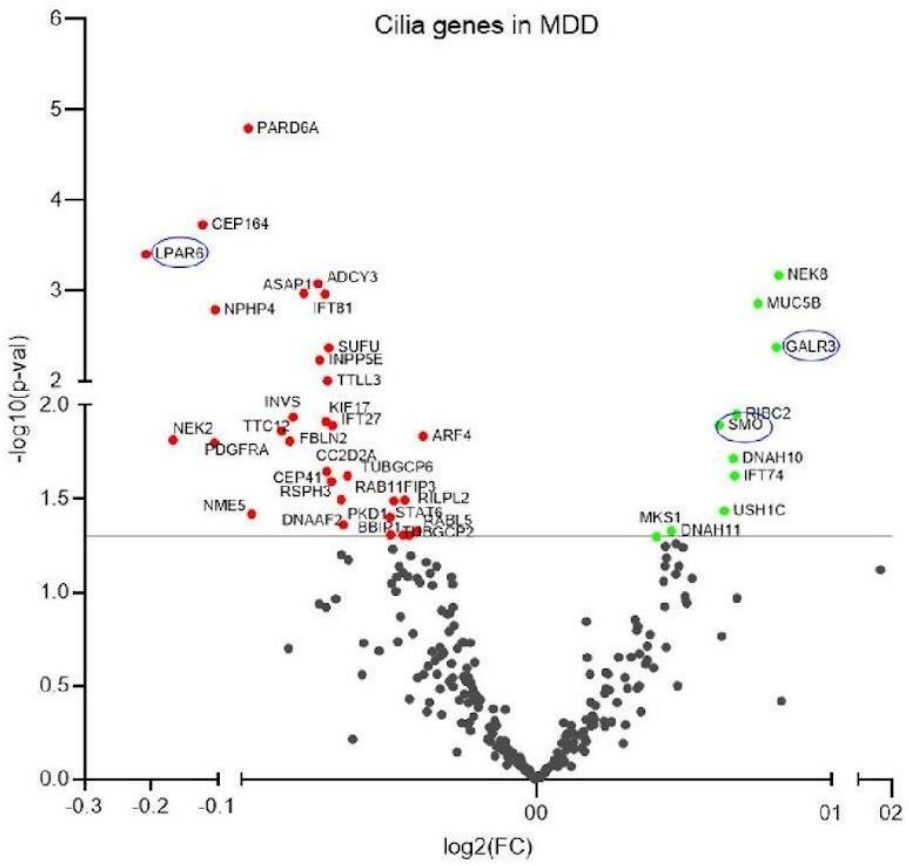

Figure 2.2. Cilia differentially expressed genes in SCZ, ASD, BP, and MDD.

a. Volcano plot showing DEGs ($P < 0.05$) in SCZ. Scattered points represent cilia genes: the x axis is the fold change while the y axis is the -log p value. Green and red dots refer to upregulated and downregulated genes respectively. Genes circled in blue represent GPCRs that localize to the cilium. b. Histogram showing the cilia genes and non-cilia genes that are differentially expressed in SCZ; Exact Fisher test OR = 1.681, $P < 0.0001$. c. Histogram showing cilia GPCR genes and non-cilia GPCR genes that are differentially expressed in SCZ; Exact Fisher test: OR: 6.873, $P = 0.0001$. d-f. Volcano plots of cilia DEGs in (d) ASD, (e) BP, and (f) MDD. Scattered points represent cilia genes: the x axis is the fold change while the y axis is the -log p value. Green and red dots refer to upregulated and downregulated genes respectively.

Several cilia DEGs overlapped across the four disorders, particularly between SCZ and each of the three other disorders (Fig. 2.3a-j). Fisher exact test revealed significant DEGs overlap

between SCZ and BP (P = 0.0009), and a trend in overlap between SCZ and ASD (P = 0.0795), and between the down regulated genes in SCZ and MDD (P = 0.07, Fig. 2.3a).

a

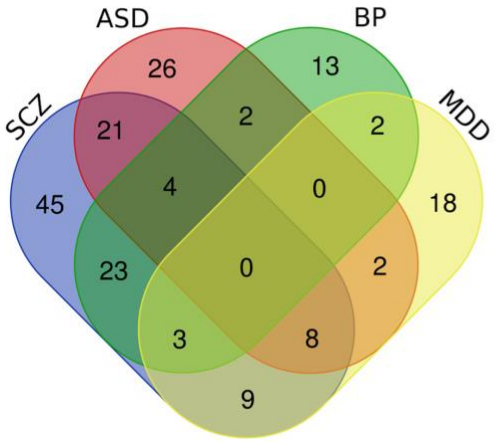

SCZ ∩ ASD *P* = 0.0795
SCZ ∩ BP *P* = 0.0009
SCZ ∩ MDD *P* = 0.61
ASD ∩ BP *P* = 0.085
ASD ∩ MDD *P* = 0.4230
BP ∩ MDD *P* = 0.2587
Downregulated SCZ ∩ downregulated MDD *P* = 0.07

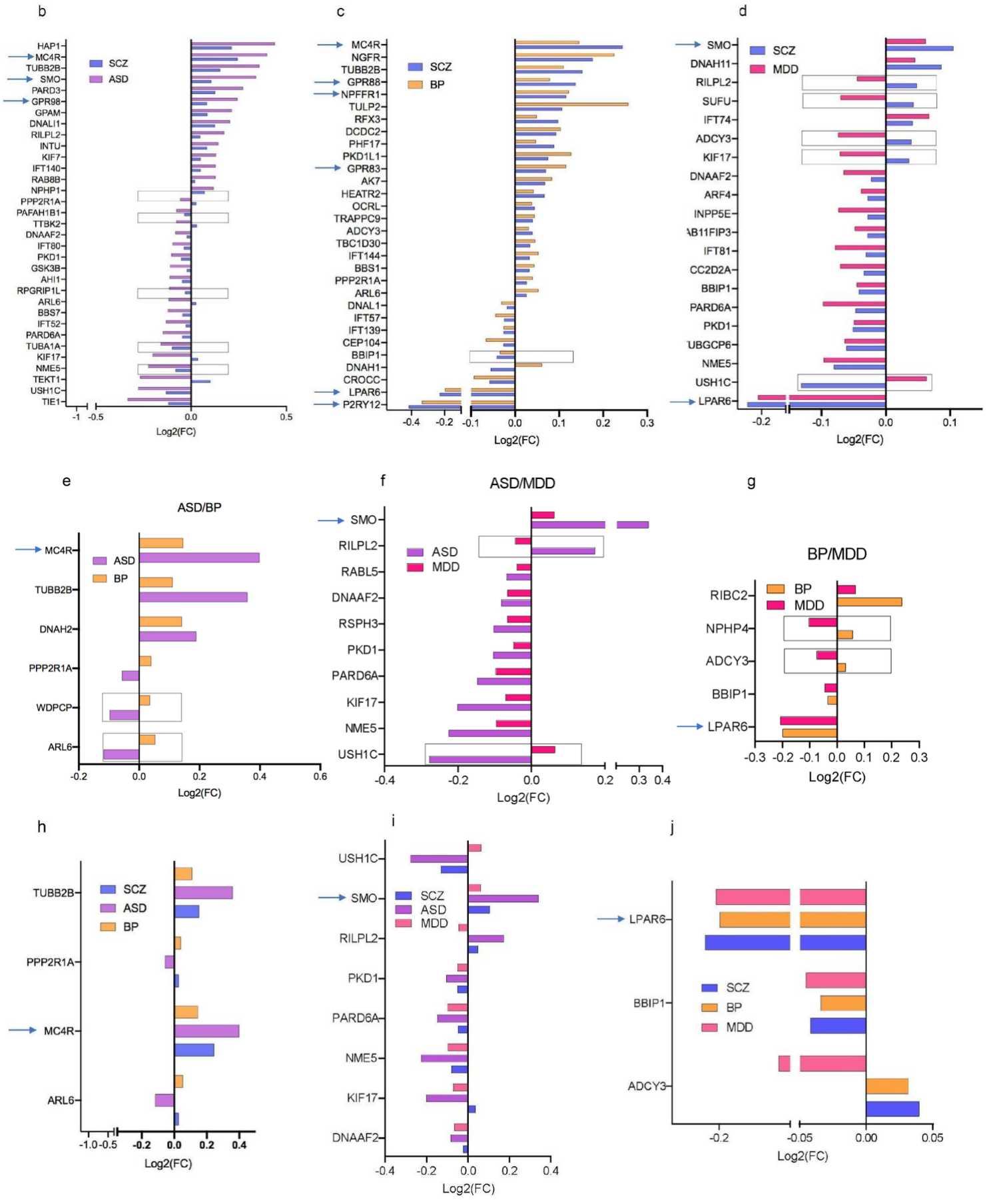
b
HAP1
MC4R
TUBB2B
SMO
PARD3
GPR98
GPAM
DNALI1
RILPL2
INTU
KIF7
IFT140
RABBB
NPHP1
PPP2R1A
PAFAH1B1
TTBK2
DNAAF2
IFT80
PKD1
GSK3B
AHI1
RPGRIP1L
ARL6
BBS7
IFT52
PARD6A
TUBA1A
KIF17
NME5
TEKT1
USH1C
TIE1
SCZ
ASD
-1 -0.5 0.0 0.5
Log2(FC)
c
MC4R
NGFR
TUBB2B
GPR88
NPFFR1
TULP2
RFX3
DCDC2
PHF17
PKD1L1
GPR83
AK7
HEATR2
OCRL
TRAPPC9
ADCY3
TBC1D30
IFT144
BBS1
PPP2R1A
ARL6
DNAL1
IFT57
IFT139
CEP104
BBIP1
DNAH1
CROCC
LPAR6
P2RY12
SCZ
BP
-0.4 -0.2 -0.1 0.0 0.1 0.2 0.3
Log2(FC)
d
SMO
DNAH11
RILPL2
SUFU
IFT74
ADCY3
KIF17
DNAAF2
ARF4
INPP5E
\B11FIP3
IFT81
CC2D2A
BBIP1
PARD6A
PKD1
UBGCP6
NME5
USH1C
LPAR6
SCZ
MDD
-0.2 -0.1 0.0 0.1
Log2(FC)
e
ASD/BP
MC4R
TUBB2B
DNAH2
PPP2R1A
WDPCP
ARL6
ASD
BP
-0.2 0.0 0.2 0.4 0.6
Log2(FC)
f
ASD/MDD
SMO
RILPL2
RABL5
DNAAF2
RSPH3
PKD1
PARD6A
KIF17
NME5
USH1C
ASD
MDD
-0.4 -0.2 0.0 0.2 0.3 0.4
Log2(FC)
g
BP/MDD
RIBC2
NPHP4
ADCY3
BBIP1
LPAR6
BP
MDD
-0.3 -0.2 -0.1 0.0 0.1 0.2 0.3
Log2(FC)
h
TUBB2B
PPP2R1A
MC4R
ARL6
SCZ
ASD
BP
-1.0 -0.5 -0.2 0.0 0.2 0.4
Log2(FC)
i
USH1C
SMO
RILPL2
PKD1
PARD6A
NME5
KIF17
DNAAF2
SCZ
ASD
MDD
-0.4 -0.2 0.0 0.2 0.4
Log2(FC)
j
LPAR6
BBIP1
ADCY3
SCZ
BP
MDD
-0.2 -0.05 0.00 0.05
Log2(FC)

Figure 2.3. Cilia DEGs overlap across the four psychiatric disorders.

(a)Venn diagram conveying overlap between significant DEGs ($P < 0.05$) within the four psychiatric disorders SCZ, ASD, BP, and MDD. b-d. Cilia DEGs overlapping between SCZ with (b) ASD, (c) BP, (d) and MDD. Genes that are differentially expressed in opposing directions are denoted with a box. GPCRs are identified by arrows. e-g. Overlap of DEGs between two disorders: (e) ASD and BP, (f) ASD and MDD, (g) BP and MDD. h-j. Overlap of DEGs among three disorders: (h) SCZ, ASD, and BP, (i) SCZ, ASD, and MDD, (j) SCZ, BP, MDD. The x axis shows Log2(FC) and along the y axis are the cilia genes. Genes that are differentially expressed in opposing directions are denoted with a box. GPCRs are identified by arrows.

Approximately 50% of ASD cilia DEGs (33 genes) including all the three differential GPCRs in ASD (MC4R, SMO, and GPR98) were also differentially expressed in SCZ (Fig. 2.3b). Around two-third of BP cilia DEGs (30 genes) including 6 GPCRs: MC4R, GPR83, GPR88, NPFFR1, P2RY12, and LPAR6 were differentially expressed in SCZ (Fig. 2.3c), and 20 MDD cilia DEGs overlapped with SCZ (Fig. 2.3d).

All cilia structural and functional compartments are associated with the four psychiatric disorders

We next identified the sub-cilia localization of cilia DEGs in the four disorders. We found that proteins encoded by the SCZ cilia DEGs were localized in almost all cilia compartments, including the axoneme (core of the cilium), basal body, ciliary membrane proteins, intraflagellar transport cargo (IFTA and IFTB), cytoskeletal motor proteins (dynein and kinesin family), BBSome (Bardet–Biedl syndrome (BBS) protein trafficking complex), and the transition zone (Fig. 2.4a). We found that 50% of the transition zone genes (33% upregulated and 16% downregulated), 40% of the axoneme genes, 38% of the BBSome complex genes, and 30% of the basal body genes were DEGs in SCZ. While 40% of IFT-A genes were DEGs in SCZ, only 6% of IFT-B genes

displayed expression changes (mainly upregulation) in this disorder. Along with the IFT-A and IFT-B gene changes, 100% of kinesin DEGs compared with 33% of dynein DEGs exhibited upregulation. Strikingly, 75% of cilia GPCRs exhibited altered expression in SCZ.

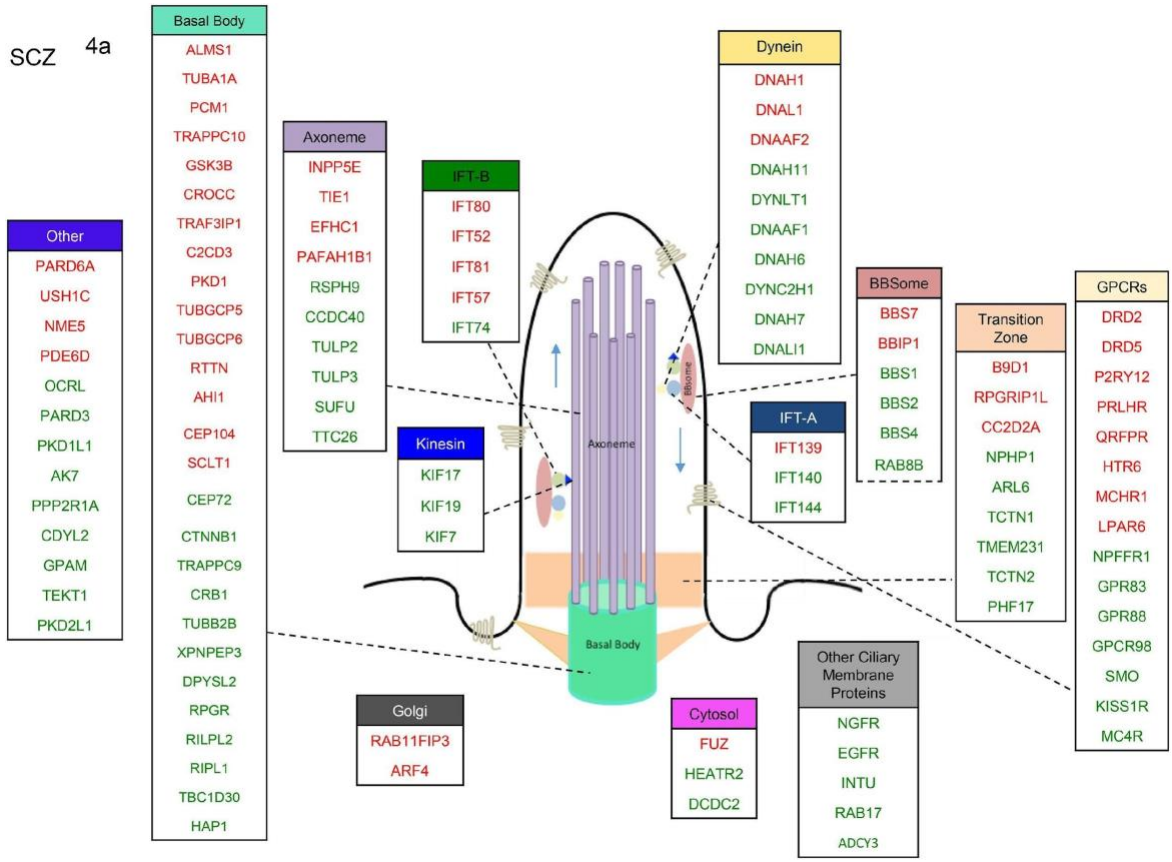

ASD

4b

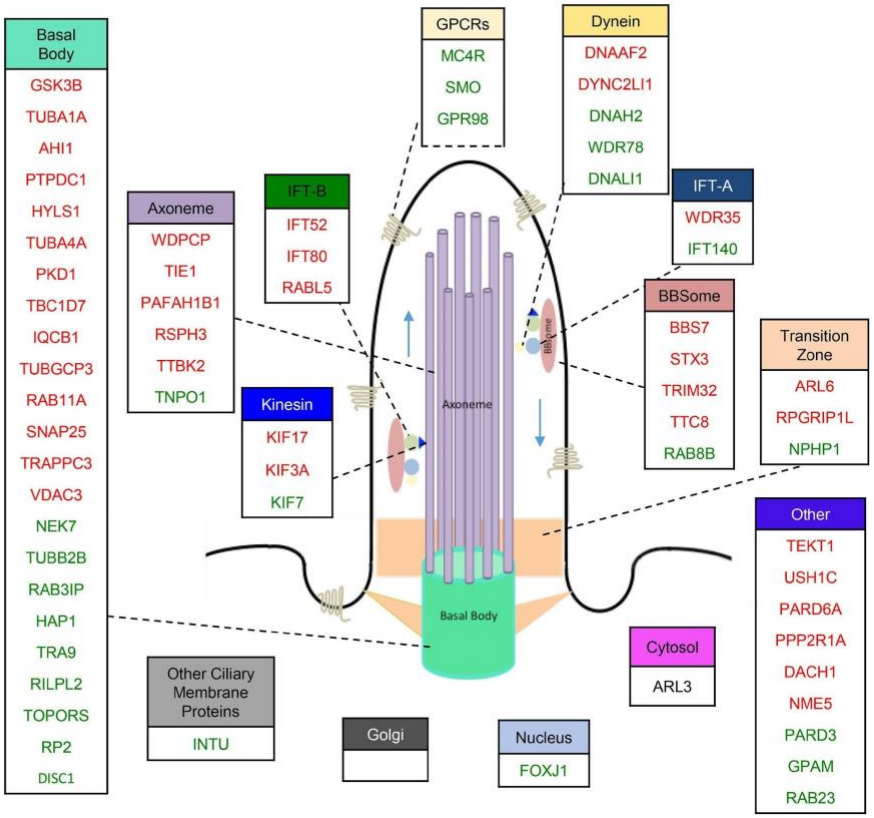
Basal Body
GSK3B
TUBA1A
AHI1
PTPDC1
HYLS1
TUBA4A
PKD1
TBC1D7
IQCB1
TUBGCP3
RAB11A
SNAP25
TRAPPC3
VDAC3
NEK7
TUBB2B
RAB3IP
HAP1
TRA9
RILPL2
TOPORS
RP2
DISC1
GPCRs
MC4R
SMO
GPR98
Dynein
DNAAF2
DYNC2LI1
DNAH2
WDR78
DNALI1
IFT-A
WDR35
IFT140
IFT-B
IFT52
IFT80
RABL5
Axoneme
WDPCP
TIE1
PAFAH1B1
RSPH3
TTBK2
TNPO1
BBSome
BBS7
STX3
TRIM32
TTC8
RAB8B
Transition Zone
ARL6
RPGRIP1L
NPHP1
Kinesin
KIF17
KIF3A
KIF7
Other
TEKT1
USH1C
PARD6A
PPP2R1A
DACH1
NME5
PARD3
GPAM
RAB23
Cytosol
ARL3
Other Ciliary Membrane Proteins
INTU
Golgi
Nucleus
FOXJ1

BP

4c

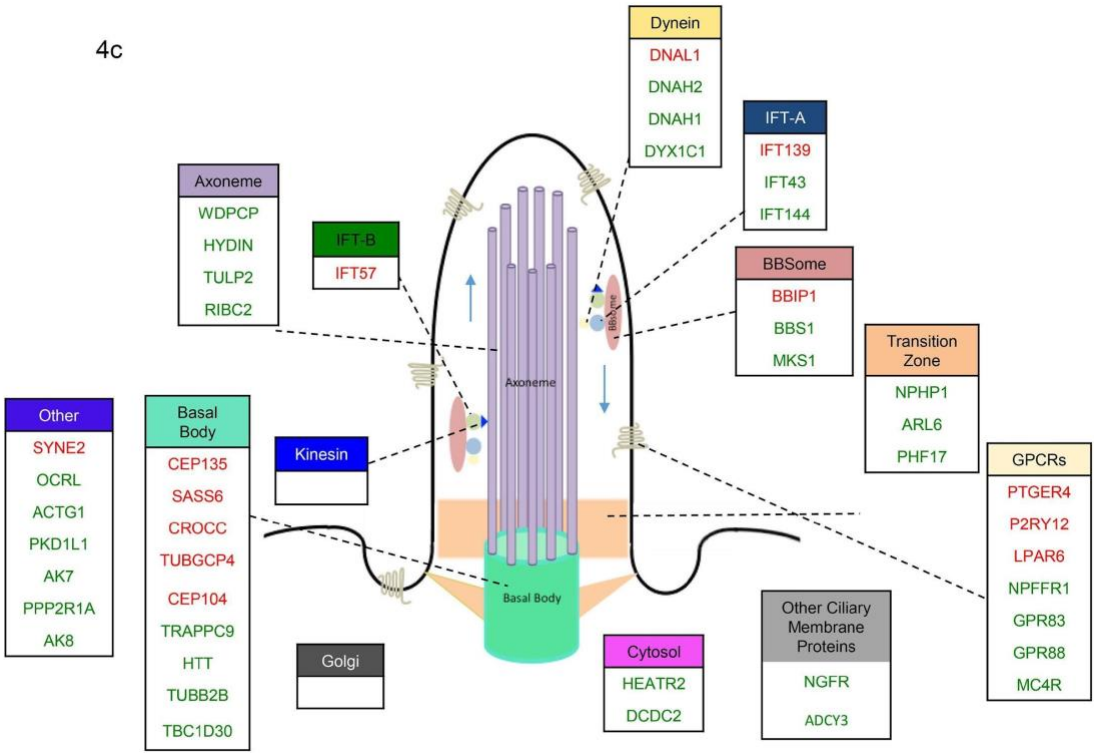
Dynein
DNAL1
DNAH2
DNAH1
DYX1C1
IFT-A
IFT139
IFT43
IFT144
Axoneme
WDPCP
HYDIN
TULP2
RIBC2
IFT-B
IFT57
BBSome
BBIP1
BBS1
MKS1
Transition Zone
NPHP1
ARL6
PHF17
Other
SYNE2
OCRL
ACTG1
PKD1L1
AK7
PPP2R1A
AK8
Basal Body
CEP135
SASS6
CROCC
TUBGCP4
CEP104
TRAPPC9
HTT
TUBB2B
TBC1D30
Kinesin
GPCRs
PTGER4
P2RY12
LPAR6
NPFFR1
GPR83
GPR88
MC4R
Golgi
Cytosol
HEATR2
DCDC2
Other Ciliary Membrane Proteins
NGFR
ADCY3

MDD

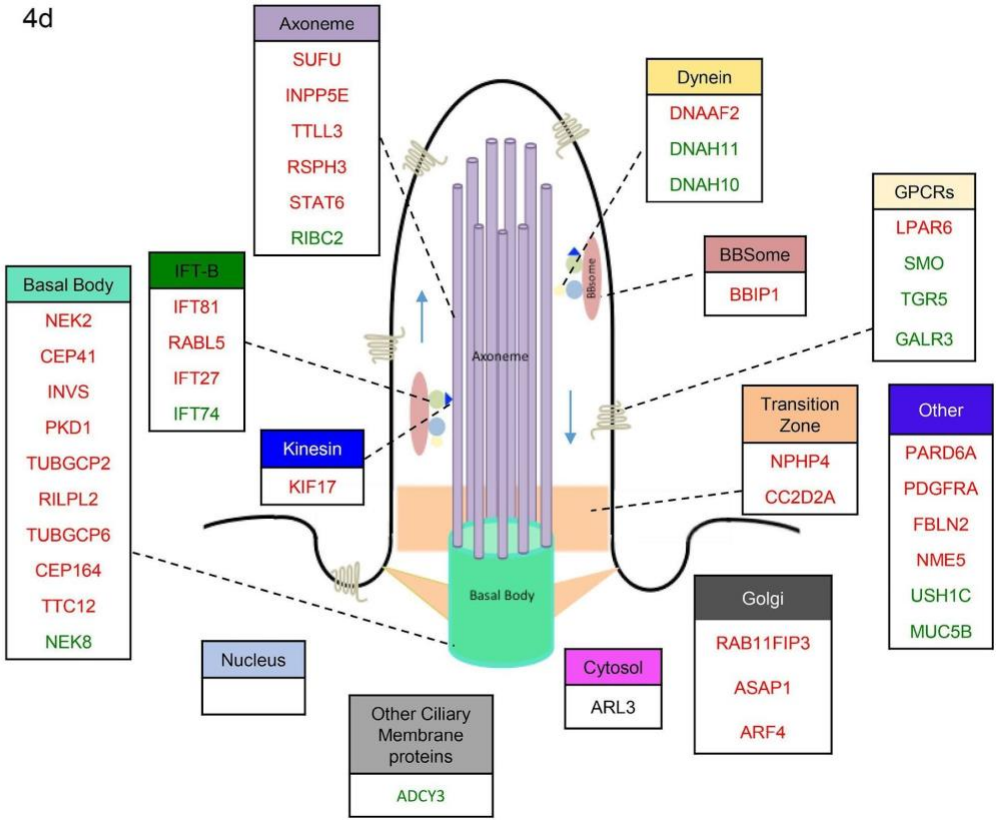

Figure 2.4. Sub-cilia localization of the genes that exhibited differential gene expression in the four disorders.

a-d. Sub-cilia localization of genes that exhibited differential gene expression in (a) SCZ, (b) ASD, (c) BP, (d) MDD. Upregulated and downregulated DEGs are in green and red respectively.

We found that 33% of IFT-A and 19% of IFT-B were DEGs in ASD, and that all IFT-B DEGs exhibited downregulation (Fig. 2.4b). Around 20% of genes localized to the cilia axoneme were DEGs in ASD, of which the vast majority exhibited downregulation. 29% of basal body genes were DEGs, and 15% of GPCRs were upregulated in ASD.

In BP, 50% of IFT-A were DEGs (two-fold more upregulated genes than downregulated), and 6% of IFT-B were downregulated (Fig. 2.4c). Aligned with these, none of the kinesin genes and 19% dynein genes were DEGs.

In MDD, 25% of IFT-B genes, 13% of kinesin genes, 14% of dynein genes, 20% of axoneme genes, 11% of transition zone genes, and 15% of GPCRs were dysregulated (Fig. 2.4d). Interestingly, 75% of genes involved in the Golgi network were downregulated in MDD.

Across the disorders, several cilia DEGs overlapped within most of the cilia structure sub-compartments.

Discussion

This is the first study that describes the association between the brain cilia' structural and functional components at the transcriptomic level and the major psychiatric disorders.

Despite the growing interest in cilia functions, very little is known about their potential involvement in psychiatric disorders. Remarkably, many of the cilia genes that have been causally associated with ciliopathies are also associated with neurological defects such as cognitive deficits [21-23]. Yet, the roles of cilia dysfunctions in the pathogenesis of psychiatric disorders have been largely overlooked.

Therefore, this study is the first step toward understanding the link between the dysregulation of the components of primary cilia and four major psychiatric disorders, namely schizophrenia, autism spectrum disorder, bipolar disorder, and major depressive disorder.

To examine whether the cilia genes are differentially expressed and identify the patterns of gene expression dysregulations in the four psychiatric disorders, we acquired transcriptomic data from the largest cohorts of cases and controls [44, 48]. We show that over 40% of the brain cilia genes are differentially expressed in SCZ, with significant enrichment of differentially expressed cilia genes in this disorder. The dysregulated cilia genes in SCZ encode proteins that are located in almost all cilia structural compartments including basal body, axoneme, cytoskeletal motor proteins (dynein and kinesin family), intraflagellar transport cargo (IFT-A and IFT-B), BBSome, and the transition zone.

Interestingly, all kinesin and kinesin-associated DEGs in SCZ were upregulated, yet most IFT-B DEGs were downregulated. Given the crucial role of the kinesin/IFT-B system in cilia anterograde transport, the dysregulation of this system may negatively affect base-to-tip transport of cilia proteins particularly cilia-associated GPCRs ([50]). Studies have shown that a complete loss of genes involved with the IFT-B complex or kinesin leads to shortening or cilia loss [51-59]. Interestingly, the retrograde system consisting of dynein and IFT-A was also dysregulated, and more than 40% of dynein and IFT-A genes, including IFT144 and IFT140, were dysregulated.

IFT-A complex is associated with dynein motor proteins, and is required for cilia function, assembly, and trafficking within cilia [60]. Mutations in the IFT-A complex subunits and the dynein retrograde motor result in shortened or swollen cilia with an accumulation of particles, including IFT-B proteins, and cause decreased retrograde transport velocities, increased ratio of anterograde to retrograde particles, and an accumulation of complex B proteins in the flagella [61-63]. This complex is particularly associated with ciliary retrograde transport, and it particularly promotes the trafficking of GPCRs [50], which were strikingly dysregulated SCZ (75% of cilia GPCRs were DEGs in SCZ).

TULP3, which encodes the axoneme protein TUB Like Protein 3 that interacts with IFT-A proteins (particularly IFT144) [24], is also upregulated along with IFT144 in SCZ. TULP3 and IFT-A proteins negatively regulate hedgehog signaling in embryonic development and brain formation [28, 50][64-65]. Therefore, TULP3/IFT-A upregulation in SCZ suggests a role for cilia components in the abnormal neurodevelopment in this disorder [50].

The transcriptomic signature of the three other psychiatric disorders ASD, BP, and MDD included many cilia genes. Remarkably, 60% of cilia DEGs were downregulated in ASD, compared to only 30% in BP and 76% in MDD. The high rates of upregulated genes and downregulated genes in bipolar mood disorders and MDD (unipolar mood disorder) respectively are very interesting, given the similarities in the clinical presentations between MDD and the depressive episodes in BP. The differences observed in the trends and directions of cilia genes' alterations in MDD and BP indicate that these two mood disorders, albeit their similar depressive symptoms, display distinct cilia transcriptomic signatures. These differences suggest discrete neuropathological mechanisms underlying these two disorders, and help develop potential classification tools, which might improve diagnostic accuracy and therapeutic precision.

Strikingly, over 50% of cilia DEGs overlap between ASD, BP, or MDD on one side with SCZ on the other side. Such large transcriptomic cross-disorder overlap suggests that dysfunctions of common cilia signaling pathways may partially underlie the pathophysiology of,

or determine susceptibility to more than one psychiatric disorder. For example, ADCY3, which was largely upregulated in SCZ and BP, exhibited downregulation in MDD. ADCY3 encodes the enzyme adenylate cyclase-3 that catalyzes the synthesis of cyclic adenosine monophosphate. ADCY3, known to be associated with ASD [66], was identified by the genome wide study (GWAS) of MDD as one of the three top associated genes [67, 68], and depressed patients display a reduction in platelet ADCY3 activity [69]. Interestingly, ADCY3 knockout mice exhibit depression-like symptoms, more REM sleep, smaller hippocampus, less synaptic activity in the hippocampus and impaired sociability [70]. Another interesting cilia gene is TUBB2B, which is upregulated in SCZ, ASD, and BP. TUBB2B encodes tubulin beta-2B chain, and the dysregulation of this gene results in malformations of development of the cortex and basal ganglia [71-75]. These effects are thought to be caused by altering tubulin heterodimer or GTP binding, and disrupting the interaction between microtubule polymers with associated proteins (e.g. kinesin), ultimately leading to changes in the dynamic properties of microtubule polymers [76, 77].

The overlap observed in cilia DEGs between the four major psychiatric disorders is aligned with the consistent GWAS data on the shared genetic susceptibility across psychiatric disorders [44][78-79]. Thus, our results suggest that shared cilia-related molecular and cellular mechanisms may partially underlie these disorders' clinical phenotypes, particularly since most shared cilia DEGs encode products known to interact or function in common biochemical pathways. Our findings, however, acknowledge the need to construct new classifications of psychiatric disorders, considering the convergence and divergence of biological mechanisms and phenotypic presentations of these disorders.

PCM1, one of the top cilia DEGs in SCZ, has recently emerged as a credible candidate for severe schizophrenia [79]. Missense mutation and polymorphisms of PCM1, have been previously associated with schizophrenia [35] [80]. PCM1, which is a DISC1- interacting protein, is involved in the maintenance of centrosome integrity and regulation of microtubule cytoskeleton and dopamine transmission [81-83]. Suppression of PCM1 affects neuronal migration and plays

a role in cortical development and genetic susceptibility to schizophrenia [36], and Pcm1+/− mice display deficits in social interaction and show significant reduction in brain volume [84].

The striking alterations in the expressions of GPCRs in the four psychiatric disorders, particularly in SCZ (75% of cilia GPCRs) indicate a crucial role for the cilia GPCRs in the pathogenesis of these disorders. Cilia-associated GPCRs regulate cilia formation, structure, and ability to respond to external stimuli [85], and therefore, are essential for correct ciliary signal transduction. The high “druggability” of GPCRs, and the advancements in the cilia targeted drug delivery [86, 87] make these receptors of great interest as druggable sites, which might lead to novel treatments and/or prevention strategies for these psychiatric disorders.

In conclusion, we demonstrate gene dysregulations of almost all structural and functional components of primary cilia in four major psychiatric disorders, and identify large transcriptomic cross-disorder overlap. Our work provides strong evidence for the potential that primary cilia have as possible pathophysiological cause or therapeutic target in psychiatric disorders.

Chapter 3: Large-Scale Analysis Reveals Spatiotemporal Circadian Patterns of Cilia Transcriptomes in the Primate Brain

Baldi, P., Alhassen, W., Chen, S., Nguyen, H., Khoudari, M., & Alachkar, A. (2021). **Large-scale analysis reveals spatiotemporal circadian patterns of cilia transcriptomes in the primate brain**. Journal of Neuroscience Research, 99, 2610–2624. https://doi.org/10.1002/jnr.24919

Abstract

Cilia are dynamic sub-cellular systems, with core structural and functional components operating in a highly coordinated manner. Since many environmental stimuli sensed by cilia are circadian in nature, it is reasonable to speculate that genes encoding cilia structural and functional components follow rhythmic circadian patterns of expression. Using computational methods and the largest spatiotemporal gene expression atlas of primates, we identified and analyzed the circadian rhythmic expression of cilia genes across 22 primate brain areas. We found that around 73% of cilia transcripts exhibited circadian rhythmicity across at least one of 22 brain regions. In 12 brain regions, cilia transcriptomes were significantly enriched with circadian oscillating transcripts, as compared to the rest of the transcriptome. The phase of the cilia circadian transcripts deviated from the phase of the majority of the background circadian transcripts, and transcripts coding for cilia basal body components accounted for the majority of cilia circadian transcripts. In addition, adjacent or functionally connected brain nuclei had large overlapping complements of circadian cilia genes. Most remarkably, cilia circadian transcripts shared across the basal ganglia nuclei and the prefrontal cortex peaked in these structures in sequential fashion that is similar to the sequential order of activation of the basal ganglia-cortical circuitry in connection with movement coordination, albeit on completely different time scales. These findings support a role for the circadian spatiotemporal orchestration of cilia genes expression in the normal physiology of the basal ganglia-cortical circuit and motor control. Studying orchestrated cilia rhythmicity in the basal ganglia-cortical circuits and other brain circuits may help develop better functional models, and shed light on the causal effects cilia functions have on these circuits and on the regulation of movement and other behaviors.

Introduction

Cilia are evolutionarily conserved organelles that protrude from the membranes of almost all cell types. The distinct designs of cilia, which served swimming through fluids in ancient unicellular organisms, were repurposed by evolution to drive a wide range of completely different functions from their original ones. These functions range from guiding a worm to explore its environment to regulating complex cognitive functions in primates. With recent discoveries highlighting the importance of primary cilia in brain function [1-6], cilia have emerged as an essential component of sensory perception and transduction signaling pathways and a crucial center for non-synaptic neuronal signaling [7]. Cilia, however, have preserved two features throughout their long evolutionary history and across all cell types: highly dynamic physical structures (length and assembly/disassembly) and the capability of sensing and transducing a variety of environmental stimuli. In this context, cilia act as cell "antennas" to sense environmental signals and transduce them into biochemical responses that regulate a wide range of cellular activities (see [8, 9] for reviews).

Numerous extracellular and environmental stimuli can be detected and transduced by cilia, including light [10] odorant [11], mechanical stimuli and fluid flow [12-14], pH [15, 16], osmolarity [17, 18], temperature [19], gravity [20], and chemical signals (signaling molecules, neurotransmitter, hormones, growth factors) [15]. Besides performing these highly specialized sensory and transducing functions, cilia also act as signaling centers that mediate cell-to-cell communication through extracellular vesicles (EVs) [21, 22]. The signal transduction properties of cilia are mediated by specific molecular receptors associated with cilia membranes, including ion channels, receptor tyrosine kinases (RTK), and G-protein-coupled receptors (GPCRs) [23-28].

Cilia are highly dynamic systems in terms of length, ultrastructural morphology, sub-compartments, and protein composition and trafficking, with the core structural and functional

components of cilia functioning in a highly coordinated manner [25, 29-31]. Many environmental stimuli that are sensed by cilia are oscillatory in nature and follow rhythmic temporal patterns of stimulation such as light--dark cycles [32, 33], temperature [34], nutrient availability [35], and gravity [36-38]. The rhythmic nature of external signals sensed by cilia alongside their highly dynamic nature led us to speculate that genes encoding cilia sub-structural and functional components are expressed in rhythmic patterns.

More precisely many functions, in which ciliary signaling is implicated, oscillate in circadian fashion, such as sleep-wake, feeding [27, 39, 40], energy homeostasis [41], metabolism [42], body temperature [43], sexual/reproductive behaviors [44, 45], and even higher brain functions related to memory, and mood and social behavior [46-48]. We speculate that genes encoding cilia structural and functional components, responsible for driving cilia oscillatory regulation of metabolic, physiological, and behavioral processes, follow rhythmic circadian patterns of expression. To test this hypothesis, we acquired transcriptomic data from the largest spatiotemporal gene expression atlas of primates to profile rhythmic brain cilia transcriptome and to define the patterns of cilia gene expression in the brain [49].

Materials and methods

Cilia genes' list

We used a list of 281 genes that were identified and verified to be cilia genes expressed in the human brain using cilia databases [50-52], as described in our recent report [53]. Briefly, we used SysCilia Gold Standard version 1 and CiliaCarta database to compile a list of gold standard cilia genes as well as CilDB database to further confirm the cilia genes. We then screened the genes to be sure that they were expressed in the brain using GTEX. It is important to note that cilia gene databases are constantly being revised, and no list can truly be considered "complete" because new cilia genes are discovered all the time. As a result, our list of cilia genes is a working list that will be revised as needed.

Cilia circadian genes data

We extracted the transcriptomic time series associated with the 281 cilia genes from the full transcriptomic time series performed in 22 baboon brain regions tissue collection was performed at the Institute of Primate Research (IPR, National Museums of Kenya, Nairobi; see the original study for full details on the protocols, ethics, sample collection, and processing; Mure et al., 2018). Brain regions included the following: amygdala (AMY), arcuate nucleus (ARC), cerebellum (CER), dorsomedial hypothalamus (DMH), habenula (HAB), hippocampus (HIP), prefrontal cortex (PRC), putamen (PUT), lateral globus pallidus (LGP), lateral hypothalamus (LH), mammillary body (MMB), medial globus pallidus (MGP), olfactory bulb (OLB), paraventricular nucleus (PVN), preoptic area (PRA), pons (PON), substantia nigra (SUN), suprachiasmatic nucleus (SCN), supraoptic nucleus (SON), thalamus (THA), ventromedial hypothalamus (VMH), and visual cortex (VIC).

Circadian analysis

For the circadian analyses, we extracted the transcriptomic time series associated with the 281 cilia genes from the full transcriptomic time series performed in 22 baboon brain regions [49] through CircadiOmics [54, 55], the largest repository of circadian omic time series datasets. We then identified which transcripts were oscillating in a circadian manner under control and experimental conditions. BIO_CYCLE [56], a deep-learning-based model developed to analyze periodicity in transcriptomic time series data, was used to identify statistically significant circadian transcripts, as well as the amplitude and the phase of their oscillations. BIO_CYCLE is trained on both synthetic and real-world biological time series data sets containing labels for periodic and aperiodic signals. A classification deep neural network (DNN) is trained to classify signals as periodic or not, and a regression DNN is trained to estimate the period, phase, and amplitude of the signal. Whether a gene is oscillating or not is determined by the p value (cutoff at 0.05) provided by BIO_CYCLE. BIO_CYCLE calculates a p value as follows: N aperiodic signals are first generated from the synthetic time series data sets, and the N output values V(i) (i = 1, …, N) of the classification DNN on these aperiodic signals are calculated. These values are used to establish the distribution for the null hypothesis. Then, the output value V of the new signal s is compared to V(i)(i = 1, …, N), producing the estimate for the probability of obtaining an output of size V or greater (p value), assuming that the signal s comes from the null distribution (the distribution of aperiodic signals). Therefore, the smaller the p value, the more likely that s is periodic. The corresponding q-values are obtained through the Benjamini and Hochberg procedure. BIO_CYCLE is publicly available from the CircadiOmics web portal at: http://circadiomics.igb.uci.edu.

Cilia circadian transcripts were grouped within four time phases of 6-hr intervals (quarter-phases), associated with their peak in gene expression: first quarter-phase (ZT0–ZT5), second quarter-phase (ZT6–ZT11), third quarter-phase (ZT12–ZT17), and fourth quarter-phase (ZT18–

ZT23). A Fisher's exact test was then used to compare the proportions of circadian cilia genes in the 22 brain regions with the brain area background circadian transcriptome. The overlap of cilia rhythmic genes across regions was determined as gene-view and region-view intersections. The distribution of cilia circadian genes across main structural and functional components of the cilia was examined. Thus, cilia genes were grouped based on their localization to the cilium, including basal body, axoneme, kinesin, dynein, IFT-A, IFT-B, transition zone, BBsome, Golgi, nucleus, cytosol, and the ciliary membrane. When localization is unknown, the genes were placed in a group labeled as “other.” The percentages of substructural cilia transcripts that exhibited circadian rhythm were calculated.

Results

Circadian oscillation of ciliary transcriptome in the brain is region-specific

All 22 brain regions reported in the primate diurnal transcriptome atlas [49] had circadian cilia transcripts (Fig. 3.1a,b,) (www.brainmaps.org) [57], and 206 cilia genes (72.8% of all cilia genes) were determined to have circadian oscillations in at least one brain region. Prefrontal cortex (PRC) exhibited the highest number of cilia circadian cycling genes (66 cilia cycling genes) followed by putamen (PUT), lateral globus pallidus (LGP) and mammillary body (MMB) (58 cilia cycling genes in each), and medial globus pallidus (MGP) (56 cilia cycling genes), accounting for 23%, 21%, 21%, and 21% of the cilia genes in PRC, PUT, LGP, and MGP respectively. Amygdala and lateral hypothalamus exhibited the lowest number of cilia circadian genes (4 cilia cycling genes in each). The overwhelming majority (greater than 99%) of the cilia rhythmic transcripts oscillate with the period of 22-24-hours (Fig. 3.1c). The rhythmic expression was region-specific and, in general, the number of cilia circadian genes in a given brain region was correlated with the number of background circadian genes in the same region (Pearson's correlation coefficient was high, r^2 = 0.966, $P < 0.0001$, Fig. 3.1d). We computed the enrichment of circadian oscillating genes in these 22 brain regions, and found that cilia circadian rhythmicity was overrepresented in 12 brain regions (Fisher's exact test, $P < 0.05$). Brain regions, in which cilia transcripts exhibited higher rhythmicity than the non-cilia transcripts, included the PRC (Odd ratio (OR)=1.8), PUT (OR=1.6), LGP (OR=1.67), MMB (OR=1.64), MGP (OR=1.5), dorsomedial hypothalamus (DMH) (OR =2.3), PVN (OR=2.2), visual cortex (VIC) (OR=1.74), suprachiasmatic nucleus (SCN) (OR=1.71), arcuate nucleus (ARC) (OR=2.38), pons (PON) (OR=1.49), and preoptic area (PRA) (OR=1.85)(Fig. 3.1e).

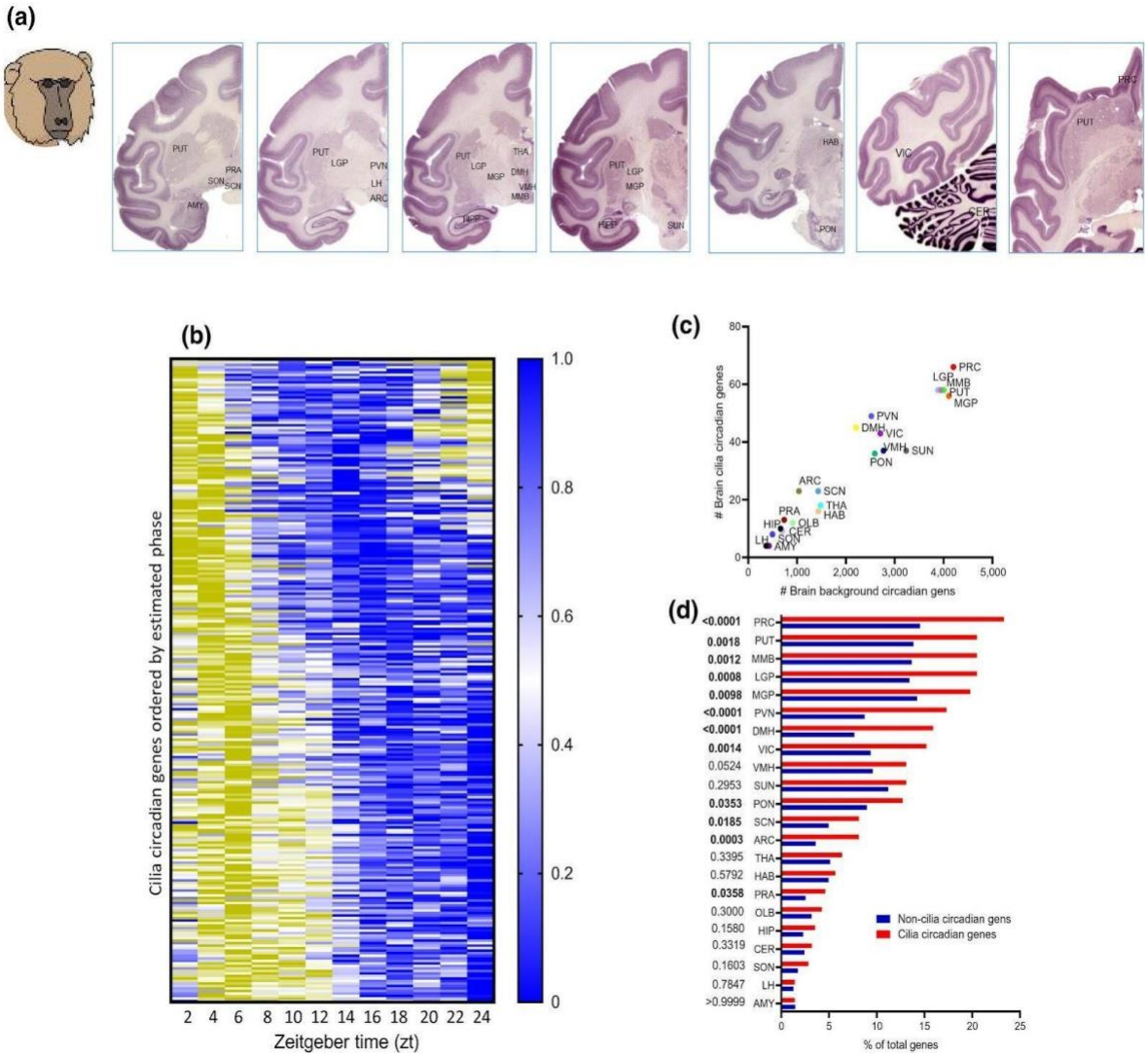

Figure 3.1. Twenty-four-hour circadian rhythms of cilia genes abundance in the brain of primates.

(a) Representative brain sections from *Macaca mulatta* brains (Brain maps, Primates: www.brainmaps.org (Mikula et al., 2007)), showing the regions and nuclei from which tissues were collected (Mure et al., 2018). AMY, Amygdala; ARC, arcuate nucleus; CER, cerebellum; DMH, dorsomedial hypothalamus; HAB, habenula; HIP, hippocampus; LGP, lateral globus pallidus; LH, lateral hypothalamus; MGP, medial globus pallidus; MMB, mammillary body;

OLB, olfactory bulb; PRA, preoptic area; PRC, prefrontal cortex; PON, pons; PUT, putamen; PVN, paraventricular nucleus; SCN, suprachiasmatic nucleus; SON, supraoptic nucleus; SUN, substantia nigra; THA, thalamus; VIC, visual cortex; VMH, ventromedial hypothalamus. (b) Heatmap representation of 24-hr oscillation of 206 circadian cilia genes in primate brain, with mean expressions ordered by phase ($p < 0.05$). Gene expressions are normalized between 0 and 1, yellow (1) indicates a peak of expression and blue (0) indicates a trough of expression. (c) Linear correlation between number of cilia circadian genes in a given brain region and the number of general circadian genes in the same region (Pearson's r, $r^2 = 0.966$, $p < 0.0001$). (d) Histogram showing the enrichment analysis (Fisher's exact test) of cilia genes that are circadian in the 22 brain regions; 12 regions exhibited significant enrichment (i.e., with overrepresented circadian cilia transcripts including: ARC, arcuate nucleus; DMH, dorsomedial hypothalamus; LGP, lateral globus pallidus; LH, lateral hypothalamus; MGP, medial globus pallidus; MMB, mammillary body; PON, pons; PRA, preoptic area; PRC, prefrontal cortex; PUT, putamen; PVN, paraventricular nucleus; SCN, suprachiasmatic nucleus; VIC, visual cortex)

We grouped the circadian ciliary genes into four 6-hour phases (quarter-phases) (Fig. 3.2a). Across all cilia circadian genes and the 22 brain regions, the combination of peak phases of expression revealed three main peaks, early afternoon (44 and 83 cilia genes peaked at ZT6 and ZT7 respectively), midnight (41 genes peaked at ZT14), and late night (39 genes peaked at ZT20) (Fig. 3.2a,b). With a few exceptions, the peak phases in each brain region were mostly bundled in one or two narrow (<6 hours) temporal intervals (Fig. 3.2c,d). In regions such as ARC, DMH, LGP, MGP, PRC, PUT, PVN, VIC, SCN, PRA, the majority of circadian genes peaked within a narrow window, whereas some regions such as PON, MMB, and SCN had transcripts that peaked within two distinct time windows (Fig. 3.2d). However, in anatomically and functionally connected regions these phase clusters were temporally close. For example, in the basal ganglia, the main phase cluster was at ZT4 for the PUT, and in the LGP and MGP, it appeared at ZT6 and ZT7

respectively. Similarly, except for the PRA, the phase clusters of the hypothalamic nuclei (ARC, DMH, SCN, and PVN) were similar (Fig. 3.2c,d).

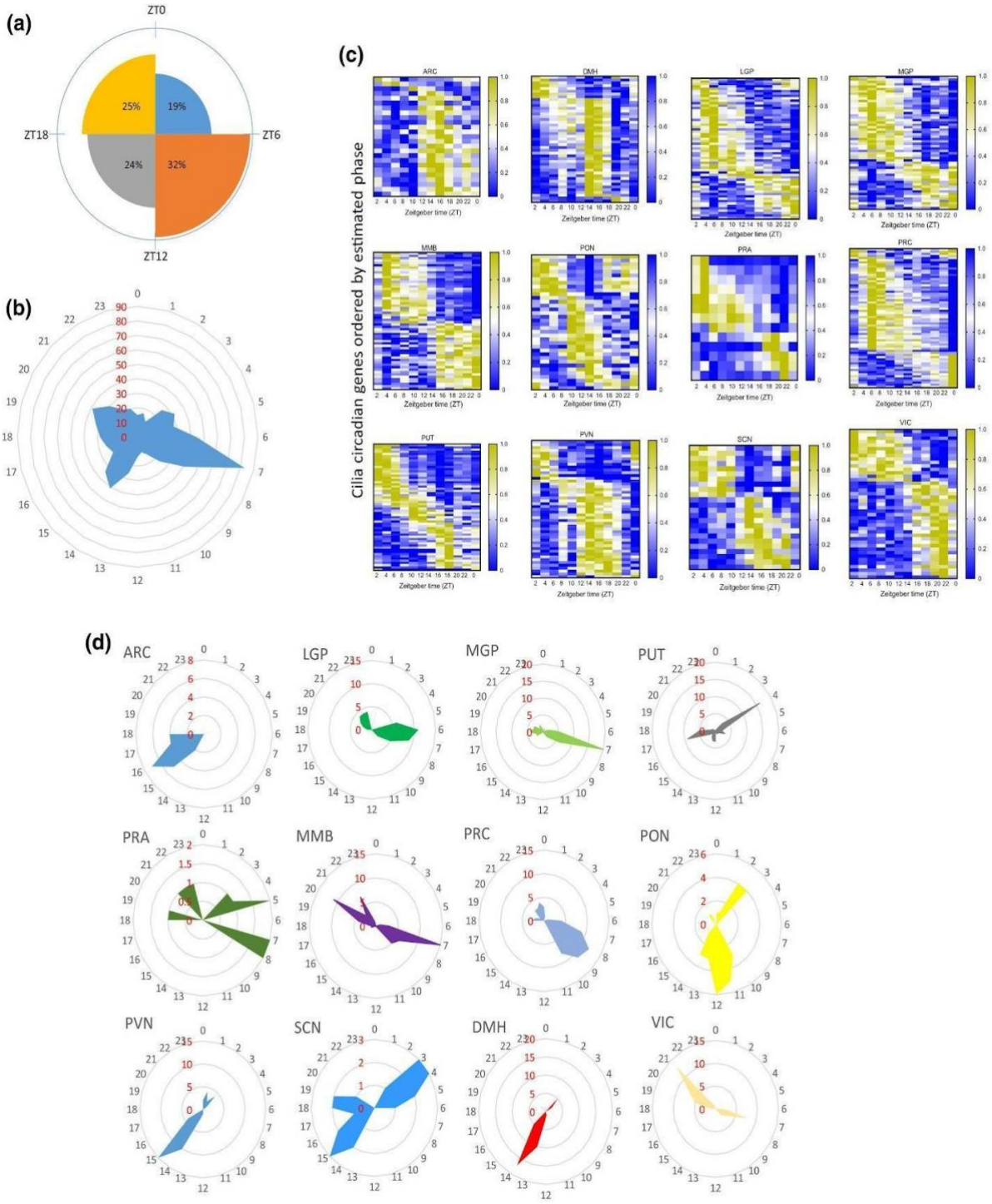

Figure 3.2. Cilia circadian gene display region-specific expression. (a) Rose diagram showing the percentage of cilia circadian genes in each of the four time phases. (b) Radial diagram of the distribution of the peak phase of expression of the circadian cilia genes in the whole brain. The radial plot displays phases (hr) on the circumference and the number of gene peaks of expression on the radius (red). (c) Heatmap representation of 24-hr oscillation of circadian cilia genes in the 12 brain regions that exhibited overrepresented circadian cilia genes in primate brain ($p < 0.05$), with mean expressions ordered by phase ($p < 0.05$). Gene expressions are normalized between 0 and 1, yellow (1) indicates a peak of expression and blue (0) indicates a trough of expression. (d) Radial plot of the distribution of the peak phase of expression of the cilia circadian genes in each of the 12 brain regions that exhibited overrepresentation (in Figure 1d). Phases (hours) are displayed on the circumference and the numbers of gene peaks of expression are displayed on the radius (red).

Overlap of expression of cilia circadian genes across brain regions

Gene view overlap

Confined expression overlap of cilia circadian genes between brain regions was observed, with no cycling genes being shared across all brain regions (Fig. 3.3a). The maximal number of regions that shared one circadian gene was 14 regions, whereas 54 cilia genes exhibited circadian oscillation only in a single brain region (Fig. 3.3a). We surveyed genes that were detected as being circadian in multiple brain regions. The gene shared in the largest number of brain regions was FOPNL (14 regions), followed by RILPL1, which was circadian in 12 brain regions, and TUBGCP2, TUBGCP6, and RAB8A, which were circadian in 9 regions (Fig. 3.3b). Out of these five genes, only FOPNL did peak within a distinct narrow interval (ZT17-ZT22) in all the 14 shared brain regions (Fig. 3.3b).

Region view overlap

Region pairwise intersection analysis revealed 184 (out of 231 possible) non-empty intersections. The size of these intersections ranged from one gene for 37 intersections to 31 genes which occurred in two intersections (Fig. 3.3c,d). PUT exhibited an overlap of its cilia circadian transcriptome with all other brain regions (21 regions), and PON, PRC, and SCN exhibited overlaps with 20 brain regions. As per the number of shared circadian genes, MGP exhibited the highest overlap in the transcripts shared (31 genes with LGP and MMB), followed by PRC which overlapped with MMB (29 genes), and with MGP and LGP (28 genes each). In turn, PUT overlapped with MMB (25 shared genes), MGP (24 genes), and LGP (23 genes) (Fig. 3.3d).

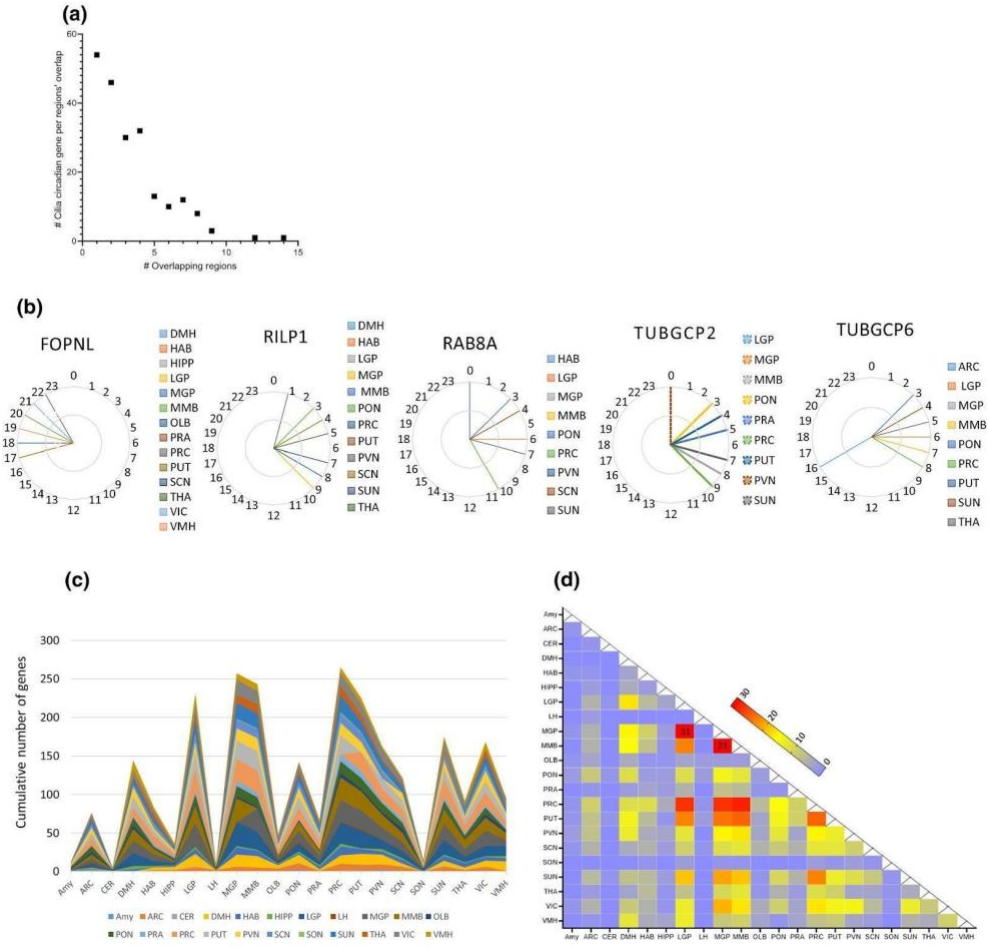

Figure 3.3. Overlap of cilia circadian transcriptome in brain nuclei/regions.

(a) Number of cilia circadian transcripts (y axis), whose expressions exhibit overlap in corresponding number of brain regions' intersections (x axis). (b) Peak expression phase of top overlapping cilia circadian genes (genes showing highest overlap among brain regions). (c) Stacked area plot showing the cumulative distribution of the overlapped genes in different brain regions. (d) Heatmap of nucleus-by-nucleus intersections of the cilia circadian genes. The size of the intersections ranged from one gene (blue) to 31 transcripts (red), which occurred in two intersections

Structural and functional organization of cilia circadian genes

We then examined the distribution of cilia circadian genes' expressions across cilia's main structural and functional components (Fig. 3.4a). We found that genes encoding the components of the basal body exhibited the highest number (61) of circadian genes (78% of total basal body genes) (Fig. 3.4a). Interestingly, 100% of genes encoding the components of the Golgi and IFT-A particles were circadian, whereas 82%, 87.5%, 67%, 73%, 60%, and 47.6% of IFT-B, kinesin, transition zone, GPCRs, axoneme, dynein respectively exhibited circadian rhythms in at least one brain region (Fig. 3.4a,b). This strongly suggests that the regulation of cilia assembly and functions have a strong circadian component.

We further analyzed the phase distributions of the genes encoding most cilia structural and functional components in the entire brain. We found that most genes were clustered in one or two narrow windows (Fig. 3.4a-n), whereas some components were widely distributed within 14-18 hours, such as the genes of the basal body and transition zone. Notably, the circadian transcripts associated with the axoneme, which gives rise to the cilia cytoskeletal structure, peaked within wide intervals. Apparently, the majority of cilia circadian transcripts that peaked at

ZT7, as noted above, encode components of the basal body, transition zone, kinesin, cilia membrane, and Golgi apparatus. Of particular interest are the temporal patterns of the transport machinery genes (kinesin, dynein, BBsomes, and IFT-A and IFT-B). The circadian genes associated with kinesin motors, which are primarily involved in anterograde trafficking, peaked during the 12-hour light phase, whereas the circadian genes associated with dynein motors, which are responsible for the retrograde transport, peaked during the 12-hour dark phase. The circadian transcripts of BBsomes and IFT-B particles peaked in the same phase as dynein in the dark phase (ZT13-ZT22). Most interestingly, most circadian genes encoding cilia GPCRs, which are transported through cilia by the kinesin-dependent trafficking machinery, peaked in a way similar to kinesin, during the light phase.

Although the abundance of rhythmic gene expression of cilia substructures components varied across brain regions, the peak phases of expression of the cilia sub-structural components were mostly consistent with their rhythmic patterns in the whole brain (Fig. 3.4a,c-n). Circadian transcripts encoding specific cilia sub-structures, however, exhibited dispersed temporal phases in different brain regions. Unlike their multi-phasic oscillating patterns in the whole brain, genes of the basal body and the transition zone tended to peak in one or two phases in different brain regions. These results support the idea that specific cilia genes oscillate in circadian manner distinctively across brain regions (Fig. 3.4a,c-n).

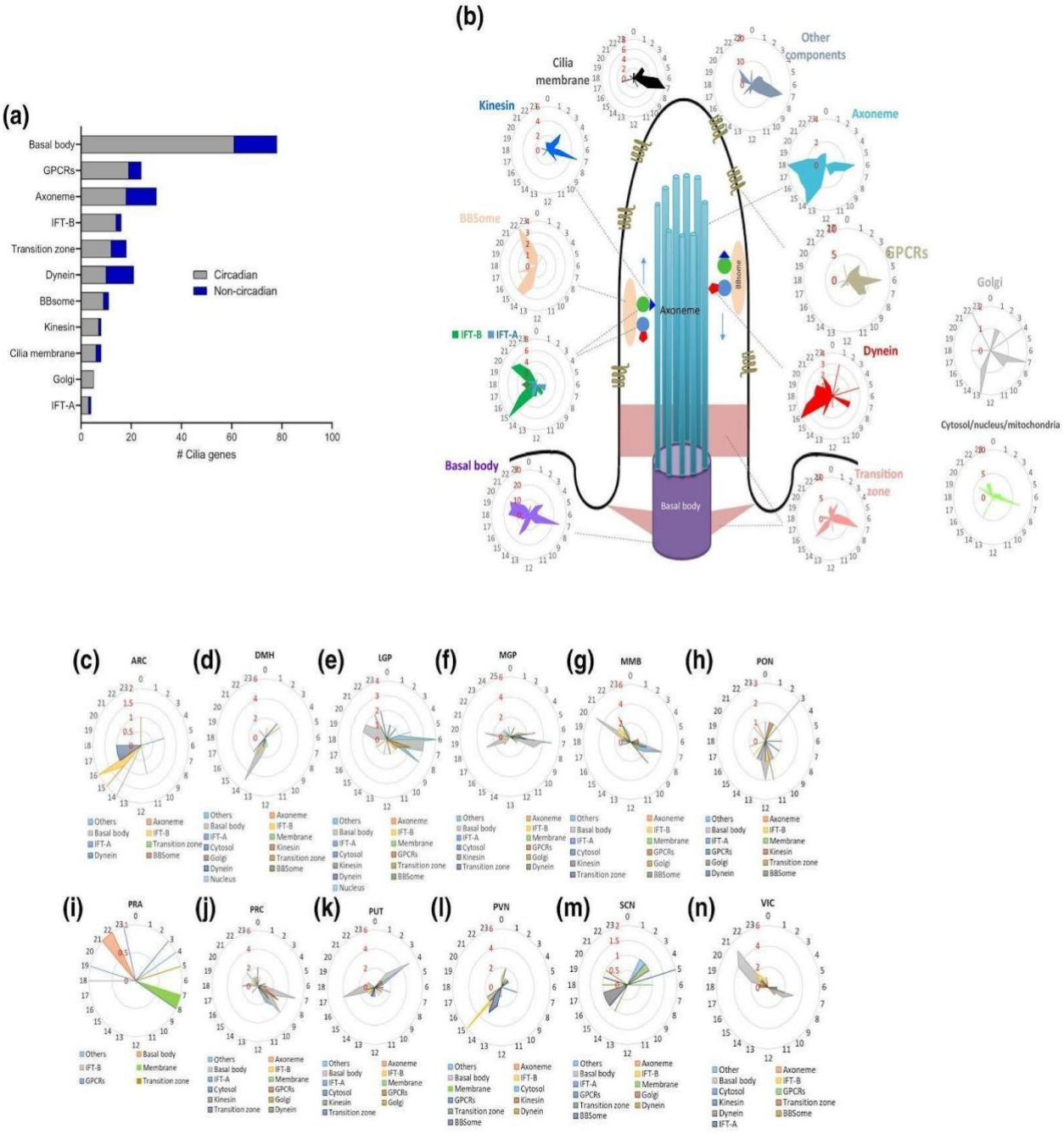

Figure 3.4. Substructural organization of cilia circadian genes. (a) Number of circadian and non-circadian genes in each of cilia substructural compartments. (b) Schematic of cilia structure and radial diagrams of the distribution of the peak phase of expression of the cilia substructural components' transcripts in the whole brain. The radial plot displays phases (hours) on the

circumference and the number of gene peaks of expression on the radius (in red). (c–n) Radial diagram of the distribution of the peak phase of expression of the circadian cilia genes in the 12 brain regions that showed significant enrichment. The radial plot displays phases (hours) on the circumference and the number of gene peaks of expression on the radius

Rhythmicity of brain circuits' functions

Given the high-level of circadian rhythmicity and confinement of shared oscillatory patterns in multiple brain nuclei, we speculated that cilia components display orchestrated oscillatory patterns in anatomically and functionally defined brain circuits. We focused on a brain circuit involved in movement control because its nuclei and structures, PUT, SUN, MGP, LGP, and PFC, share the highest number of circadian cilia transcripts. Notably, PUT, LGP, MGP, and SUN shared 10 cilia circadian genes (Fig. 3.3d, 3.5a). These four nuclei collectively form the basal ganglia, a set of subcortical nuclei that are mainly responsible for motor control and motor learning, in addition to other functions such as executive functions and emotions. Circadian genes in the PUT, the input region of the basal ganglia, peaked mostly at two sharp phases: ZT4 (first half of the morning) and ZT17 (around midnight), whereas LGP and MGP genes peaked within 1-2 hours of PUT cilia genes peaking (ZT6-ZT7 and ZT17-ZT20). Interestingly, nine out of the ten shared circadian transcripts among the basal ganglia structures (B9D1, C21ORF2, CCDC28B, FUZ, PARD6A, PKD1, RILPL1, TUBGCP2, and TUBGCP6) peaked at ZT4 in the PUT and ZT6-ZT8 in the other regions. All these nine genes were also rhythmic in the PRC and peaked there at ZT9-ZT10. The tenth common gene (PCM1) in the basal ganglia nuclei peaked at ZT17 in the PUT and at ZT18- ZT20 in the three other nuclei, maintaining a 12-hours phase shift with respect to the other nine genes in the four basal ganglia structures.

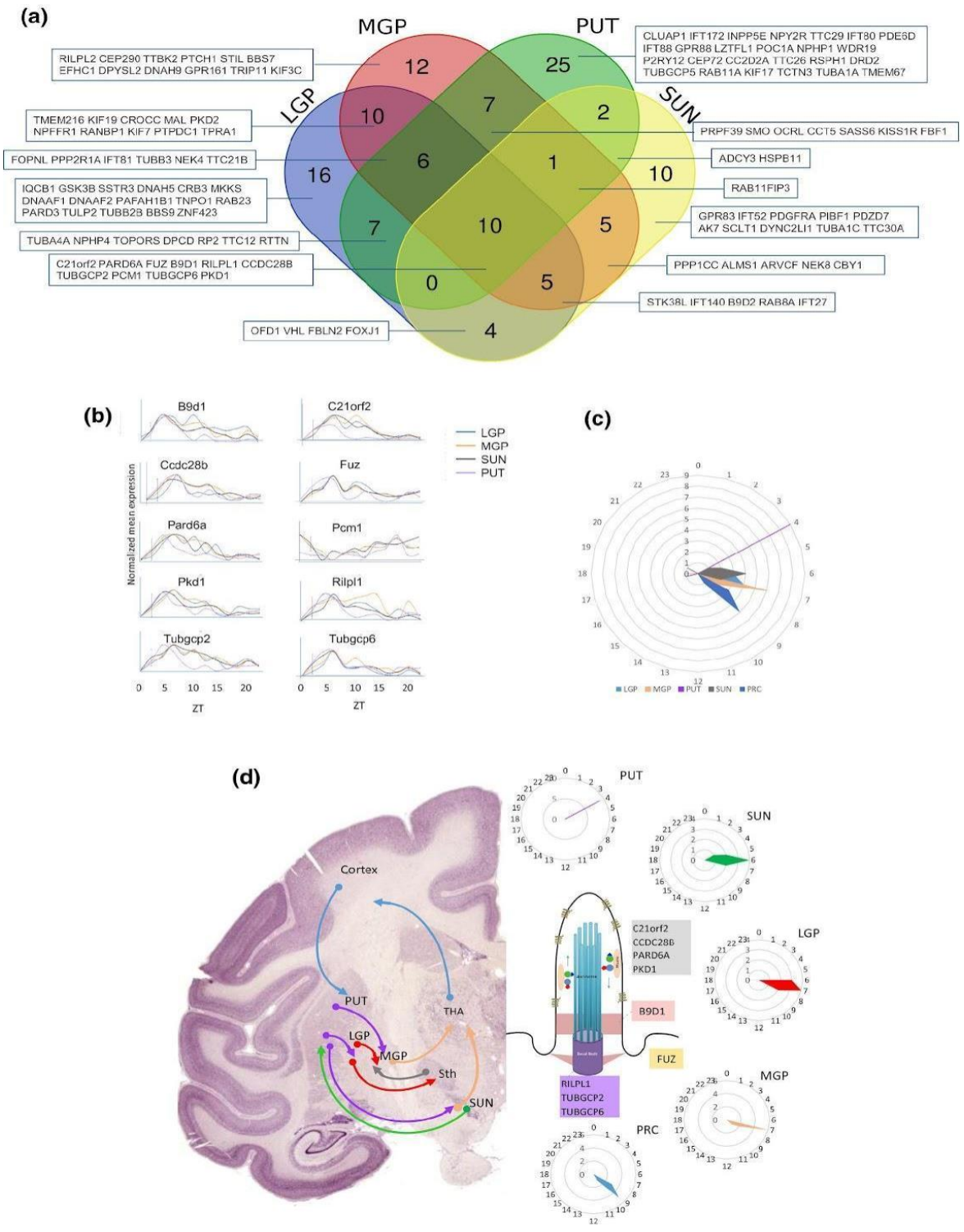

Figure 3.5. Rhythmicity of the nuclei/regions of the basal ganglia-cortex circuit. (a) Venn diagram showing the overlap between the cilia circadian genes identified in the motor control

circuit (nuclei of the basal ganglia and PRC). The overlapping transcripts are shown in boxes. (b) Twenty-four-hour oscillating cilia genes in the basal ganglia nuclei, displayed as normalized expression levels. (c) Radial plot of the distribution of the peak phase of expression of the cilia circadian genes in each of the five brain regions of the motor control circuit. Phases (hours) are displayed on the circumference and the numbers of gene peaks of expression are displayed on the radius. (d) Schematic diagram illustrating the arrangement of information flow through the cortical-basal ganglia-cortical circuit in primate brain (left), and the peak phase of the nine overlapping genes in the nuclei/regions of the circuit (right), with their localized expression in the cilia substructures (middle)

Discussion

This study presents a systematic evaluation of rhythmicity and spatiotemporal expression patterns of cilia genes in 22 baboon brain regions. To examine whether cilia associated genes oscillate in a circadian manner in various brain areas, we acquired publicly available transcriptomic data from the largest spatiotemporal gene expression atlas of a primate [49].

Around 73% of cilia transcripts exhibited circadian rhythmicity across at least one of the 22 brain regions reported in the primate diurnal transcriptome atlas [49], and in 12 brain regions cilia circadian transcripts were statistically overrepresented compared to the brain circadian background transcriptome, supporting the notion that cilia are highly dynamic and circadian systems.

Cilia circadian genes follow distinct rhythmic patterns

To our surprise, cilia circadian transcripts did not strictly follow the rhythmic fashion of the majority of the background circadian transcriptomes. For example, in contrast to many circadian transcripts which tend to peak in the early morning [49], cilia rhythmic transcripts tend to peak during the early afternoon at ZT7 (83 transcripts). Furthermore, there were a few major differences in the rhythmic patterns between cilia genes and the background of all circadian transcripts in specific brain regions [49]. For example, contrary to the expression patterns of the majority of background circadian genes in the PVN, which peaked in the early morning (first quarter-phase), cilia circadian genes peaked at ZT14-15 (third quarter-phase) in this region. In addition, unlike the majority of ARC background rhythmic transcriptomes, which peaked within three phases (first, third and fourth quarter-phases), cilia rhythmic genes in this region peaked only within a 4-hour interval (ZT14-18) [49]. On the other hand, cilia circadian transcripts in the SCN (master clock) had peaks distributed across three phases (the first, third, and fourth quarter-phases), compared to the majority of background circadian transcripts, which peaked mainly in the first quarter-phase [49]. These discrepancies raise the question of whether the gene expression of cilia circadian

components is regulated in a specific way that is different from the background oscillating transcriptomes.

Rhythmicity of cilia structural and functional components

The primary cilia's core structure comprises 9+0 axoneme that consists of doublet microtubules nucleating and extending from the basal body through the ciliary transition zone [58, 59]. The basal body is a centriolar structure composed of a radial array of nine triplet microtubules and comprised of a mother and daughter centrioles [60, 61]. Genes coding for the basal body components produced the largest fraction of circadian transcripts in each of the 22 brain regions. The peak phases of circadian genes encoding components of axoneme, basal body, and transition zones were dispersed, with the majority of genes peaking at ZT4, ZT7, ZT14, and ZT16-18. This strongly suggests that cilia assembly/disassembly and length, which are governed by axoneme and basal body components, might also oscillate following similar rhythmic patterns to that of axoneme, basal body components.

Ciliogenesis, elongation, and maintenance are contingent on the proper function of the intraflagellar transport (IFT) machinery [62]. IFT is associated with a bidirectional transport process that relies on kinesin and dynein molecular motors, IFT particle sub-complexes (A and B), and IFT-associated proteins (e.g. Bardet–Biedl syndrome (BBS) proteins) [63, 64]. Kinesin-dependent motors, associated with IFT-B particles, traffic cargo (e.g. axonemal components and receptors) towards the tip of the cilia. In contrast, dynein-mediated retrograde motor, associated with IF-A particles, recycles components back to the base [63-65]. Circadian genes encoding components of kinesin peaked in the light phase (ZT0-ZT11), whereas those encoding dynein components peaked in the dark phase (ZT12-ZT23). Unexpectedly, genes encoding IFT-B particles peaked, unlike kinesin, in the dark phase, along with other components of the IFT system (BBsomes). Although the number of rhythmic genes encoding IFT-B particles seem to be higher than that of IFT-A, rhythmic IFT-A genes acccounted for 100% of the entire brain IFT-A genes, whereas rhythmic IFT-B genes accounted for 82% of brain IFT-B genes.

Ciliary GPCRs play essential roles in the signal transduction mediated by neuronal cilia. Interestingly, cilia rhythmic GPCRs included receptors that bind to known neurotransmitters/ neuropeptides (DRD2, KISSR1, SMO, MCHR1, SSTR3, GALR3, GALR2, DRD5, and HTR6) as well as orphan receptors (GPR88, GPR161, GPR83) [27, 66-69]. Signaling through these cilia GPCRs has been implicated in numerous physiological functions such as movement control, feeding behavior, cognitive processes, wake/sleep, and reproduction [24, 27, 66, 70, 71]. Cilia receptors recruit kinesin/IFT-B transport machinery for their trafficking to the cilia membrane [72, 73]. Therefore, peaking of the brain cilia primarily in the light phase (ZT2-3, ZT7, and ZT8-9) and the similar rhythmic patterns of GPCRs and IFT-B particles are, thus, not surprising.

Cilia circadian transcripts exhibit higher overlap in adjacent and functionally connected nuclei

Despite the limited overlap of cilia circadian genes between regions, nuclei with anatomical and/or functional connectivity exhibited higher overlap than non-connected regions. For example, cilia rhythmic genes in the hypothalamic nuclei including SCN, PVN, ARC, and DMH shared peaking in the third quarter-phase (early evening (ZT14-16)). On the other hand, cilia cycling genes in the anatomically and/or functionally connected nuclei of basal ganglia (PUT, LGP, MGP, and SUN) and the PFC peaked in the light phase when the animal is awake. Interestingly, the amygdala, which is involved in emotional behaviors and fear response, and the cerebellum showed the lowest overlap of cilia rhythmic genes with any other brain regions.

The fact that physiological functions that are regulated by cilia follow circadian patterns raises the questions of whether the circadian rhythm of cilia gene expressions regulates circadian rhythmicity of these functions or that cilia gene expressions follow the physiological needs associated with the different brain regions. For example, the expression levels of specific cilia genes such as MC4R, MCHR1, and ADCY3 directly alter feeding behavior [74, 75]. On the other hand, cilia length is controlled by the feeding status (they are shorter in fasted mice than fed mice)

[76, 77]. Given that feeding behavior is regulated by a number of hypothalamic orexigenic and anorexic neuropeptides, the circadian rhythm of cilia gene expressions in different brain regions may simply follow the circadian expressions of these hypothalamic neuropeptides.

Basal ganglia as a model of brain rhythmic functional circuit

The dynamic organization and spatio-temporal coordination of activities within and across different parts of the basal ganglia-cortex loop are at the basis of motor initiation, coordination and learning [78]. Remarkably, the nine shared cilia rhythmic genes in the basal ganglia nuclei and the PRC peaked in these structures in a sequential fashion, as in a wave: PUT (ZT4) → SUN (ZT6) → LGP/MGP (ZT7) → PRC (ZT9). This order is interesting, as it is the same order of activation, albeit on a completely different time scale, of the basal ganglia-cortical circuitry connected with movement coordination.

The PUT, with caudate (CA), is the main input to the basal ganglia, whereas the MGP and pars reticulata of the SUN (SUNr) represent the output stations of the basal ganglia. Interestingly, the PUT was the only nucleus that shared rhythmic cilia genes with all the other brain regions, whereas MGP shared the highest number of cilia rhythmic genes with other brain regions (31 genes with each of LGP and MMB, 28 with PRC, 27 with PUT, 21 with SUN, and 20 with VIC).

The basal ganglia control movement by regulating motor planning, sequencing, feedback processing and learning; by acting as a coincidence detector of cortical and thalamic input [79-82]. According to the functional circuit model of the basal ganglia, information about movement is collected from the cortex, processed in the PUT/CA, and then transmitted to the output structures of the basal ganglia (SUNr/MGP), through two pathways, the direct and indirect pathways (for review [83-86]). The direct pathway projects monosynaptically to the output nuclei of the basal ganglia, whereas the indirect pathway projects to the output regions, bisynaptically (via LGP) and trisynaptically (via LGP and the subthalamic nucleus (STN)). When the animal is not moving, PUT/CA neurons are mute, while neurons in the output regions of the basal ganglia

are tonically active. The firings of the SUNr/MGP drive an inhibitory (GABAergic) tone on the ventral thalamic nucleus, which in turn project back to the cortex. Apparently, the spatiotemporal expressions of circadian cilia genes in the basal ganglia neurons follow the sequential order of this circuitry while controlling movement, though on different time scales. The highly coordinated rhythmicity of cilia genes in the basal ganglia and the peaking of these genes during the light phase suggest an essential role for cilia genes in the control of motor sequencing and activity. In support of this notion, many GPCRs in the basal ganglia that are involved in motor control (including D2 and D1 dopamine receptors) are localized on the cilia membrane [25, 27, 87]. The pars compacta of the SUN (SUNc) sends dopaminergic projections to the PUT/CA, which stimulates the direct pathway via D1 receptors and inhibits the indirect pathway via D2 receptors. Interestingly, D2 but not D1 receptors displayed circadian rhythms in the PUT, suggesting a key role for cilia rhythmicity in the function of the indirect pathway of the basal ganglia (for review: [86, 88]).

The basal ganglia circuit is believed to perform central clock functions in the brain [89, 90] and its role in timing is thought to result from the dopaminergic projection from the SUNc to the PUT/CA. SUNc and PUT/CA are the two basal ganglia regions that are necessary for interval timing [91]. It is accepted now that the pacemaker pulses are action potentials of dopaminergic neurons, and that dopamine controls the clock speed [92-94]. Thus, the increases in synaptic dopamine in the PUT/CA result in a faster internal clock process, whereas the decreases in PUT/CA synaptic dopamine slow down the clock speed [92-94].

Dysfunctions of the basal ganglia underlie a spectrum of movement disorders including Parkinson's disease, which results from the degeneration of dopaminergic neurons in the SUNc, and Huntington's disease, which results from the degeneration of projection neurons in the PUT/CA. Of great interest, patients in both disorders exhibit profound difficulty in performing rhythmic movements and show decreased ability to calculate the timing of the initiation and termination of voluntary actions, especially for sequential movements [95-97]. The rhythmicity of

cilia genes encoding therapeutic targets (Dopamine receptors) for Parkinson's disease and Huntington's disease suggests that the therapeutic efficacies might be influenced by the time-of-day of administration of the corresponding drugs.

We speculate that spatiotemporal orchestration of cilia gene expression in the basal ganglia, particularly in the SUN, PUT, LGP, and MGP, is essential to maintain normal physiology of the basal ganglia-cortical circuit and proper motor control, and that abnormal orchestration of cilia genes might contribute to the pathophysiology of several neurological and psychiatric disorders.

Further mechanistic studies are warranted to better characterize and understand cilia rhythmicity in the basal ganglia-cortical circuits and other brain circuits, which in turn may help develop better functional models, and shed light on the causal effects cilia functions have on these circuits and on the regulation of movement and other behaviors.

Chapter 4: Regulation of Brain Primary Cilia Length by MCH Signaling: Evidence from Pharmacological, Genetic, Optogenetic, and Chemogenic Manipulations

Alhassen W, Kobayashi Y, Su J, Robbins B, Nguyen H, Myint T, Yu M, Nauli SM, Saito Y, Alachkar A. **Regulation of Brain Primary Cilia Length by MCH Signaling: Evidence from Pharmacological, Genetic, Optogenetic, and Chemogenic Manipulations**. Mol Neurobiol. 2022 Jan;59(1):245-265.

Abstract

The melanin-concentrating hormone (MCH) system is involved in numerous functions, including energy homeostasis, food intake, sleep, stress, mood, aggression, reward, maternal behavior, social behavior, and cognition. In rodents, MCH acts on MCHR1, a G protein-coupled receptor, which is widely expressed in the brain and abundantly localized to neuronal primary cilia. Cilia act as cells' antennas and play crucial roles in cell signaling to detect and transduce external stimuli to regulate cell differentiation and migration. Cilia are highly dynamic in terms of their length and morphology; however, it is not known if cilia length is causally regulated by MCH system activation in vivo. In the current work, we examined the effects of activation and inactivation of MCH system on cilia lengths by using different experimental models and methodologies, including organotypic brain slice cultures from rat prefrontal cortex (PFC) and caudate–putamen (CPu), in vivo pharmacological (MCHR1 agonist and antagonist GW803430), germline and conditional genetic deletion of MCHR1 and MCH, optogenetic, and chemogenetic (designer receptors exclusively activated by designer drugs (DREADD)) approaches. We found that stimulation of MCH system either directly through MCHR1 activation or indirectly through optogenetic and chemogenetic-mediated excitation of MCH-neuron, caused cilia shortening, detected by the quantification of the presence of ADCY3 protein, a known primary cilia marker. In contrast, inactivation of MCH signaling through pharmacological MCHR1 blockade or through genetic manipulations — germline deletion of MCHR1 and conditional ablation of MCH neurons — induced cilia lengthening. Our study is the first to uncover the causal effects of the MCH system in the regulation of the length of brain neuronal primary cilia. These findings place MCH system at a unique position in the ciliary signaling in physiological and pathological conditions and implicate MCHR1 present at primary cilia as a potential therapeutic target for the treatment of pathological conditions characterized by impaired primary cilia function associated with the modification of its length.

Introduction

Melanin-concentrating hormone (MCH), a 19 amino acid hypothalamic neuropeptide, is involved in numerous functions, including food intake, energy homeostasis, arousal, sleep, learning and memory, cognition, emotions, and maternal behavior [4, 13, 14, 18, 22, 23, 34, 35, 60, 63, 64, 82]. Dysregulation of the MCH system has been linked to psychiatric and neurological disorders such as depression anxiety and, most recently, schizophrenia and Alzheimer's disease [58, 83].

MCH exerts its actions through activating the G protein- coupled receptor (GPCR) MCHR1 that is widely distributed throughout the brain [68, 69]. MCHR1 couples to Gi/o and Gq, resulting in the activation of signaling pathways, including Ca^{2+} mobilization, ERK phosphorylation, and inhibition of cyclic AMP generation. MCHR1 receptors are abundantly found in neuronal primary cilia [8, 26, 43], protrusions from the cell bodies of neurons that act as antennas for cells. Cilia are responsible for signaling functions, including detecting and transducing external stimuli crucial for maintaining homeostasis (see [10, 85], for reviews). Despite the limited understanding of primary cilia functions, their abundant distribution throughout the brain and correlation of cilia dysfunctions to some cognitive diseases and behavioral abnormalities suggest an essential role for cilia in brain functions. A few G protein-coupled receptors (GPCRs) have been shown to selectively localize to cilia including somatostatin receptor 3 (SSTR3), serotonin receptor 6 (5HTR6), and melanocortin receptors (MC4R) [9, 15, 27, 37, 59, 81].

We recently showed that dysregulations of cilia genes, including ciliary GPCRs, are associated with major psychiatric disorders, including schizophrenia, autism, major depressive disorder, and bipolar disorder [3]. Therefore, MCHR1 localization on cilia membranes might be the basis of the uniqueness of these receptors in regulating ciliary signaling. In support of this notion, in vitro studies demonstrated that MCH treatment shortened the length of cilia in human retinal pigmented epithelial (hRPE1) cells transfected with MCHR1. Additionally, the reduction in cilia length was mediated via Gi/o-Akt pathway [75]. A recent study by the Saito group

demonstrated that treatment of hippocampus slice cultures with MCH induced cilia shortening in the CA1 region [43]. Moreover, their results revealed a marked increase in MCH mRNA expression in the lateral hypothalamus of fasting mice which correlated with a reduction of MCHR1-positive cilia lengths in the hippocampal CA1 region [43]. Therefore, we aim to establish the causal relationship between MCH system signaling and cilia length. We examined how manipulating the MCH system affects cilia integrity in multiple mouse brain regions. We used multiple techniques to manipulate the MCH system, including pharmacological, genetic, optogenetic, and chemogenetic approaches to determine how alterations in the MCH system affect cilia length.

Materials and Methods

Ex Vivo *Studies Rat Brain Slice Culture from the Striatum (Caudate/ Putamen (CPu)) and Prefrontal Cortex (PFC)*

For rat brain slices, Wistar rats (Charles River Japan, Yokohama, Japan) were maintained in a room under a 12 h light:12 h darkness cycle and controlled temperature (23 to 25 °C), with water and food available ad libitum. All experimental protocols were reviewed by Hiroshima University Animal Care Committee and met the Japanese Experimental Animal Research Association standards, as defined in the Guidelines for Animal Experiments (1987). We established rat CPu and PFC slice culture method for clear detection of primary cilia and ciliary MCHR1 based on a previous study [43]. The 11-day-old rats were anesthetized with 5% isoflurane and decapitated for slice culture preparation. Brains were removed, embedded in agarose, and dissected into 200 μm coronal slices using a McIlwain tissue chopper (The Mickle Laboratory Engineering, Surrey, UK). The CPu and PFC (Paxinos, 2007) slices were trimmed from the same individual brain slice in ice-cold dissection buffer (2.5 mM KCl, 0.05 μM CaCl2, 1.7 mM NaH2PO4, 11 mM glucose, 20 mM HEPES, 8 mM NaOH, 18 mM NaCl, 0.23 M sucrose, and penicillin G sodium/streptomycin sulfate (PG/SM)). The four CPu slices and eight PFC slices were placed on separate Millicell Cell Culture inserts (PICM0RG50; Merck Millipore, Germany) in 35-mm petri dishes. Each 35-mm petri dish contained 1 ml of starter medium comprising 50% MEM (GIBCO, Grand Island, NY, USA), 25% normal horse serum, 25% Hanks' balanced salt solution, 36 mM glucose, and PG/ SM. CPu and PFC slices were placed on each membrane and maintained at 37 °C in a 5% CO2 incubator. After 1 day, the medium was changed to neurobasal medium (21,103–049; Gibco) containing 1.2% B27 serum-free supplement (17,504–044; Gibco), 25 mM GlutaMAX I (Gibco), and PG/SM (Slice-GM). One-third of the Slice-GM was changed every 72 h. CPu and PFC slices were treated with MCH (30 nM, Peptide Research Institute, Osaka, Japan) on days 14 and 7 of culture, respectively.

Immunohistochemical staining of each slice was performed by placing Millicell Cell Culture inserts in 6-well culture plates. After MCH treatment, the slices were fixed for 3 h at 4 °C in fresh 4% paraformaldehyde, washed with PBS, heated (70 °C for 20 min) in 10% Histo VT One (Nacalai Tesque, Kyoto, Japan) in PBS for anti- gen retrieval, and blocked with PBS containing 5% horse serum and 0.1% Triton X-100 for 2 h. The slices were then incubated with rabbit anti-rat adenylate cyclase 3 (ADCY3, RPCA-ACIII; Encor Biotechnology, Alachua, FL, USA; 1:5000) and goat anti-human MCHR1 (goat anti-human MCHR1; C-17, sc-5534; Santa Cruz Biotechnology; 1:300) primary antibodies overnight at 4 °C. The bound antibodies were detected by incubation with Alexa Fluor 488-conjugated donkey anti-rabbit IgG (A21206, Thermo Fisher Scientific, Rockford, IL, USA; 1:300) or Alexa Fluor 546-conjugated donkey anti-goat IgG (A11056, Thermo Fisher Scientific; 1:300) secondary antibodies for 2 h at room temperature. Each brain slice was cut out from the Millicell Cell Culture inserts using a scalpel together with the Millicell membrane and then mounted with VECTOR Shield.

Microscopic Images and Analysis

The length of primary cilium, which is labeled both with MCHR1/ADCY3, was measured with a BZ-9000 fluorescence microscope (Keyence, Osaka, Japan) using PhotoRuler ver. 1.1 software (the Genus Inocybe, Hyogo, Japan). A minimum of 80 cilia per treatment were obtained from at least three independent experiments, and the values are presented as means ± SEM. Numerical data are shown as scatter plot (boxplots and bee swarms) for the cilia length distributions in each group.

In Vivo Studies

All experimental procedures were approved by the Institutional Animal Care and Use Committee of the University of California, Irvine, and were performed in compliance with national and institutional guidelines for the care and use of laboratory animals. Animal genetic background and treatments are summarized in Table 4.1.

Experiment	Genetic background	Route of administration	Vendor
MCH	Swiss Webster	Intracerebroventricular injection	Charles River
GW803430	Swiss Webster	Intraperitoneal injection	Charles River
Optogenetics pMCHCre	C57BL/6	Stereotaxic injection of AAV	Tg(pMCH-cre)1Lowl/J mice, Jackson Laboratories
Chemogenics pMCHCre	C57BL/6	Stereotaxic injection of AAV, and intraperitoneal injection of CNO	Tg(pMCH-cre)1Lowl/J mice, Jackson Laboratories
lDTR pMCHCre	C57BL/6	Intraperitoneal injection of DT	Tg(pMCH-cre)1Lowl/J mice, Jackson Laboratories
MCHR1 KO	BL6-Taconic	N/A	Dr. Su Qian (Merck, Rahway, NJ)

Table 4.1. Mouse genetic background and routes of drug/virus administrations

Pharmacological Manipulations Chronic Intracerebroventricular (i.c.v) Administration of MCH

Eight-week-old Swiss Webster male mice (*n* = 16) underwent stereotaxic surgery to implant a stainless steel guide cannula into the lateral ventricles (20-gauge guide cannulas with 2.5-mm custom-cut depth, PlasticsOne). Animals were anesthetized with 2% isoflurane anesthesia (Institutional Animal Care and Use Committee guide- lines) and were secured in a Kopf stereotaxic instrument. Guide cannula was implanted at − 0.22 mm posterior to bregma, 1.0 mm lateral, and 2.3 mm below the skull surface (G. Paxinos, 2001). Animals were then allowed to recover for 1 week with a dummy cannula in place before injections. Animals were then infused with either vehicle (phosphate-buffered saline (pH 7.4)) with 0.2% bovine serum albumin or MCH peptide (1 nmol) dissolved in the same vehicle for 7 consecutive days using a 50 µl Hamilton Microsyringe. MCH (1 nmol) was dissolved in phosphate-buffered saline (pH 7.4) with 0.2% bovine serum albumin. The dose of MCH was determined by previously reported findings [70].

Following the last injection, 9–10-week-old mice were anesthetized with isoflurane and perfused intracardially with saline and 4% paraformaldehyde.

Intraperitoneal Administration of MCHR1 Antagonist GW 803430

Eight-week Swiss Webster male mice were administered intraperitoneally (i.p.) 3 mg/kg (*n* = 8) MCH1R antagonist GW803430 or vehicle (*n* = 8) for 7 consecutive days [31, 70]. GW80343 was dissolved in a vehicle made in 2% Tween 80 with acetic acid. This dose was selected based on previous receptor occupancy studies demonstrating that near-complete blockade of the MCH system is achieved following i.p. administration at the 3 mg/kg dose [31, 70]. Following the final injection at 9–10 weeks old, animals were perfused transcardially for tissue fixation.

Genetic Manipulation

Germline MCHR1 Knockout (MCHR1 KO) and MCH Conditional Knockout (MCHcKO) mice

MCHR1 KO male mice were generated as previously described [49]. Pmch- Cre/ + ,iDTR/$^{+}$ mice were generated as described previously [2]. Briefly, PmchCre mice (Tg(pMCH-cre)1Lowl/J mice, Jackson Laboratories, Bar Harbor, Maine, USA) that express Cre-recombinase (Cre) under the MCH promoter [45] were bred with homozygous inducible diphtheria toxin receptor iDTR/$^{+}$ mice (from Dr. Satchidananda Panda and originally generated in the lab of Dr. Ari Waisman), rendering MCH neurons in these mice sensitive to diphtheria toxin (DT) [2, 17, 70, 83]. The resulting iDTR^{+}PmchCre^{+} (iDTR^{+}/Cre^{+}) and their control littermate iDTR^{+}PmchCre^{-}(iDTR^{+}/Cre^{-}) mice were injected twice in 4 days with the diphtheria toxin (DT) (16 μg/kg, i.p.), which then produces profound ablation of MCH neurons.

Optogenetic Stimulation of MCH Neurons

Surgery

AAV5-EF1a-DIO-ChR2-T159c-eYFP (titer, ≥ 1 × 10^{13} vg/mL) is an EF1a-driven, Cre-dependent, humanized channelrhodopsin E123T/T159C mutant fused to EYFP for optogenetic activation (pAAV-Ef1a- DIO hChR2 (E123T/T159C)-EYFP was a gift from Karl Deisseroth (Addgene viral prep # 35,509-AAV5; http:// n2t.net/addgene:35509; RRID: Addgene_35509) [50]. AAV5-EF1a-

DIO-ChR2-T159c-eYFP was stereotaxically injected into the lateral hypothalamus (flat skull coordinates from bregma: anteroposterior, − 1.30 mm; mediolateral, + 1 mm; and dorsalventral, − 5.20 mm) of 8-week-old male transgenic C57BL/6 PmchCre + (*n* = 8) and PmchCre- animals (*n* = 8), (Jackson Laboratories, Bar Harbor, Maine, USA) that express Cre-recombinase (Cre) under the MCH promoter. Each mouse received one injection of 800 nl in each lateral hypothalamus. At this time, the high-power LED fiber cannula (core diameter 200 μm, outer diameter 225 μm, length 2.5 mm, numerical aperture 0.66, Prizmatix, Israel) was implanted in the lateral hypothalamus at − 5.0 mm slightly above the injection site. The cannula light irradiance was adjusted to 6 mW before implantation. An additional hole was drilled on the opposite side for stainless steel holding screws. The fiber was fixed with dental cement holding the fiber and screw to the skull. The skin was closed with silk sutures. Animals were allowed to recover for 1 week before the start of the experiments. Correct fiber placement and injection site were ascertained postmortem on coronal brain sections.

Animals were habituated to the connection of the fiber patch cords to their cannulas inside their home cage for 1 h for 3 days. On the fourth day, animals were connected to the fiber patch cord and were tested in their home cage on feeding behavior. Animals were exposed to a 460 nm blue led light source to excite ChR2 at a specific stimulation paradigm: 10 Hz, 10 ms pulse 1 s, repeated every 4 s for 10 min. Feeding behavior was tracked and recorded. Twenty-four hours after feeding behavior test, mice were exposed to blue light at 10 ms pulse 1 s repeated every 4 s for 30 min and were intracardially perfused 90 min post light exposure.

Designer Receptors Exclusively Activated by Designer Drug (DREADD)-Based Chemogenetic Stimulation of MCH Neurons

AAV8-hSyn-DIO-hM3D(Gq)-mCherry (titer, 4.8 × 10^{12} GC/mL) (pAAV-hSyn-DIO-hM3D(Gq)- mCherry was a gift from Bryan Roth (Addgene viral prep #44,361-AAV8; http://n2t.net/addgene: 44,361; RRID:Addgene_44361)) was stereotaxically injected into the lateral hypothalamus (flat skull coordinates from bregma: anteroposterior, − 1.30 mm;

mediolateral, ± 1 mm; and dorsal ventral, − 5.20 mm) (G. Paxinos, 2001) of 8-week-old male transgenic C57BL/6 PmchCre + (*n* = 8) and PmchCre- animals (*n* = 8). This virus is a Syn-driven, Cre-dependent, hM3D(Gq) receptor with an mCherry reporter for CNO-induced neuronal activation [46]. Using this virus in mice that express Cre in MCH neurons allows precise expression of DREADD in the lateral hypothalamus and activates MCH neurons directly via CNO. Mice received two injections (both hemispheres; 0.6 nl), and then 1 week post-surgery animals were injected with one dose of CNO (1 mg/kg) and perfused 90 min after CNO injection.

Immunohistochemistry

Immunofluorescent staining was carried out as previously reported [65]. Briefly, 9–10-week-old animals were perfused transcardially under isoflurane anesthesia with saline followed by 4% paraformaldehyde in phosphate buffer saline. Brains were removed, and 30 µm coronal brain sections were dissected. The MCH-neuron ablation was verified by visualizing MCH neurons using rabbit polyclonal anti-MCH antibody (1:150,000, anti- body courtesy of W. Vale, Salk Institute, La Jolla, CA, USA) as previously described [70]. A goat anti-rabbit (1:500,Thermo Fisher) was used to visualize MCH immunoreactivity. For the cilia study, three to five sections were selected from each region of interest according to the mouse brain atlas (G. Paxinos, 2001). Primary cilia were stained with ADCY3 (rabbit, 1:500; Santa Cruz Biotechnology) and the secondary antibody donkey anti-rabbit Alexa 546 (Thermo Fisher Scientific). For c-Fos immunohistochemistry, mice were perfused 90 min after stimulation, and brain sections were stained with rabbit anti-c-Fos antibody (1:500, Invitrogen). Nuclei were stained with 4′,6-diamidino-2-phenylindole (DAPI) solution (1:10,000) and mounted with Aquamount mounting solution. Four to six brains from each group were used for quantification. For each brain, we used four to six non-consecutive sections per region of interest. Quantification of primary cilia was based solely on ADCY3 immunofluorescence positive signals. Each section was imaged bilaterally, thus giving 2 images quantifying a total of 10 images per region per brain. Cilia were counted in the bilateral areas of each section, and each brain was given one averaged cilia length

value for each region. Image acquisition was carried out using a confocal laser microscope. Images were captured using Leica Sp8 TCS confocal microscope (UCI optical biology core facility). Cilia length was measured using ImageJ [71] in all cells in each section, and the mean values of three sections per brain of 3–5 brains were calculated. A number of cilia in specific regions of the brain were also counted and referred to as cilia density per field. All cilia measurements were performed by two persons blind to the experiment conditions using cilia length cutoff of 0.5 μm. A total of 16 animals were used per experiment (8 control and 8 experimental groups), and 3–5 animals per group were used for analysis. Additional animals were used to account for any margins of error that may occur during perfusions, cutting, etc.

Statistical Analysis

GraphPad Prism (GraphPad Software, Inc.) was used for statistical analysis, and all data were presented as mean ± standard error mean (SEM). Student's unpaired *t* test was used to analyze the results. *P* value < 0.05 was considered statistically significant.

Results

MCH Shortens Cilia Length in the Rat Organotypic Striatum and Prefrontal Cortex Culture

Immunohistochemical analyses in the brains of rats showed that ADCY3/MCHR1 double-positive neuronal primary cilia were localized in discrete regions, including CPu and cerebral cortex [26]. Cilia MCHR1 merge with ADCY3 was also observed in cultured slices derived from the rat CPu and PFC (Fig. 4.1a, c). The neuronal cilia length in the CPu slices was 10.30 ± 0.23 μm (mean ± SEM), and MCH treatment for 18 h decreased this length by 23.0% (7.90 ± 0.28 μm, unpaired *t* test, $P < 0.01$) (Fig. 4.1b). We observed a similar effect of MCH in rat PFC slice cultures. Exposure to MCH led to neuronal cilia shortening by 31% (4.39 ± 0.12 μm vs 3.05 ± 0.06 μm; mean ± SEM, unpaired *t* test, $P < 0.01$) (Fig. 4.1d).

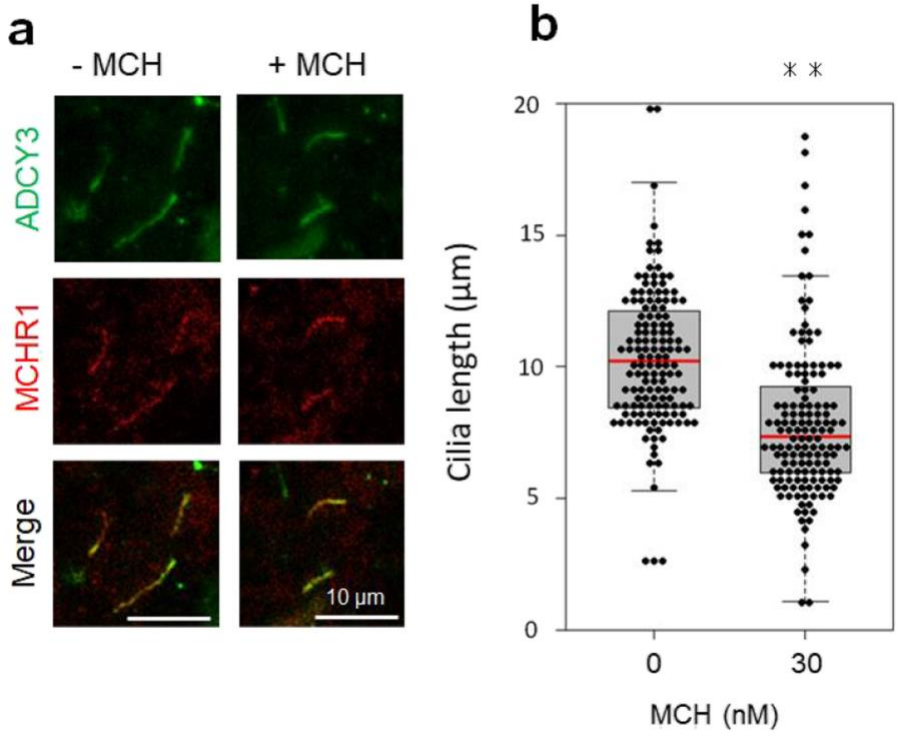

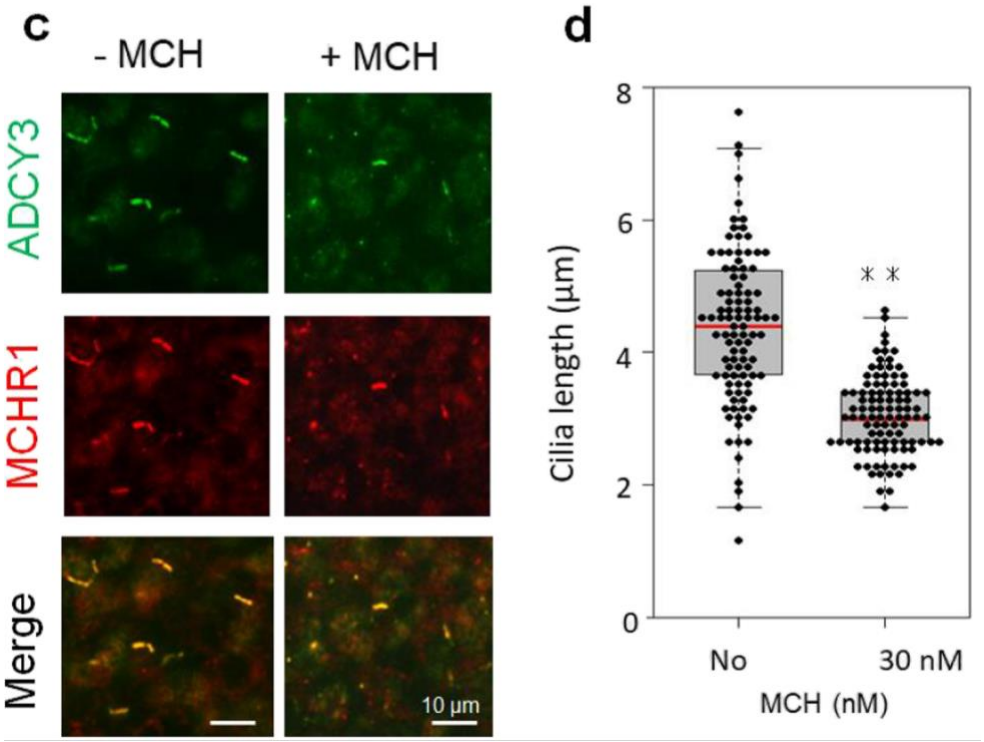

Figure 4.1. MCH treatment leads to cilia length shortening in cultured brain slices. CPu and PFC slices were treated with MCH on days 14 or 7 of culture, respectively.

a, **b** Rat CPu slice cultures were treated with vehicle or 30 nM MCH for 18 h. **c**, **d** Rat PFC slice cultures were treated with vehicle or 30 nM MCH for 6 h. **a**, **c** Primary cilia were co-labeled with antibodies against ADCY3 (green) and MCHR1 (red). Scale bars = 10 µm. **b**, **d** The scatter plot represents cilium lengths measured using ADCY3/MCHR1 double labeling in randomly selected fields; at least 80 cilia per group in both CPu slices (**b**) and PFC slices (**d**) were evaluated, respectively. Primary cilia were significantly shorter in MCH-treated cultures than in control cultures for both CPu slices and PFC slices. Unpaired *t* test, $^{**}P < 0.01$. Data are presented as means ± SEM

Activation of the MCH System Shortens Cilia Length in the Mouse Brain MCHR1 Agonist Shortens Cilia in the Mouse Brain

The central (i.c.v.) administration of MCH in adult mice for 7 consecutive days caused a significant decrease in the cilia length in several regions of the brain, including the hippocampus, striatum, prefrontal cortex (PFC), and nucleus accumbens (NAc) (Fig. 4.2a). In the PFC, administration of MCH caused a 42% reduction in cilia length (4.96 ± 0.30 μm in the PFC of the animals administered vehicle, $n = 4$, compared to 2.85 ± 0.1 μm in mice treated with MCH, $n = 4$, $t = 6.433$, $P = 0.0007$, unpaired t test) (Fig. 4.2b-d). In the CA1, administration of MCH caused a 33% shortening in cilia length (10.18 ± 0.30 μm in the CA1 of the animals administered vehicle, $n = 4$, com- pared to 6.743 ± 0.23 μm in mice treated with MCH, $n = 4$, $t = 8.436$, $P = 0.0002$, unpaired t test) (Fig. 4.2e-g). In the CPu, administration of MCH, $n = 5$, caused a 37% reduction in cilia length (5.04 ± 0.17 μm compared to 8.005 ± 0.2 μm in the CPu of the animals administered vehicle, $n = 5$, $t = 10.03$, $P < 0.0001$, unpaired t test) (Fig. 4.2h-j). In the NAc, administration of MCH caused a reduction in cilia length by 32% (8.287 ± 0.67 μm in the NAc of the animals administered vehicle, $n = 4$, compared to 5.566±0.33μm when given MCH, $n=4$, $t=3.648$, $P = 0.0107$, unpaired t test) (Fig. 4.2k-m). Chronic MCH administration caused a significant decrease in cilia density per field in the PFC ($t = 3.849$, $P = 0.0085$), CA1 ($t = 3.141$, $P = 0.02$), CPu ($t = 4.224$, $P = 0.0055$), and NAc ($t = 3.766$, $P = 0.0093$).

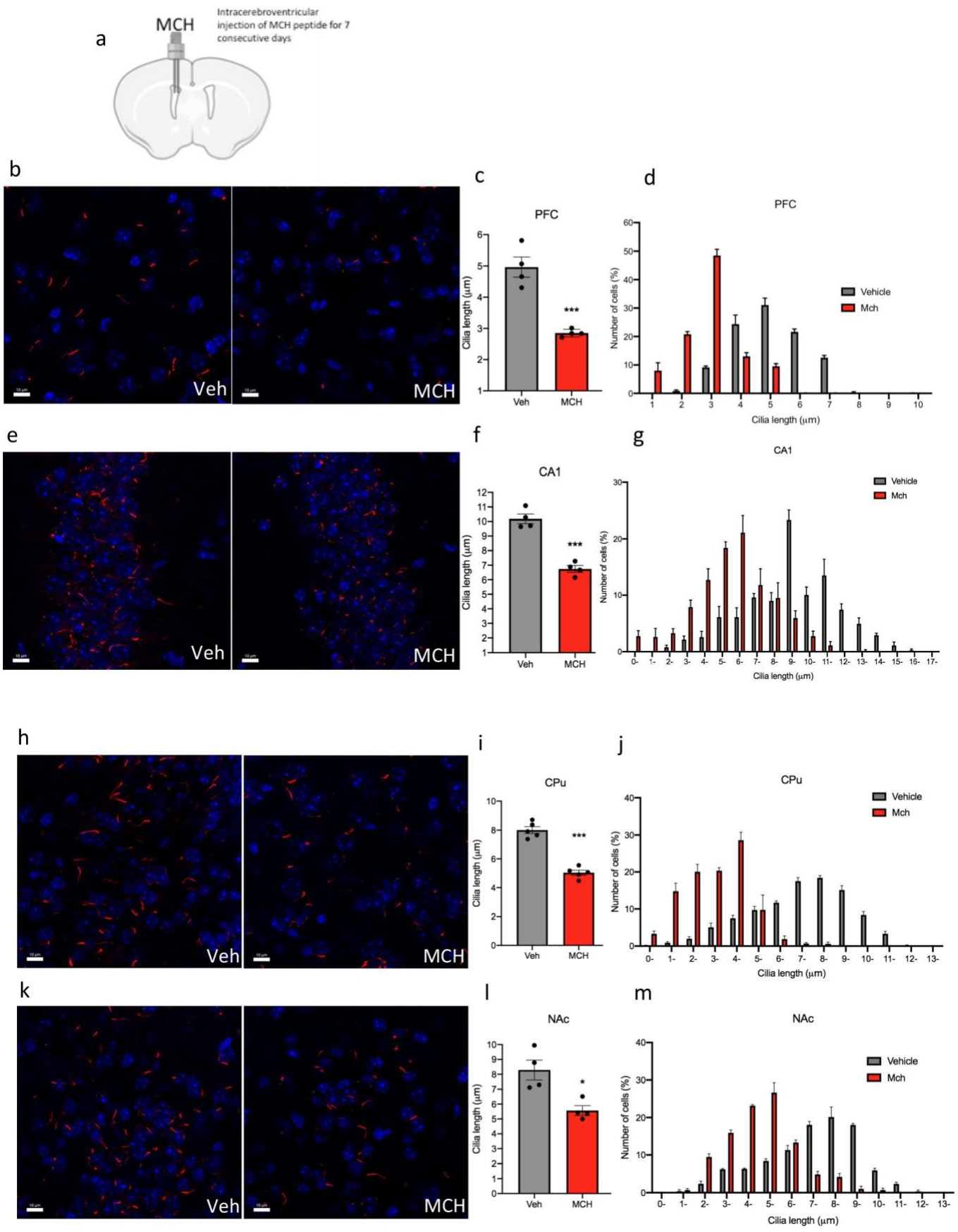
a
MCH
Intracerebroventricular injection of MCH peptide for 7 consecutive days
b
Veh
MCH
c
PFC
Cilia length (µm)
***
Veh
MCH
d
PFC
Number of cells (%)
Vehicle
Mch
Cilia length (µm)
e
Veh
MCH
f
CA1
Cilia length (µm)
***
Veh
MCH
g
CA1
Number of cells (%)
Vehicle
Mch
Cilia length (µm)
h
Veh
MCH
i
CPu
Cilia length (µm)
***
Veh
MCH
j
CPu
Number of cells (%)
Vehicle
Mch
Cilia length (µm)
k
Veh
MCH
l
NAc
Cilia length (µm)
*
Veh
MCH
m
NAc
Number of cells (%)
Vehicle
Mch
Cilia length (µm)

Figure 4.2. Chronic intracerebroventricular administration of MCH to mice shortens cilia length.

a. Schematic representation of chronic intracerebroventricular administration of MCH peptide. Male mice were administered with vehicle or MCH (1 nmol). Diagram was created with BioRender.com webpage. b, e, h, k Immunostaining of ADCY3 labeled in red fluorescence and counterstained with DAPI (blue) in the b PFC, e CA1, h CPu, and k NAc in animals administered with MCH or vehicle (scale bar = 10 μm, magnification = 63 ×). c, e, g, i Quantification of the length of ADCY3 + primary cilia (μm) in the c PFC, e CA1, g CPu, and (i) NAc in animals administered with MCH or vehicle, ***$P < 0.0007$ and **$P < 0.01$. d, g, j, m Cilia were grouped by length (μm) and plotted against the number of cells (%) in the d PFC, g CA1, j CPu, and m NAc

Optogenetic and Chemogenic Excitation of MCH Neurons Shortens Cilia Length

Optogenetic stimulation of MCH neurons was applied to one hemisphere of the brain at 460 nm blue led light at 10 Hz 10ms pulse 1s repeated every 4s for 10 min, based on previously reported rates, at which MCH neurons fire [33, 39] (Fig. 4.3a). Expression of ChR2 in the LH MCH neurons was confirmed using double immunostaining of GFP (green) and MCH (red) in Pmch-Cre + and PmchCre- mice (Fig. 4.3b). Co-expression of GFP fluorescence (green) and c-Fos immunofluorescence (red) identifies cells recently activated neurons in PmchCre + and PmchCre- mice (Fig. 4.3c). Optogenetic stimulation of MCH neurons in PmchCre + mice caused a significant bilateral decrease in cilia length compared to PmchCre- mice (control) in the CA1, striatum, PFC, and NAc. In the PFC, cilia lengths were shortened by 59% in PmchCre + mice compared to PmchCre- following optogenetic stimulation of MCH neurons (6.497 ± 0.6 μm in PmchCre- mice, $n = 4$, compared to 2.635 ± 0.23 μm in PmchCre + mice, $n = 4$, $t = 6.319$, $P = 0.0007$, unpaired t test) (Fig. 4.3d-f). In the CA1, stimulating MCH neurons caused a significant reduction in cilia length by 34% (3.823 ± 0.33 μm in PmchCre- mice, $n = 4$, compared to 2.536±0.14 μm in PmchCre+ mice, $n=4$, $t=3.535$, $P = 0.0123$, unpaired t test) (Fig. 4.3g-i). In the CPu, stimulating

MCH neurons caused a significant shortening of cilia length by 56% (6.065 ± 0.45 μm in PmchCre- mice, n = 5 compared to 4.031 ± 0.4 μm in PmchCre + mice, n = 5, t = 3.520, P = 0.0078, unpaired t test (Fig. 4.3k-l). In the NAc stimulating MCH neurons caused significant reduction in cilia length by 20% (7.442 ± 0.46 μm in PmchCre- mice, n = 4, compared to 5.952 ± 0.34 μ in PmchCre + mice, n = 4, t = 2.593, P = 0.0410, unpaired t test) (Fig. 4.3m-o). PmchCre + mice also exhibited more food intake than PmchCre- mice when exposed to blue light. Over the observed 10 min, PmchCre + mice aver- aged 74.13 s of feeding, while PmchCre- mice averaged 7.413 s (t = 7.027, P < 0.001). Stimulating MCH neurons via optogenetics caused a significant decrease in cilia density per field in the PFC (t = 3.789, P = 0.0091), CA1 (t = 6.324, P = 0.0007), and CPu (t = 5.656, P = 0.0013).

a

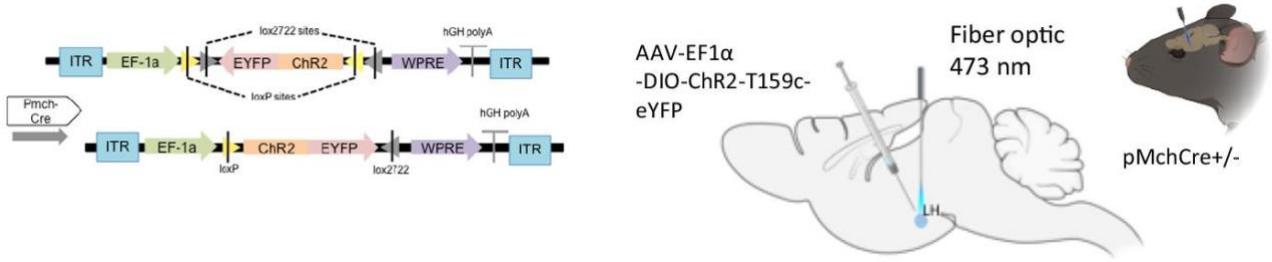

b

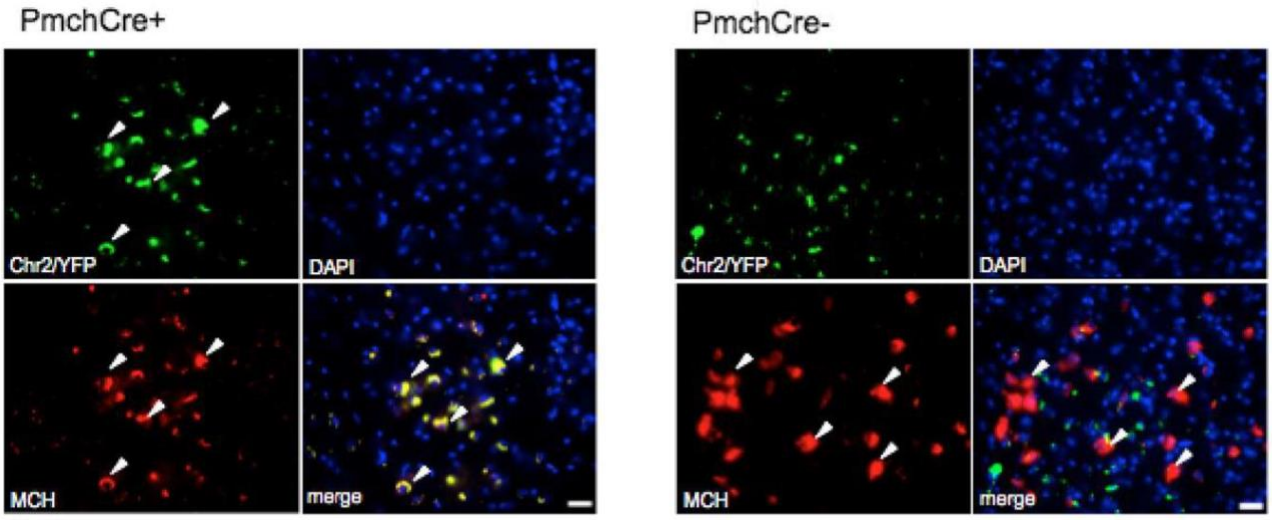

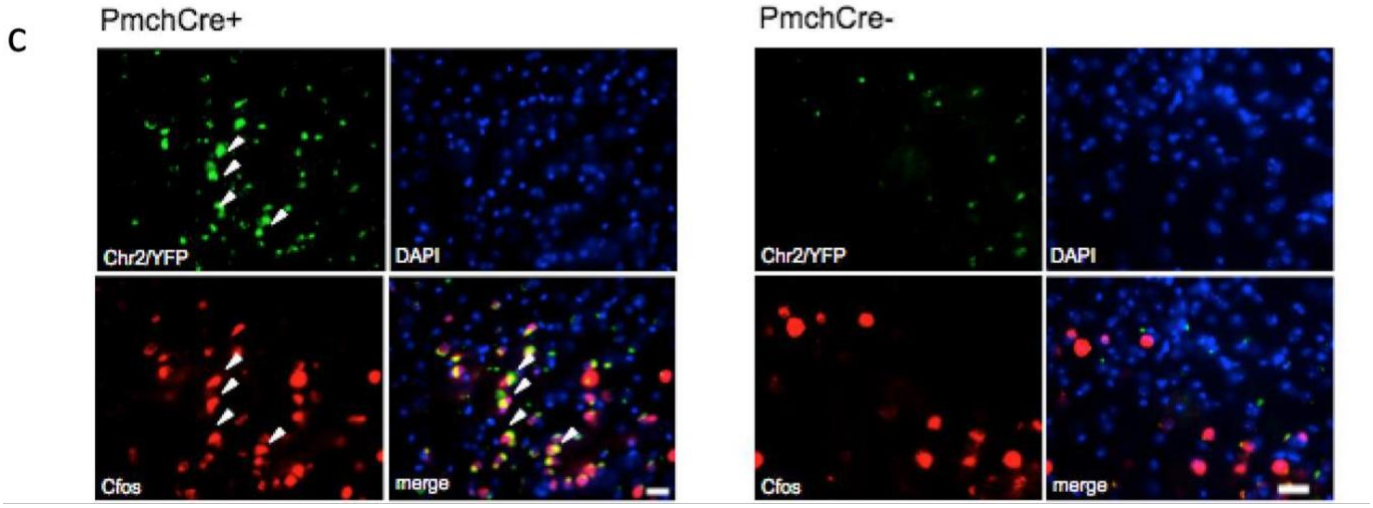
c
PmchCre+
PmchCre-
Chr2/YFP
DAPI
Cfos
merge
Chr2/YFP
DAPI
Cfos
merge

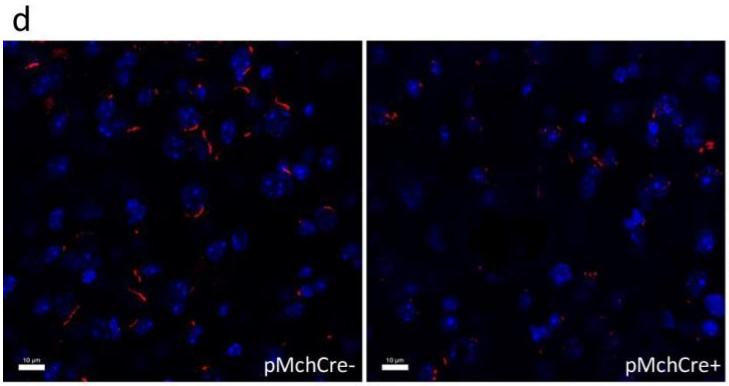
d
pMchCre-
pMchCre+

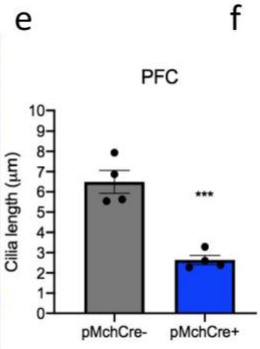
e
PFC
Cilia length (μm)
***
pMchCre-
pMchCre+

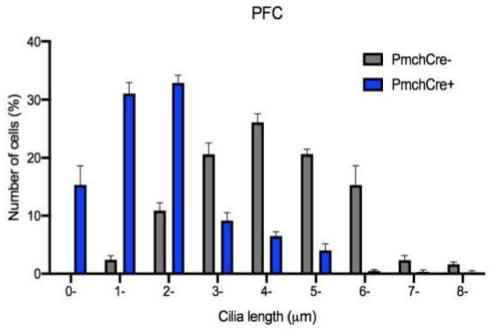
f
PFC
PmchCre-
PmchCre+
Number of cells (%)
Cilia length (μm)

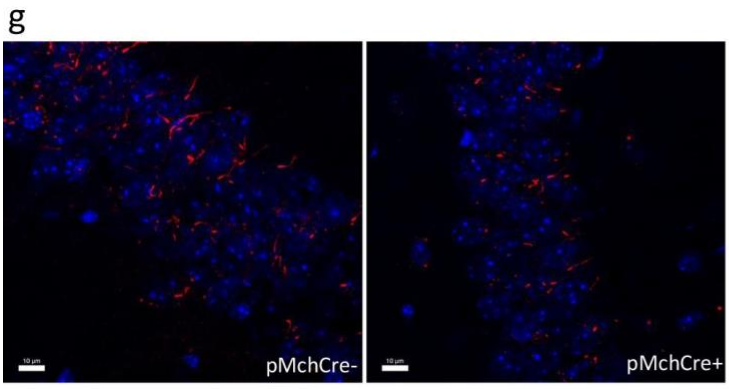
g
pMchCre-
pMchCre+

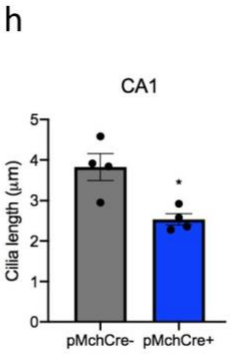
h
CA1
Cilia length (μm)
*
pMchCre-
pMchCre+

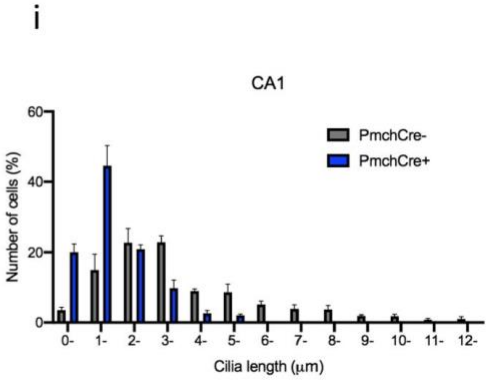
i
CA1
PmchCre-
PmchCre+
Number of cells (%)
Cilia length (μm)

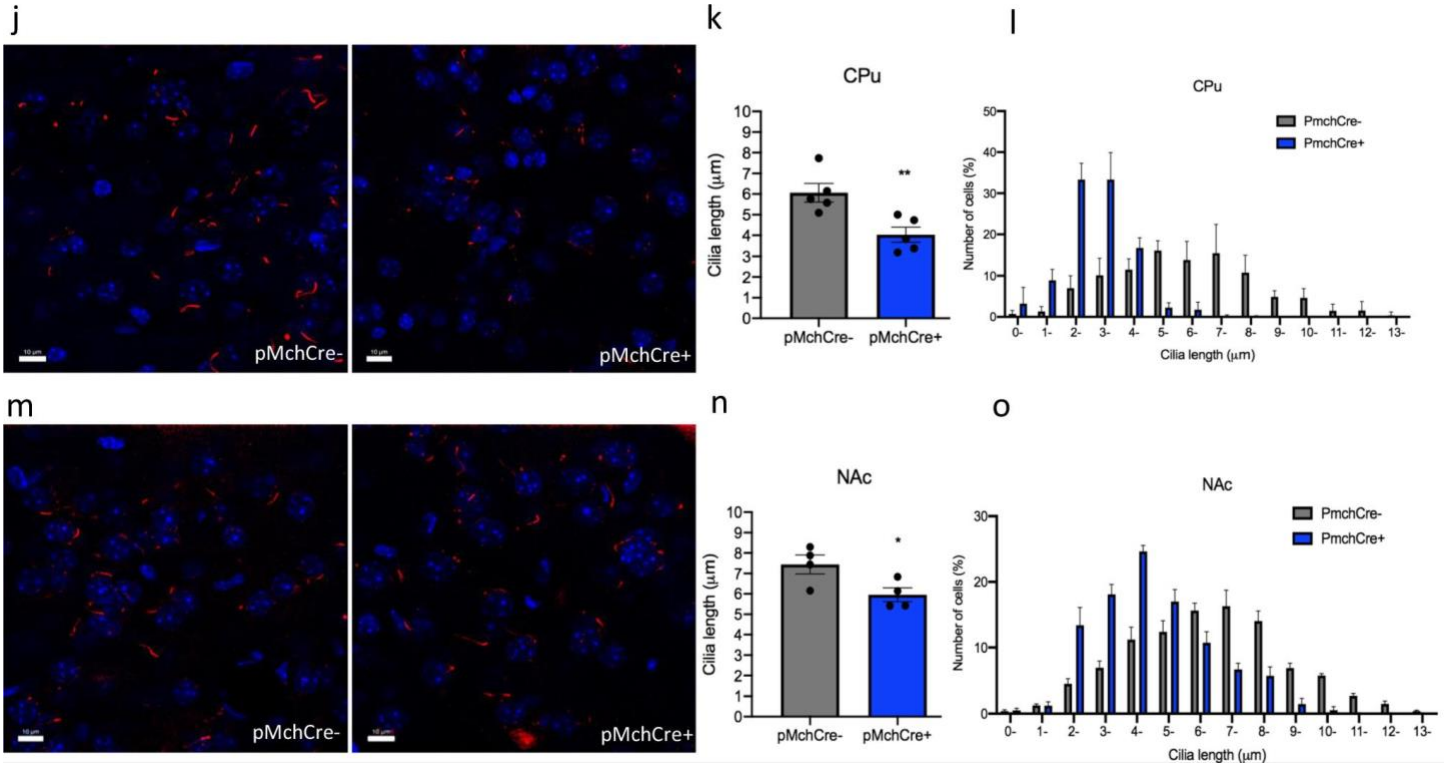

Figure 4.3. Optogenetic stimulation of MCH shortens cilia length.

a Experimental approach. Adult PmchCre + and PmchCre- mice were stereotaxically injected with AAV-EF1α-DIO-ChR2-T159c-eYFP in the lateral hypothalamus (LH). A fiber cannula was then placed in the LH slightly above the injection site. Diagram was created with BioRender.com webpage. **b** Coexpression of ChR2 (green) containing neurons in the lateral hypothalamus and MCH immunofluorescence (red) and counterstained with DAPI (blue) in PmchCre + and PmchCre- mice. (scale bar = 10 µm, magnification = 40 ×). **c** ChR2 fluorescence (green) and c-Fos immunofluorescence (red) identifies cells recently activated in PmchCre + and PmchCre- mice (scale bar = 10 µm). **d**, **g**, **j**, **m** Immunostaining of ADCY3 labeled in red fluorescence in the **d** PFC, **g** CA1, **j** CPu, and **m** NAc after blue light activation in PmchCre + and PmchCre- mice (scale bar = 10 µm). **e**, **h**, **k**, **n** Quantification of the length of ADCY3 + primary cilia (µm) in the **e**PFC, **h** CA1, **k** CPu, and **n** NAc, $*P < 0.05$, $**P < 0.01$, and $***P < 0.001$. **f**, **I**, **l**, **o** Cilia were

grouped by length (μm) and plotted against the number of cells (%) in the **f** PFC, **i** CA1, **l** CPu, and **o** NAc

DREADD expression in MCH neurons was confirmed by double immunostaining of mCherry fluorescence (red) identifying DREADD-expressing neurons and MCH staining (green) (Fig. 4.4a,b). Co-expression of mCherry fluorescence (red) identifies DREADD-expressing neurons, and c-Fos immunofluorescence (green) confirmed cells recently activated in PmchCre + and PmchCre- mice (Fig. 4.4c). DREADD hM3Dq-mediated chemogenic activation of MCH neurons in PmchCre + adult mice caused a significant decrease in cilia length compared to PmchCre- adult mice in both hemi- spheres of the brain in several regions of the brain, including the CA1, striatum, PFC, and NAc. In the PFC, stimulating MCH neurons in PmchCre- mice caused a 40% decrease in cilia length (5.226 ± 0.4111 μm in PmchCre- mice, n = 4, com- pared to 3.125 ± 0.3080 μm in PmchCre + mice, n = 4, t = 4.090, P = 0.0064, unpaired t test) (Fig. 4.4d-f). In the CA1, stimulating MCH neurons in PmchCre- mice caused a 39% decrease in cilia length (6.079 ± 0.3029 μm in PmchCre- mice, n = 4, com- pared to 3.699 ± 0.3173 μm in PmchCre + mice, n = 4, t = 5.426, P = 0.0016, unpaired t test) (Fig. 4.4g-i). In the CPu, stimulating MCH neurons in PmchCre- mice caused a 40% decrease in cilia length (6.792 ± 0.3493 μm in PmchCre- mice, n = 4, com- pared to 4.059 ± 0.4322 μm in PmchCre + mice, n = 4 (t = 4.918, P = 0.0027, unpaired t test) (Fig. 4.4j-l). In the NAc, stimulating MCH neurons in PmchCre- mice caused a 32% decrease in cilia length (9.240 ± 0.4591 μm in PmchCre- mice, n = 4, com- pared to 6.267 ± 0.1699 μm in PmchCre + mice, n = 4, t = 6.073, P = 0.0009, unpaired t test) (Fig. 4.4m-o). Activation of MCH neurons via chemogenetics caused a significant decrease in cilia density per field in the PFC (t = 4.092, P = 0.0064) and CA1 (t = 3.613, P = 0.0112).

a

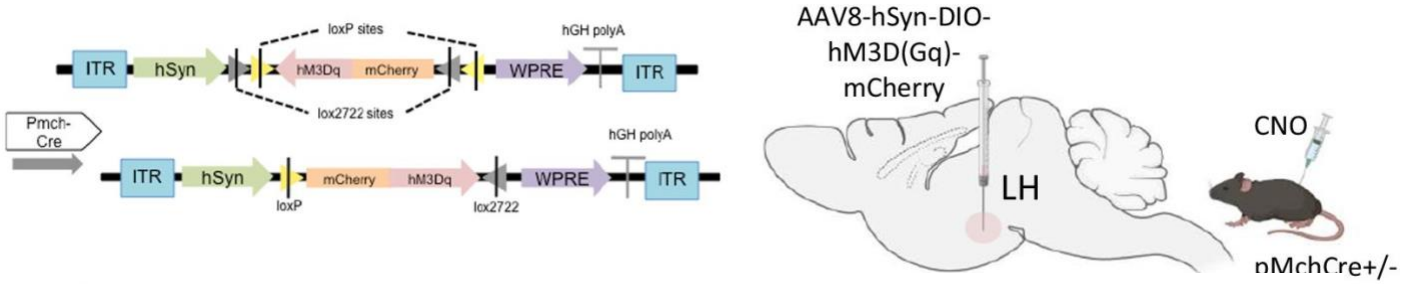
loxP sites
hGH polyA
ITR
hSyn
hM3Dq
mCherry
WPRE
ITR
lox2722 sites
Pmch-Cre
hGH polyA
ITR
hSyn
mCherry
hM3Dq
WPRE
ITR
loxP
lox2722
AAV8-hSyn-DIO-hM3D(Gq)-mCherry
LH
CNO
PmchCre+/-

b

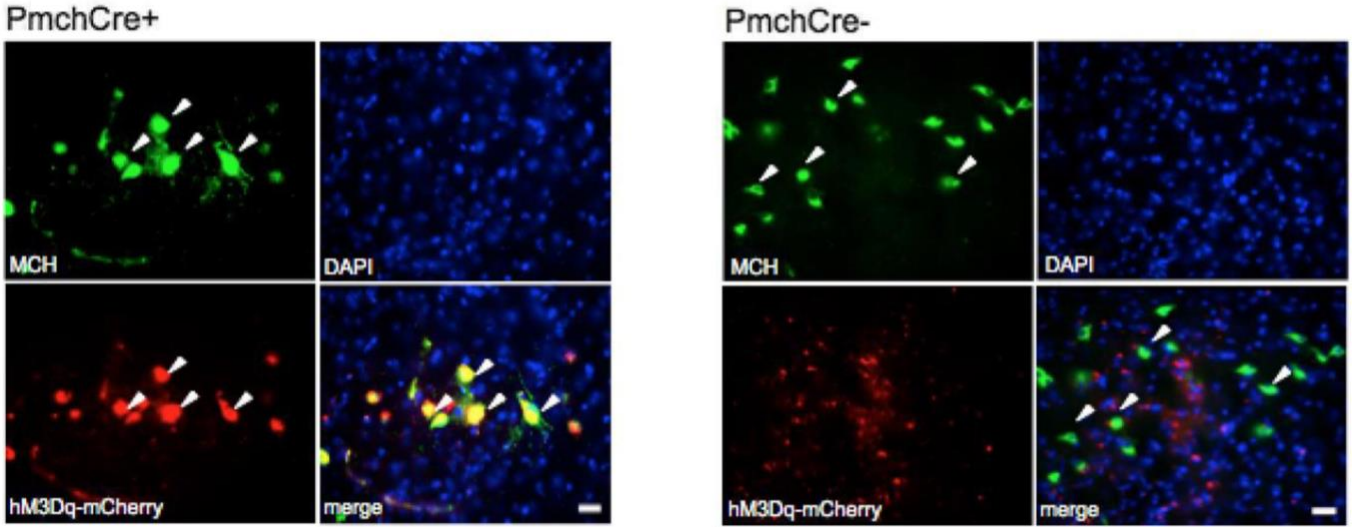
PmchCre+
MCH
DAPI
hM3Dq-mCherry
merge
PmchCre-
MCH
DAPI
hM3Dq-mCherry
merge

c

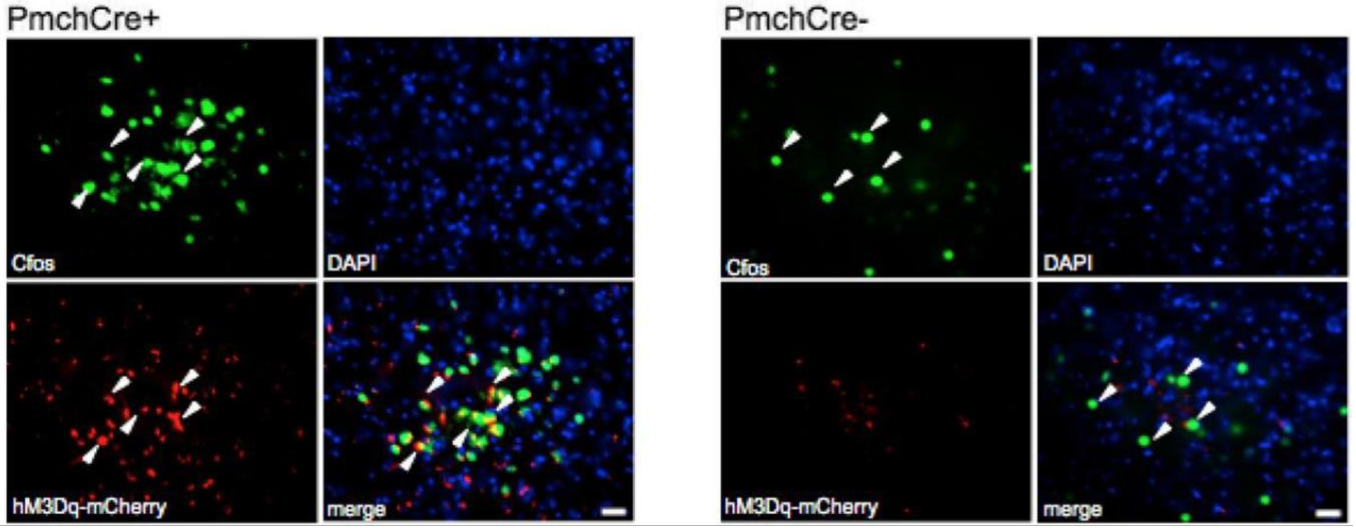
PmchCre+
Cfos
DAPI
hM3Dq-mCherry
merge
PmchCre-
Cfos
DAPI
hM3Dq-mCherry
merge

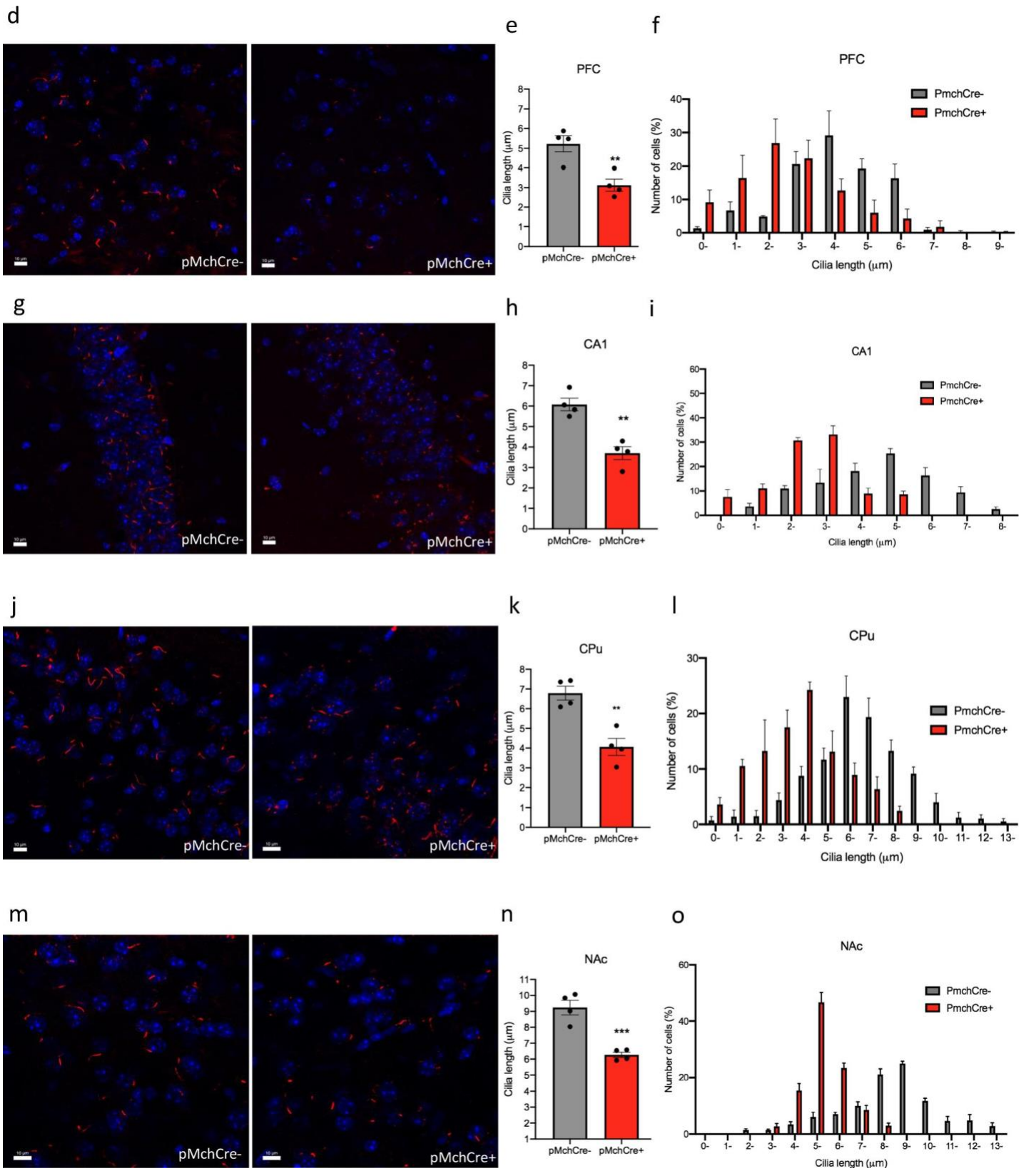
d
pMchCre-
pMchCre+
e
PFC
Cilia length (μm)
**
pMchCre-
pMchCre+
f
PFC
PmchCre-
PmchCre+
Number of cells (%)
Cilia length (μm)
g
pMchCre-
pMchCre+
h
CA1
Cilia length (μm)
**
pMchCre-
pMchCre+
i
CA1
PmchCre-
PmchCre+
Number of cells (%)
Cilia length (μm)
j
pMchCre-
pMchCre+
k
CPu
Cilia length (μm)
**
pMchCre-
pMchCre+
l
CPu
PmchCre-
PmchCre+
Number of cells (%)
Cilia length (μm)
m
pMchCre-
pMchCre+
n
NAc
Cilia length (μm)
***
pMchCre-
pMchCre+
o
NAc
PmchCre-
PmchCre+
Number of cells (%)
Cilia length (μm)

Figure 4.4. Chemogenic excitation of MCH shortens cilia length.

a. Experimental approach. Adult PmchCre + and PmchCre- mice underwent bilateral stereotaxic injection in the lateral hypothalamus with AAV-hSyn-DIO-hM3D(Gq)-mCherry to express DREADD in Cre-expressing MCH neurons. Clozapine-N-oxide (CNO) was delivered intraperitoneally to stimulate MCH neurons. Diagram was created with BioRender.com webpage. b Co-expression of mCherry fluorescence (red) identifying DREADD-expressing neurons and MCH immunofluorescence (green) and counterstained with DAPI (blue) in PmchCre + and PmchCre- mice (scale bar = 10 μm, magnification = 40 ×). c mCherry fluorescence (red) identifies DREADD-expressing neurons, and c-Fos immunofluorescence (green) identifies cells recently activated in PmchCre + and PmchCre- mice (Scale bar = 10 μm). d, g, j, m Immunostaining of ADCY3 labeled in red fluorescence in the d PFC, g CA1, j CPu and m NAc via CNO-dependent activation of Gq signaling in PmchCre + and PmchCre- mice (scale bar = 10 μm). e, h, k, n) Quantification of the length of ADCY3 + primary cilia in the e PFC, hCA1, k CPu, and n NAc, $^{**}P < 0.01$ and $^{***}P < 0.001$. f, i, l, o Cilia were grouped by length (μm) and plotted against the number of cells (%) in the f PFC, i CA1, l CPu, and o NAc

Inactivation of the MCH System Increases Cilia Length in the Mouse Brain

MCHR1 Antagonist Lengthens Cilia

The administration of GW803430 via intraperitoneal injection in adult mice for 7 consecutive days caused a significant increase in the cilia length in multiple brain regions, including the CA1 of the CA1, striatum, PFC, and NAc (Fig. 4.5a). Administration of GW803430 caused an increase in cilia length in the PFC by 42% (3.935±0.42μm in the PFC of the animals administered vehicle, $n = 4$, compared to 6.845 ± 0.3 μm in mice treated with GW803430, $n = 4$, $t = 5.646$, $P = 0.0013$, unpaired t test) (Fig. 4.5b- d). GW803430 administration caused an increase in cilia length in the CA1 by 28% (6.103 ± 0.5 μm in the animals administered vehicle, $n = 4$,

compared to 8.595 ± 0.55 μm in mice treated with GW803430, n = 4, t = 3.4, P = 0.0145, unpaired t test) (Fig. 4.5e-g). The administration of GW803430 caused lengthening in cilia in the CPu by 33% (7.30±0.50 μm, n=4, compared to 4.84 ± 0.24 μm in the CPu of the animals administered vehicle, n = 4, t = 4.583, P = 0.0038, unpaired t test) (Fig. 4.5h-j). GW803430 increased cilia length in the NAc by 17% (7.544 ± 0.22 μm in the NAc of the animals administered vehicle, n = 4, compared to 9.190 ± 0.17 μm in mice treated with GW803430, n = 4, t = 5.992, P = 0.0010, unpaired t test (Fig. 4.5k- m). Administration of GW803430 resulted in no significant difference in cilia density per field in the PFC, CA1, CPu, and NAc.

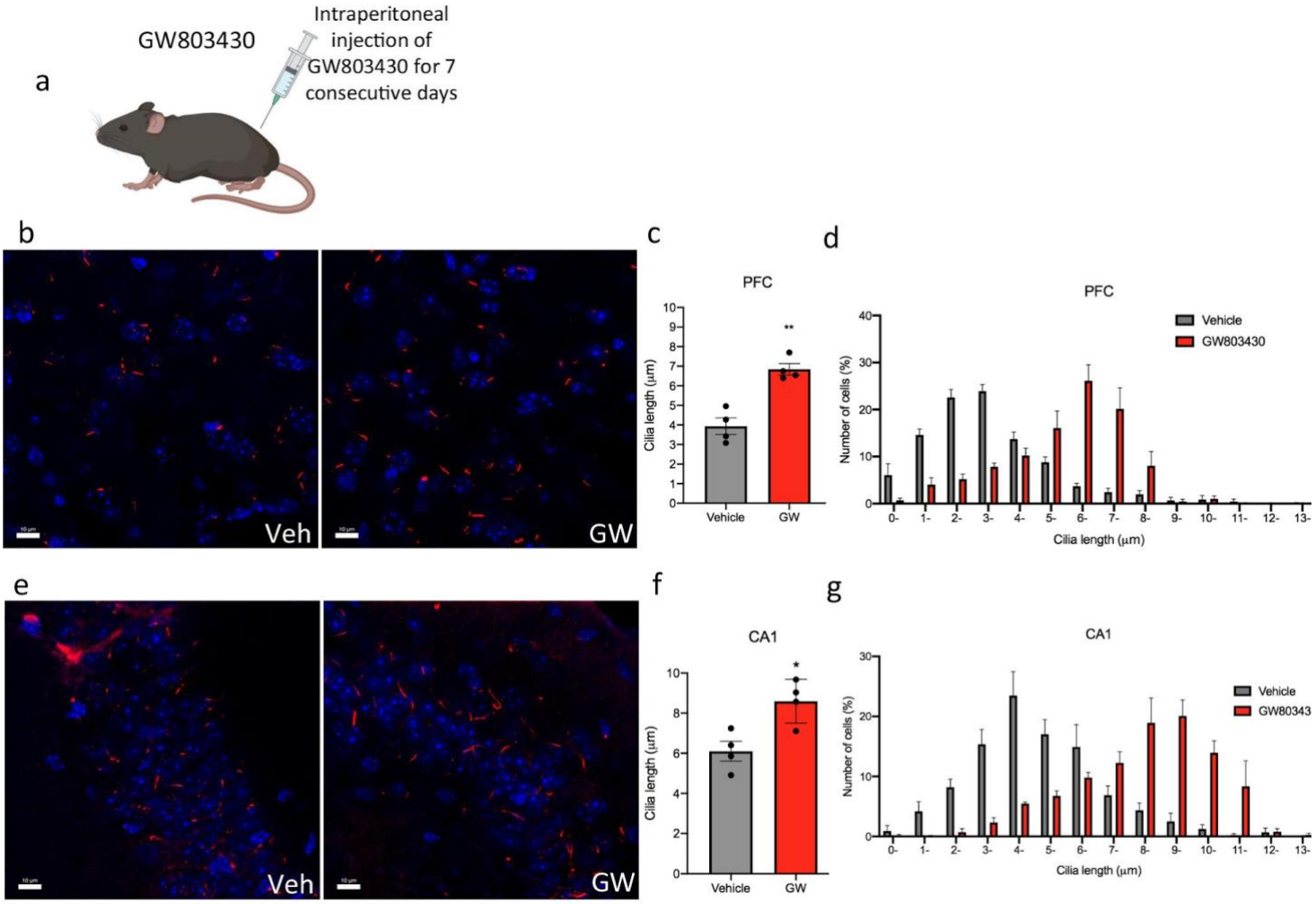

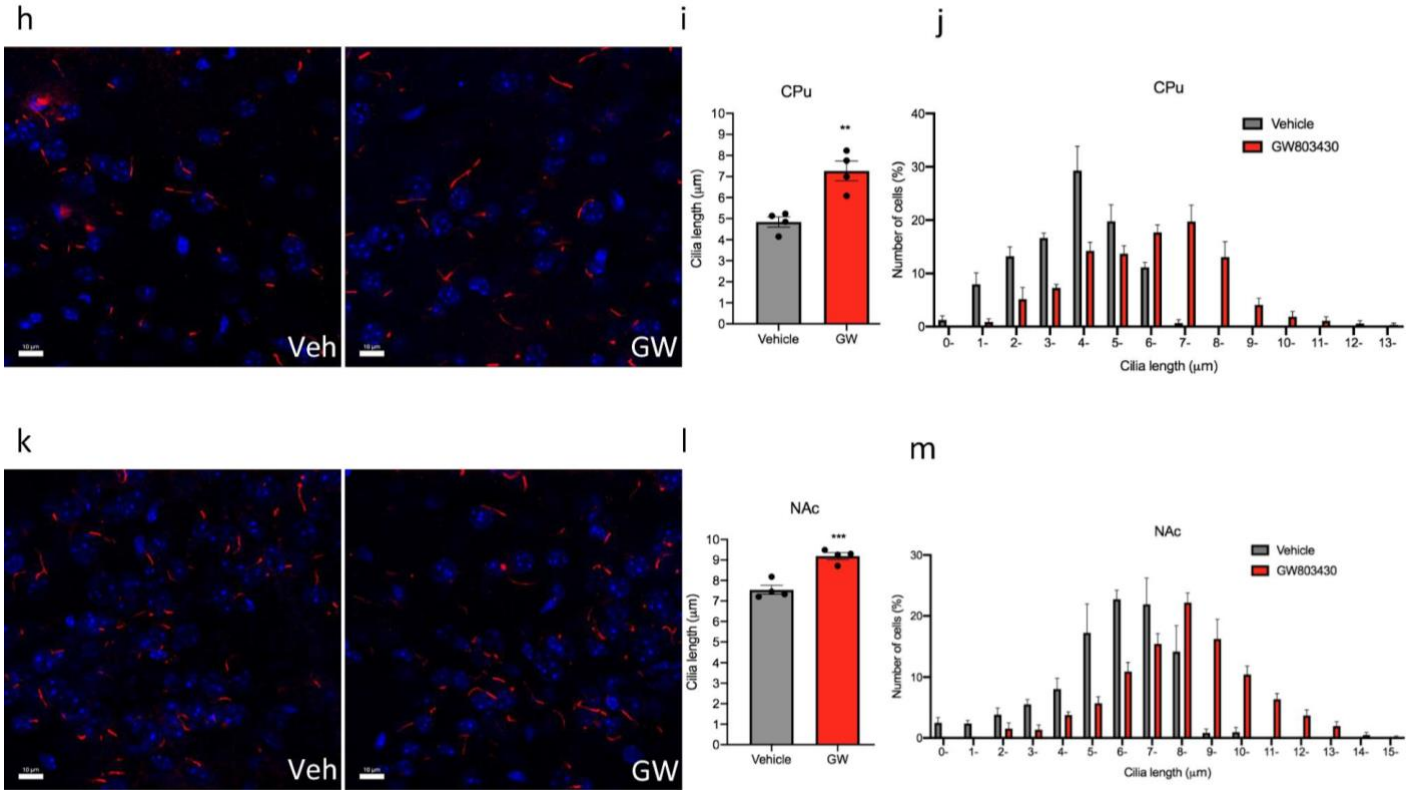

Figure 4.5. Systemic administration of the GW803430 (MCHR1 antagonist) to mice increases cilia length.

a. Schematic representation of systemic administration of GW803430 or vehicle for 7 consecutive days in adult mice. Diagram was created with BioRender.com webpage. b, e, h, k Immunostaining of ADCY3 labeled in red fluorescence in the b PFC, e CA1, h CPu, and k NAc in animals administered with GW803430 or vehicle (scale bar = 10 µm). c, f, I, l Quantification of the length of ADCY3 + primary cilia in the cPFC, f CA1, i CPu, and l NAc in animals administered with GW803430 or vehicle, $*P < 0.05$, $**P < 0.01$, and $***P < 0.001$. d, g, j, mCilia were grouped by length (µm) and plotted against the number of cells (%) in the d PFC, g CA1, j CPu, and m NAc

Cilia Length Is Increased in MCH and MCHR1 Deficit Mice

To assess MCH-neuron ablation extent following DT injection into IDTR + PmchCre- and IDTR + Pmch- Cre- mice, MCH neurons were visualized and counted using rabbit polyclonal anti-MCH antibody (Fig. 4.6a,b), and only mice that exhibited over 90% ablation of MCH neurons were used in the study. The conditional ablation of MCH neurons in adult mice (MCH-cKO) caused a significant increase in the cilia length in several regions of the brain including CA1, striatum, and PFC and NAc (Fig. 4.6a,b). In the PFC of MCH-cKO mice, cilia length increased by 19% (5.03 ± 0.32 μm in IDTR + Pmch- Cre- mice, n = 3, compared to 6.185 ± 0.04609 μm in IDTR+PmchCre+mice, n=3 t=3.539, P=0.024, unpaired t test) (Fig. 4.6c-e). In the CA1 of IDTR + MCH- cKO mice, cilia length increased by 24% (6.24 ± 0.23 μm in IDTR + PmchCre- mice, n = 3, compared to 8.209 ± 0.07566 μm in IDTR + PmchCre + mice, n = 3, t = 8.265, P = 0.0012, unpaired t test) (Fig. 4.6f-h). In the CPu of MCH-cKO mice, cilia length increased by 29% (5.242 ± 0.2518 μm IDTR + PmchCre- mice, n = 3, com- pared to 7.373 ± 0.6131 μm in IDTR + PmchCre + mice, n = 3 (t = 3.215, P = 0.0324, unpaired t test) (Fig. 4.6i-k). In the NAc of MCH-cKO mice, cilia length increased by 23% (5.239 ± 0.4177 μm in IDTR + PmchCre- mice, n = 3, compared to 6.823 ± 0.3695 μm in IDTR + Pmch- Cre + mice, n = 3 (t = 2.841, P = 0.0456, unpaired t test) (Fig. 4.6l-n). MCH-cKO mice resulted in a significant increase in cilia density per field in the CA1 (t = 6.516, P = 0.0006) and the NAc (t = 5.047, P = 0.0023).

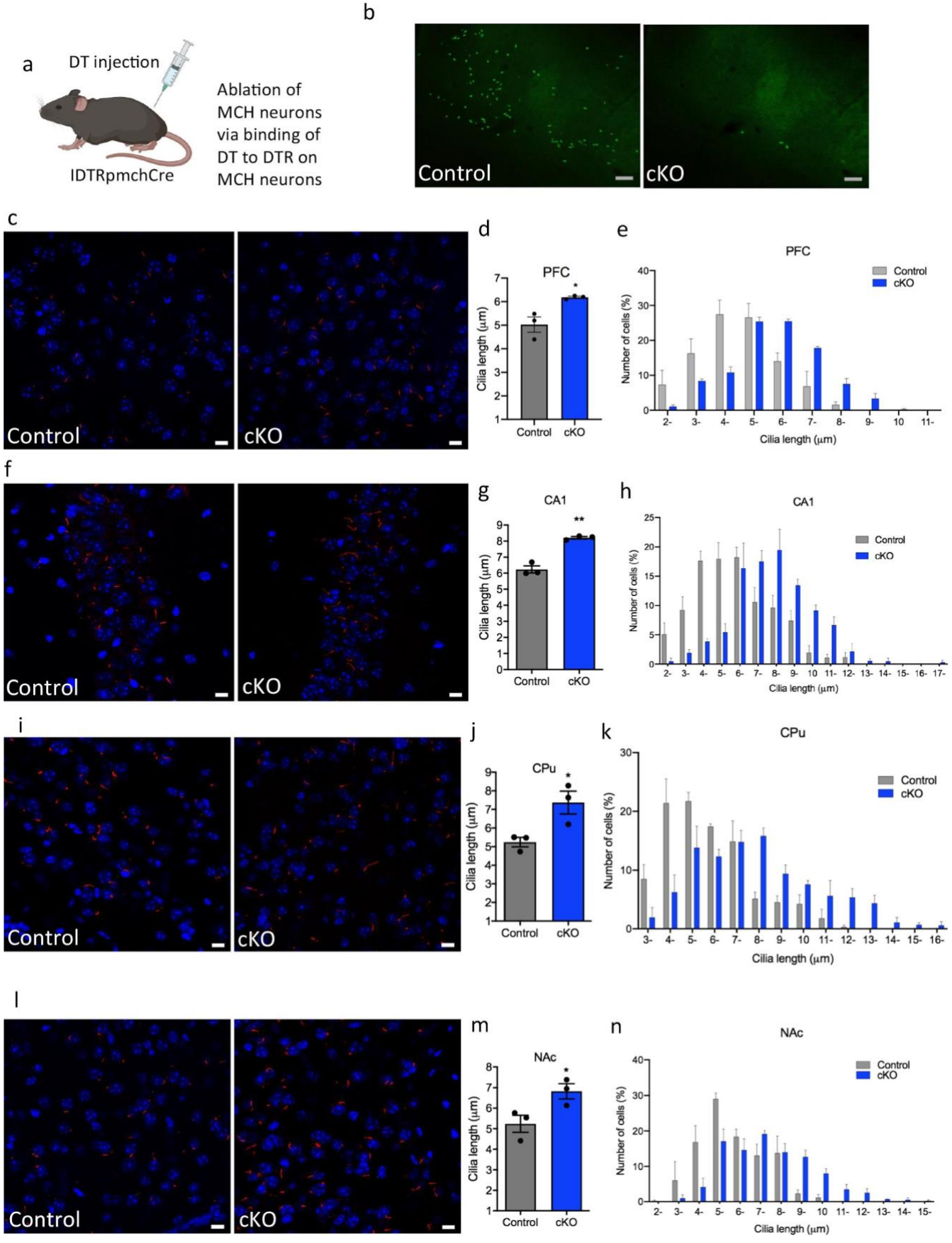
a
DT injection
IDTRpmchCre
Ablation of MCH neurons via binding of DT to DTR on MCH neurons
b
Control
cKO
c
Control
cKO
d
PFC
Cilia length (μm)
Control
cKO
e
PFC
Control
cKO
Number of cells (%)
Cilia length (μm)
f
Control
cKO
g
CA1
Cilia length (μm)
Control
cKO
h
CA1
Control
cKO
Number of cells (%)
Cilia length (μm)
i
Control
cKO
j
CPu
Cilia length (μm)
Control
cKO
k
CPu
Control
cKO
Number of cells (%)
Cilia length (μm)
l
Control
cKO
m
NAc
Cilia length (μm)
Control
cKO
n
NAc
Control
cKO
Number of cells (%)
Cilia length (μm)

Figure 4.6. Cilia length is increased in MCH deficit mice.

a Schematic representation of how the MCH cells are ablated through DTR. IDTR mice were crossed with PmchCre mice rendering offspring mice with Cre-expressing MCH neurons sensitive to DT. Diagram was created with BioRender.com webpage. **b** MCH immunoreactivity (GFP) in the lateral hypothalamus of IDTRPmchCre- and IDTRPmchCre + mice following DT injection (scale bar = 100 μm, magnification = 10 ×). **c**, **f**, **l**, **l** Immunostaining of ADCY3 labeled in red fluorescence and counterstained with DAPI (blue) in IDTRPmch + and IDTRPmch- mice in the **c** PFC, **e** CA1, **g** CPu, and **i**NAc (scale bar = 10 μm, magnification = 63 ×). **d**, **g**, **j**, **m** Quantification of cilia length (μm) in the **d** PFC, **f** CA1, **h** CPu, and **j** NAc, **P* < 0.05 and ***P* < 0.01. **e**, **h**, **k**, **n** Cilia were grouped by length (μm) and plotted against the number of cells (%) in the **e** PFC, **h**CA1, **k** CPu, and **n** NAc

Germline deletion of MCHR1 in mice caused a significant increase in the cilia length in several brain regions, including CA1, CPu, PFC, and NAc. In the PFC of MCHR1 KO mice, there was an increase in cilia length by 41% (3.8±0.1 μm in WT mice, *n*=4, com- pared to 6.50 ± 0.09 μm in the MCHR1KO mice, $n = 5$, $t = 20.15$, $P < 0.0001$, unpaired *t* test) (Fig. 4.7a-c). In the CA1 of the hippocampus of MCHR1 KO mice, cilia were 22% longer than in WT mice (2.8 ± 0.03 μm in the CA1 of the WT mice, $n = 4$, compared to 3.6 ± 0.10 μm. 0.1 μm in the MCHR1KO mice, $n = 5$, $t = 6.712$, $P = 0.0003$, unpaired *t* test) (Fig. 4.7d-f). In the CPu of the MCHR1 KO mice, $n = 5$, cilia length increased by 17% (9.5 ± 0.3 μm compared to 7.9 ± 0.3 μm in WT mice, $n = 4$, $t = 3.952$, $P = 0.005$, unpaired *t* test) (Fig. 4.7g-i). In the NAc of the MCHR1 KO mice, cilia length increased by 25% (7.60 ± 0.50 μm in the NAc of the WT mice, $n = 4$, compared to 10.19 ± 0.50 μ in MCHR1KO mice, $n = 5$, $t = 4.434$, $P = 0.003$, unpaired *t* test) (Fig. 4.7j-l). MCHR1KO mice caused a significant increase in cilia density per field in the CA1 ($t = 3.884$, $P = 0.0081$).

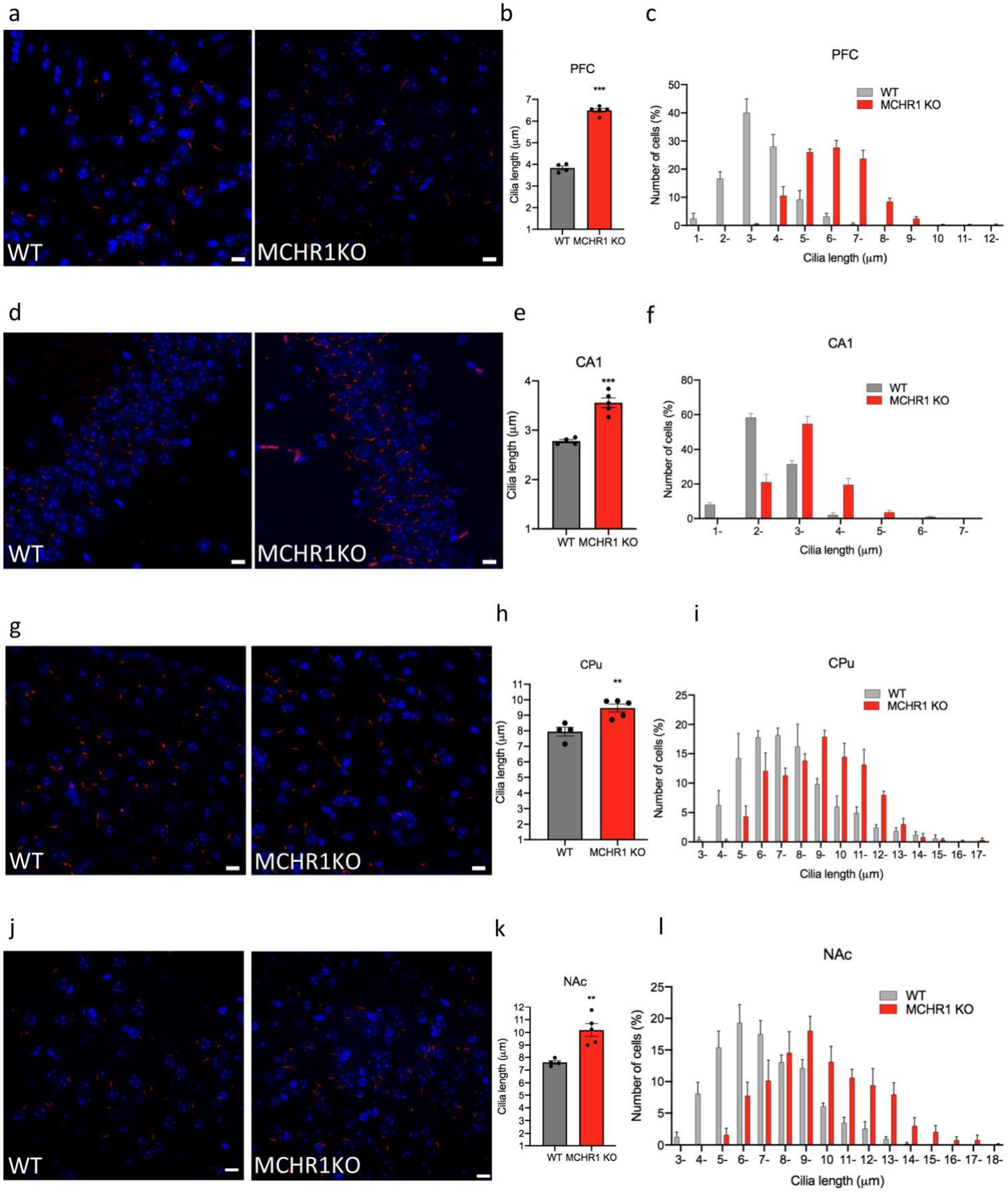
a
b
c
WT
MCHR1KO
PFC
***
Cilia length (μm)
WT MCHR1 KO
PFC
WT
MCHR1 KO
Number of cells (%)
1- 2- 3- 4- 5- 6- 7- 8- 9- 10 11- 12-
Cilia length (μm)
d
e
f
WT
MCHR1KO
CA1
***
Cilia length (μm)
WT MCHR1 KO
CA1
WT
MCHR1 KO
Number of cells (%)
1- 2- 3- 4- 5- 6- 7-
Cilia length (μm)
g
h
i
WT
MCHR1KO
CPu
**
Cilia length (μm)
WT MCHR1 KO
CPu
WT
MCHR1 KO
Number of cells (%)
3- 4- 5- 6- 7- 8- 9- 10 11- 12- 13- 14- 15- 16- 17-
Cilia length (μm)
j
k
l
WT
MCHR1KO
NAc
**
Cilia length (μm)
WT MCHR1 KO
NAc
WT
MCHR1 KO
Number of cells (%)
3- 4- 5- 6- 7- 8- 9- 10 11- 12- 13- 14- 15- 16- 17- 18-
Cilia length (μm)

Figure 4.7. Cilia length is increased in MCHR1 knockout animals.

Immunostaining of ADCY3 labeled in red fluorescence and counterstained with DAPI (blue) in the a PFC, d CA1, g CPu, and j NAc in MCHR1 KO or WT mice (scale bar = 10 μm, magnification = 63 × . b, e, h, k Quantification of the length of ADCY3^{+} primary cilia (μm) in the b PFC, e CA1, h CPu (CPu), and k NAc in MCHR1 KO or WT mice, $^{**}P < 0.01$ and $^{***}P < 0.001$. c, f, I, l Cilia were grouped by length (μm) and plotted against the number of cells (%) in the cPFC, f CA1, i CPu, and l NAc

Discussion

In this study, we established the causal effects of MCH signaling pathways on cilia length. We first showed that MCH treatment causes cilia shortening in the striatal and cortical brain slice cultures. We then demonstrated that the stimulation of the MCH system through direct agonist activation of the MCHR1 or via optogenetic and chemogenic excitation of MCH neurons causes a significant decrease in cilia length. In contrast, the inactivation of the MCH system through pharmacological blockade of MCHR1 or genetic manipulation (MCHR1 germline deletion or MCH neurons' conditional ablation) causes a significant increase in cilia length.

MCHR1 is widely distributed throughout the brain, with high density in the CPu, NAc, CA1 of the hippocampus, and the PFC [40, 68]. Therefore, we focused on these regions in examining the effects of MCH system activation and inactivation on cilia length. Consistent with previous reports, we found that cilia length differed among brain regions [11, 36, 43, 51, 74]. Interestingly, we also found that cilia length differs among mouse strains. This observation warrants further investigation to determine whether such variabilities in cilia length correlate with genotypic or phenotypic characteristics of these different strains.

The various manipulation approaches allowed us to (1) recapitulate conditions used previously to substantiate MCH physiological functions; (2) differentiate between the effects of MCH neurons and MCHR1 manipulation; (3) distinguish the effects of acute versus chronic activation/inactivation of MCH system; and (4) determine the effects of early-life versus adult stage MCH system manipulations.

The role of MCH in regulating a wide variety of physiological functions such as feeding, obesity, reward, and sleep has been established using pharmacological and genetic manipulations [19, 20, 30, 41, 73]. For example, central chronic infusions of MCH had long been shown to induce mild obesity in wild-type mice [32]. In contrast, subchronic administration of MCHR1 antagonists and MCHR1/MCH genetic deletion are known to produce anti-obesity effects in mice [31, 49]. The ciliopathy Bardet-Biedl syndrome (BBS) is characterized by obesity, and

mutations affecting the mouse orthologs of BBS- associated genes disrupt the localization of MCHR1 [9, 87]. Thus, failure of MCHR1 to reach the cilium could potentially be associated with failure in the MCHR1 signaling pathway in the cilia, leading to obesity in BBS [28, 77].

Given that MCH neurons synthesize and release other neurotransmitters/neuropeptides, including gamma-aminobutyric acid (GABA), neuropeptide E-I (NEI), and neuropeptide G-E (NGE) [53, 61], it is important to distinguish the selective role of the activation of MCHR1 present on neuronal primary cilia from the activation or inactivation of MCH neurons releasing MCH or other neurotransmitter, in regulating primary cilia length. Hence, MCHR1 pharmacological activation by MCH intracerebral infusion, the blockade of the receptors by GW803430 systemic treatment and MCHR-1 germline deletion, allowed the exploration of the selective role of MCHR1. In parallel, optogenetic and DREADD stimulation of the MCH neurons and IDTR-dependent ablation of MCH neurons allowed for exploring the role of MCH neurons. Optogenetics and DREADD technologies have also been previously used to explore MCH neurons' role in sleep, reward, and feeding [12, 25, 52].

Previous reports demonstrated distinctive effects of acute versus chronic activations of MCH systems on body weight [72]. Therefore, we examined the effects of acute (optogenetic and chemogenetic stimulation) and chronic activations (MCH i.c.v. administration for 7 days) of the MCH system on cilia length. We previously showed that developmental and adulthood inactivation of the MCH system in mice leads to distinct behavioral deficits. For example, germline MCHR1 deletion but not adult IDTR- dependent ablation of MCH neurons caused olfactory impairment and social deficits [83]. Therefore, we examined the effects of germline MCHR1 deletion and adulthood conditional MCH ablation on cilia length.

Strikingly, we found that the different MCH system manipulations produced consistent patterns of alterations in cilia length. The activation of MCH system consistently shortened cilia length, while the inactivation of MCH system lengthened cilia length. The findings that both acute and chronic activation of MCH system shortened cilia length and that both early-life and adulthood

inactivation of the MCH system lengthened cilia substantiate the dynamic nature of the cilia system and suggest that cilia's morphology undergoes rapid changes in response to its environment. Most importantly, our findings provide the first evidence for the direct and moment-to-moment regulation of the brain cilia structure by the MCH system.

Unexpectedly, unilateral optogenetic stimulation of MCH neurons in the lateral hypothalamus caused bilateral shortening of cilia length in the PFC, CA1, CPu, and NAc. This finding may suggest that MCH neurons project ipsilaterally and contralaterally to these brain regions. Another explanation might be that MCH activation may produce ipsilateral modifications of other neurotransmitter systems, which may result in contralateral shortening of cilia length. It is well-established that MCH neurons innervate serotonergic neurons in the raphe nucleus and regulate the activity of these neurons [24, 78]. Indeed, specific MCH-regulated functions are mediated through the serotonin system [48, 79]. Thus, the activation of MCH neurons may regulate cilia indirectly through its interaction with the serotonin system. Interestingly, MCHR1 and 5-HT6 are among the very few GPCRs that preferentially localize to primary cilia [6], and the inhibition of 5-HT6 receptors is known to shorten cilia length [16, 41]. Another possible explanation for the bilateral modifications of the cilia length could be that the stimulation of MCH neurons induces the release of MCH to the ventricular system, thus allowing MCH to reach distant targets via the cerebrospinal fluid causing cilia shortening throughout the brain [55, 76].

While cilia shortening effects of MCH system activation is not unexpected, and is, indeed, consistent with previous in vitro studies, the effect of MCH signaling on cilia retraction is surprising. However, taking in consideration our threshold that was setup for measuring cilia length (> 0.5 μm), it is possible that MCH system activation reduced cilia length to levels that were below this threshold.

A possible mechanism for MCH-induced cilia shortening is through a Gi/o-dependent Akt pathway [36, 75]. The ciliary MCHR1-Gi/o pathway seems to result in a series of downstream signal cascades that lead to increasing the depolymerization of cytosolic tubulin, increasing

soluble tubulin levels in the cell body and increase actin filaments [36, 75]. A very recent study by Dr. Saito group demonstrated that the PDZ and LIM domain-containing protein 5 (PDLIM5) is the most important crucial factor in MCHR1-mediacted cilia shortening and discovered that the actin-binding protein alpha-actinin 1/4 is the main downstream target of the PDLIM5 signaling pathway that mediate MCHR1-induced cilia shortening [26].

Defects in the assembly such as cilia shortening have been shown to cause a range of severe diseases and developmental disorders called ciliopathies, which are associated with neurological deficits such as abnormal cortical formation and cognitive deficits [38, 66, 80]. We have recently shown that brain cilia genes were differentially expressed in major psychiatric disorders, including schizophrenia, autism spectrum disorder, depression, and bipolar disorder [3]. On the other hand, evidence from our own work and others strongly support an essential role for the MCH system, particularly MCHR1, in the pathophysiology of schizophrenia. We showed that MCHR1 mRNA is decreased in the PFC of patients with schizophrenia [83]. We also demonstrated that genetic manipulation of the MCH system via the deletion of MCHR1 and the conditional ablation of MCH neurons resulted in behavioral abnormalities mimicking schizophrenia-like phenotypes, including repetitive behavior, social impairment, impaired sensorimotor gating, and disrupted cognitive functions [84]. We also showed that MCHR1 germline deletion causes alterations in depressive-like behavior that is sex-dependent [83]. These same genetic models were used in our current study to examine the consequences of this genetic manipulation on cilia length. In both IDTR + PmchCre + and MCHR1KO animals, we found a significant increase in cilia in all regions, including the PFC, CA1, CPu, and NAc. Our previous and current data may point to the role of ciliary MCHR1 in the pathophysiology of psychiatric disorders such as schizophrenia and depression. Together, our previous and current studies point at the cilia elongation as a possible mechanism through which MCH system dysregulation causes social and cognitive deficits in mice and is associated with psychiatric disorders in humans [3, 83]. Our results also prompt the question on whether selective targeting of cilia MCHR1 might

offer a novel approach to treat psychiatric disorders. Indeed, studies have demonstrated that some pharmacological agents can alter cilia length. For example, lithium, a mood stabilizer that is used in treatment of bipolar disorder and acute mania, increases MCHR1-positive cilia length in several cell types, including neuronal cells, the dorsal striatum, and NAc [51].

Since our analysis of cilia length was mainly based on the quantification of ADCY3 positive signals and not in MCHR-1 positive ones, and given that some brain cilia do not express MCHR1, further studies are needed to determine whether cilia length is regulated by MCH signaling in MCHR1-expressing neurons that have MCHR1-negative cilia. On the other hand, as our study was conducted on male mice, it is of particular importance to investigate the sex difference in cilia length as a response to MCH system manipulation particularly due to the sexually dimorphic expression of MCH in rodent brain [67]. Given the high dynamic nature of cilia, it would also be interesting to investigate whether the estrous cycle in female mice affects cilia morphology and length.

Unexpectedly, we found that within the same strains, the vehicle-treated animals in the two pharmacological manipulations exhibited different cilia lengths. For example, the average cilia length was 4.84 ± 0.24 μm in the CPU of animals treated with the vehicle of GW803430, compared to 8.005 ± 0.2 μm in animals treated with the vehicle of MCH. While the reasons for these differences in cilia lengths are not fully under- stood, this finding substantiates the well-established highly dynamic features of cilia structure and morphology [5, 7, 21, 42, 47, 54, 56, 57, 86]. Given that the control animals, despite being from the same sex, strain, and age, underwent different experimental procedures, the variability in cilia length among the control animals might be attributed to factors related to the experimental designs. Some of these factors might be (1) the composition of vehicles administered, (2) the route of administration, and (3) the exposure to stereotactic surgery and anesthetic agents. First, while the MCH vehicle was composed of phosphate-buffered saline with 0.2% bovine serum albumin, GW803430 dissolving vehicle was composed of 2% Tween 80 with acetic acid. Second, since MCH does not cross the blood–brain

barrier, intracerebroventricular route was used for direct injection of MCH into the cerebrospinal fluid in the ventricles. MCHR1 antagonist GW803430, on the other hand, was administered via intraperitoneal route. The vehicles and routes of administration were selected based on previously characterized pharmacological and behavioral profiles [1, 70]. Lastly, unlike the animals injected with GW803430, MCH-injected animals underwent stereotactic surgery for cannula implantation and had been administered isoflurane to induce anesthesia. These factors may have contributed to the variability in cilia lengths in the control animals, thus, further investigation is necessary to determine whether these effects are sufficient to influence changes in cilia length.

In conclusion, our present study has established the causal regulatory effects of the MCH system signaling on cilia length. The findings of this study are significant because (1) they show for the first time in vivo that primary cilia length can be regulated by the MCH signaling, proving the link between GPCRs and cilia length regulation and (2) they implicate ciliary MCHR1 as a potential therapeutic target for the treatment of pathological conditions characterized by impaired cilia function.

Chapter 5: Cilia in the Striatum Mediate Timing-Dependent Function

Alhassen W, Alhassen S, Chen J, Monfared RV, Alachkar A. **Cilia in the Striatum Mediate Timing-Dependent Functions**. Mol Neurobiol. 2023 Feb;60(2):545-565. doi: 10.1007/s12035-022-03095-9. Epub 2022 Nov 2. PMID: 36322337; PMCID: PMC9849326.

Abstract

Almost all brain cells contain cilia, antennae-like microtubule-based organelles. Yet, the significance of cilia, once considered vestigial organelles, in the higher-order brain functions is unknown. Cilia act as a hub that senses and transduces environmental sensory stimuli to generate an appropriate cellular response. Similarly, the striatum, a brain structure enriched in cilia, functions as a hub that receives and integrates various types of environmental information to drive appropriate motor response. To understand cilia's role in the striatum functions, we used loxP/Cre technology to ablate cilia from the dorsal striatum of male mice and monitored the behavioral consequences. Our results revealed an essential role for striatal cilia in the acquisition and brief storage of information, including learning new motor skills, but not in long-term consolidation of information or maintaining habitual/learned motor skills. A fundamental aspect of all disrupted functions was the "time perception/judgment deficit." Furthermore, the observed behavioral deficits form a cluster pertaining to clinical manifestations overlapping across psychiatric disorders that involve the striatum functions and are known to exhibit timing deficits. Thus, striatal cilia may act as a calibrator of the timing functions of the basal ganglia-cortical circuit by maintaining proper timing perception. Our findings suggest that dysfunctional cilia may contribute to the pathophysiology of neuro-psychiatric disorders, as related to deficits in timing perception.

Introduction

Primary cilia, antennae-like microtubule-based organelles emanating from the cell surface, function as a signaling hub that senses environmental sensory stimuli and transduces them to generate appropriate cellular responses [1–4]. As an essential center for non-synaptic neuronal communications, cilia signaling is achieved through specific receptors and downstream pathways' components such as the Sonic Hedgehog (Shh) signaling pathway, G-protein-coupled receptors (GPCRs), and ion channels [5–12].

Cilia's dynamic structure, reflected by the vibrant length, morphology, and protein composition, allows cilia to quickly respond to environmental stimuli such as light, mechanical stimuli, pH, and chemical signals (signaling molecules, neurotransmitters, and nutrients) [13–19]. Although most ciliopathies are associated with cognitive impairments, cilia have only been scarcely investigated for their roles in higher- order cognitive functions [20–25]. We recently showed dys- regulations of genes associated with cilia's structural and functional components in four psychiatric disorders: schizophrenia, autism, bipolar disorder, and major depressive disorder [26]. Furthermore, many dysregulated cilia genes overlapped across these psychiatric disorders, indicating that common cilia signaling pathways' dysfunctions may underlie some pathophysiological aspects of these psychiatric disorders.

Like cilia, though at larger spatial and organizational scales, the striatum, which comprises the primary input station to the basal ganglia, functions as a hub receiving and integrating various environmental information, including contextual, motor, and reward [27–31]. Striatal neurons process the information and project to the output structures of the basal ganglia, substantia nigra pars reticulata (SNr)/medial globus pallidus (GPm) (for review [32–35]). The striatum is enriched in cilia [36, 37]. Furthermore, a number of cilia-associated GPCRs are expressed in the striatum (e.g., dopamine receptors, serotonin receptor 6 (5-HT6), melanin-concentrating hormone receptor 1 (MCHR1), and the orphan receptors GPR88) [5–10, 38–56].

As a central part of cortico-basal ganglia-thalamic-cortico circuits, the striatum controls various executive functions, including motor movements, planning, decision-making, working memory, and attention [57–60]. Dysfunctions of cortico-basal ganglia-thalamic circuits are involved in several neurological and psychiatric (neuro-psychiatric) disorders such as attention-deficit hyperactivity disorder (ADHD), Hunting- ton's disease (HD), Parkinson's disease (PD), schizophrenia (SCZ), autism spectrum disorder (ASD), Tourette syndrome (TS), and obsessive–compulsive disorder (OCD) [61–76]. The overlap in clinical features of these disorders suggests common signaling pathways that may underlie some pathophysiological aspects of these neuro-psychiatric disorders. Hence, it is tempting to ask whether cilia in the striatum mediate some of its functions and whether cilia are involved in psychiatric disorders associated with striatum dysfunctions.

According to our recent study, the striatum was the only brain structure that shared rhythmic cilia genes with every other brain region studied [18]. The spatiotemporal expressions of circadian cilia genes in the basal ganglia-cortical neurons follow the same sequential order of this circuitry in controlling movement, though on different time scales. Therefore, this study aims to examine the behavioral consequences of cilia ablation in the striatum and explore whether abnormal striatal cilia are a unifying pathophysiological factor in striatum-associated neuropsychiatric disorders. For this purpose, we used the loxP/Cre conditional deletion system to selectively delete the intraflagellar transport (IFT88) gene, an essential factor for primary cilia formation, from the dorsal striatum. We then monitored the behavioral phenotypes resulting from striatal cilia ablation, focusing on neuropsychiatric phenotypes/manifestations of the striatum functional domains.

Materials and Methods

Animals

The IFT88fl mice possess *loxP* sites flanking exons 4-6 of the intraflagellar transport 88 (IFT88) gene (Jackson Laboratories, #022,409). All experimental procedures were approved by the Institutional Animal Care and Use Committee of the University of California, Irvine, and were performed in compliance with national and institutional guidelines for the care and use of laboratory animals. The experimental design is illustrated in Fig. 5.1a. Only male mice were used in this study.

Genotyping

The genotyping protocol was provided by Jackson Laboratory (JAX). DNA was extracted from mice using the following protocol. One millimeter of the tip of the tail was cut and digested in lysis buffer along with proteinase K overnight followed by isopropanol to precipitate the DNA, and ethanol to wash the pellet, and finally dissolved in TE buffer. DNA concentration and purity were checked. The DNA was used for the following PCR reaction. The following primers were used Forward 5′-GACCACCTTTTT AGCCTCCTG, Reverse 5′-AGGGAAGGGACTTAGGAA TGA. Amplification was performed using KAPA2GFast HotStart PCR kit (Roche Cat. No 07960930001). Touch- down cycling was performed and ran on a 1% agarose gel with the homozygous at ~ 410 bp, heterozygous at 365 bp and ~ 410 bp, and wildtype at 365 bp.

Stereotaxic Surgery

Eight-week-old male *Ift88fl* mice were subjected to stereotaxic surgery along with wild-type littermates. Mice were anesthetized with 2% isoflurane and mounted on the stereotaxic frame. The skin between the eyes and ears was shaved, and an incision was made to uncover the skull and reveal bregma. A small hole was drilled bilaterally, and all mice received 0.5 µl of the adenovirus expressing Cre: AAV.CamKII.HI.GFP-Cre.WPRE.SV40 (titer 2.4 × $10^{\wedge 13}$ G.C./ml, serotype AAV9), which was bilaterally injected into the dorsal segment of the rostral striatum, at the stereotaxic coordinates anteroposterior at 1.3 mm, mediolateral at ± 1.3 mm, and dorsoventral

at 3.2 mm (Fig. 6.1b). AAV.CamKII.HI.GFP-Cre.WPRE.SV40 was a gift from James M. Wilson (Addgene viral prep # 105,551-AAV9 http://n2t.net/addgene:105551; RRID:Addgene_105551). The skin was sutured with silk non-absorbable sutures, and mice were allowed a week to recover before behavioral experiments. After the last behavioral experiment at approximately 16 weeks old, mice were perfused, and AAV infection was analyzed.

Behavioral Experiments

Two weeks after the surgery, mice were tested in a battery of behavioral paradigms in the following order (Fig. 5.1a): locomotion and stereotypy/open field, rotarod, grooming, social interaction and novelty, spontaneous T-maze alternation, novel object/location recognition, prepulse inhibition, forced swim, hot plate, and contextual fear conditioning. The sequence of specific assays spaced by 3–6 days inter-assay interval was adapted from previously published reports [77–79].

Locomotor Activity Test and Open Field

The locomotor activity and open field assays were carried out as we previously described [78]. The experiment is divided into two phases of a total of 90 min experiment, which is divided into 30 min acclimation and 60 min locomotor activity test [78]. Animals were placed in a 40 × 40 cm locomotion chamber (Med Associates, Inc.), and their activity was logged every 5 min, over the assay duration using Activity Monitor 5 software (Med Associates, Inc.).

Open field assay was carried out in the first 10 min after placing the mice into the chambers, and the distance traveled and activity time in the central and peripheral zones were recorded and analyzed using Activity Monitor 5 software.

Rotarod Test

In order to evaluate motor coordination, mice were subjected to the rotarod assay. Animals were placed on an elevated rotating rod divided into 5 lanes with trip plates below each lane to stop the timer when a subject falls. Each trial is 420 s with a starting speed at 4 RPM that continues

to incrementally speed up to 60 RPM. Animals were subjected to 3 trials with 15 min between each trial. Data were analyzed based on latency and speed to fall over each trial.

T-maze Spontaneous Alternation

Mice were placed in the entrance at the base of the T-maze. Mice were acclimated at the base of the T-maze for 30 sec. After acclimation, the doors were opened, and animals were free to explore either the left or right arm of the maze. After a choice had been made, the door was closed, allowing the animal to explore the sidearm chosen for 30 sec. Mice were then returned to the maze base to start the subsequent trial. Eight total trials were carried out with 7 possible alternations, and the alternation percentage was calculated as 100x (number of alternations/7). The time taken to make the alter- nation decision was recorded as well.

Self-Grooming Behavioral Assay

Mice were placed in an empty cage for 20 min. They were first allowed to acclimate to the environment for 10 min and then were monitored for grooming activity for the last 10 min. Time spent grooming over the 10 min was recorded. Videos were recorded, and grooming was manually scored for grooming activities such as licking, face swiping, scratching, or nibbling. Each video was scored by three persons blinded to the animal genotype, and the average of the scores was recorded.

Social Interaction and Social Novelty

The 3-chamber box used for these assays is a rectangular plexiglass box consisting of a left, middle, and right chamber with removable doors, which separate the chambers. Empty mesh wire cups were placed in the middle of both the left and right chambers. In the social interaction assay, mice were allotted 5 min to explore the middle chamber. After 5 min, a control mouse of the same gender, age, and strain as the experimental mouse was placed inside one of the cups in either the right or left chamber. The doors were then removed, allowing the experimental mice to explore all three chambers for 10 min. The total time experimental mice spent inter- acting with both the empty cup and the control mouse cup was recorded.

Immediately following the social interaction assay, the social novelty assay began. The experimental mouse was returned to the middle chamber, and a new control mouse was placed underneath the empty cup. Doors were removed, and the experimental mouse was allotted 10 min to explore all three chambers. The total time experimental mice spent interacting with the mouse from the social interaction assay and the novel mouse was recorded. ANY-maze software (Stoelting, Wood Dale, IL, USA) was used to record and analyze these interactions.

Novel Object Recognition

Novel object recognition (NOR) consists of a training and testing phase. All mice were handled for 1–2 min a day for 3 days prior to the training phase. Mice were then allowed to habituate to the experimental apparatus, a rectangular box for 3 consecutive days without the presence of objects. During the training phase, mice were exposed to two identical objects in the apparatus and allowed to explore for 10 min. After 24 h, mice were subjected to the testing phase, where they were allotted 5 min to explore the apparatus with the familiar object and a novel object. The total time each subject mouse spent interacting with both the familiar and novel object was recorded individually. ANY-maze software (Stoelting, Wood Dale, IL, USA) was used to document and analyze these interactions.

Novel Location Recognition

Novel location recognition (NLR) consists of the training and testing phase. All mice were handled for 1–2 min a day for 3 days prior to the training phase. Mice were then allowed to habituate to the experimental apparatus, a rectangular box for 3 consecutive days without the presence of objects. During the training phase, mice were exposed to two identical objects in the apparatus and allowed to explore for 10 min. After 24 h, mice were subjected to the testing phase, where one location of the object is moved. Mice were allotted 5 min to explore the apparatus with the familiar location and a novel location. The total time each subject mouse spent interacting with both the familiar and novel location was recorded individually. ANY-maze software (Stoelting, Wood Dale, IL, USA) was used to document and analyze these interactions.

Forced Swim

Mice were placed in a cylinder containing water at 25 °C for 6 min. Mice were recorded, and following the assay, the last 4 min were scored and analyzed. The immobility time or time the mice spent floating was recorded. ANY- maze software was used to record and analyze immobility time (Stoelting Co.).

Prepulse Inhibition

Mice were habituated to the startle chambers for 5 min with 65 dB of background noise. The PPI sessions consisted of 5 trials, either no stimulus (65 dB), 3 prepulse (20-ms pre- pulse at 68 dB, 71 dB, or 77 dB, a 100-ms interstimulus interval, followed by a 40-ms duration startle stimulus at 120 dB. The amount of prepulse inhibition was calculated as a percentage score for each acoustic prepulse intensity: % PPI = 100 - ([(startle response for prepulse + pulse trials) / (startle response for pulse − alone trials)] X 100).

Hot Plate

Mice were habituated to the hot plate with no heat to establish a baseline. Following the habituation, mice were subjected to a 52 °C hot plate, and were monitored for an initial response of either a rear paw lift, paw shake, or paw lick in response to the heat or once the cutoff time was reached. Once the initial response was seen, the time was recorded, and animals were returned to their home cage.

Contextual Fear Conditioning

This assay consists of a training and a testing session 24 h following the training session. On day 1, mice were placed in the conditioning chamber for 3 min, received a 2-s 0.7 mA foot shock at 2.5 min, and were placed back into their home cage on day 2, animals were returned to the same chamber for 5 min without shock. Freezing behavior was measured pre- and post-shock sessions and was scored as freezing (1) or not (0) within a 5-s interval and calculated as 100x (the number of intervals of freezing / total intervals).

Immunohistochemistry

Ninety minutes after the fear conditioning assay, mice were anesthetized with isoflurane and transcardially perfused with saline and 4% paraformaldehyde (PFA). Brains were harvested, kept in PFA overnight, and switched to 30% sucrose. Brains were coronally sectioned at 20 μm using a microtome. Using the Allen Brain Atlas, 3–4 sections were selected from specific regions of interest. Sections were blocked with goat serum in PBS with 0.3% Triton X-100 for 1 h. Next, brain sections were incubated in blocking buffer with the primary antibody, either cFos, 1:500 (Abcam cFos ab190289 Rb pAb to cFos Lot#: GR339395) or ADCY3, 1:500 (LSBIO-C204505 ADCY3 Lot#: 193037). Following the primary antibody incubation, sections were washed with PBS and then incubated with the secondary antibody, 1:500 (Invitrogen AlexaFluor546 goat anti-rabbit ref: A101035 Lot: 2,273,730), and DAPI, 1:10,000 (Thermo Scientific Ref: 62,248 Lot: WF3296471). Sections were washed with PBS and mounted on slides. Images were carried out using the Leica SP8 confocal microscope with a 63 × objective lens (UCI optical biology core facility) for visualizing cilia, and Keyence BZ-9000 microscope with a 10x objective lens for visualizing cFos positive neurons.

Image Analysis

cFos positive neurons and ADCY3 were counted bilaterally, and the mean of the three sections per 4–6 brains was calculated. All image analysis and cell counts were performed in Fiji (ImageJ). Automatic particle quantification and analysis methods were used for counting cFos labeled neurons. Briefly, images were opened in Fiji, and color channels were split into the appropriate color. Color images were then converted to grayscale. All regions were defined with specific dimensions across all images for cohesiveness. Once in gray- scale, a threshold was set to highlight fluorescent particles and create a binary image. The "analyze particle" function was used to select the size of particles and set the circularity of the particles. Cilia length was measured using the line measurement tools in Fiji, and the length unit was converted from pixels to micron.

Statistical Analysis

GraphPad Prism (GraphPad Software, Inc.) was employed to perform statistical analysis. Data were presented as means ± S.E.M. Results were analyzed using student *t*-test or ANOVA followed by the appropriate post hoc comparisons, and $P < 0.05$ was considered statistically significant.

Results

Selective Deletion of Cilia in the Striatum

To examine the physiological role of primary cilia in the striatum, we used the conditional deletion system and disrupted intraflagellar transport (IFT) machinery by deleting the Ift88 gene. Stereotactic infusion of IFT88fl/fl mice with AAV.CamKII.HI.GFP-Cre into the striatum (Bregma level 1.3 mm, ± 1.3 mm, 3.2 mm) resulted in mice with primary cilia deficiency exclusively in the dorsal part of the rostral striatum (Fig. 5.1b).

Cilia deletion from the dorsal-rostral striatum did not affect the number of striatal neurons, indicating that the dorsal-rostral striatum of IFT88-KO mice is intact, and the neurons were viable. Next, we performed a coexpression analysis of primary cilia with GFP-Cre via immunohistochemistry, using an antibody against ADCY3, a well-known marker of primary cilia. While the numbers of neurons expressing primary cilia and the cilia length were comparable in caudal striatum and nucleus accumbens between the control and IFT88-KO mice, these numbers were markedly reduced in the dorsal-rostral striatum of IFT88-KO mice (Fig. 5.1c–j). Furthermore, comparable body weights and normal response to nociceptive stimulus (hot plate) confirmed that the IFT88-KO mice have normal gross growth and well-being (Fig. 5.1k, l).

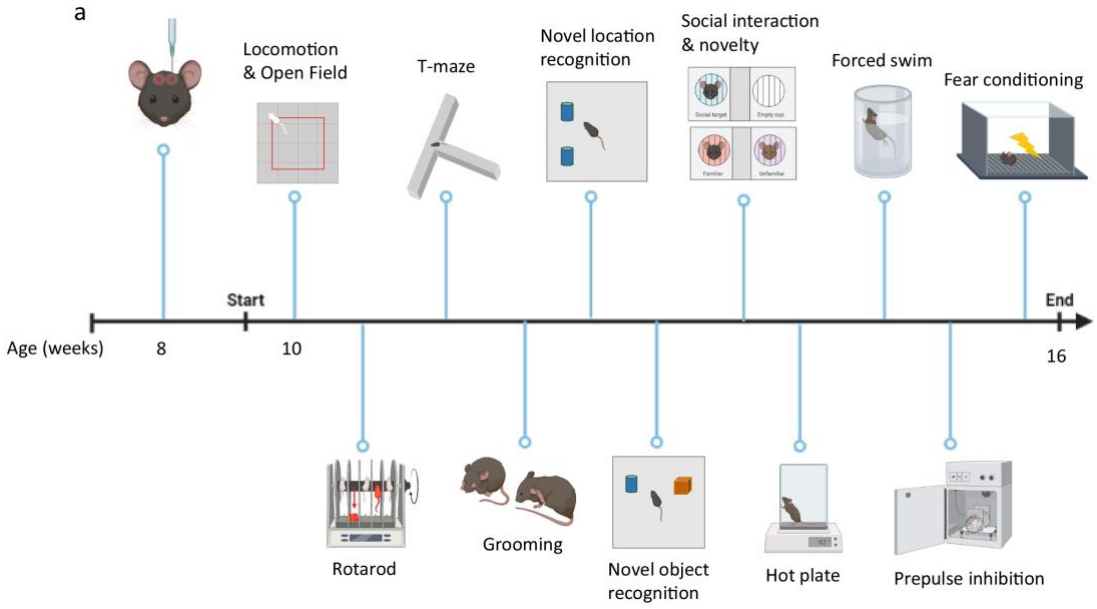

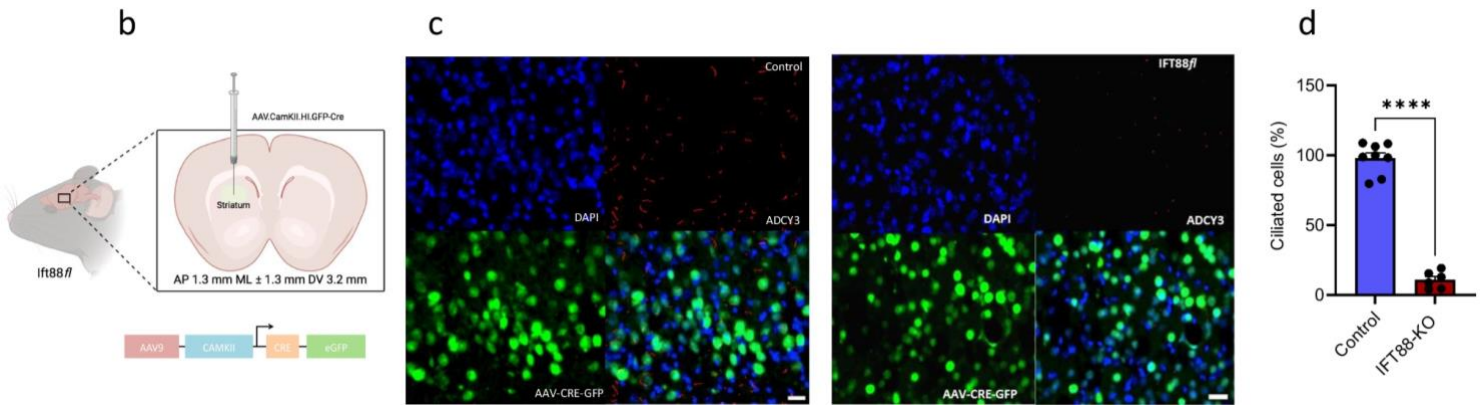

Figure 5.1. Selective cilia deletion in the striatum and confirmation of mice's normal gross growth and well-being.

a Schematic view of experimental design and behavior assays performed and their sequence. Diagram was created with the BioRender.com webpage. **b** Schematic showing bilateral viral injection into the dorsal striatum. **c** and **d** Verification of cilia removal in ciliated neurons of the striatum using immunostaining of ADCY3. Scale bar = 10 µm. **c** Representative images of ADCY3 immunostaining showing the intact cilia in the control mice and the conditional ablation of cilia in the dorsal striatum neurons of *Ift88*^{fl} mice (counterstained with DAPI, blue); **d** Quantification of the ciliated cells in the rostral-dorsal striatum ($n = 8$ control, 6 IFT88-KO). Unpaired *t*-test ($t = 17.26$, $P < 0.0001$) ****$P < 0.0001$. Data are presented as means ± S.E.M. Scale bar = 10 µm. **e–g** ADCY3 immunostaining in the caudal striatum. **e** Representative images of ADCY3 immunostaining in the caudal striatum showing that the selective removal of cilia from the dorsal rostral striatum does not affect **f** the number of ciliated cells ($t = 0.30$, $P > 0.05$) or **g** the cilia length ($t = 0.30$, $P > 0.05$, $n = 4$) in the caudal striatum. Scale bar = 10 µm. **h–j** ADCY3 immunostaining in the ventral striatum (nucleus accumbens). **h** Representative images of ADCY3 immunostaining in the ventral striatum showing that the selective removal of cilia from the rostral striatum does not affect **i** the number of ciliated neurons ($t = 0.52$, $P > 0.05$) or **j** the cilia length ($t = 0.08$, $P > 0.05$, $n = 4$) in the ventral striatum. Scale bar = 10 µm. **k** Effect of cilia removal on

body weight to confirm normal gross growth ($n = 8$ control, 6 IFT88-KO). Unpaired *t*-test ($t = 0.2463$, $P = 0.8096$) revealed no significant difference in body weight. ns, not significant. Data are presented as means ± S.E.M. **I** Verification of well-being ($n = 8$ control, 6 IFT88-KO). Unpaired *t*-test ($t = 0.2060$, $P = 0.8403$) showed normal response to nociceptive stimulus. ns, not significant. Data are presented as means ± S.E.M

Primary Cilia in the Striatum Are Required to Maintain Normal Motor Coordination But Not the Spontaneous Motor Activity

Although the striatum is identified as a brain site for motor control timing, it is unknown whether striatum primary cilia play a role in regulating motor functions. To address this question, spontaneous motor activity and motor coordination were monitored in IFT88-KO mice. After the habituation period, IFT88-KO mice displayed similar locomotor activity to the control mice, measured by distance traveled (Fig. 5.2a, b). However, the locomotor activity in the first 10 min after placing mice into the open box was significantly lower in the IFT88-KO than in the control mice. In addition, IFT88-KO mice showed a reduced latency to fall and a lower rotation speed at which they fall in the rotarod test (Fig. 5.2c, d), indicating an impairment of motor coordination in the IFT88- KO mice. This may also be interpreted as impairment of procedural learning as trial 1 shows IFT88-KO mice just as coordinated as the control mice.

Ablation of Primary Cilia in the Striatum Increases Repetitive Behavior and Impairs Sensorimotor Gating

The IFT88-KO mice showed a higher level of compulsive grooming than the control mice (Fig. 5.2e), indicating an enhanced compulsive, repetitive behavior in these animals. Grooming was measured as the time mice spent face swiping, paw licking, rubbing of the head and ears, and cleaning the entire body. IFT88-KO mice also exhibited reduced values of prepulse inhibition of the startle reaction at 71 dB and 77 dB prepulses, as well as the average prepulse, although the startle reactions were comparable to those in the control mice (Fig. 5.2f, g). The average PPI

value was also lower in IFT88-KO mice than the control ones. These results indicate that ablation of cilia in the striatum causes a deficit in sensorimotor gating without affecting the startle reaction.

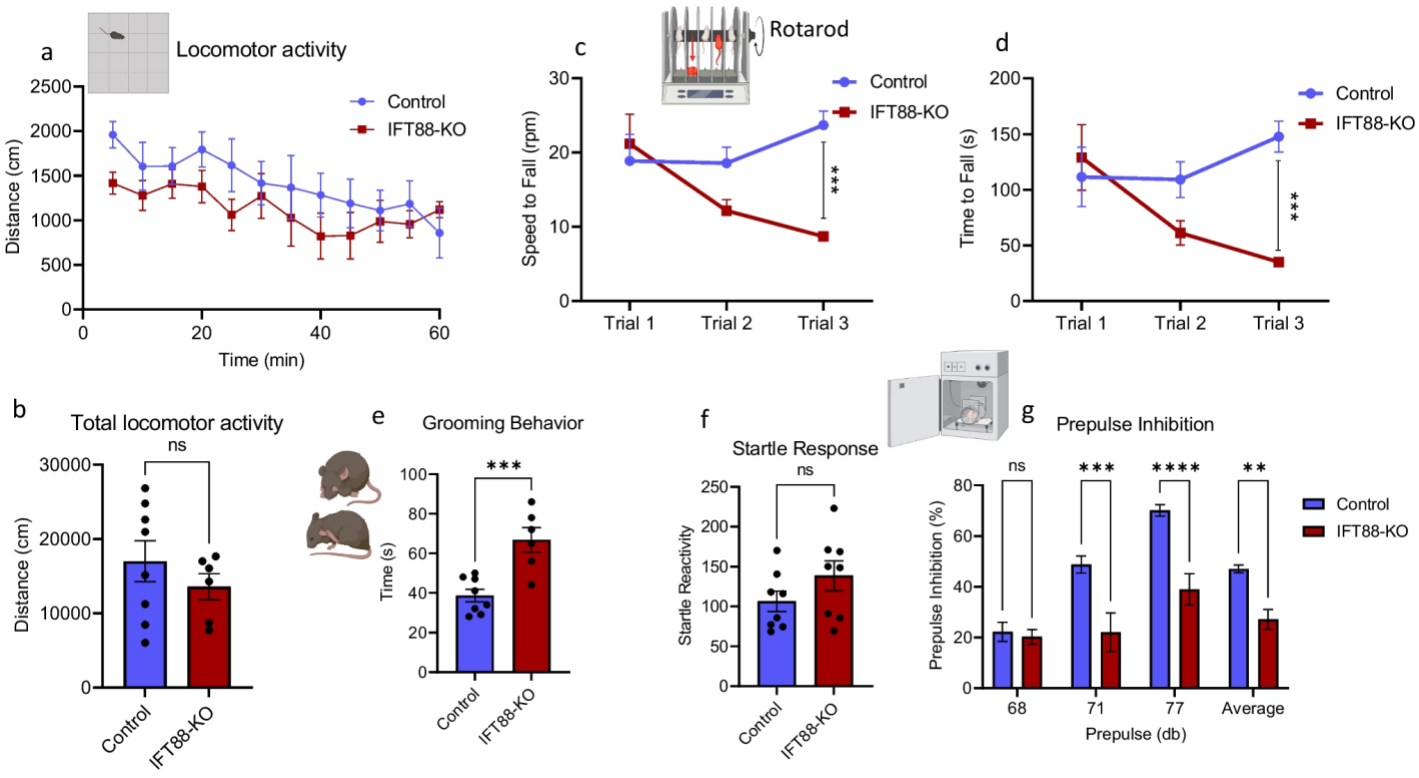

Figure 5.2. Primary cilia ablation in the striatum affects motor and sensorimotor-related behaviors.

a Distance traveled in the last 60 min of the locomotor assay ($n = 8$ control, 6 IFT88-KO). Two-way ANOVA ($F_{(11,\ 144)} = 0.4143$, $P > 0.05$) followed by Bonferroni's post hoc test showed that IFT88-KO mice displayed similar locomotor activity to the control mice; ns, not significant. **b** Total locomotor activity in the locomotor assay. Unpaired *t*-test ($t = 0.9608$, $P = 0.3556$), ns, not significant. Data are presented as means ± S.E.M. **c** and **d**Motor skill learning on the accelerated rotarod. **c** Speed to fall in rotarod assay ($n = 8$). Two-way ANOVA (cilia removal factor: $F_{(1,42)} = 9.399$, $P = 0.0038$, trial factor $F_{(2,42)} = 1.927$, $P > 0.05$) followed by Bonferroni post hoc test: IFT88-KO vs control, $^{**}P < 0.001$. Data are presented as means ± S.E.M; **d** Latency to fall in rotarod assay ($n = 8$). Two-way ANOVA (cilia removal factor: $F_{(1,42)} = 9.246$, $P = 0.0041$, trial factor:

$F_{(2,42)} = 1.93$, $P > 0.05$) followed by Bonferroni post hoc test: IFT88-KO vs control, ***$P < 0.001$. Data are presented as means ± S.E.M. **e** Repetitive behavior in grooming behavior assays ($n = 8$ control, 6 IFT88-KO), unpaired *t*-test ($t = 4.357$, $P = 0.0009$), IFT88-KO vs control. Data are presented as means ± S.E.M. **f** and **g** Performance of mice in PPI assay. **f** Startle reactivity in prepulse inhibition assay ($n = 8$), unpaired *t*-test ($t = 1.424$, $P = 0.1763$), ns, not significant. **g**Prepulse inhibition in PPI assay ($n = 8$), two-way ANOVA (cilia removal factor: $F_{(1,56)} = 41.69$, $P < 0.0001$, prepulse intensity factor: $F_{(3,56)} = 19.55$, $P < 0.0001$), control vs IFT88-KO, **$P < 0.01$, ***$P < 0.001$, ****$P < 0.0001$. Data are presented as means ± S.E.M

Primary Cilia in the Striatum Are Not Involved in Anxiety, Sociability, and Depressive-Like Behaviors

To test whether cilia ablation affects anxiety-like behavior, we used open field assay, which is based on the assumption that mice placed in a new environment tend to avoid open space and, therefore, spend more time in the peripheral than central arenas. Cilia ablation did not affect anxiety-like behavior, revealed by the longer times spent in the peripheral than central arenas in IFT88-KO mice, which were comparable to those in the control mice (Fig. 5.3a). Although the total distance and the distance traveled in the peripheral zone were significantly lower in the IFT88-KO mice than the control mice (Fig. 5.3b, c), this does not indicate an altered anxiety-related behavior; rather, it reflects a slower response to the new environment. The immobility time in the forced swim test, which measures helplessness behavior, was similar in the control and IFT88-KO mice (Fig. 5.3d). Furthermore, IFT88-KO mice showed normal social behavior, revealed by spending significantly more time with a stranger mouse than an empty cup (Fig. 5.3e, f). These results indicate that cilia ablation in the striatum does not affect anxiety, sociability, and depressive-like behavior.

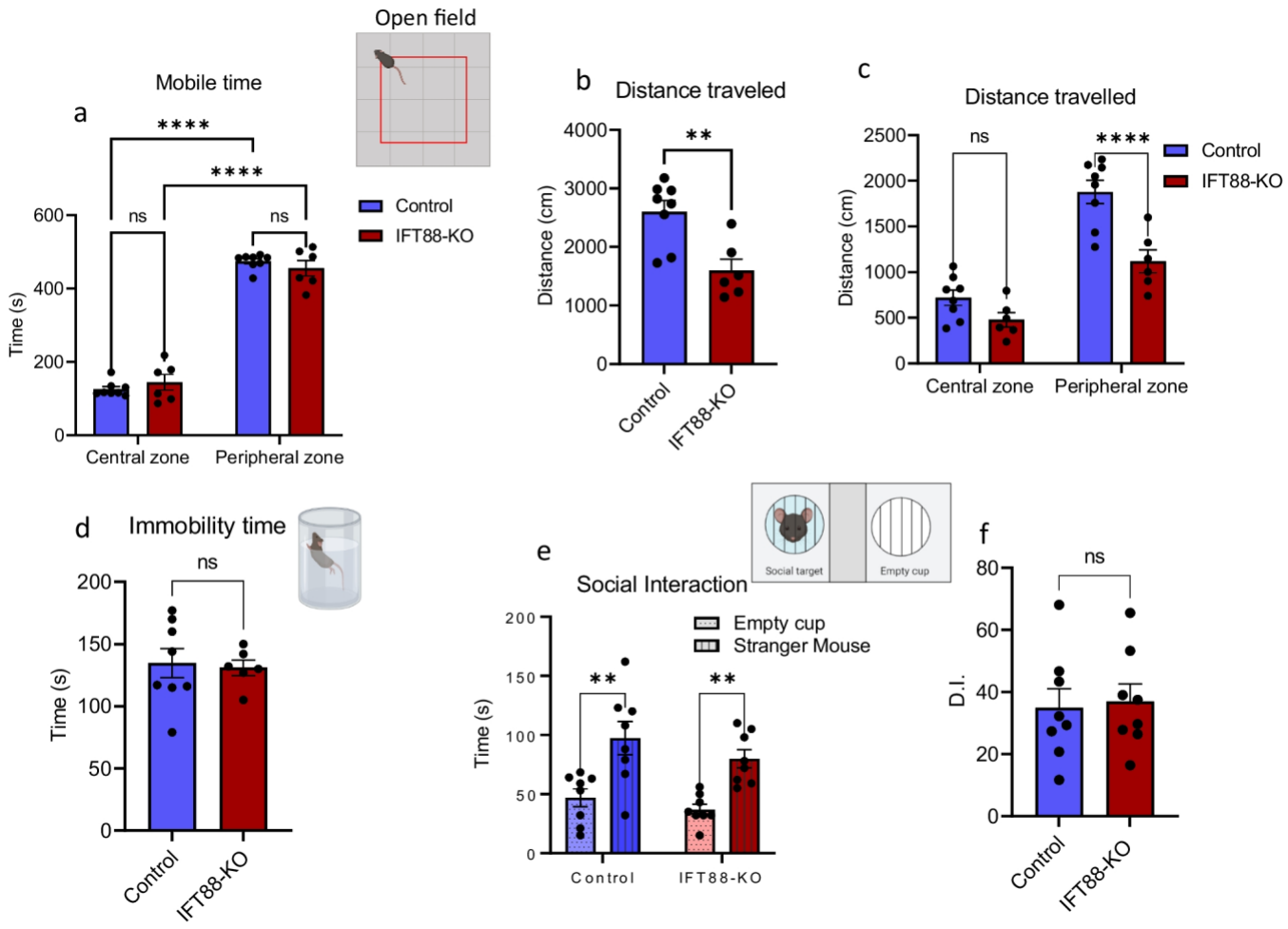

Figure 5.3. Primary cilia removal in the dorsal striatum does not affect anxiety, sociability, and depressive-like behaviors.

a Time spent in central vs time in peripheral zones in open field assay ($n = 8$ control, 6 IFT88-KO), two-way ANOVA (cilia removal factor: $F_{(1,24)} = 0.00$, $P > 0.999$, zone factor: $F_{(1,24)} = 538.1$, $P < 0.0001$) followed by Bonferroni post hoc test. ****$P < 0.0001$. Data are presented as means ± S.E.M. b Total distance traveled in open field assay, unpaired *t*-test ($t = 3.598$, $P = 0.0037$), IFT88-KO vs control, **$P < 0.01$. Data are presented as means ± S.E.M. c Distance traveled in central vs time in peripheral zones in open field assay ($n = 8$ control, 6 IFT88-KO), two-way ANOVA (cilia removal factor: $F_{(1,24)} = 21.1$, $P = 0.0001$, zone factor: $F_{(1,24)} = 68.31$, $P < 0.0001$), followed by Bonferroni post hoc test, ****$P < 0.0001$. e Social

interaction ($n = 8$), two-way ANOVA (cup factor: $F_{(1,28)} = 26.25$, $P < 0.0001$, cilia removal factor: $F_{(1,28)} = 2.28$, $P = 0.1420$); Empty cup vs stranger mouse, $^{**}P < 0.0001$. Data are presented as means ± S.E.M. f Social interaction discrimination index, unpaired *t*-test ($t = 0.2422$, $P = 0.8121$), control vs IFT88-KO, ns, not significant. Data are presented as means ± S.E.M

Primary Cilia in the Striatum Are Required for Spatial Working Memory But Not Other Memory Types

We examined the effects of cilia ablation in the striatum on different types of memories, including spatial working memory, social recognition memory, object recognition memory, spatial memory (location recognition), and con- textual memory. Spatial working memory was tested in the T-maze paradigm, which is based on the mice' tendency to repeatedly alternate between the right and left arms in order to optimize their navigation of their environment [80]. The short-term social memory (social recognition) was tested using the three-chamber assay, which is based on the instinctive tendency of mice to investigate and spend more time with unfamiliar social subjects (strange mouse) than familiar ones [81]. Long-term memory formation involves encoding, short-term memory consolidation (storage), and long-term memory reconsolidation and retrieval [82] and is usually tested in mice 24 h after conditioning [71].

The spatial working memory was significantly impaired in the IFT88-KO mice, revealed by the higher incorrect choices in these mice than in the control mice (Fig. 5.4a). Associated with working memory impairment in IFT88-KO, the latency for decision-making was significantly longer in these mice compared with the control mice (Fig. 5.4b). Interestingly, while the ablation of primary cilia in the striatum did not affect social behavior, it caused an impairment in social recognition memory (Fig. 5.4c, d), as reflected by the similar time IFT88-KO mice spent with the old and new stranger mice.

Ablation of primary cilia in the striatum did not affect the object recognition memory, as evidenced by the more time mice spent with the novel object than the old object (Fig. 5.4e, f).

Similarly, in the novel location recognition assay, IFT88- KO spent more time with the novel location than the old location (Fig. 5.4g, h), indicating a normal spatial memory. In addition, the contextual memory, measured using the fear conditioning test, was intact in the IFT88-KO mice, as revealed by the similar freezing time on the test day compared with the control mice (Fig. 5.4i).

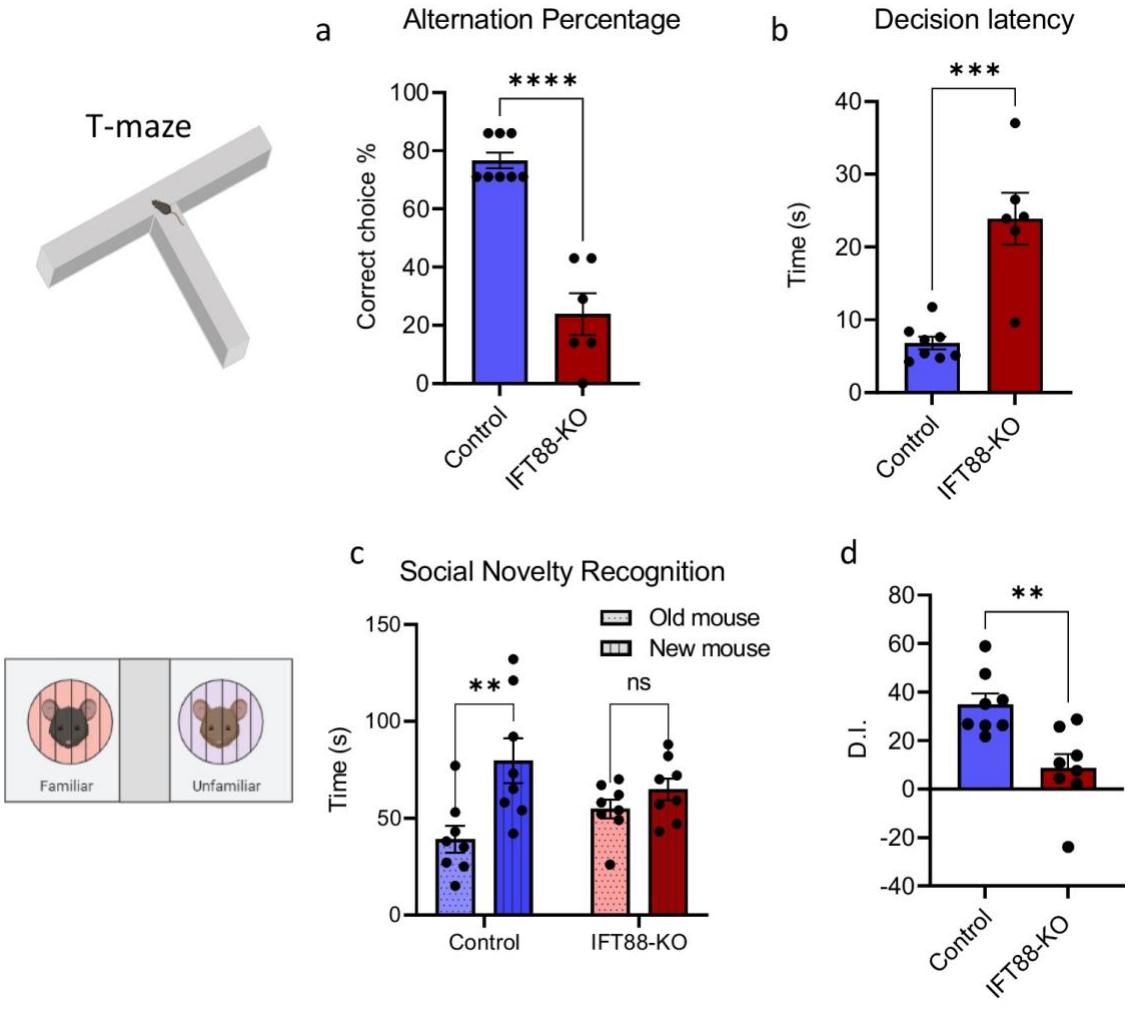

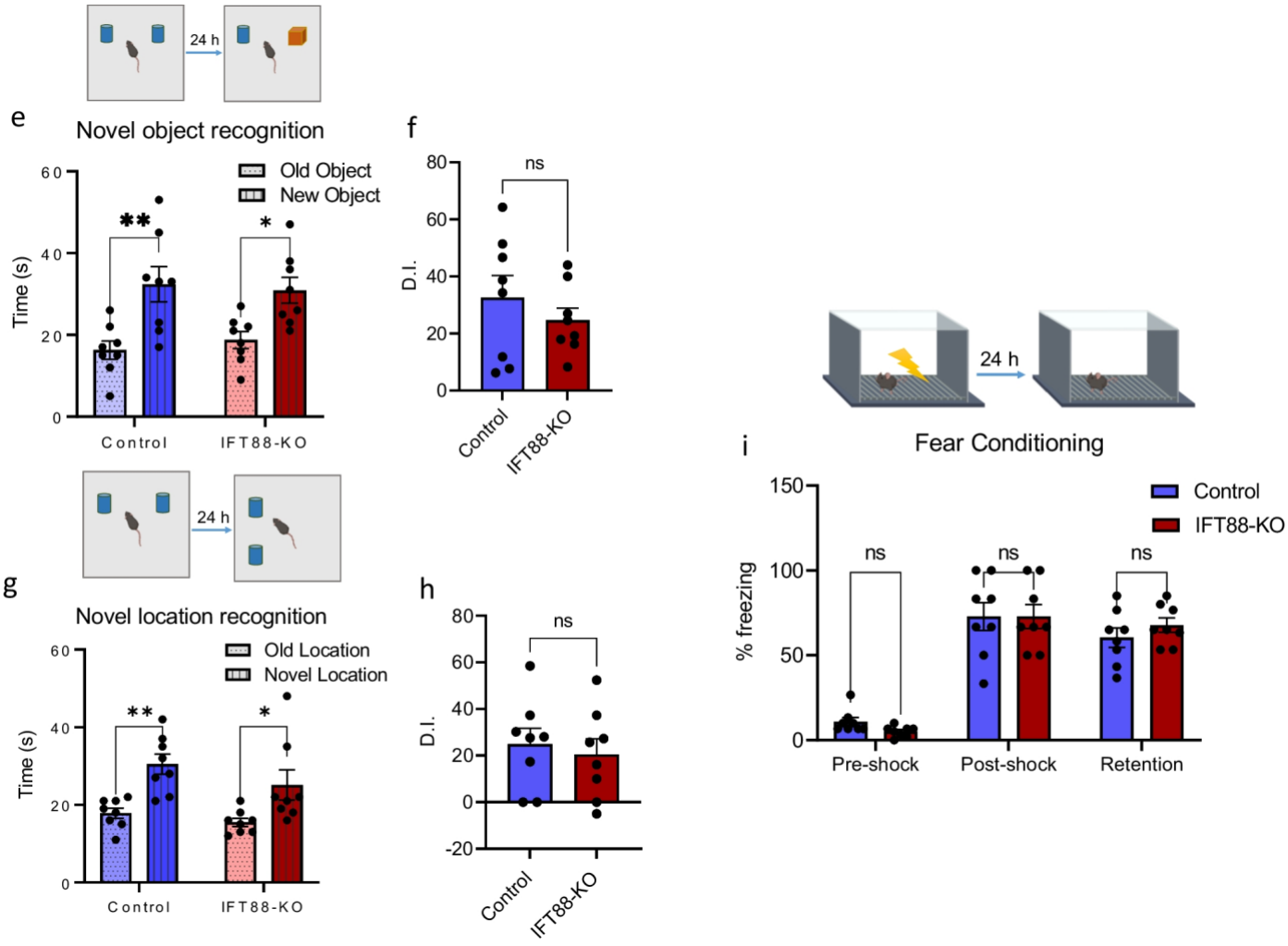

Figure 5.4. Primary cilia in the striatum are required for spatial working memory but not other memories.

a Spatial working memory alteration percentage in T-maze ($n = 8$ control, 6 IFT88-KO), unpaired t-test ($t = 7.679$, $P < 0.0001$), control vs IFT88-KO, ****$P < 0.0001$, bDecision latency in T-maze test ($n = 8$ control, 6 IFT88-KO), unpaired t-test ($t = 5.295$, $P = 0.0002$), control vs IFT88-KO, ***$P < 0.001$, c social novelty recognition ($n = 8$), two-way ANOVA (cilia removal factor: $F_{(1,28)} = 10.90$, $P = 0.0026$, novel mouse factor: ($F_{(1,28)}$, $P = 0.9612$), followed by Bonferroni post hoc test: old mouse vs new mouse, **$P < 001$, ns, not significant. Data are presented as means ± S.E.M. d Discrimination index in social novelty recognition ($n = 8$), unpaired t-test ($t = 3.604$, $P = 0.0029$), control vs IFT88-KO, **$P < 0.01$. e Novel object recognition ($n = 8$), two-

way ANOVA (object factor: $F_{(1,28)} = 21.24$, $P < 0.0001$, cilia removal factor: $F_{(1,28)} = 0.02662$, $P = 0.8716$): old object vs new object: *$P < 0.05$, **$P < 0.01$. Data are presented as means ± S.E.M. f Discrimination index in novel object recognition ($n = 8$), unpaired *t*-test ($t = 0.90$, $P = 0.38$), control vs IFT88-KO, ns, not significant. Data are presented as means ± S.E.M. g Novel location recognition ($n = 8$), two-way ANOVA (object factor: $F_{(1,28)} = 20.30$, $P < 0.0001$, cilia removal factor: $F_{(1,28)} = 0.2.46$, $P = 0.8716$): *$P < 0.05$, **$P < 0.01$. h Discrimination index in novel location recognition ($n = 8$), unpaired *t*-test ($t = 0.46$, $P = 0.65$), control vs IFT88-KO, ns, not significant. i Fear conditioning ($n = 8$), two-way ANOVA ($P > 0.05$) followed by Bonferroni post hoc test: control vs. IFT88-KO. ns, not significant. Data are presented as means ± S.E.M

Neural Activity Is Changed in Striatal Input and Output Nuclei Pathways

The expression of the immediate-early gene cFos was used as a molecular marker of neural activity. We examined cFos immunoreactivity (number of cFos-positive cells) in structures that are parts of striatal circuits and those known to project to or receive projections from the striatum (Fig. 5.5a, b). First, the rostral dorsal striatum, but not the caudal striatum of IFT88-KO mice, exhibited a significant decrease of cFos immunoreactivity (Fig. 5.5c, d). Within the basal ganglia circuit, there was a trend for cFos immunoreactivity reductions in the output regions (SNr and the GPm), but not in the nuclei of the indirect pathway structures (lateral globus pallidus and subthalamic nucleus) (Fig. 5.5c, d). The main input regions to the striatum include the dopaminergic neurons of the substantia nigra pars compact (SNc) and the glutamatergic neurons of the cortices. While IFT88-KO mice exhibited significant decreases in cFos immunoreactivity in several cortices, including the prefrontal cortex, primary motor area, secondary motor area, and somatosensory area, there was a trend for cFos decrease in the SNc, albeit not significant (Fig. 5.5c, d).

a

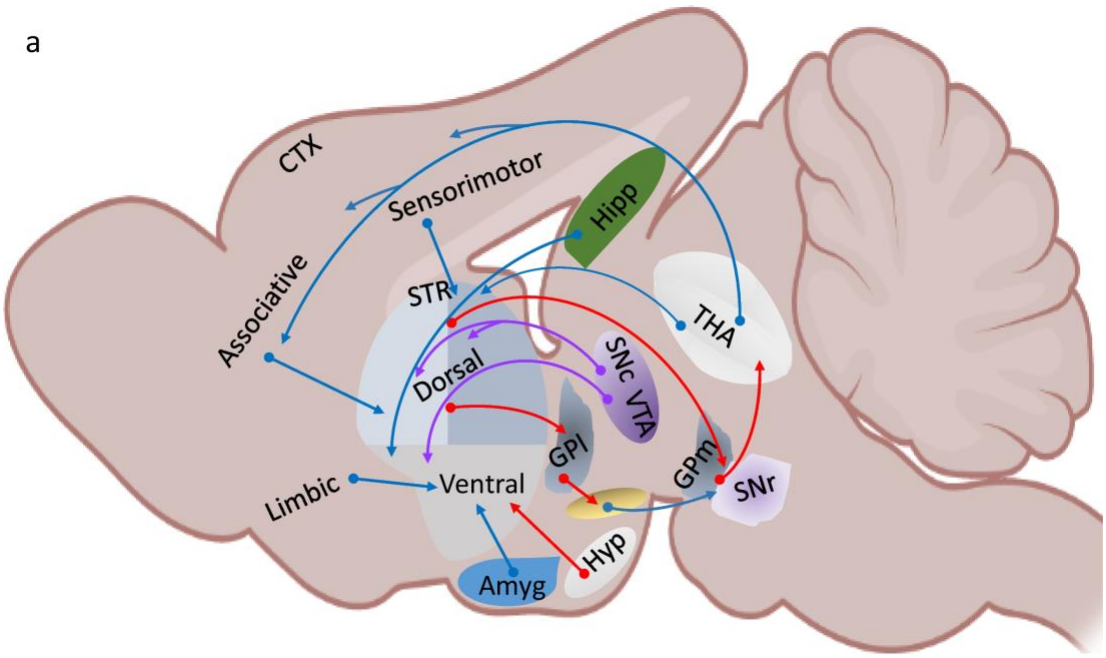
CTX
Sensorimotor
Associative
Hipp
STR
THA
Dorsal
SNc VTA
GPl
GPm
SNr
Limbic
Ventral
Hyp
Amyg

b

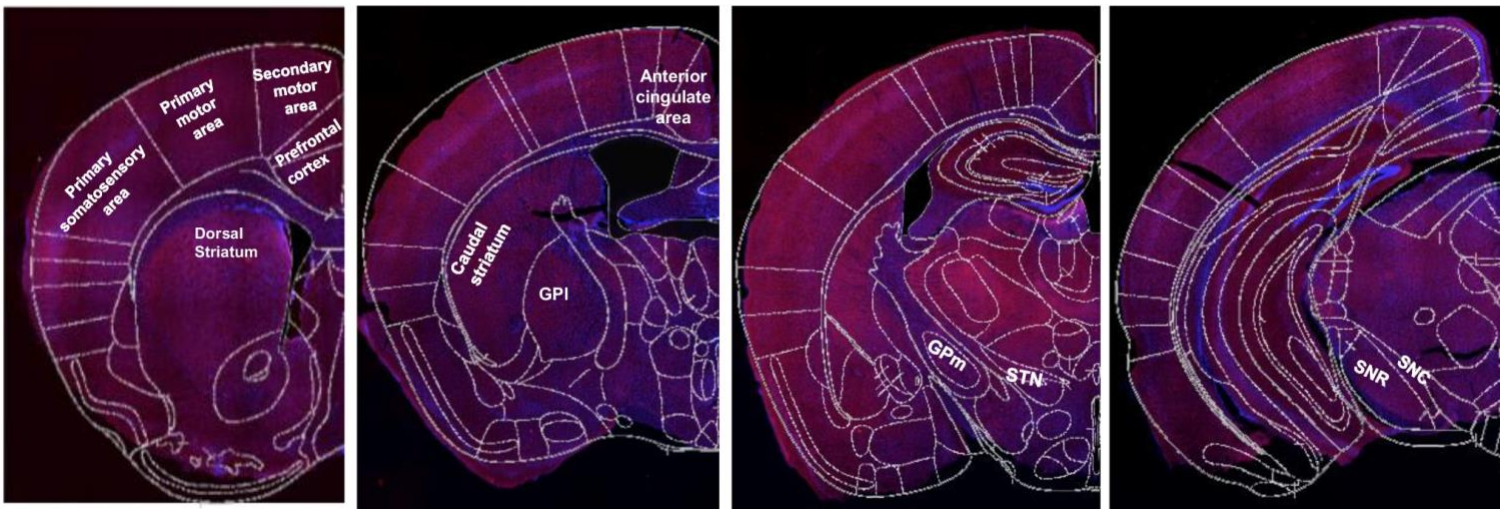
Primary somatosensory area
Primary motor area
Secondary motor area
Prefrontal cortex
Dorsal Striatum
Anterior cingulate area
Caudal striatum
GPl
GPm
STN
SNR
SNC

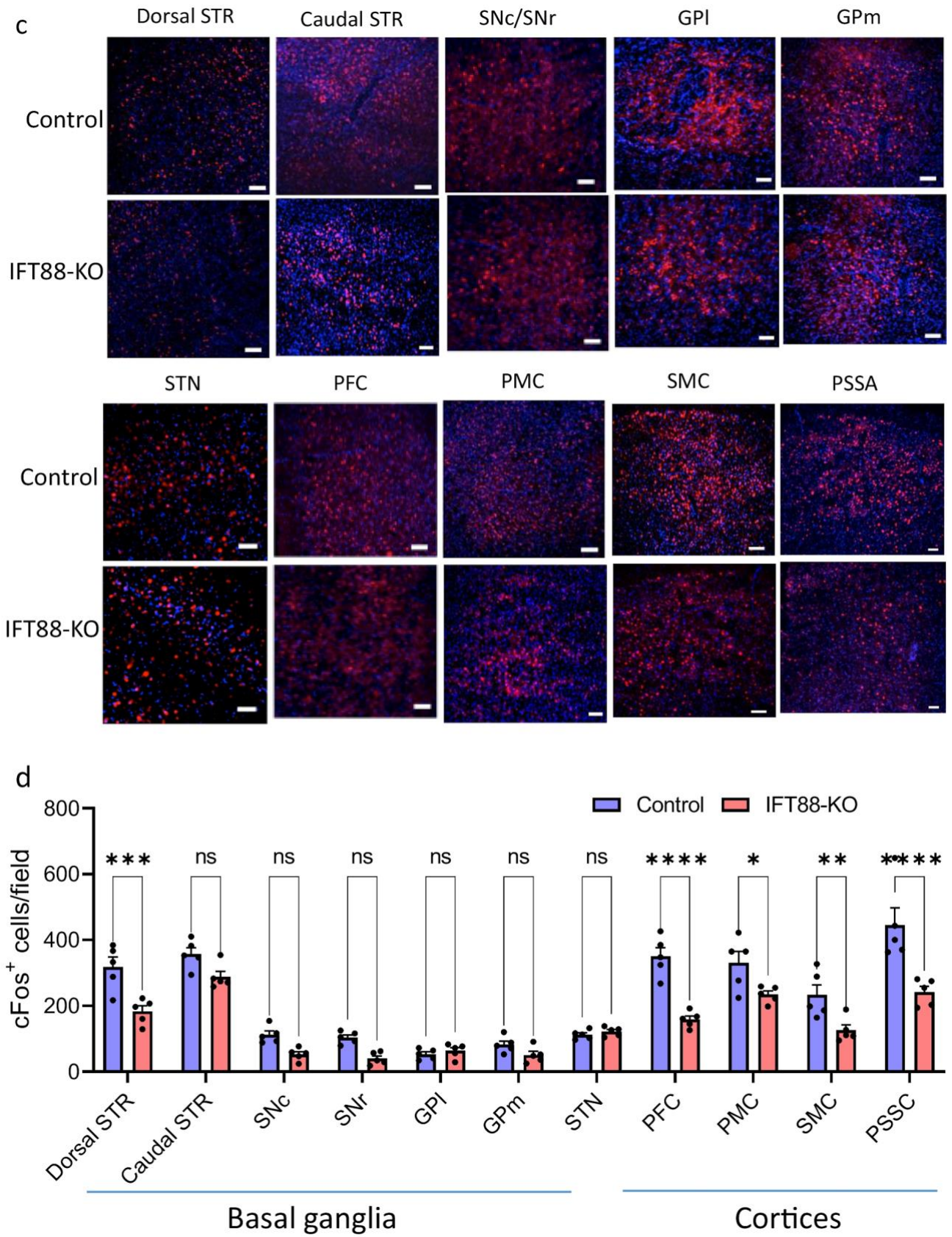
c
Dorsal STR
Caudal STR
SNc/SNr
GPl
GPm
Control
IFT88-KO
STN
PFC
PMC
SMC
PSSA
Control
IFT88-KO
d
Control
IFT88-KO
cFos+ cells/field
800
600
400
200
0
***
ns
ns
ns
ns
ns
ns
****
*
**
****
Dorsal STR
Caudal STR
SNc
SNr
GPl
GPm
STN
PFC
PMC
SMC
PSSC
Basal ganglia
Cortices

Figure 5.5. Effects of cilia removal in the dorsal striatum on cFos expression in the striatum, its input and output structures.

a Schematic view of neuronal circuits in mice brain. Amy, amygdala; CTX, cortex; GPL, lateral globus pallidus; GPm, medial globus pallidus; Hipp, hippocampus; Hyp, hypothalamus; SNc, substantia nigra pars compacta; SNr, substantia nigra pars reticulata; STN, subthalamic nucleus; STR, striatum; THA, thalamus; VTN, ventral tegmental area. Diagram was created with the BioRender.com webpage. bcFos immunostaining in four levels of the mouse brain. c Representative images of cFos immunostaining in the striatum and its input and output structures: striatum (STR), substantia nigra pars compacta (SNc), substantia nigra pars reticulata (SNr), lateral globus pallidus (GPl), medial globus pallidus (GPm), subthalamic nucleus (STN), prefrontal cortex (PFC), primary motor cortex (PMC), secondary motor cortex (SMC), primary somatosensory area (PSSA). Scale bar = 10 μm. d Quantification of the cFos-positive cells in the control and IFT88-KO mice. Two-way ANOVA, control vs IFT88-KO ($F_{(1,88)} = 94.28$, $P < 0.0001$), *$P < 0.05$, **$P < 0.01$, ***$P < 0.001$, ****$P < 0.0001$, ns, not significant. Data are presented as means ± S.E.M; $n = 3$ sections of 5 mice per group

Discussion

In this study, we examined the role of cilia in the striatum using a selective conditional deletion system. Our data provide the first evidence for the essential role of striatal primary cilia in specific functions of the striatum, namely, sensorimotor and executive functions.

Methodological Considerations

To examine whether striatal cilia mediate some of the striatum functional domains, we used loxP/Cre technology to selectively delete IFT88, an essential protein for cilia genesis, from the dorsal striatum. The deletion of IFT88 resulted in cilia ablation in the dorsal striatum, as evidenced by the profound decrease in ADCY3-immunostaining. We monitored the behavioral phenotypes resulting from

striatal cilia ablation, focusing on neuropsychiatric phenotypes related to three striatum functional domains: the sensorimotor, associative, and limbic domains. The sensorimotor domain is essential for habitual behaviors that are automatically evoked, whereas the associative (cognitive) domain is responsible for driving consciously formed actions and goal- directed behaviors. The dorsal striatum mediates these two functional domains, whereas the limbic domain, associated with motivational and affective behaviors, is sited in the ventral striatum (nucleus accumbens in rodents) [83–88].

Cilia in the Dorsal Striatum Are Necessary for Sensorimotor Learning and Execution of Goal-Directed Behaviors, But Not Affective Behaviors

Cilia ablation from the dorsal striatum did not affect spontaneous motor in mice, evidenced by the normal locomotor activity in the IFT88-KO mice. However, motor activity was lower in IFT88-KO directly after placing them into the open field apparatus, indicating that their reactions to a new environment are diminished. Interestingly, the performance of cilia-ablated mice in the first trial of the rotarod assay was comparable to that of the control mice, indicating that cilia-ablated mice can walk normally on the rotarod. In contrast to the control group, however, in the second and third trials, cilia-ablated mice' performance not only did not improve but also

worsened. The proper performance in rotarod assay reflects motor coordination and learning, which are dependent on striatal function in processing and integrating new sensory information and coordinating the time sequence of motor response [89–92]. Our findings indicate an essential role for striatal cilia in acquiring new motor skills learning, but not in maintaining habitual or already learned motor skills. While we cannot make a concrete conclusion on whether this function of cilia is mediated through processing and integrating new sensory information or by coordinating the time sequence of motor response, we speculate that cilia might be involved in both mechanisms.

In support of this assumption, we found that cilia ablation in the striatum impaired sensorimotor gating, as revealed by the reduced PPI levels [93]. Sensorimotor gating, a largely striatum-thalamus-dependent phenomenon, represents the ability of the brain to respond to a sensory stimulus by sup- pressing a motor response. Through this mechanism, the brain filters irrelevant sensory information input, prior processing and transmitting to motor output systems. The PPI deficits in cilia-ablated mice further support an essential role for cilia in the sensorimotor integration process and motor executing actions.

The role of cilia in sensorimotor functions is further evidenced by our finding that cilia-ablated mice exhibited excessive repetitive behavior, revealed by increased self-grooming. Repetitive behaviors result from excessive automatized actions or exaggerations of habitual behaviors, for which the dorsal striatum plays an essential role [94–96]. Our results, thus, indicate that these actions of the dorsolateral striatum are mediated through its primary cilia. One important question posed by our findings is whether the failure of acquiring new motor skills in cilia-ablated mice is causally correlated with their enhanced repetitive behavior. Robust evidence, lending a premise to this posit, is that repetitive behaviors arise from the inflexibility in switching and transitioning between habitual and novel motor behavioral patterns [97–99]. Accordingly, cilia may provide an adaptation mechanism that adjusts the transition of habitual behaviors to repetitive behaviors.

We tested the effects of cilia ablation in the striatum on the three types of memory: working memory, short-term memory, and long-term memory. Our results reveal that striatal cilia ablation impairs spatial working memory and short-term social memory and delays decision and task execution in the working memory test but does not affect any long-term memory types.

Working memory encodes and stores information in its temporal context and permits its further manipulation to guide decision-making and behavior execution [100, 101]. The dorsal striatum is involved in the initial storage of temporal information in working memory, and dysfunctions of the striatum or dopaminergic projections to the striatum are known to impair the execution of working memory [102–104]. The striatum also plays an essential role in social recognition, in which different sensory cues are acquired for coding social information [105–107]. Taken together, our results indicate that cilia in the striatum are essential for initial acquisition and brief storage of information but not for its long-term consolidation or retrieval. Our results also suggest that cilia are key components of brain networks for action selection and timing of the decision process. Previous studies have shown that cilia removal from the hippocampus and cortex resulted in deficits in fear conditioning memory [23, 108]. However, our finding of the lack of an impact of cilia loss from the rostral striatum on the contextual fear memory does not seem to contradict with these previous results, since the hippocampus and cortex rather than the striatum are known to be involved in contextual fear memory formation.

Dorsal Striatal Cilia Ablation Does Not Affect Limbic Functional Domains

Cilia ablation in the dorsal striatum did not impair motivational and affective functions, as revealed by the normal sociability, anxiety, nociception, and depressive-like behaviors in the cilia-ablated mice. These results are interesting, though not surprising, given that the dorsal striatum has a minor role in these functions compared with the ventral striatum (nucleus accumbens in rodents), which is the main site for limbic functional domains [109–111].

Striatal Cilia Ablation Alters Neuronal Activities in Striatum Input Structures

Associated with the behavioral phenotype induced by striatal cilia ablation, cFos expression, as a marker for neural activity, was altered in the dorsal striatum itself and in the cortical structures that project to the dorsal striatum, including nuclei of sensorimotor and associative cortical-basal ganglia-thalamic-cortical circuits. The striatum receives projections from the cortex, thalamus, and SNc [28, 31, 112], and its neurons project to the outputs of the basal ganglia SNr/GPm via the direct and indirect pathways via GPl and the sub- thalamic nucleus (STN) (for review [32–35]). The primary motor cortex is responsible for generating the signals that control movement execution, whereas the secondary motor areas control motor planning. The thalamus, a main output target of the basal ganglia, is under the inhibitory (GABAergic) tone of the SNr and GPm, and in its turn projects, using glutamate transmitter, back to the cortex [113–116]. On the other hand, the dopaminergic neurons of the SNc project to the striatum, stimulating the direct pathway through D1 receptors and inhibiting the indirect pathway via D2 receptors. Surprisingly, none of the basal ganglia structures that receive projections from the striatum showed altered cFos expression. This finding is interesting and, together with the finding of decreased cFos in the cortical regions, indicates that cilia removal from the striatum decreases the activity of presynaptic neurons projecting to the striatum more than neurons that receive projections from the cilia-ablated neurons. It is noteworthy, however, that cFos expression was analyzed in mice' brains 90 min after the fear conditioning retrieval test. Given that cilia-ablated mice showed normal performance in this assay, the profound changes in cFos expressions in several brain regions suggest that striatal cilia ablation caused alteration in the constitutive cFos levels [117, 118].

Striatal Cilia as a Modulator of Timing Perception

An interesting observation made of the reconciliation of our results is that the disrupted functions in striatum cilia-ablated mice share a common fundamental aspect: “impaired time perception,” i.e., losing the ability of quick and timely adjustment of behavior in response to

changing environmental cues and, thus, failing to maintain appropriate, goal-directed motor response [119]. Time perception is embedded in the processing and integration of environmental sensory information and in motor and executive actions. Timing judgment allows for the timely selection of appropriate responses to the environment sensory. In this sense, prepulse inhibition of startle reaction, repetitive motor, and motor coordination all involve a sequence of motor actions, for which execution requires precise timing and coordination, usually in the millisecond timescale. Therefore, the exclusive impairments of these functions in cilia-ablated mice may indicate a disruption of time judgment and adjustment, which may impede the successful execution of these motor activities [120–125]. Time perception is also critical for cognitive processes. Successful performance of working memory, attention, decision-making, and executive function requires accurate and precise timing judgment, usually within a millisecond to minute timescale [126–133]. In the context of working memory, the encoding, maintenance, and synchronization of stimulus attributes are presented in specific temporal sequences [134, 135]. Memory formation begins when environmental stimuli first elicit a timing mechanism, in which information about elapsed time is stored in working memory or short term. When the stimulus ends or another event happens, the value of that duration is stored in long-term memory [100, 136]. The impairments of working memory and the delay in the decision and executive function in cilia-ablated mice further support the speculation of interval timing disruption in these mice. This speculation is in line with the known role of the basal ganglia circuit in performing central clock functions in the brain [137, 138]. Particularly, the SNc and striatum are the two basal ganglia regions necessary for interval timing and are parts of cortical-basal-ganglia circuits that form neuronal clocks [139–146]. These circuits coordinate the estimation and reproduction of time, wherein dopamine modulates the clock speed and timing judgment functions [147–149]. For example, increased dopamine levels result in a faster internal clock process, whereas decreased dopamine slows down the clock speed [147–149]. Furthermore, dysfunctions of the striatum have been shown to cause impairments of interval- timing judgments, particularly as related to the

spatial working memory [104, 150–152]. Interestingly, we recently found that most cilia transcripts in the primate basal ganglia-cortical circuit are circadian, and they peak in a sequential pattern similar to the sequential order of activation of structures of this circuit during movement coordination albeit on completely different time scales. Taken together, our findings, in line with robust evidence from the literature, suggest a critical role for striatal cilia in the brain's central clock function.

Implications of Cilia Dysfunctions in Neuropsychiatric Disorders

Intriguingly, the distinctive behavioral phenotype induced by striatal cilia ablation in mice appears to pertain to clinical manifestations of specific neurological and psychiatric disorders related to both the striatum functions and timing deficits. We base our view on the following notions: 1-The behavioral deficits in cilia-ablated mice represent a cluster that extensively overlaps across specific disorders, including SCZ, PD, HD, ASD, OCD, ADHD, and TS, with some of these deficits more significant in particular disorders than in others. Motor coordination deficits, for example, are the main features of PD and HD but are also observed in TS, ASD, OCD, SCZ, and ADHD [153–162]. On the other hand, repetitive behavior is a common feature of ASD, TS, OCD, and SCZ but is also found in ADHD and PD [163–174]. While sensorimotor gating deficit is a characteristic feature of SCZ, it is also observed in ASD, HD, PD, ADHD, OCD, and TS [175–187]. Furthermore, social recognition memory is impaired in ASD, SCZ, and OCD [188–193]. Lastly, decision execution and working memory deficits are common features in SCZ, ASD, ADHD, PD, HD, and OCD [194–204]. 2- Dysfunctions of the striatum, as a target of dopaminergic pathways and an essential part of the cortico-basal ganglia-thalamic circuits, underlie fully or partially the pathophysiology of these neuro-psychiatric disorders [61–76]. 3- A common feature of striatum-related disorders and the seven discussed disorders is a profound decrease in patients' ability to accurately calculate the timing of the initiation and termination of voluntary actions [205–220]. While time perception deficits have been extensively studied in the PD, SCZ,

ADHD, and HD individuals, timing judgment deficits in ASD, OCD, and TS have recently begun to receive attention [205–220].

It is also important to note that it is possible that the disruption of cilia may alter the morphology and function of other parts of the neuron, and thus, the manipulation might cause some indirect effects on neuron morphology, which may alter connectivity or excitability. Based on our findings and the discussion above, we propose a model in which cilia in the striatum act as a calibrator of the timing function of the basal ganglia-cortical circuit by maintaining proper timing perception. According to this model, abnormal cilia functions might be a unifying factor contributing to the pathophysiology of neurological and psychiatric disorders, particularly as related to the deficits in timing judgment.

In conclusion, our findings shed light on the roles that striatal cilia may play in timing-dependent functions. These findings enhance our understanding of brain function in the context of the crucial roles played by this previously unappreciated organelle and may open new avenues for therapeutic intervention through cilia-targeted therapies.

Chapter 6: Behavioral deficits induced by time-dependent Ciliary MCHR1 deletion

Abstract

Primary cilia are microtubule-based organelles that protrude from the surface of most mammalian cells and function as important signaling centers. The melanin-concentrating hormone receptor 1 (MCHR1) is a G protein-coupled receptor that is expressed in several regions of the brain, including the primary cilia of some neurons. The role of MCHR1 in primary cilia is not yet fully understood, but it has been implicated in various physiological processes such as regulation of appetite and energy balance, as well as behaviors related to reward, motivation, and mood.

To better understand the role of ciliary MCHR1 in social and cognitive deficits, we used an inducible knockout model of ciliary MCHR1. Our study aimed to investigate whether the deletion of ciliary MCHR1 would result in similar behavioral deficits as seen in MCH/MCHR1 deletion mice models. In our model, we found that the deletion of ciliary MCHR1 led to normal sociability, but an increase in hyperactivity, deficits in cognition, and sensorimotor gating.

Interestingly, we observed that the timing of the deletion of ciliary MCHR1 had an impact on the behavioral outcomes. In mice with late deletion of ciliary MCHR1, we observed an increase in hyperactivity, deficits in cognition, and sensorimotor gating, whereas in mice with early deletion, we observed deficits in both social and cognitive function as well as sensorimotor gating deficits. These findings suggest that ciliary MCHR1 may play a critical role in the development of social and cognitive behavior.

Furthermore, we were able to use our model to quantify the amount of ciliary and non-ciliary MCHR1 that localizes to primary cilia to better understand the role they play in the deficits seen. Our results showed that ciliary MCHR1 levels were significantly reduced in the knockout mice, whereas non-ciliary MCHR1 levels were unchanged. This finding supports the idea that ciliary MCHR1 may be crucial for the proper functioning of primary cilia. Our study has important implications for our understanding of the role of the MCH system in neurodevelopmental processes and its contribution to the pathogenesis of schizophrenia. We have shown that the

disruption of the MCH system interferes with neurodevelopmental processes, which may contribute to the pathogenesis of schizophrenia. These findings suggest that targeting the MCH system, particularly ciliary MCHR1 at specific ages, may be a potential therapeutic strategy for treating the social and cognitive deficits associated with schizophrenia.

Introduction

Melanin concentrating hormone (MCH) is a neuropeptide that is primarily produced in the lateral hypothalamus and zona incerta of the brain[1, 2]. The MCH system is involved in regulating various physiological processes, including food intake, energy balance, and arousal [3-6]. MCH acts through the G protein-coupled receptors, MCHR1, which is widely expressed throughout the central nervous system [7]. The MCH system has been implicated in various diseases, such as obesity, depression, and sleep disorders, making it a potential therapeutic target [8-15].

In addition the MCH system has also been implicated in cognitive processes. MCH has been shown to affect learning and memory in animal models, with MCH-deficient mice exhibiting improved memory performance in certain tasks [16-19]. Furthermore, MCH receptors have been found in areas of the brain associated with cognitive processes, such as the hippocampus and prefrontal cortex [20]. This suggests that the MCH system may play a role in modulating cognitive function and could potentially be targeted for cognitive enhancement. Studies in animal models have suggested that MCHR1 may be involved in learning, memory, and attention. For example, MCHR1 knockout mice exhibited impaired spatial learning and memory [21-23]. Another study found that blocking MCHR1 improved attention in rats [24]. The exact role of MCHR1 in cognitive function in humans is still unclear.

In addition to cognition, MCHR1 has also been implicated in social behavior. Studies in animal models have suggested that MCHR1 may play a role in regulating social behavior, such as aggression and social recognition. MCHR1 knockout mice exhibited increased aggression and impaired social recognition [17, 23, 25-27]. As well, blocking MCHR1 reduced aggression in rats [28]. The exact mechanisms by which MCHR1 regulates social behavior are not yet fully understood and more research is needed to better understand this relationship.

The MCH system has also been found to be involved in schizophrenia [23]. The study found that individuals with schizophrenia had lower levels of MCHR1 in certain brain regions and that these deficits were associated with cognitive impairments, particularly in memory and social

functioning. Additionally, the study found that MCHR1 deficits were also associated with abnormal sensorimotor gating, which is a common feature of schizophrenia. The vast majority of our understanding of the MCH system was obtained from studying germline MCHR1 knockout mice and conditional MCH-cell ablation using inducible diphtheria toxin receptors (iDTR) system to induce selective death of MCH neurons [29]. While the germline KO approach provides crucial insights on the functions of MCH system and serves as a valuable reference and guide for research questions, it has its own limitations as the developmental compensatory mechanisms for the deletion of MCHR1 gene might mask or change the behavioral phenotypes. Also it is difficult to determine the selective and temporally distinct roles of the MCH system in social and cognitive functions at different stages of animal life. While the iDTR-induced ablation of MCH neurons provides an important tool for identifying the selective and temporally distinct roles of MCH system, however, this selectivity is eliminated by the fact that by inducing the death of MCH neurons that co-express other neurotransmitters such as GABA, orexin, histamine etc, these neurotransmitter systems are impacted and thus the ultimate phenotype is not solely due to the MCH ablation. Therefore, this study will enable us to induce ciliary MCHR1 deletion at different stages of life. These findings suggest that the MCH system may be a potential target for the development of new treatments for schizophrenia. However, more research is needed to fully understand the role of the MCH system in schizophrenia and how it may be targeted for therapeutic intervention.

Recent studies have also demonstrated that the MCHR1 receptor localizes to cilia in various cell types, including neurons [30-32]. Cilia are hair-like structures that extend from the surface of cells and are involved in various cellular processes, including signal transduction. The localization of MCHR1 to cilia suggests that it may play a role in cilia-mediated signaling pathways. Additionally, mutations in cilia-related genes have been linked to various diseases, such as obesity and ciliopathies [33-37]. Therefore, understanding the role of MCHR1 in cilia-mediated

signaling may provide new insights into the pathogenesis of these diseases, and how they relate to the MCH system.

Cilia dysfunction has been associated with the development of several neurological disorders, such as schizophrenia and bipolar disorder. Studies have suggested that disruptions in cilia function could result in alterations in signaling pathways in the brain, which may contribute to the development of these disorders. For instance, research has shown that mutations in genes that regulate cilia function are related to abnormalities in brain structure and function, as well as cognitive deficits [38].

The increasing evidence on cilia in the brain highlights the importance of these structures in sustaining brain function. Dysfunctions in cilia and associated signaling pathways may contribute to the development of various neurological disorders. Further studies are required to fully comprehend the role of cilia in these disorders and to identify potential targets for therapeutic intervention. The localization of the MCHR1 receptor and other proteins to cilia suggests that these systems may be promising targets for the development of novel treatments for neurological disorders [39-42]. Thus we used an inducible mouse Mchr1-CreER model coupled with IFT88 fl to study the role of ciliary melanin concentrating hormone (MCH) signaling in the developing brain to understand the responsibility of MCHR1s' localization to cilia. We hypothesize that timing of ciliary MCHR1 dysregulation in the early stage of postnatal development contributes to the pathogenesis of schizophrenia-like behavior.

Materials and Methods

Generation of MCHR1CreER x IFT88fl mice

We received the inducible mouse MCHR1-CreER model from the Berbari lab[43]. They generated a BAC transgenic mouse where the Mchr1 promoter drives expression of tamoxifen inducible CreER recombinase. Mchr1CreER positive mice were bred with IFT88*fl* mice that have loxp sites that flank the exons 4-6 of the intraflagellar transport 88 gene (IFT88). This will result in the deletion of exon 4-6 in the tissues upon activation of the estrogen receptor expressed on Cre. Upon tamoxifen injection i.p, tamoxifen-bound Cre-ER dissociates from HSP90, translocates into the nucleus, and carries out site-specific recombination between flanking loxP sites. All experimental procedures were approved by the Institutional Animal Care and Use Committee of the University of California, Irvine, and were performed in compliance with national and institutional guidelines for the care and use of laboratory animals.

Genotyping

For the Mchr1CreER, we used two primers with the following sequences: 5′-GCAAACGGACAGAAGCATTT and 5′-GCGGTAGAGGAAGACCCTTT. The PCR program consisted of an initial step of heating the mixture at 95°C for 2 minutes, followed by 35 cycles of heating at 95°C for 15 seconds, annealing at 57°C for 30 seconds, and elongation at 72°C for 1 minute. Finally, there was a last elongation step at 72°C for 1 minute. As for the RosaLacZ, we used three primers with sequences 5′- GCG AAG AGT TTG TCC TCA ACC, 5′- AAA GTC GCT CTG AGT TGT TAT, and 5′- GGA GCG GGA GAA ATG GAT ATG. The PCR program consisted of the initial denaturation at 94°C for 2 minutes. The denaturation step is at 94°C for 20 seconds, annealing at 65°C for 15 seconds with a temperature decrease of 0.5°C per cycle. For elongation 68°C for 10 seconds with for 10 cycles, with a touchdown protocol. Next, at 94°C for 15 seconds., 60°C for 15 seconds, 72°C for 10 seconds, repeating for 28 cycles, and 72°C for 2 minutes. For IFT88*fl,* the following PCR reaction was conducted using KAPA2GFast HotStart PCR kit (Roche Cat. No 07960930001) with the Forward primer 5′-GACCACCTTTTT AGCCTCCTG and the

Reverse primer 5′-AGGGAAGGGACTTAGGAA TGA. Touch-down cycling was performed, and the PCR product was analyzed on a 1% agarose gel. The genotypes were identified as homozygous at ~ 410 bp, heterozygous at 365 bp and ~ 410 bp, and wildtype at 365 bp [43].

Tamoxifen administration

Tamoxifen administration was done as previously mentioned [43]. Briefly, to activate CreER recombinase, groups of mice were administered intraperitoneal injections of 20 mg/ml tamoxifen (Sigma Aldrich, St. Louis, MO) that was dissolved in corn oil (Sigma Aldrich, St. Louis, MO). Adult mice were given injections for five consecutive days with a dosage of 150 mg/kg. Meanwhile, mice at P21 were administered a single 50 µL injection for two consecutive days to induce the recombinase.

Behavioral Assays

7-week-old mice underwent a series of behavioral tests two weeks after the tamoxifen injections, 21 day old mice were left until they were 8 weeks old to start behavioral tests. The behavioral tests included locomotion, rotarod, social interaction, spontaneous T-maze alternation, novel object recognition, and prepulse inhibition.

Locomotor Activity

The procedure for the locomotor activity was based on our previous studies[44-46]. Briefly, the experiment consisted of two phases: a 30-minute acclimation phase followed by a 60-minute locomotor activity test [78]. Mice were placed in a locomotion chamber (40 × 40 cm, Med Associates, Inc.), and their movements were recorded every 5 minutes using Activity Monitor 5 software (Med Associates, Inc.).

Rotarod Test

Rotarod test was performed as previously mentioned [44]. Briefly, to assess the motor coordination of mice, they underwent the rotarod test, which involved placing them on a raised rotating rod consisting of 5 lanes, each with a trip plate below to halt the timer when the subject falls. The test comprised three 420-second trials with a starting speed of 4 RPM that gradually

increased to 60 RPM. A 15-minute interval was given between each trial, and the data were examined based on the latency and speed of the falls in each trial.

Spontaneous T-maze Alternation

Spontaneous t maze alternation was performed as previously mentioned [44]. The mice were placed in the entrance of the T-maze and allowed to acclimate for 30 seconds. Subsequently, the doors were opened, providing the animals access to either the left or right arm of the maze. Once a decision had been made, the door was closed, and the mice were allowed to explore the chosen side arm for 30 seconds. After that, the mice were returned to the maze base to commence the next trial. A total of eight trials were conducted, and the percentage of alternations was determined as 100 times the number of alternations divided by seven. Additionally, the time taken to make an alteration decision was recorded.

Social Interaction

Social interaction was performed as previously mentioned [44]. The three-chamber box utilized in these assays is a rectangular plexiglass box with separable doors that divide the left, middle, and right chambers. To create an environment for social interaction, empty mesh wire cups were placed in the middle of the left and right chambers. The social interaction assay began with the experimental mice exploring the middle chamber for 5 minutes. After that, a control mouse of the same gender, age, and strain as the experimental mouse was placed inside one of the cups in either the right or left chamber, and the experimental mice were allowed to explore all three chambers for 10 minutes. The total duration of time that the experimental mice spent interacting with the empty and control mouse cups was documented. The social novelty assay followed immediately after the social interaction assay, with a new control mouse placed underneath the empty cup. The experimental mice were allotted 10 minutes to explore all three chambers, and the total time they spent interacting with the mouse from the social interaction assay and the novel mouse was documented. ANY-maze software (Stoelting, Wood Dale, IL, USA) was utilized to record and analyze these interactions.

Novel Object Recognition

The novel object recognition (NOR) paradigm consists of the training and the testing phase. Prior to training, all mice were handled for 1-2 minutes per day for three days. Then, they were allowed to habituate to the rectangular box apparatus for three consecutive days without objects. During the training phase, mice were given 10 minutes to explore two identical objects in the box. After 24 hours, the testing phase began, during which mice were given 5 minutes to explore the box containing one familiar and one novel object. The total time spent by each mouse interacting with both objects was recorded individually [44]. The software ANY-maze (Stoelting, Wood Dale, IL, USA) was used to document and analyze these interactions.

Prepulse Inhibition

The mice underwent a 5-minute acclimation period in the startle chambers with a background noise of 65 dB. The PPI session consisted of five trials, including no-stimulus trials, prepulse trials, and startle trials. The no-stimulus trials involved only background noise, while startle trials included a 40-millisecond startle stimulus at 120 dB (p120). The prepulse trials consisted of a 20-millisecond prepulse at 68 dB (pp3), 71 dB (pp6), or 77 dB (pp12) with a 100-millisecond interstimulus interval, followed by a 40-millisecond startle stimulus at 120 dB. The test sessions started with five presentations of the p120 trial, followed by ten presentations of various trials in a pseudorandom order, with an intertrial interval of 8 to 23 seconds (mean 15 seconds) and ended with five presentations of the p120 trial. The PPI percentage score was calculated for each acoustic prepulse intensity, which is % PPI = 100-([(startle response for prepulse + pulse trials)/ (startle response for pulse-alone trials)] × 100). The magnitude of the response was calculated as the average response to all of the startle or prepulse trials [23].

Immunohistochemistry

Ninety minutes following the last behavioral assay, mice were anesthetized with isoflurane and transcardially perfused with saline and 4% paraformaldehyde (PFA). The brains were then harvested and kept in PFA overnight, after which they were switched to 30% sucrose. Using a

microtome, brains were coronally sectioned at 30 µm. From specific regions of interest, 3-4 sections were chosen with the help of the Allen Brain Atlas. These sections were blocked with goat serum in PBS with 0.3% Triton X-100 for 30 minutes. Subsequently, the brain sections were incubated in blocking buffer with anti-MCHR1, (rabbit pAB; 1:250 dilution; catalog #711649, Thermo Fisher Scientific)

and anti-adenylate cyclase 3, (ACIII; 1:1000 dilution; chicken polyclonal antibody (pAb); CPCA-ACIII, Encor) in 4°C overnight. After primary antibody incubation, the sections were washed with PBS and then incubated with the secondary antibody, goat conjugated Alexa Fluor 647 and 488 (1:500; Thermo Fisher Scientific) and DAPI, 1:10,000 (Thermo Scientific Ref: 62,248 Lot: WF3296471) for 1 hour shielded from light. The sections were then washed with PBS and mounted on slides. Images were carried out using the Leica SP8 confocal microscope with a 63x objective lens (UCI optical biology core facility) [42].

Data Analysis

We performed statistical analysis using GraphPad Prism software. We presented the data as means with SEM. We analyzed the results of locomotor activity, stereotypic behavior, marble burying, NOR, and NOL assays using Student unpaired t-test. We analyzed social behavior, PPI, and fear conditioning data using 2-way ANOVA, followed by the Bonferroni post hoc comparison. We considered a P value less than 0.05 as statistically significant.

Results

Animals

To examine the physiological role of ciliary MCHR1, we generated MCHR1CreERxIFT88fl mice, which upon intraperitoneal injection of tamoxifen, tamoxifen-bound Cre-ER dissociates from HSP90, translocates into the nucleus, and carries out site-specific recombination between flanking loxP sites thus allowing us to specifically delete ciliary MCHR1 by the dysregulation of the IFT88 gene responsible for ciliogenesis. Using tamoxifen, we controlled the timing of the deletion at 7 weeks and early on at 21 days of age and tested the animals to see the difference in social and cognitive deficits (Fig. 6.1).

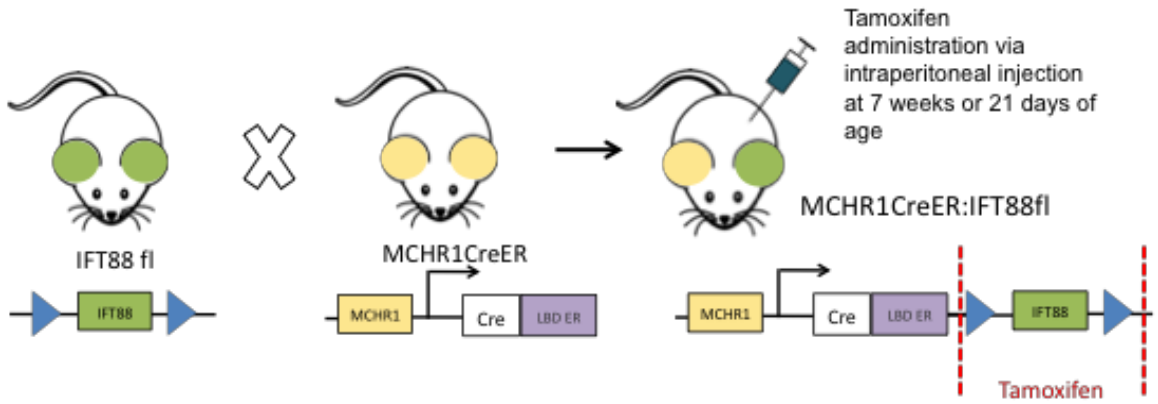

Figure 6.1. Animal model.

We have animals that have loxp sites that flank the exons 4-6 of the intraflagellar transport 88 gene (IFT88 (Jackson Laboratories, #022,409). These mice are bred with our MCHR1CreER mice (a generous gift from the Berbari Lab), which will result in the deletion of exon 4-6 in the tissues upon activation of the estrogen receptor expressed on Cre. Upon tamoxifen injection i.p, tamoxifen-bound Cre-ER dissociates from HSP90, translocates into the nucleus, and carries out site-specific recombination between flanking loxP sites. Tamoxifen will be injected at 7 weeks old and 21 days old separately and once 8 weeks old will be subjected to social and cognitive behaviors.

Validation of MCHR1 antibody and ciliary deletion

First, we confirmed the validity of the MCHR1 antibody in our MCHR1KO model (Fig. 6.2a,b). GPCRs are the biggest drug targets however are difficult targets to generate antibodies for, thus confirming using a MCHR1KO mouse model gives clarity to the specificity of the antibody. We collected regions from the CA1 hippocampus and nucleus accumbens from WT and MCHR1KO animals and confirmed that the antibody was indeed specific to the MCHR1 as there was no staining in the KO animals in multiple regions.

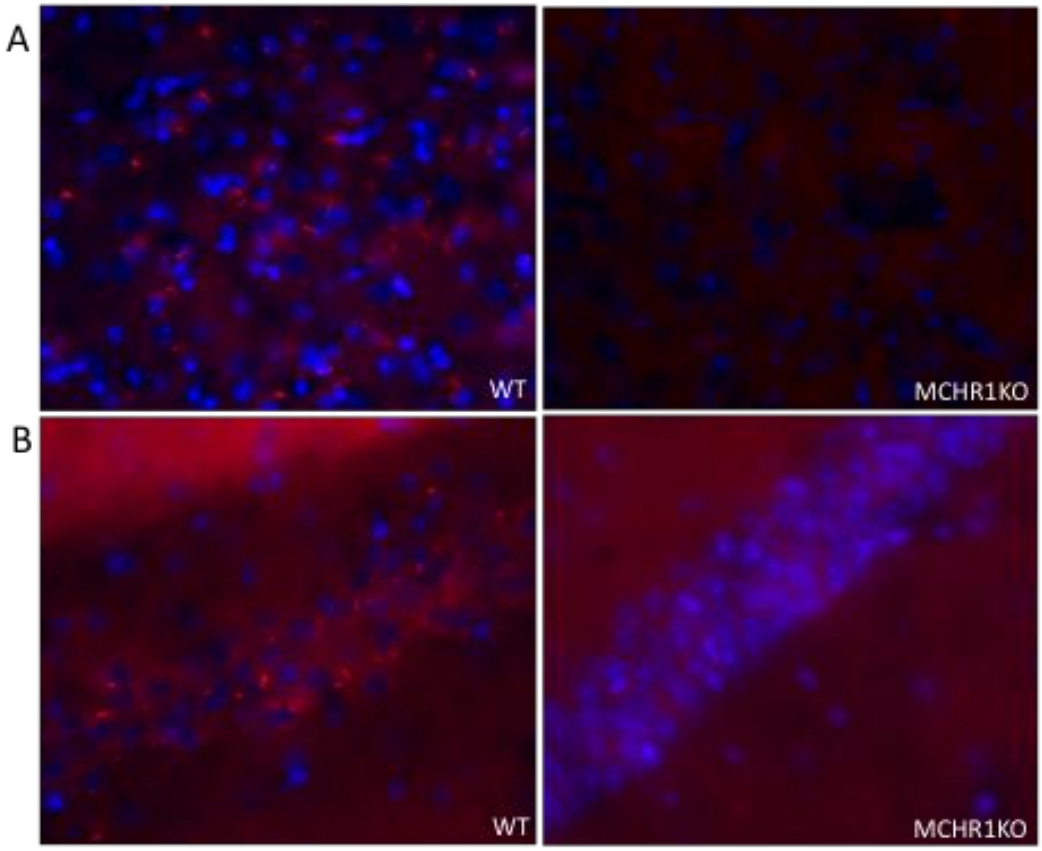

Figure 6.2. MCHR1 antibody validation.

WT animals showed MCHR1 positive cells in the (a) nucleus accumbens and (b) CA1 in the hippocampus while MCHR1ko animals showed no MCHR1 positive cells.

Following all the behavioral assays we performed coexpression analysis of primary cilia and MCHR1 via immunohistochemistry, using an ADCY3 antibody and MCHR1 antibody to confirm

removal of ciliary MCHR1 in both 7 week and 21 day group mice in the nucleus accumbens and CA1 of the hippocampus (Fig. 6.3, 6.4). Although MCH and MCHR1 display sexual dimorphism, we only observed male mice in these experiments. In both age dependent deletions we observed in multiple regions that the WT animals had coexpression of both ciliary MCHR1 and ADCY3 while the MCHR1CreERxIFT88fl animals showed ciliary MCHR1 deletion. Interestingly, we do see some cilia intact stained by ADCY3 as well as MCHR1 that localize to the cell membrane and not directly to cilia. Quantification of the percentage of ciliary MCHR1 in the control and CKO mice. Two-way ANOVA, WT vs MCHR1CreERxIFT88fl CA1, Nac ($F_{(1,63)} = 218.2$, $P < 0.0001$), ****$P < 0.0001$. Quantification of the percentage of ciliary MCHR1 in the control and CKO mice. Two-way ANOVA, WT vs MCHR1CreERxIFT88fl ($F_{(1,60)} = 557.3$, $P < 0.0001$), ****$P < 0.0001$. Data are presented as means ± S.E.M.

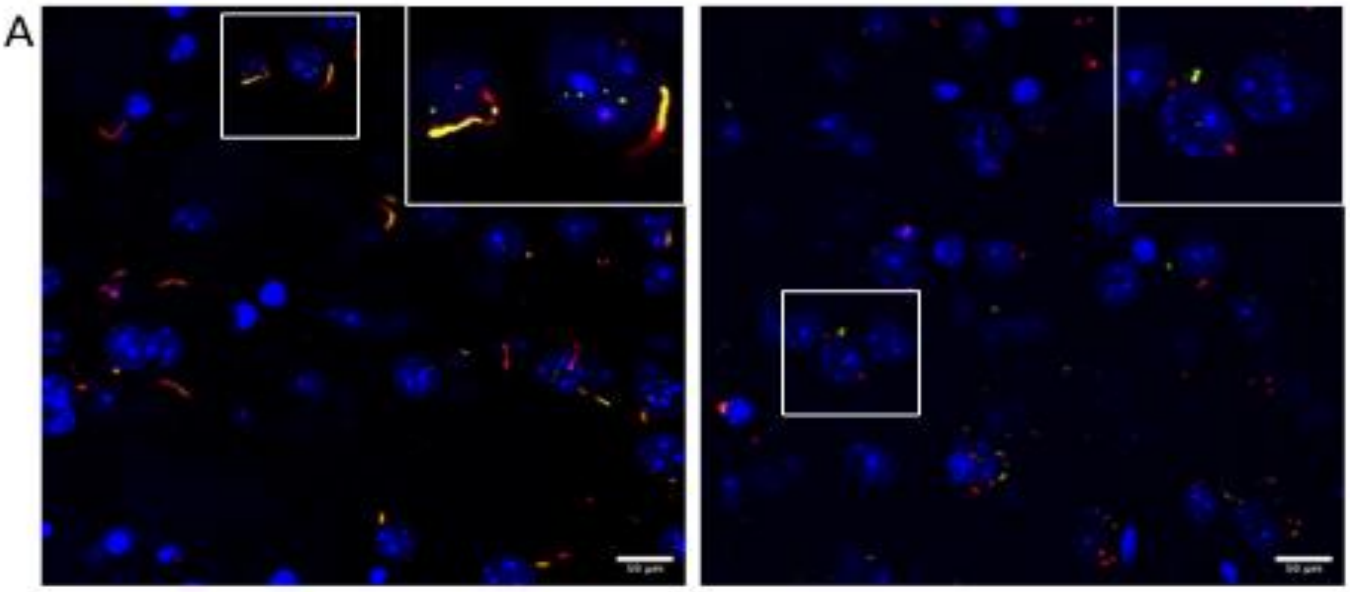

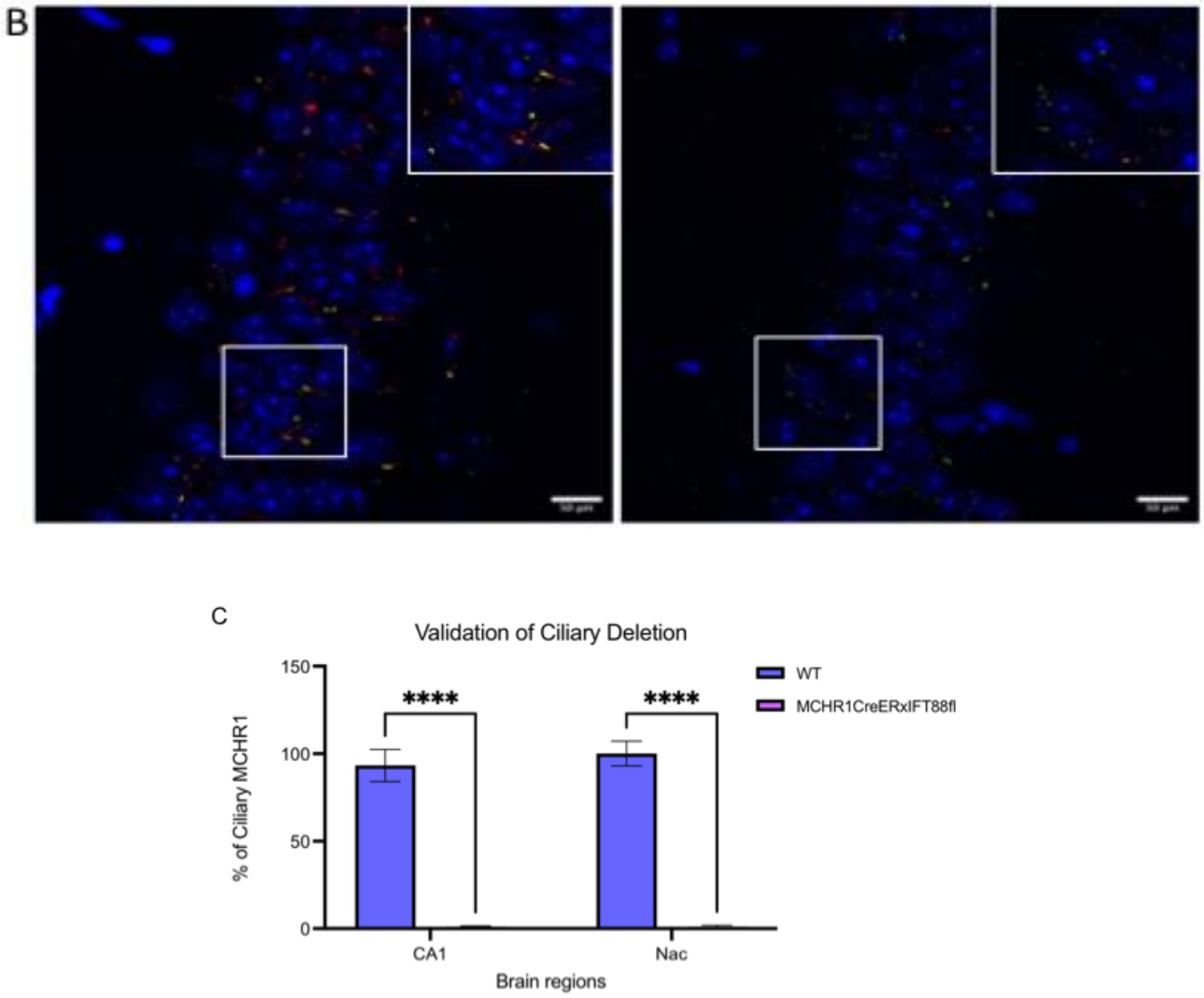

Figure 6.3. Validation of deletion of ciliary MCHR1 in the nucleus accumbens and hippocampus in 7-week animals.

MCHR1CreERxIFT88fl (right panels) and WT mice (left panels) were injected with Tamoxifen for 5 days to remove ciliary MCHR1. Verification of ciliary MCHR1 removal in the (a) nucleus accumbens and (b) CA1 of the hippocampus using immunostaining showing ciliary MCHR1 (red) and ADCY3 (green) in both the control animals and conditional knockout animals (counterstained with DAPI, blue). Scale bar=50 μm. (c) Quantification of the percentage of ciliary MCHR1 in the

control and CKO mice. Two-way ANOVA, WT vs MCHR1CreERxIFT88fl CA1, Nac ($F_{(1,63)} = 218.2$, $P < 0.0001$), ****$P < 0.0001$.

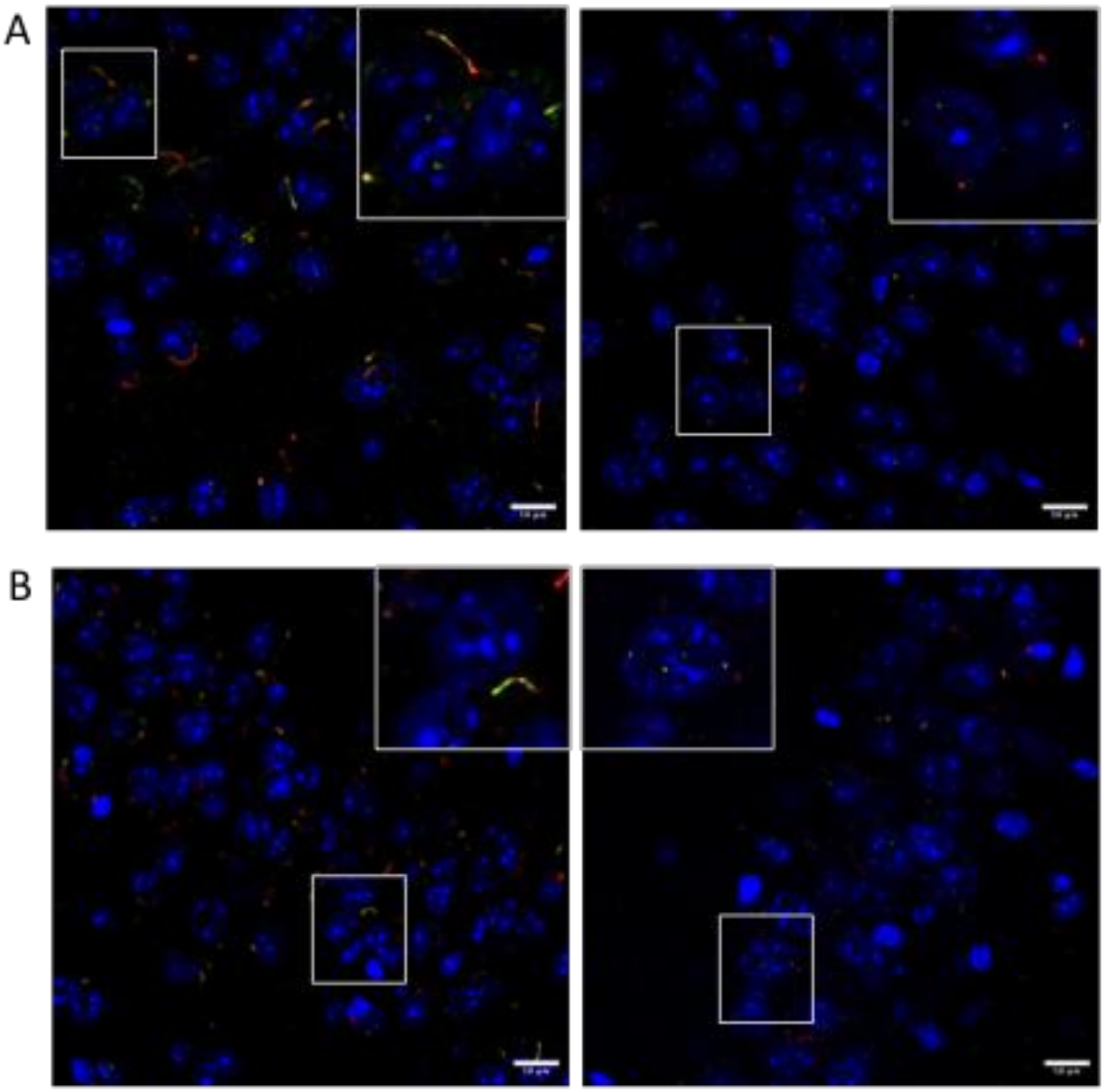

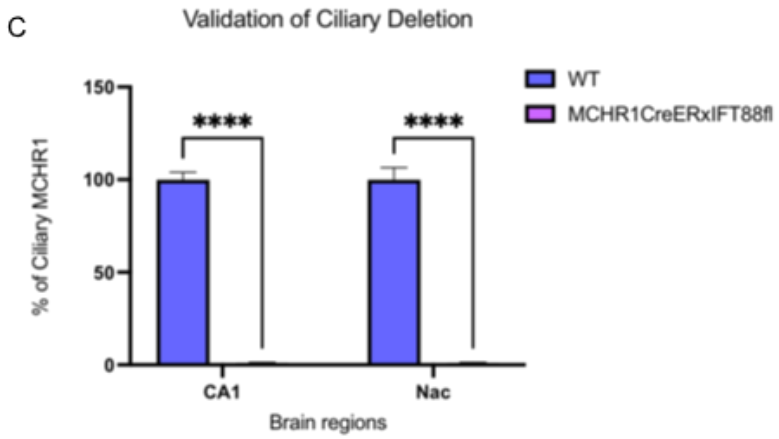

Figure 6.4. Validation of deletion of ciliary MCHR1 in the nucleus accumbens and hippocampus in 21 day animals.

MCHR1CreERxIFT88fl mice were injected with Tamoxifen for 2 days to remove ciliary MCHR1. Verification of ciliary MCHR1 removal in the (a) nucleus accumbens and (b) CA1 of the hippocampus using immunostaining showing ciliary MCHR1 (red) and ADCY3 (green) in both the control animals and conditional knockout animals (counterstained with DAPI, blue). Scale bar=50 μm. (c) Quantification of the percentage of ciliary MCHR1 in the control and CKO mice. Two-way ANOVA, WT vs MCHR1CreERxIFT88fl ($F_{(1,60)} = 557.3$, $P < 0.0001$), ****$P < 0.0001$. Data are presented as means ± S.E.M.

Deletion of ciliary MCHR1 at 7 weeks of age resulted in increased hyperactivity

Mice were subjected to multiple behavioral assays following 2 weeks of the start of injections to understand the physiological role of ciliary MCHR1. Previous studies have shown that MCH cko and MCHR1KO animals resulted in increased hyperactivity which we were able to confirm in our model that ciliary MCHR1 is responsible for the hyperactivity seen. The average distance traveled over 60 minutes was significantly increased compared to the control mice (Fig. 6.5).

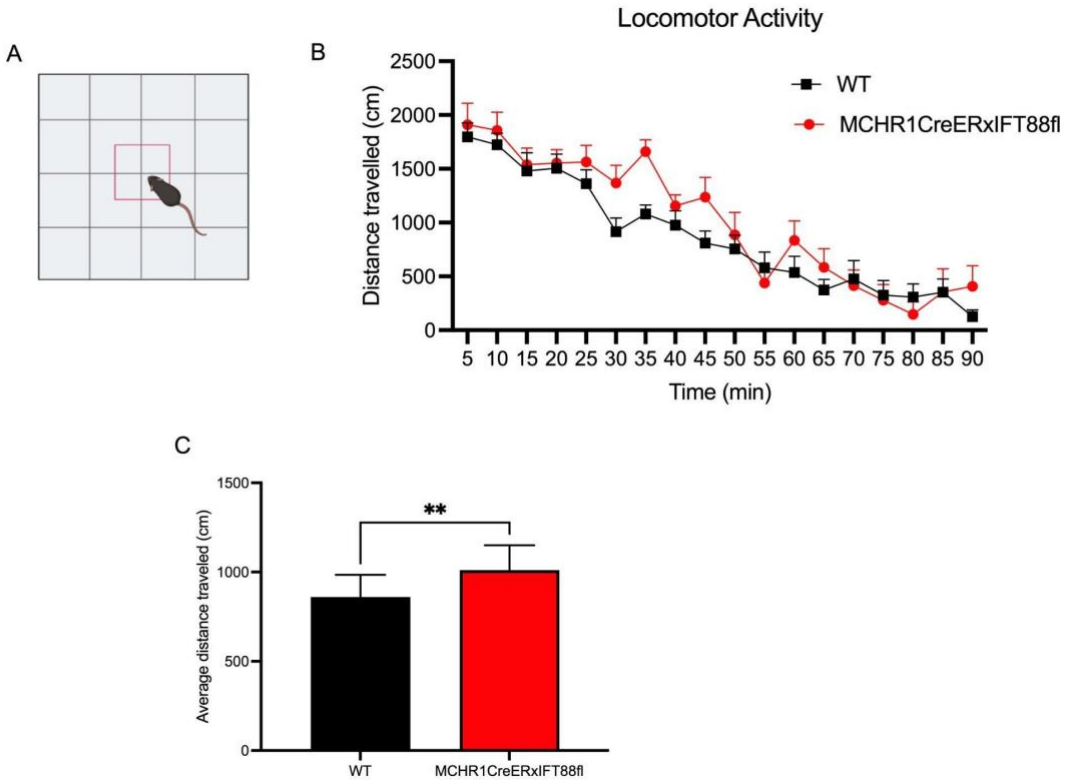

Figure 6.5. Deletion of ciliary MCHR1 at 7 weeks of age in mice resulted in a significant increase in spontaneous motor activity however normal non-spontaneous activity.

A. Schematic of the open field assay that the mice were allowed to explore for 90 minutes. B. Total distance traveled for the 90 min of the locomotor assay. C. Average distance traveled in 60 minutes of locomotion test. (Unpaired *t*-test **P=0.0062 t=3.121, n=8 WT, 7 MCHR1CreERxIFT88fl) Data are presented as means ± S.E.M.

Mice did not display any other differences in the locomotor activity. Mice were subjected to the rotarod assay and showed no impairments of motor coordination as they showed similar latency to fall and speed at which they fall in the rotarod test (Fig. 6.6). Mice also showed an increase in latency and speed to fall overtime following the 3 trials showing they have no impairments in procedural learning

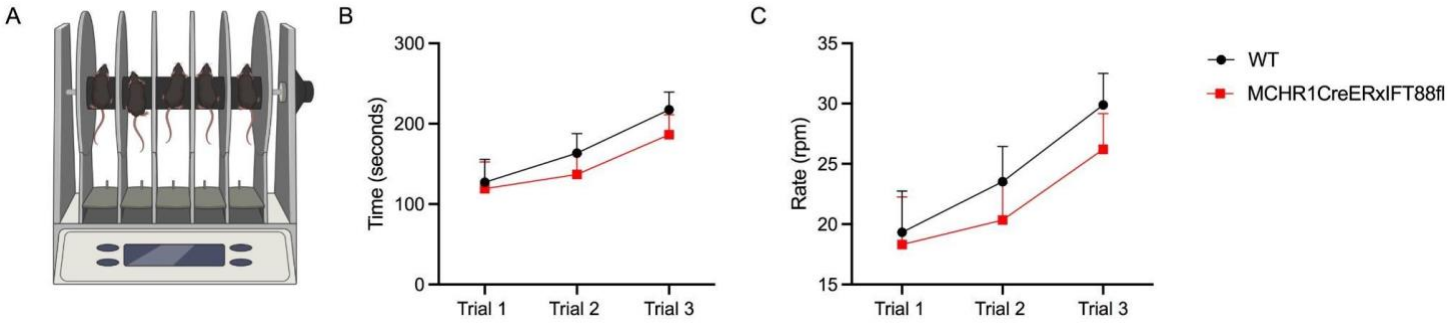

Figure 6.6. Deletion of ciliary MCHR1 at 7 weeks of age in mice resulted in normal motor coordination.

A. Schematic of the rotarod assay. B. Latency to fall in rotarod assay ($n = 8$). Two-way ANOVA (ko removal factor: $F_{(2,39)} = 4.372$, $P = 0.0194$, trial factor: $F_{(1,39)} = 1.030$, $P=0.3165$) followed by Bonferroni post hoc test: KO vs control, ns, not significant, P>0.9999. C. Speed to fall in rotarod assay ($n = 8$). Two-way ANOVA (removal factor: $F_{(2,39)} = 4.593$, $P = 0.0162$, trial factor $F_{(1,39)} = 1.014$, $P=0.3202$ followed by Bonferroni post hoc test: KO vs control, ns, not significant, P>0.9999. Data are presented as means ± S.E.M.

Deletion of ciliary MCHR1 at 7 weeks of age resulted in normal sociability

To test whether ciliary MCHR1 is responsible for social behaviors. Mice were subjected to the social interaction assay (Fig 6.7a). Removal of ciliary MCHR1 resulted in normal social behavior as the mice spent more time with the unfamiliar mouse than the empty cup (2-way ANOVA, genotype effect: $F_{1,26} = 4.830$, P=0.0371, genotype effect × cup interaction $F_{1,26} = 0.001425$, P=0.9702. Bonferroni post hoc test: empty cup vs unfamiliar mouse, wild type: $t = 3.4$, $P=0.0044$, KO: $t = 3.129$, $P=0.0086$ ($n = 8$ and 8 for wild type and KO, respectively). Although there was no significant difference between the amount of time spent with both the empty cup and unfamiliar mouse, they did spend more time with the mouse thus concluding that ciliary MCHR1 ablation at 7 weeks does not affect sociability.

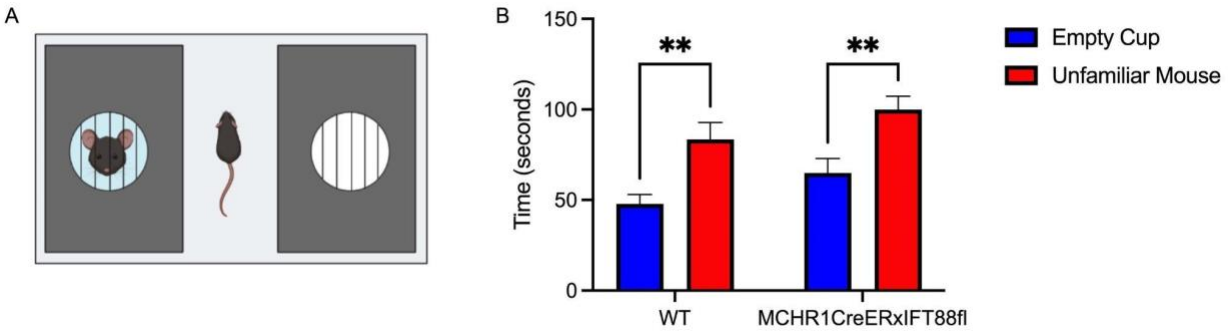

Figure 6.7. Deletion of ciliary MCHR1 at 7 weeks of age resulted in normal sociability.

A. Schematic of the social interaction assay. B. Time mice spent interacting with empty cup and control mice in social interaction test: 2-way ANOVA, genotype effect: $F_{1,26} = 4.830$, P=0.0371, genotype effect × cup interaction $F_{1,26} = 0.001425$, P=0.9702. Bonferroni post hoc test: empty cup vs unfamiliar mouse, wild type: t = 3.4, *P* =0.0044, KO: t = 3.129, *P* =0.0086 (n = 8 and 8 for wild type and KO, respectively).

Deletion of ciliary MCHR1 at 7 weeks of age resulted deficits in working and object recognition memory

We examined the effects of ciliary MCHR1 deletion at 7 weeks of age and found deficits in spatial working memory and object recognition memory. The T-maze paradigm was utilized to evaluate spatial working memory, taking advantage of mice's natural inclination to alternate between the right and left arms in order to efficiently navigate their surroundings. The spatial working memory was significantly impaired in the mice that had their ciliary MCHR1 deleted at 7 weeks. These mice displayed a lower alternation percentage because they had higher incorrect choices compared to the control mice. These mice took the same amount of time to make the incorrect decision compared to the control mice. Alternation percentage in t-maze (n=8) unpaired t-test

(t = 3.48 P =0.0041), control vs KO, P= 0.0041 Decision latency in T-maze test (*n* = 8), unpaired *t*-test (*t* = 0.3432 *P* = 0.7369), control vs KO, *P*= 0.7369 (Fig. 6.8).

Figure 6.8. Deletion of ciliary MCHR1 at 7 weeks of age resulted in deficits in working memory.

A. Schematic of the Spontaneous T-maze behavioral assay. B. Alternation percentage in t maze (n=8) unpaired t-test (t = 3.48 P =0.0041), control vs KO,P= 0.0041. C. Decision latency in T-maze test (*n* = 8), unpaired *t*-test (*t* = 0.3432 *P* = 0.7369), control vs KO, *P*= 0.7369.

The novel object recognition paradigm looks at long term memory, as mice are tested 24 hours after conditioning. Ciliary MCHR1 deletion at 7 weeks showed deficits in object recognition memory, as evidence mice spent about the same amount of time with both the new and old object compared to the control animals.

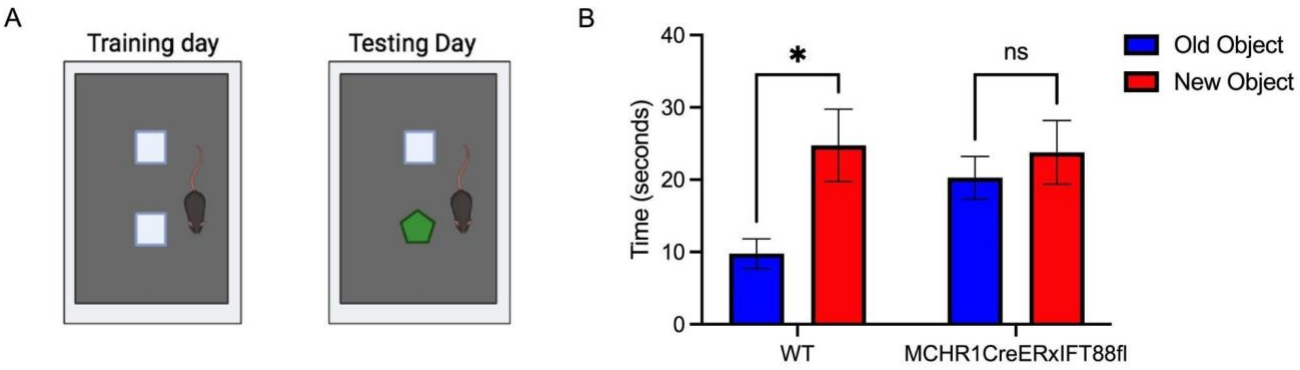

Figure 6.9. Deletion of ciliary MCHR1 at 7 weeks of age resulted in deficits in long term recognition memory.

A. Schematic of the novel object recognition paradigm. B. Novel object recognition (*n* = 8), two-way ANOVA (object factor: $F_{(1,28)} = 1.590$, P=0.2178, cilia removal factor: $F_{(1,28)} = 5.981$, P=0.0210): old object vs new object: P=0.0210. Data are presented as means ± S.E.M.

Deletion of ciliary MCHR1 at 7 weeks of age resulted in sensorimotor gating deficits.

To test for sensorimotor gating deficits, mice are subjected to the prepulse inhibition assay where we look at their startle reaction to a weak stimulus (prepulse) following a stronger subsequent startle response (pulse). Ciliary MCHR1 deletion at 7 weeks seems to exhibit significant reduction in inhibition at both 71 dB and 77dB compared to the control mice. These results indicate that ciliary MCHR1 may be responsible for the sensorimotor gating mechanism (Fig. 6.10).

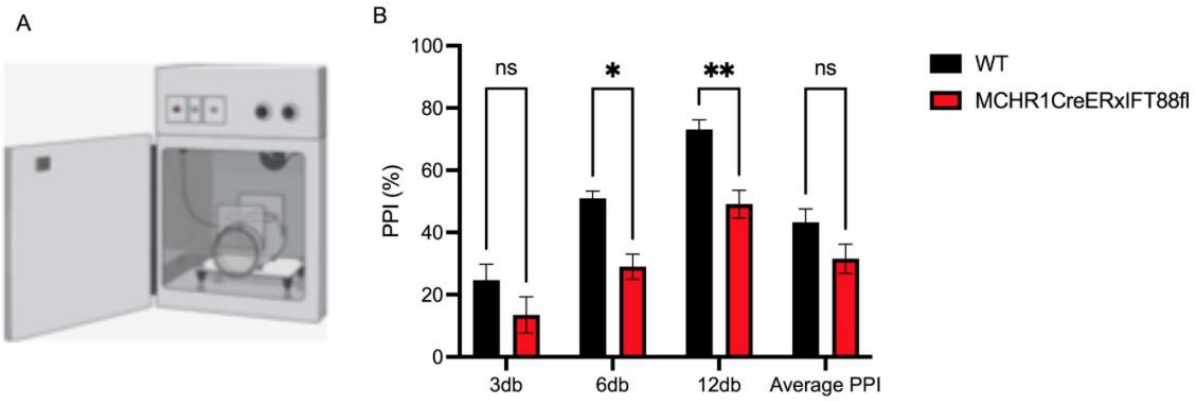

Figure 6.10. Deletion of ciliary MCHR1 at 7 weeks of age resulted in deficits in sensorimotor gating.

A. Schematic of the Prepulse inhibition paradigm. B. Prepulse inhibition ratio in mice: 2-way ANOVA, genotype effect ($F_{3,36} = 0.9461$, $P = 0.4286$), prepulse intensity effect ($F_{1,36} = 37.84$, $P<0.0001$) and genotype x prepulse intensity ($F_{3,36} = 0.04810$, $P = 0.9858$) followed by Bonferroni post hoc test: WT vs KO 3db, $P = 0.0329$, WT vs KO 6db, $P = 0.0192$, WT vs KO 12db, $P = 0.0107$, WT vs KO, Average PPI, $P=0.0094$.

Deletion of ciliary MCHR1 at 21 days of age resulted in increased hyperactivity

Mice were subjected to multiple behavioral assays upon reaching 9 weeks of age to understand the physiological role of ciliary MCHR1. Previous studies have shown that MCH cko and

MCHR1KO animals resulted in increased hyperactivity which we were able to confirm in our model that ciliary MCHR1 is responsible for the hyperactivity seen regardless of the age at which ciliary MCHR1 is deleted. The average distance traveled over 60 minutes was significantly increased compared to the control mice (Fig. 6.11).

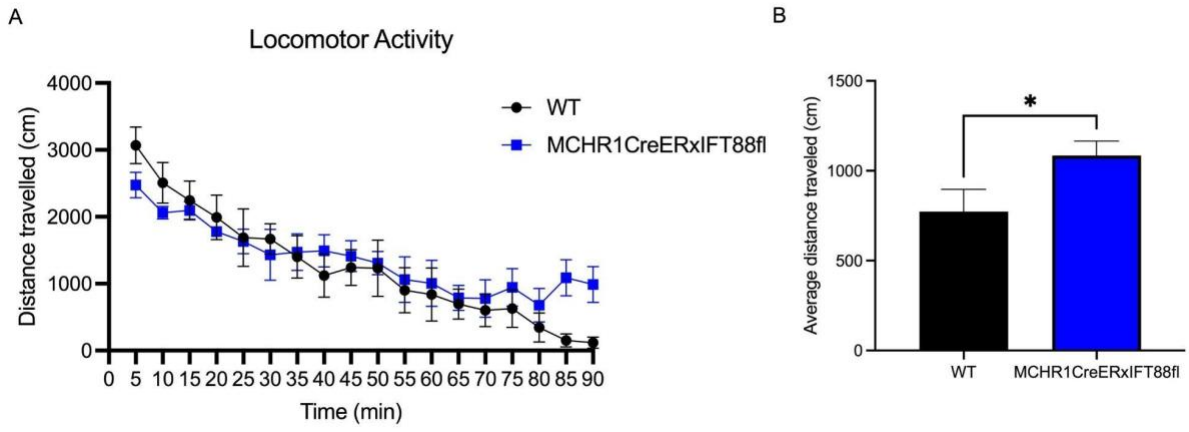

Figure 6.11. Deletion of ciliary MCHR1 at 21 days of age in mice resulted in a significant increase in spontaneous motor activity however normal non-spontaneous activity.

A. Total distance traveled for the 90 min of the locomotor assay b. Average distance traveled in 60 minutes of locomotion test. (Unpaired *t*-test *P=0.0464 t=2.111, n=6 WT n=5 KO) Data are presented as means ± S.E.M.

Mice did not display any other differences in the locomotor activity. Mice were subjected to the rotarod assay and showed no impairments of motor coordination as they showed similar latency to fall and speed at which they fall in the rotarod test (Fig. 8.12). Mice also showed an increase in latency and speed to fall overtime following the 3 trials showing they have no impairments in procedural learning.

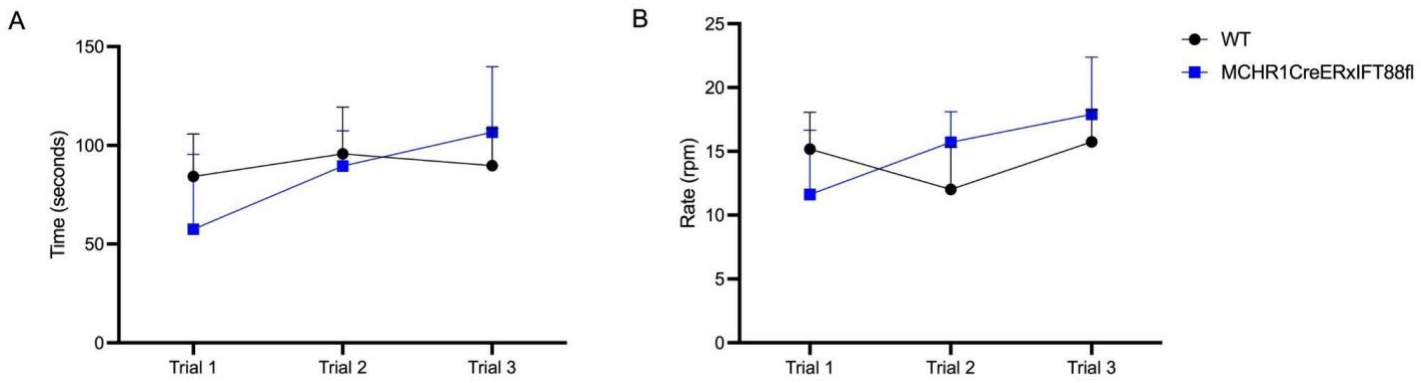

Figure 6.12. Deletion of ciliary MCHR1 at 21 days of age in mice resulted in normal motor coordination.

A. Latency to fall in rotarod assay ($n = 6$, 5). Two-way ANOVA (ko removal factor: $F_{(1,27)} = 0.06304$, $P = 0.8037$, trial factor: $F_{(2,27)} = 0.3570$, $P=0.7031$) followed by Bonferroni post hoc test: KO vs control, ns, not significant, P>0.9999. C. Speed to fall in rotarod assay ($n = 8$). Two-way ANOVA (removal factor: $F_{(1,27)} = 0.07204$, $P = 0.7904$, trial factor $F_{(2,27)} = 0.5682$, $P=0.5732$ followed by Bonferroni post hoc test: KO vs control, ns, not significant, P>0.9999. Data are presented as means ± S.E.M.

Deletion of ciliary MCHR1 at 21 days of age resulted in social deficits

To test whether ciliary MCHR1 is responsible for social behaviors. Mice were subjected to the social interaction assay. Removal of ciliary MCHR1 at 21 days of age resulted in deficits in social behavior as the mice spent the same amount of time with the unfamiliar mouse as the empty. Thus concluding that ciliary MCHR1 ablation at 21 days affects sociability (Fig 6.13).

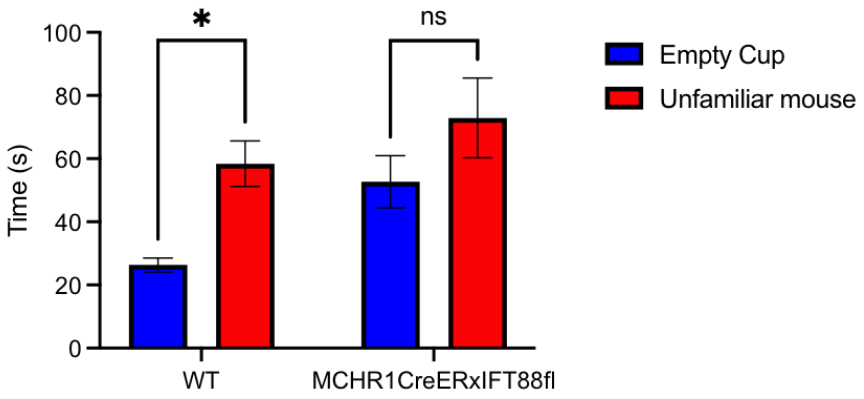

Figure 6.13. Deletion of ciliary MCHR1 at 21 days of age resulted in social impairments.

Time mice spent interacting with empty cup and control mice in social interaction test: 2-way ANOVA, genotype effect: $F_{1,18} = 6.559$, $P = 0.0196$, genotype effect × cup interaction $F_{1,18} = 0.5517$, P=0.4672 . Bonferroni post hoc test: empty cup vs unfamiliar mouse, wild type: $t = 2.978$, P =0.0483, KO: $t = 0.51$, $P > .05$.***$P < .001$ (n =6 and 5 for wild type and KO, respectively).

Deletion of ciliary MCHR1 at 21 days of age resulted deficits in working and object recognition memory

We examined the effects of ciliary MCHR1 deletion at 21 days of age and found deficits in spatial working memory and object recognition memory. The T-maze paradigm was utilized to evaluate spatial working memory, taking advantage of mice's natural inclination to alternate between the right and left arms in order to efficiently navigate their surroundings. The spatial working memory was significantly impaired in the mice that had their ciliary MCHR1 deleted at 21 days. These mice displayed a lower alternation percentage because they had higher incorrect choices compared to the control mice. These mice took the same amount of time to make the incorrect decision compared to the control mice (Fig. 6.14).

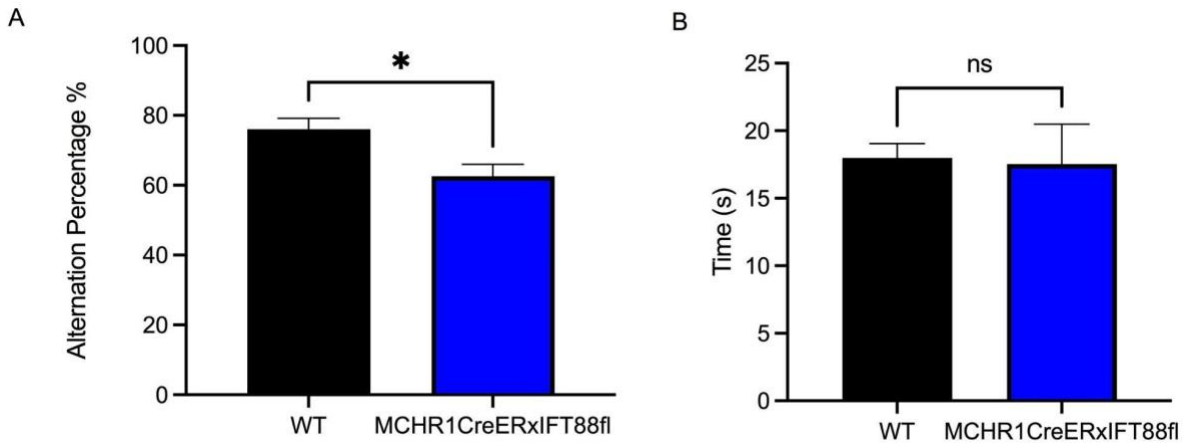

Figure 6.14. Deletion of ciliary MCHR1 at 21 days of age resulted in deficits in working memory.

A. Alternation percentage in t maze (n=6,5) unpaired t-test (t =2.870, *P* =0.0185 control vs KO, P=0.0185. C. Decision latency in T-maze test (*n* = 6,5), unpaired *t*-test (*t = 0.1507, P= 0.8835*), control vs KO, *P*= 0.8835, ns, not significant. Data are presented as means ± S.E.M.

The novel object recognition paradigm looks at long term memory, as mice are tested 24 hours after conditioning. Ciliary MCHR1 deletion at 21 days showed deficits in object recognition memory, as evidence mice spent more time with old objects than the new object compared to the control animals (Fig. 6.15).

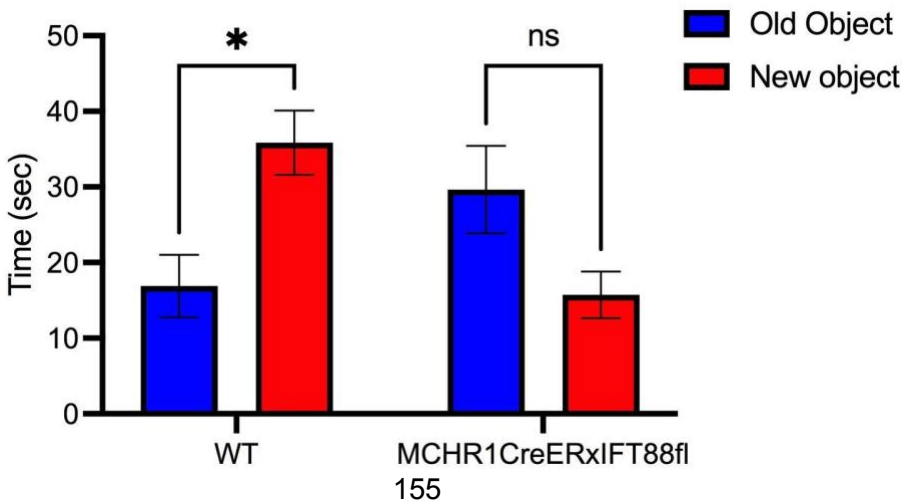

Figure 6.15. Deletion of ciliary MCHR1 at 21 days of age resulted in deficits in long-term recognition memory.

Novel object recognition (n = 6,5), two-way ANOVA (object factor: $F_{(1,18)} = 0.3282$, $P < 0.0001$, cilia removal factor: $F_{(1,18)} = 0.7067$, $P = 0.4116$): old object vs new object: P=0.0304. Data are presented as means ± S.E.M.

Deletion of ciliary MCHR1 at 21 days of age resulted in sensorimotor gating deficits.

To test for sensorimotor gating deficits, mice are subjected to the prepulse inhibition assay where we look at their startle reaction to a weak stimulus (prepulse) following a stronger subsequent startle response (pulse). Ciliary MCHR1 deletion at 21 days exhibits a significant reduction in inhibition at 68 dB, 71 dB and 77dB compared to the control mice. These results indicate that ciliary MCHR1 may be responsible for the sensorimotor gating mechanism (Fig. 6.16).

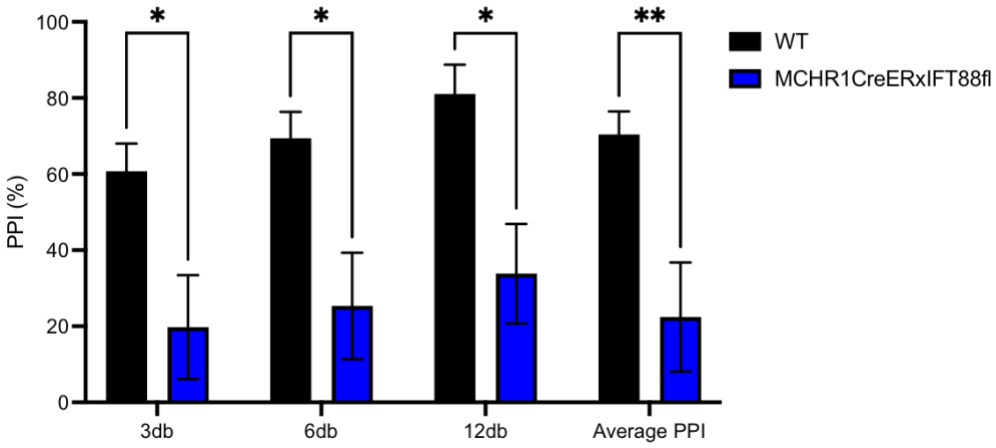

Figure 6.16. Deletion of ciliary MCHR1 at 21 days of age resulted in deficits in sensorimotor gating.

Prepulse inhibition ratio in male: 2-way ANOVA, genotype effect ($F_{3,36} = 0.9461$, $P = 0.4286$), prepulse intensity effect ($F_{1,36} = 37.84$, P<0.0001) and genotype x prepulse intensity

($F_{3,36}$ =0.04810, P = 0.9858) followed by Bonferroni post hoc test: WT vs KO 3db, P = 0.0329, WT vs KO 6db, P =0.0192, WT vs KO 12db, P =0.0107 WT vs KO Average PPI, P=0.0094.

Discussion

In this study we examined the role of time-dependent ciliary MCHR1 deletion using an inducible ciliary MCHR1 knockout model through CreER. This data provides confirmation of previous studies done on MCHR1 knockout models and conditional knockout models of the MCHR1 system, however is the first to uncover the role of the MCHR1 that localize to cilia specifically compared to those on the cell membrane. We provide evidence that the timing of the deletion of ciliary MCHR1 is important for social behaviors however it is not dependent on memory, hyperactivity, and sensorimotor gating. Our results also may be different than those published because it may be that both ciliary MCHR1 and those localized to the membrane are both responsible for the same thing and thus deleting a majority of them may result in partially seeing the effects in the behavioral paradigms. Our data also quantifies the localization of MCHR1 to cilia versus those binding to the cell membrane.

Methodological Considerations

This is the first inducible ciliary MCHR1 deletion model that uses tamoxifen to promote the deletion. There are many studies that have shown adverse effects of tamoxifen in behavioral assays in normal conditions. Tamoxifen is a selective estrogen receptor modulator (SERM) that is commonly used in mouse models to induce conditional gene knockout or overexpression [42]. Tamoxifen is known to interact with estrogen receptors in the brain, and as a result, it may have effects on mouse behavior. Studies have shown that tamoxifen can affect mouse behavior in a number of ways, although the exact effects may depend on a variety of factors, including the dose, duration of treatment, and specific behavioral test used. Some of the effects of tamoxifen on mouse behavior may include: (1) Anxiety-like behavior: Tamoxifen treatment has been shown to increase anxiety-like behavior in mice in some studies [47, 48]. For example, tamoxifen-treated mice may spend less time in the open arms of an elevated plus maze or have reduced exploration in a novel environment [49]. (2) Depression-like behavior: this may manifest as reduced motivation to explore or decreased preference for sucrose, which is commonly used as a measure

of reward sensitivity [50]. (3) Learning and memory: tamoxifen-treated mice may have impaired spatial learning and memory in the Morris water maze [50]. (4) Motor function: studies have reported reduced locomotor activity or impaired motor coordination in tamoxifen-treated mice [50]. In our model both the control and experimental animals are injected with tamoxifen, thus in some assays we see a trend that is not significant and may be a result because of the administration of tamoxifen rather than the deletion of ciliary MCHR1. We confirmed the deletion of ciliary MCHR1 through the immunostaining of both MCHR1 and ADCY3, which have been previously shown as the standard staining to quantify cilia expression. We showed a significant decrease in both MCHR1 and ADCY3 staining in multiple brain regions providing evidence that the mice indeed lacked ciliary MCHR1. We monitored the behavioral phenotypes resulting in ciliary MCHR1 ablation focusing on social and cognitive function as well as sensorimotor learning.

It is important to note that we found and confirmed with previous studies that a majority of MCHR1 localizes to primary cilia and thus the deletions we have seen of the MCH system may be linked to ciliary dysfunction. While it is difficult to recapitulate the human psychopathological phenotypes of schizophrenia in rodents, a number of behavioral patterns have been validated and historically accepted as translational models between rodents and humans. Locomotor hyperactivity, augmented stereotypic, and repetitive behaviors are widely used to evaluate the positive symptoms of schizophrenia [51-55]. Abnormal social interaction and communication are the main features of the negative symptoms of schizophrenia [56-58]. In mice, social behavior and social recognition are tested in the three chambers sociability assay [59]. Cognitive deficits are commonly evaluated using a wide range of assays such as T-maze (working memory), the novel object recognition (neutral memory), novel location recognition (spatial memory), fear conditioning (emotional memory) [60-63]. Impairment of prepulse inhibition of startle, which is present in patients with schizophrenia, reflects an inability to filter non-relevant sensory information [64], and tested in mice using the test of prepulse inhibition of acoustic startle [59].

Late deletion of ciliary MCHR1 results in normal sociability but deficits in cognitive function and sensorimotor learning while early deletion of ciliary MCHR1 resulted in deficits in both social and cognitive function as well as sensorimotor learning.

We produced MCHR1CreERxIFT88fl mice to investigate the physiological function of ciliary MCHR1. By administering tamoxifen through injection, the tamoxifen-bound Cre-ER separates from HSP90, moves into the nucleus, and executes targeted recombination between adjacent loxP sites. As a result, we can delete ciliary MCHR1 specifically by disrupting the IFT88 gene, which is responsible for cilia formation. We employed tamoxifen to control the timing of the deletion, either at 7 weeks or 21 days of age, and evaluated the animals for any differences in social and cognitive deficiencies.

We discovered that in both early and late deletion of ciliary MCHR1, resulted in a notable rise in spontaneous motor activity, but their non-spontaneous activity remained normal. Previous studies have investigated the relationship between the MCH system and locomotor activity and discovered that the deletion or antagonism of MCHR1 can lead to an increase in locomotor activity in a novel environment [65-67]. It is known that many GPCRs localize primarily to cilia just like MCHR1 for example some dopamine receptors [40, 68]. We need to consider that the deletion of ciliary MCHR1 is removing cilia in this model and thus, other receptors that localize may be removed and cause deficits seen. Previous studies found that when MCHR1 was deleted specifically in the dopamine D1 receptor-expressing neurons in the striatum, the mice showed increased locomotor activity and decreased anxiety-related behavior [69]. These findings suggest that ciliary MCHR1 plays a role in regulating locomotor activity in mice.

We discovered that in late deletion of ciliary MCHR1 resulted in normal sociability however early deletion of ciliary MCHR1 resulted in social deficits. We have previously found the germline deletion of MCHR1, but not ablation of MCH neurons during the adult stage, affected social behavior in mice in the three chambers sociability test [23]. Previous studies have also shown that mice lacking the MCHR1 gene displayed reduced social interaction compared to normal mice,

suggesting that the gene plays a role in the regulation of social behavior in mice. They also discovered that the deletion of the gene led to alterations in the levels of brain monoamines, such as dopamine and serotonin, which are involved in the regulation of social behavior [27]. There is evidence that primary cilia play a modulatory role in dopamine and serotonin signaling in the brain [70-78]. Some research found that ciliary dysfunction in a specific subset of neurons in mice led to alterations in dopamine signaling and behavior [70, 79]. Others found that ciliary defects in the brain led to alterations in serotonin signaling and social behavior in mice [80, 81]. Primary cilia regulate the number of neurons in brain areas involved in social behavior [82]. It is possible that timing of ciliary MCHR1 deletion plays a role in regulating social deficits.

Early and late deletion of ciliary MCHR1 resulted in deficits in working memory and long-term spatial recognition memory. Studies in rodents have shown that deletion of the mchr1 gene can result in various cognitive and memory deficits, including deficits in spatial learning and memory, fear conditioning, cognitive flexibility, and object recognition memory [23, 83]. These findings suggest that the MCH system, which includes the MCHR1 receptor, plays an important role in cognitive and memory processes in rodents. There is also some evidence to suggest that primary cilia may be involved in memory processes [84]. Previous studies found that primary cilia in the hippocampus, a brain region critical for learning and memory, are required for the formation and maintenance of long-term memories in mice. Others found that a genetic mutation that disrupts primary cilia function is associated with impairments in memory and learning in humans. These findings suggest that primary cilia may be an important target for understanding the neural mechanisms underlying cognitive and memory processes [84-88].

We discovered that in both early and late deletion of ciliary MCHR1, resulted in sensorimotor gating function. Sensorimotor gating refers to the ability of the brain to filter out irrelevant sensory information, and deficits in sensorimotor gating are thought to underlie some of the cognitive and behavioral symptoms of schizophrenia [89]. Studies have found that deletion of MCHR1 or ablation of MCH neurons can result in significant deficits in PPI and administering MCHR1

antagonists improves sensorimotor gating deficits in models of schizophrenia [22, 90-93]. Both early and late ciliary MCHR1 deletion mouse models display PPI deficit phenotypes suggests that the MCH system plays a critical role in preattentive information processing.

Many in vivo and in vitro studies have shown evidence that MCHR1 localizes primarily to cilia [32, 94-96]. Previously we investigated the effects of MCH on ciliary length and found that MCH treatment resulted in a significant increase in cilia length in these cells. [82]. Another important study showed that MCHR1 is widely distributed in the cilia of neurons throughout the CNS in mice in a sex-independent manner, providing further evidence for the importance of MCHR1 localization to cilia in CNS function [32]. We were prompted to inquire about the extent of MCHR1 localization to primary cilia and whether the observed behavioral effects arise indirectly from cilia or from MCHR1 localized to the cell membrane. Here we aimed to investigate the effect of the timing of ciliary MCHR1 ablation on the localization of MCHR1 to primary cilia and its colocalization with ACY3 cilia in the hippocampus and nucleus accumbens. The percentage of cells expressing ciliary MCHR1, non-ciliary MCHR1, ACY3 cilia, and colocalization of cells expressing both ciliary MCHR1 and ACY3 cilia or non-ciliary MCHR1 and ACY3 cilia was quantified. Control animals showed that ciliary MCHR1 was more abundant in the nucleus accumbens than in the hippocampus, while non-ciliary MCHR1 was more abundant in the hippocampus than in the nucleus accumbens. Additionally, there was more colocalization of ciliary MCHR1 and ACY3 cilia on cells than non-ciliary MCHR1 and ACY3 in both regions of the brain. These findings suggest that the localization of MCHR1 to primary cilia varies across different regions of the brain, however the majority of cilia contain MCHR1. The present study sheds light on the relationship between primary cilia and MCHR1, but it is worth noting that the quantification of ciliary MCHR1 may be subject to some uncertainty. Specifically, we do not know the extent to which MCHR1 is present on cilia versus on the cell membrane, which could affect the accuracy of our measurements. Further research using advanced imaging techniques or other approaches will be needed to clarify the precise localization of MCHR1 in these structures. Taken together,

our results indicate that the disruption of the MCH system interferes with neurodevelopmental processes, which may contribute to the pathogenesis of schizophrenia.

Chapter 7: Future Direction: In vivo and in vitro binding of MCH fragment analogues

Abstract

Mammalian melanin concentrating hormone (MCH) is a neuropeptide produced in the lateral hypothalamus that plays a role in the regulation of feeding behavior and energy homeostasis. Abnormalities in MCH signaling have been associated with a number of physiological and pathological conditions from metabolic dysfunction to depression, anxiety or even schizophrenia-like phenotypes. This project aims to design MCH analogues with improved binding affinity for MCH receptors, which could potentially lead to new therapies. The project will involve both in vitro binding techniques and in vivo intracerebroventricular injection of MCH and MCH analogues in mice, followed by measurement of body weight and analysis of cilia length, which has been shown to mediate MCH-MCHR1 binding. We found an MCH fragment analogue with a reduced number of amino acids and molecular weight showed potential to bind in vivo. This MCH fragment analogue had a potency comparable to the full MCH peptide, and caused cilia shortening in the adult mouse brain, which was reversed when administered with an MCHR1 antagonist. We also found that when administered i.c.v similarly to MCH the mice gained weight and when given simultaneously with an antagonist resulted in weight loss. Overall this study shows the potential of MCH fragment analogues being treatments for ciliopathies or psychiatric disorders and we are testing these peptides in vitro and in vivo in the hope that these can be developed as drugs that cross the blood brain barrier.

Introduction

Mammalian melanin concentrating hormone (MCH) is a cyclic nineteen amino acid neuropeptide found in the brain with the native sequence: Asp-Thr-Met-Arg-Cys-Met-Val-Gly-Arg-Val-Tyr-Arg-Pro-Cys-Trp-Glu-Val[1, 2]. MCH is a neurotransmitter that exerts its action to the endogenous G protein coupled receptor MCHR1 [3]. MCH is highly produced in the lateral hypothalamus and zona incerta and is involved in regulating feeding behavior and energy homeostasis [3-5]. It has been shown to play a role in the regulation of mood, anxiety, and stress [6, 7] and is related to a number of physiological and pathological conditions including obesity, metabolic syndrome, depression, and addiction [8-19]. Melanin-concentrating hormone receptor 1 (MCHR1) localizes to primary cilia in hypothalamic neurons, and thus primary cilia play a role in regulating MCHR1 signaling [20-22]. Primary cilia negatively regulate MCHR1 signaling in hypothalamic neurons, suggesting that disruption of this regulation could contribute to the development of metabolic disorders [23-25]. Studies have injected MCH intracerebroventricularly (i.c.v) and found that there is an increase in food intake and body weight gain[8-13, 26-33]. We have previously found that stimulation of MCH system either directly through MCHR1 activation or indirectly through optogenetic and chemogenetic-mediated excitation of MCH-neuron, caused cilia shortening and inactivation of MCH signaling through pharmacological MCHR1 blockade or through genetic manipulations induced cilia lengthening [21].

MCH is a relatively large molecule, with a molecular weight of about 1.7 kDa and as a result, it is not able to cross the blood-brain barrier (BBB) by passive diffusion, which only allows for the passage of small, lipophilic molecules [34-37]. In addition to its size, MCH is also subject to active transport mechanisms that prevent its entry into the brain[38, 39]. The BBB is lined with specialized cells called endothelial cells, which are tightly connected by tight junctions that restrict the movement of substances between them Studies have shown that MCH is actively transported out of the brain by a protein called P-glycoprotein (P-gp), which is expressed on the luminal side of the BBB endothelial cells [40]. P-gp acts as an efflux pump, actively transporting molecules out

of the brain and back into the bloodstream [41]. This mechanism helps to maintain the concentration of MCH in the brain at a constant level and prevent its accumulation. MCH has been shown to affect the permeability of the BBB and can indirectly influence brain function, however it is not able to cross the BBB itself due to its size and active transport mechanisms [37].

Thus, MCH analogues have been studied for their potential as therapeutic agents in various disease states, including obesity, depression, and addiction [42-44]. In one study, researchers designed a series of MCH analogues with modifications to the C-terminus, which is thought to be important for receptor binding and activation [45]. They found that the modified analogues had enhanced binding affinity and biological activity compared to the native MCH peptide and that elimination of substituents from both the carboxy- and amino-termini while keeping the disulfide linked ring-possessed equipotency to the native sequence. They investigated the effects of modifying specific amino acid residues in the MCH peptide sequence and found that replacing the tryptophan with a phenylalanine residue led to a significant reduction in receptor binding affinity, suggesting that the tryptophan residue is important for MCH receptor binding [4, 44, 45]. A study investigated the effects of an MCH analogue on food intake and body weight in rats and found that the analogue significantly reduced food intake and body weight gain compared to control animals, suggesting that it may have potential as a therapeutic agent for obesity [46]. By identifying specific amino acid residues that are important for receptor binding and activity, we hope to develop MCH analogues that are more selective and potent in their actions, with fewer side effects than existing treatments. The goal of this study is to identify MCH analogues that bind to MCHR1 similarly to MCH in vivo that are smaller and can potentially cross the blood brain barrier.

Materials and Methods

Peptide Synthesis

MCH fragment analogues were designed based on previously published data [4, 44, 45]. The native sequence of MCH in salmonid is the following Asp-Thr-Met-Arg-Cys-Met-Val-Gly-Arg-Val-Tyr-Arg-Pro-Cys-Trp-Glu-Val while the mammalian sequence is as follows Asp-Phe-Asp-Met-Leu-Arg-Cys-Met-Leu-Gly-Arg-Val-Tyr-Arg-Pro-Cys-Trp-Gln-Val. Peptide 1-3 were designed based on the mammalian sequence and peptide 4 was designed based on the salmonid sequence. Following the design, peptides were sequenced via Biosynth. The following sequences are as followed, peptide 1: H-Cys-Tyr-Arg-Pro-Cys-Trp-Gln-Val-OH with the molecular weight: 1052.3, peptide 2: H-Cys-Val-Tyr-Arg-Pro-Cys-Trp-OH with the molecular weight: 924.1, peptide 3: H-Cys-Tyr-Arg-Pro-Cys-Trp-Gln-OH with the molecular weight: 953.1, and peptide 4: H-Cys-Met-Val-Gly-Arg-Val-Tyr-Arg-Pro-Cys-Trp-OH with the molecular weight: 1367.7 (Fig. 7.1).

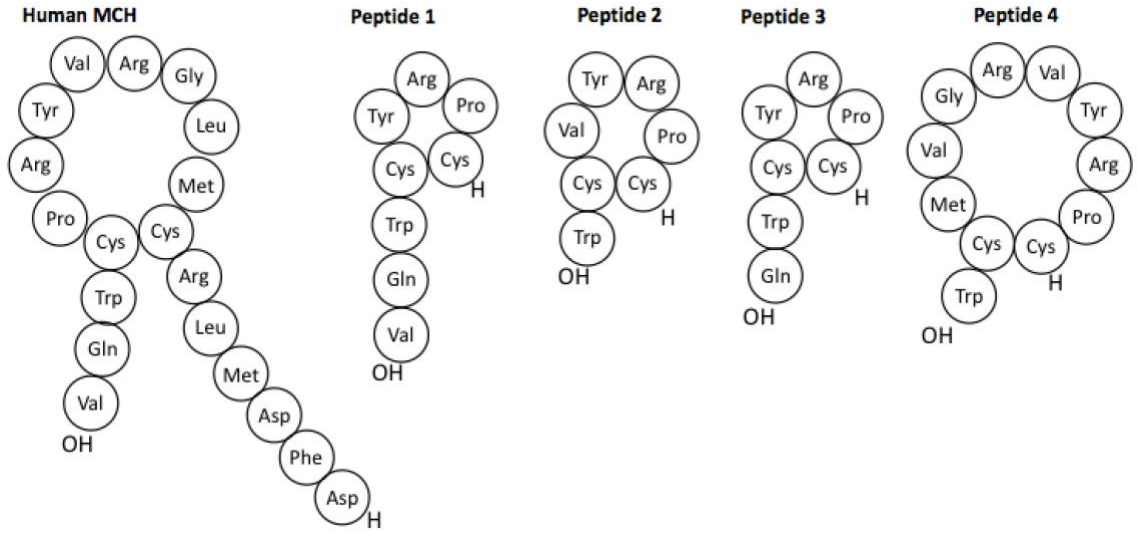

Figure 7.1. Structure of MCH and MCH fragment analogues

(left to right) Human MCH is a 19 amino acid sequence with a disulfide bridge. Peptide 1 is a 8 amino acid sequence with a disulfide bridge and the smallest ring. Peptide 2 is a 7 amino acid sequence with a disulfide bridge and a larger ring. Peptide 3 is a 7 amino acid sequence with a

disulfide bridge and the same ring in peptide 1. Peptide 4 is a 11 amino acid sequence with a disulfide bridge and the largest ring amongst all peptides designed.

Transiently transfected HEK293T cells with MCHR1

pGloSensor-22F cells were transiently transfected with human MCHR1 plasmid using jetPRIME transfection reagent using standard conditions of 1:2 DNA to jetPRIME ration (w/v) for 1 µg of DNA use 2 µg of jetPRIME. After 24 hours of incubation in 37°C with 5-10% CO_2 cells are used in the camp or FLIPR assay.

cAMP assay cells in suspension in 96-well plate format

Cells are washed with PBS, and are detached using 0.05% trypsin. Cells are pelleted and resuspended in CO_2 –independent medium, 10% FBS, and the GloSensor camp reagent. Cells are incubated for 2 hours at room temperature and inverted every 15 minutes to prevent settling of the cells. Cells are then transferred to a 96 well plate and luminescence was measured using the MicroBeta2 2450 Microplate counter. All incubations were done in triplicates. Results were analyzed using an in-house coded cAMP Data Process Analyzer where the maximum peak is averaged among each triplicate ran.

Intracerebroventricular Administration of Peptides

All experimental procedures were approved by the Institutional Animal Care and Use Committee of the University of California, Irvine, and were performed in compliance with national and institutional guidelines for the care and use of laboratory animals. 9-10 week old Swiss Webster mice underwent stereotaxic surgery to implant a stainless steel guide cannula into the lateral ventricles (20 gauge guide cannulas with 2.5-mm custom-cut depth, PlasticsOne). Animals were anesthetized with 2% isoflurane anesthesia (Institutional Animal Care and Use Committee guidelines) and were secured with the stereotaxic instrument. Guide cannula was implanted at -

0.22mm posterior to bregma, 1.0 mm lateral, and 2.3 mm below the skull surface. Post-surgery animals were allowed to recover for one week with a dummy cannula in place before injections. Animals were then infused with vehicle, MCH peptide (1nmol), Peptide 1 (10nmol), or Peptide 1 (10nmol) and GW803430 intraperitoneal (3mg/kg), for 7 consecutive days using a 10 µl Hamilton microsyringe. The dose of MCH was determined by previous reported findings[13, 21, 47, 48]. Following the final injection animals were perfused transcardially under isoflurane anesthesia with saline followed by 4% paraformaldehyde in phosphate buffer saline. Brains were removed and coronal brain sections (30 µm) were cut [21].

Immunohistochemistry

Immunofluorescent staining was carried out as previously reported [21, 49]. Briefly, 11-week-old animals were perfused transcardially under isoflurane anesthesia with saline followed by 4% paraformaldehyde in phosphate buffer saline. Brains were harvested and dissected 30 µm coronally. The MCHR1 deletion was verified by visualizing MCHR1 neurons using rabbit polyclonal anti-MCHR1 antibody (1:200). Primary cilia were stained with ADCY3 goat anti-chicken (1:1000). Three to five sections were selected from each region of interest according to the mouse brain atlas. Nuclei were stained with 4′,6-diamidino-2-phenylindole (DAPI) solution (1:10,000) and mounted with Aqua-mount mounting solution. For each brain, we used four to six non-consecutive sections per region of interest. Quantification of primary cilia was based solely on ADCY3 immunofluorescence positive signals. Cilia were counted in the bilateral areas of each section, and each brain was given one averaged cilia length value for each region. Image acquisition was carried out using a confocal laser microscope. Images were captured using Leica Sp8 TCS confocal microscope (UCI optical biology core facility).

Cilia length automation analysis

Cilia length was measured using FIJI in all cells in each section, and the mean values of three sections per brain of 3–5 brains were calculated. A number of cilia in specific regions of the brain were also counted and referred to as cilia density per field.

Results

MCH and Peptide 1 bind to MCHR1 and inhibit cAMP accumulation

Molecular characterization of MCHR1 has been previously proven to show MCH activates MCHR1 related pathways through both Gαi and/or Gαq proteins and thus using inhibition of forskolin-stimulated camp accumulation in HEK cells transfected with both MCHR1 and pGloSensor induced inhibition of adenylate cyclase when incubated with MCH or Peptide 1 (Fig. 7.2). Varying doses of MCH (0.001 nM, 0.005 nM, 0.01 nM, 0.05 nM, 0.1 nM, 0.5 nM, 1 nM, 5 nM, 10 nM, 50 nM, 100 nM, 500 nM, and 1μM) were tested and plotted as the log of the agonist vs. the response in luminescence (rlu) resulting in an EC50 of 0.4302 to 1.517 nM (Fig. 7.2a) Varying doses of Peptide 1 (0.01 nM, 0.05 nM, 0.1 nM, 0.5 nM, 1 nM, 5 nM, 10 nM, 50 nM, 100 nM, 500 nM, and 1μM) were tested and plotted as the log of the agonist vs. the response in luminescence (rlu) resulting in an EC50 of 6.524 to 25.15 nM (Fig. 7.2b). All peptides were tested for binding in the cAMP assay however peptide 1 showed the best binding and EC50 amongst the 4 tested thus we decided to use peptide 1 for the in vivo studies.

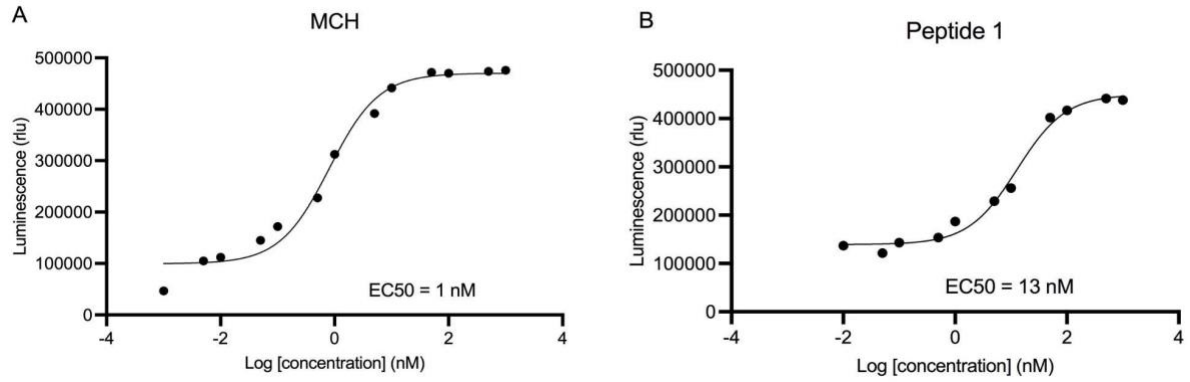

Figure 7.2. cAMP accumulation of MCH and Peptide 1

HEK cells transiently transfected with MCHR1 and pGloSensor induced inhibition of adenylate cyclase when incubated with (A) MCH or (B) Peptide 1 in a dose dependent manner with EC50 respectively at approximately 1 nM and 13 nM.

Intracerebroventricular Administration of MCH and Peptide 1 showed an increase in weight and a decrease in weight when given GW803430

Mice underwent stereotaxic surgery for cannula implantation and were allowed one week to recover. Following the recovery, Mice were administered vehicle, MCH, or Peptide 1 via ICV, while another group was administered Peptide 1 and GW803430 intraperitoneally for 7 days. Mice were weighed from day 0-day 7. Mice given vehicle exhibited on average 0.7 grams of weight gain over 7 days of administration. Mice given MCH exhibited on average 2.4 grams of weight gain over 7 days of administration 2- way ANOVA, adjusted P value< 0.0001) (Bonferroni's multiple comparisons test). Mice given Peptide 1 exhibited on average 2.075 grams of weight gain over 7 days of administration (2- way ANOVA, adjusted P value= 0.0033) (Bonferroni's multiple comparisons test). Mice given Peptide 1 and GW803430 exhibited on average 0.975 grams of weight loss over 7 days of administration (2- way ANOVA, adjusted P value= 0.0048) (Bonferroni's multiple comparisons test) (Fig. 7.3).

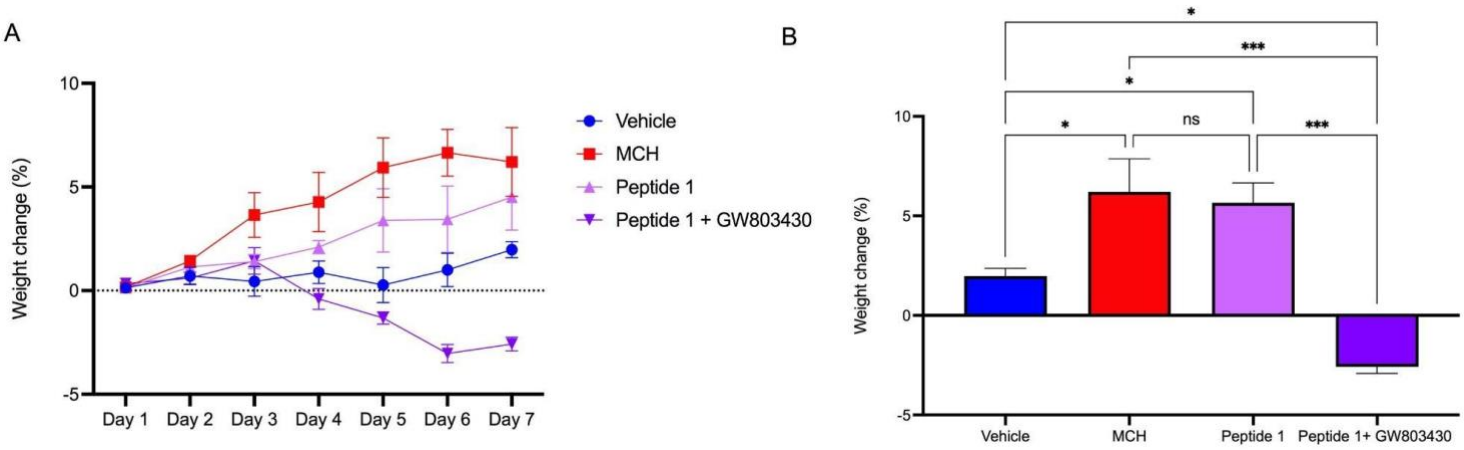

Figure 7.3. Body weight (grams) over 7 days of ICV administration of peptides

A,B. Over 7 days of intracerebroventricular administration of MCH and peptide 1, mice showed a significant increase in body weight (%), while given an MCHR1 antagonist, and peptide 1, mice showed a significant decrease in weight. (2- way ANOVA, adjusted P value< 0.0001, F(18, 77)= 4.493). Mice given MCH (2- way ANOVA, adjusted P value< 0.0001) (Bonferroni's multiple

comparisons test). Mice given Peptide 1 (2- way ANOVA, adjusted P value= 0.0033) (Bonferroni's multiple comparisons test). Mice given Peptide 1 and GW803430 (2- way ANOVA, adjusted P value= 0.0048) (Bonferroni's multiple comparisons test).

MCH and Peptide 1 shorten cilia length and MCHR1 antagonist GW803430 administered with Peptide 1 lengthens cilia in the mouse brain

As previously reported, we confirmed that intracerebroventricular administration of MCH in adult mice for 7 consecutive days caused a 43.5% decrease in the cilia length (2.495 ± 0.4493 μm) in the striatum (CPU) and a 34.3% decrease in cilia length (2.4. ± 0.2283 μm) in the hippocampus (CA1). Intracerebroventricular administration of Peptide 1 in adult mice for 7 consecutive days caused a 43.7% decrease in the cilia length (2.488 ± 0.4493 μm) in the striatum (CPU) and a 33.1% decrease in cilia length (2.441. ± 0.2283 μm) in the hippocampus (CA1). Intracerebroventricular administration of Peptide 1 and intraperitoneal injection of GW803430 in adult mice for 7 consecutive days caused a 52.6% increase in the cilia length (6.742 ± 0.4493 μm) in the striatum (CPU) and a 34% increase in cilia length (4.882 ± 0.2283 μm) in the hippocampus (CA1) (Fig. 7.4).

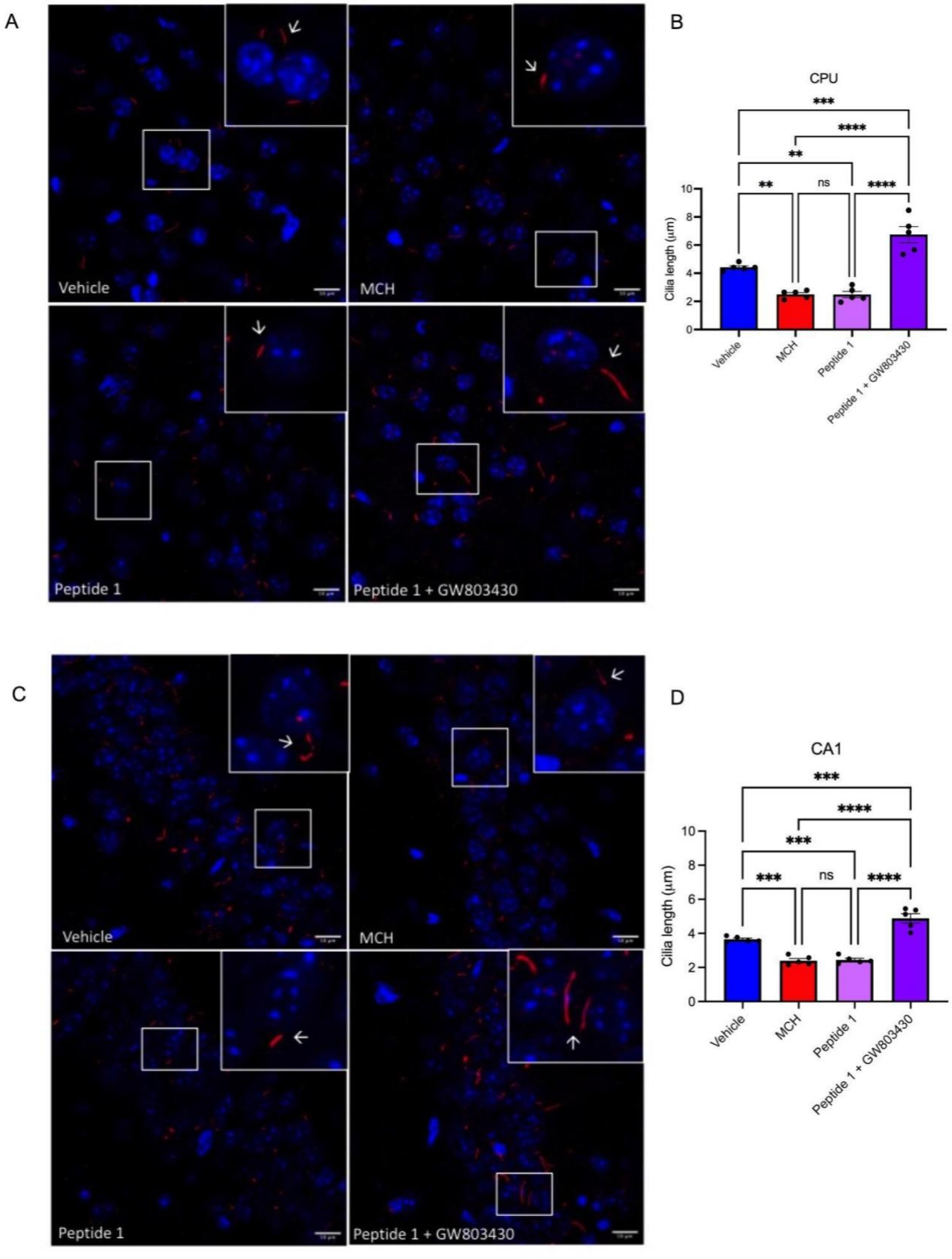
A
Vehicle
MCH
Peptide 1
Peptide 1 + GW803430
B
CPU
Cilia length (µm)
Vehicle
MCH
Peptide 1
Peptide 1 + GW803430
C
Vehicle
MCH
Peptide 1
Peptide 1 + GW803430
D
CA1
Cilia length (µm)
Vehicle
MCH
Peptide 1
Peptide 1 + GW803430

Figure 7.4. Chronic intracerebroventricular administration of MCH and Peptide 1 shorten cilia length and MCHR1 antagonist GW803430 administered with Peptide 1 lengthens cilia

A. Immunostaining of ADCY3 labeled in red fluorescence and counterstained with DAPI (blue) in the CPU in animals administered with MCH or vehicle (scale bar = 50 μm, magnification = 63x) B. Quantification of cilia length (μm) in the CPU in animals administered either vehicle, MCH, Peptide 1, or Peptide 1+GW803430. One way-ANOVA F (3, 16) = 40.42 ****P<0.0001 post hoc Tukey's multiple comparisons test, Vehicle vs. MCH **P=0.0029, Vehicle vs. Peptide 1 **P=0.0028**,** Vehicle vs. Peptide 1 + GW803430 ***P=0.0005, MCH vs. Peptide 1, ns, not significant P>0.9999, MCH vs. Peptide 1 + GW803430, ****P<0.0001, Peptide 1 vs. Peptide 1 + GW803430, ****P<0.0001. C. Immunostaining of ADCY3 labeled in red fluorescence and counterstained with DAPI (blue) in the CA1 in animals administered with MCH or vehicle (scale bar = 50 μm, magnification = 63x) D. Quantification of cilia length (μm) in the CA1 in animals administered either vehicle, MCH, Peptide 1, or Peptide 1+GW803430. One way-ANOVA F (3, 16) = 53.29 ****P<0.0001 post hoc Tukey's multiple comparisons test, Vehicle vs. MCH ***P=0.0003, Vehicle vs. Peptide 1 ***P=0.0004**,** Vehicle vs. Peptide 1 + GW803430 ***P=0.0003, MCH vs. Peptide 1, ns, not significant P>0.9978, MCH vs. Peptide 1 + GW803430, ****P<0.0001, Peptide 1 vs. Peptide 1 + GW803430, ****P<0.0001.

Discussion

In this study we were able to design MCH fragment analogues that proved to bind to MCHR1 both in vitro and in vivo. We first showed that the fragment analogues bind to MCHR1 showing cAMP accumulation in HEK cells transiently transfected with MCHR1. We then demonstrated that the peptide with the most potential to bind in vivo, was one that had (1) a 58% less amino acids comparable to the full MCH peptide, (2) had the smallest cyclic ring that was 50% smaller than the full MCH peptide, (3) was 56% smaller in molecular weight than the full MCH peptide. Although the EC_{50} found was 10 fold greater than MCH, it was still in the nanomolar range which is a great potency considering the alterations made to the original sequence. We took this peptide in vivo to confirm the binding via intracerebroventricular infusion and analyzed binding secondary through the regulation of cilia length as previously proven [21, 49]. Here we confirmed that i.c.v administration of MCH causes cilia shortening in multiple regions in the brain including the CPU and CA1. Similarly, Peptide 1 caused cilia shortening in the adult mouse brain after 7 days of consecutive administration. Interestingly we found that administering Peptide one via i.c.v infusion simultaneously with GW803430 (MCHR1 antagonist) resulted in cilia lengthening in both the CPU and CA1 in adult mouse brains.

Ciliopathies are a group of severe diseases and developmental disorders caused by defects in the assembly, such as cilia shortening, which can lead to neurological deficits like abnormal cortical formation and cognitive deficits [24, 50-54]. Brain cilia genes are differentially expressed in major psychiatric disorders like schizophrenia, autism spectrum disorder, depression, and bipolar disorder [55-57]. In particular, the MCH system, specifically MCHR1, has been shown to play an essential role in the pathophysiology of schizophrenia [58]. Studies have demonstrated that the deletion of MCHR1 and MCH neurons can result in behavioral abnormalities that mimic schizophrenia-like phenotypes, including repetitive behavior, social impairment, impaired sensorimotor gating, and disrupted cognitive functions. Additionally, MCHR1 germline deletion causes alterations in depressive-like behavior that is sex-dependent.

These results suggest that ciliary MCHR1 may play a role in the pathophysiology of psychiatric disorders such as schizophrenia and depression and that cilia elongation could be a possible mechanism through which MCH system dysregulation causes social and cognitive deficits[58]. Thus selective targeting of cilia MCHR1 may offer a novel approach to treat psychiatric disorders, as studies have shown that pharmacological agents like lithium used to treat depression can alter cilia length [59].

MCHR1 belongs to the GPCR family, which forms the largest class of membrane proteins in the human genome with >800 GPCRs [60]. GPCRs contain druggable sites located on the outer cell surface membrane that are accessible to pharmacological agents. The high "druggability" of GPCRs makes these receptors of great interest as pharmacological targets, with approximately 35% of approved drugs target GPCRs so far. The orexigenic actions of MCHR1 have made it an attractive target for treatment of obesity, and for this purpose, several small-molecule MCH1R antagonists were developed and proved to successfully reduce food intake and body weight in preclinical studies [61]. A number of these antagonists were tested in clinical trials [62-64]. However, targeting MCHR1 with pharmacological agents that activate these receptors was never tried. We have an opportunity to use drugs that act on MCHR1 (particularly agonists), to reverse the behavioral deficits previously seen. Previous studies have shown that intracerebroventricular (i.c.v) administration of MCH in the brain reduced, while MCHR1 antagonist (GW3430) increased repetitive behavior, assessed using marble burying test [65]. Furthermore, a recent study showed that intranasal administration of MCH enhanced memory retention and impairment in Alzheimer's mouse models [66]. Therefore, using drugs that act on MCHR1 (particularly MCH peptide like peptide 1 shown in this study), and/or increasing the expression of PMCH and MCHR1 in the brain, may be most effective at reversing the behavioral deficits.

This is a promising study however preliminary and requires more to be done to understand whether peptide 1 is able to cross the blood brain barrier as the reason why no one is using MCH

clinically is because MCH does not readily cross the blood brain barrier [37]. Future work involves doing an intraperitoneal injection of the peptide and testing animals in behavioral assays to see if the deficits of social and cognitive and sensorimotor gating are reversed. We will need to determine an appropriate dose response as well as timing and frequency of injection. If these fail we can also approach this problem by creating small cilia targeted nanoparticles that are loaded with antibody targeting MCHR1 with the delivery of MCH or MCH fragment analogues. This would also allow us to better understand the underlying deficits and provide potential use of MCH fragment analogues to treat ciliopathies or psychiatric disorders such as schizophrenia.

Chapter 8: Conclusions and Perspectives

Recent research has focused on the potential of the melanin-concentrating hormone (MCH) system as a target for the treatment of various diseases. The MCH system is a complex network of neurons and receptors in the brain that has been implicated in regulating a wide range of physiological functions and behaviors, including sleep, feeding, metabolism, reward, anxiety, depression, and learning. This thesis delves into various aspects of cilia, ranging from their links to psychiatric disorders, circadian rhythm, lifespan, Age-Disease Interactions, and timing, to exploring the role of the MCH system in social and cognitive functions in mice. Further we explore the development of MCH fragment analogues that may reverse the deficits seen in ciliopathies and psychiatric disorders.

We first investigated the role of cilia dysfunctions in major psychiatric disorders (SCZ, ASD, BP, MDD) in chapter 2 and found that almost all sub-cilia structural and functional compartments were dysregulated. In SCZ, genes of 75% of cilia GPCRs and 50% of transition zone proteins were differentially expressed. Our findings suggest that cilia components may represent novel therapeutic targets for these disorders and may represent a shared mechanism across them.

Chapter 3 covered the topics of cilia and circadian rhythm. Cilia are sub-cellular systems with coordinated structural and functional components that sense circadian environmental stimuli. Using computational methods and primate brain gene expression atlas, we found that around 73% of cilia transcripts exhibited circadian rhythmicity across 22 brain regions, with 12 regions significantly enriched with circadian oscillating transcripts. The basal ganglia-cortical circuit and motor control appear to be dependent on spatiotemporal orchestration of cilia genes, particularly in SUN, PUT, LGP, and MGP. Dysregulation of cilia genes may contribute to neurological and psychiatric disorders. Further mechanistic studies are needed to understand cilia rhythmicity and its effects on brain circuits and behaviors.

Our study in Chapter 4 provides a novel discovery that highlights the role of the melanin-concentrating hormone (MCH) system in regulating the length of primary cilia in the brain. This finding establishes a crucial link between the modulation of G protein-coupled receptors and the regulation of cilia length, shedding new light on the intricate mechanisms governing ciliary function. The study suggests that ciliary MCHR1 could be a potential therapeutic target for treating pathological conditions that involve impaired cilia function. In conclusion, the study establishes the causal regulatory effects of the MCH system signaling on cilia length, which is significant because it provides new insights into the mechanisms of cilia regulation and identifies a potential therapeutic target for treating cilia-related pathological conditions.

Chapter 5 involved an in-depth analysis of the function of cilia in the striatum. Cilia are microtubule-based organelles found in almost all brain cells that act as sensory hubs to generate an appropriate cellular response. The striatum, a brain structure enriched in cilia, receives and integrates various types of environmental information to drive appropriate motor response. Our study using mice with ablated cilia in the dorsal striatum found that cilia play an essential role in learning new motor skills and time perception, but not in maintaining habitual/learned motor skills. These findings suggest that dysfunctional cilia may contribute to the pathophysiology of neuro-psychiatric disorders related to deficits in timing perception. Our study highlights the potential importance of striatal cilia in timing-dependent functions and could lead to new therapeutic approaches targeting cilia.

Chapter 6 of our study centered on investigating the function of ciliary MCHR1, a G protein-coupled receptor that is expressed in primary cilia of specific neurons, in relation to social and cognitive impairments. Using an inducible knockout model of ciliary MCHR1, we found that its deletion resulted in normal sociability but an increase in hyperactivity, deficits in cognition, and sensorimotor gating. The timing of the deletion had an impact on the behavioral outcomes, with late deletion causing hyperactivity and deficits in cognition and sensorimotor gating, while early

deletion resulted in deficits in both social and cognitive function and sensorimotor gating. We also found that ciliary MCHR1 levels were significantly reduced in knockout mice, supporting the idea that it is crucial for proper primary cilia functioning. These findings suggest that targeting ciliary MCHR1 at specific ages may be a potential therapeutic strategy for treating the social and cognitive deficits associated with schizophrenia.

In the conclusive Chapter 7, our primary aim was to advance the development of therapeutic interventions through the design of analogues of melanin-concentrating hormone (MCH) that exhibit superior binding affinity for MCH receptors. In vitro and in vivo experiments were conducted to measure the binding potency of MCH analogues and their effects on cilia length and body weight. An MCH fragment analogue showed potential to bind in vivo and caused cilia shortening, which was reversed with an MCHR1 antagonist. Additionally, the analogue resulted in weight gain when administered alone, but weight loss when given with an antagonist. These findings suggest that MCH fragment analogues could be potential treatments for ciliopathies or psychiatric disorders.

GPCRs are highly druggable targets, with around 30–40% of drugs available in the market and the vast majority of therapeutic strategies for psychiatric disorders targeting GPCRs. Therefore, the developments of cilia-associated GPCRs targeted drug delivery might lead to novel treatments or prevention strategies for cilia-associated psychiatric and neurological disorders, should the treatments be administered at the proper age. Although there are some shortcomings in the research done and many challenges that still need to be pursued, the MCH system and the development of novel pharmacotherapies targeting this system holds great promise for the treatment of a variety of diseases, including ciliopathies and psychiatric disorders. Further research is needed to fully understand the complex interplay between the MCH system and ciliary signaling pathways and to develop safe and effective drugs that can target this system specifically. Nevertheless, these findings offer new hope for patients with ciliopathies and highlight the potential for MCHR1 as a therapeutic target in the treatment of these debilitating conditions.

References

Chapter 1 References

1. Fitzsimons LA, Brewer VL, Tucker KL: **Hedgehog Morphogens Act as Growth Factors Critical to Pre- and Postnatal Cardiac Development and Maturation: How Primary Cilia Mediate Their Signal Transduction**.*Cells* 2022, **11**(12).

2. Wachten D, Mick DU: **Signal transduction in primary cilia - analyzing and manipulating GPCR and second messenger signaling**. *Pharmacol Ther* 2021, **224**:107836.

3. Shao YY, Wang L, Welter JF, Ballock RT: **Primary cilia modulate Ihh signal transduction in response to hydrostatic loading of growth plate chondrocytes**. *Bone* 2012, **50**(1):79-84.

4. Kim HR, Richardson J, van Eeden F, Ingham PW: **Gli2a protein localization reveals a role for Iguana/DZIP1 in primary ciliogenesis and a dependence of Hedgehog signal transduction on primary cilia in the zebrafish**. *BMC Biol* 2010, **8**:65.

5. Armengot M, Milara J, Mata M, Carda C, Cortijo J: **Cilia motility and structure in primary and secondary ciliary dyskinesia**. *Am J Rhinol Allergy* 2010, **24**(3):175-180.

6. Bennett HW, Gustavsson AK, Bayas CA, Petrov PN, Mooney N, Moerner WE, Jackson PK: **Novel fibrillar structure in the inversin compartment of primary cilia revealed by 3D single-molecule superresolution microscopy**. *Mol Biol Cell* 2020, **31**(7):619-639.

7. Kiesel P, Alvarez Viar G, Tsoy N, Maraspini R, Gorilak P, Varga V, Honigmann A, Pigino G: **The molecular structure of mammalian primary cilia revealed by cryo-electron tomography**. *Nat Struct Mol Biol* 2020, **27**(12):1115-1124.

8. McMurray RJ, Wann AK, Thompson CL, Connelly JT, Knight MM: **Surface topography regulates wnt signaling through control of primary cilia structure in mesenchymal stem cells**. *Sci Rep* 2013, **3**:3545.

9. Poole CA, Jensen CG, Snyder JA, Gray CG, Hermanutz VL, Wheatley DN: **Confocal analysis of primary cilia structure and colocalization with the Golgi apparatus in chondrocytes and aortic smooth muscle cells**. *Cell Biol Int* 1997, **21**(8):483-494.

10. Ta CM, Vien TN, Ng LCT, DeCaen PG: **Structure and function of polycystin channels in primary cilia**. *Cell Signal* 2020, **72**:109626.

11. Vorobyeva AG, Saunders AJ: **Amyloid-beta interrupts canonical Sonic hedgehog signaling by distorting primary cilia structure**. *Cilia* 2018, **7**:5.

12. Lee JH, Gleeson JG: **The role of primary cilia in neuronal function**. *Neurobiol Dis* 2010, **38**(2):167-172.

13. Grisanti L, Revenkova E, Gordon RE, Iomini C: **Primary cilia maintain corneal epithelial homeostasis by regulation of the Notch signaling pathway**. *Development* 2016, **143**(12):2160-2171.

14. Bishop GA, Berbari NF, Lewis J, Mykytyn K: **Type III adenylyl cyclase localizes to primary cilia throughout the adult mouse brain**. *J Comp Neurol* 2007, **505**(5):562-571.

15. Sipos E, Komoly S, Acs P: **Quantitative Comparison of Primary Cilia Marker Expression and Length in the Mouse Brain**. *J Mol Neurosci* 2018, **64**(3):397-409.

16. Song Q, Gleeson JG: **Primary Cilia and Brain Wiring, Connecting the Dots**. *Dev Cell* 2019, **51**(6):661-663.

17. Sterpka A, Chen X: **Neuronal and astrocytic primary cilia in the mature brain**. *Pharmacol Res* 2018, **137**:114-121.

18. Tereshko L, Turrigiano GG, Sengupta P: **Primary cilia in the postnatal brain: Subcellular compartments for organizing neuromodulatory signaling**. *Curr Opin Neurobiol* 2022, **74**:102533.

19. Paridaen JT, Huttner WB, Wilsch-Brauninger M: **Analysis of primary cilia in the developing mouse brain**. *Methods Cell Biol* 2015, **127**:93-129.

20. Park SM, Jang HJ, Lee JH: **Roles of Primary Cilia in the Developing Brain**. *Front Cell Neurosci* 2019, **13**:218.

21. Green JA, Mykytyn K: **Neuronal primary cilia: an underappreciated signaling and sensory organelle in the brain**. *Neuropsychopharmacology* 2014, **39**(1):244-245.

22. Guemez-Gamboa A, Coufal NG, Gleeson JG: **Primary cilia in the developing and mature brain**. *Neuron* 2014, **82**(3):511-521.

23. Huang JG, Shen CB, Wu WB, Ren JW, Xu L, Liu S, Yang Q: **Primary cilia mediate sonic hedgehog signaling to regulate neuronal-like differentiation of bone mesenchymal stem cells for resveratrol induction in vitro**. *J Neurosci Res* 2014, **92**(5):587-596.

24. Sasai N, Briscoe J: **Primary cilia and graded Sonic Hedgehog signaling**. *Wiley Interdiscip Rev Dev Biol* 2012, **1**(5):753-772.

25. Breunig JJ, Sarkisian MR, Arellano JI, Morozov YM, Ayoub AE, Sojitra S, Wang B, Flavell RA, Rakic P, Town T: **Primary cilia regulate hippocampal neurogenesis by mediating sonic hedgehog signaling**. *Proc Natl Acad Sci U S A* 2008, **105**(35):13127-13132.

26. Carballo GB, Honorato JR, de Lopes GPF, Spohr T: **A highlight on Sonic hedgehog pathway**. *Cell Commun Signal* 2018, **16**(1):11.

27. Martin A, Hedinger C, Haberlin-Jakob M, Walt H: **Structure and motility of primary cilia in the follicular epithelium of the human thyroid**. *Virchows Arch B Cell Pathol Incl Mol Pathol* 1988, **55**(3):159-166.

28. Shiba D, Takamatsu T, Yokoyama T: **Primary cilia of inv/inv mouse renal epithelial cells sense physiological fluid flow: bending of primary cilia and Ca2+ influx**. *Cell Struct Funct* 2005, **30**(2):93-100.

29. Raychowdhury MK, McLaughlin M, Ramos AJ, Montalbetti N, Bouley R, Ausiello DA, Cantiello HF: **Characterization of single channel currents from primary cilia of renal epithelial cells**. *J Biol Chem* 2005, **280**(41):34718-34722.

30. Zhang MZ, Mai W, Li C, Cho SY, Hao C, Moeckel G, Zhao R, Kim I, Wang J, Xiong H *et al*: **PKHD1 protein encoded by the gene for autosomal recessive polycystic kidney disease associates with basal bodies and primary cilia in renal epithelial cells**. *Proc Natl Acad Sci U S A* 2004, **101**(8):2311-2316.

31. Ocbina PJ, Eggenschwiler JT, Moskowitz I, Anderson KV: **Complex interactions between genes controlling trafficking in primary cilia**. *Nat Genet* 2011, **43**(6):547-553.

32. Westlake CJ, Baye LM, Nachury MV, Wright KJ, Ervin KE, Phu L, Chalouni C, Beck JS, Kirkpatrick DS, Slusarski DC *et al*: **Primary cilia membrane assembly is initiated by Rab11 and transport protein particle II (TRAPPII) complex-dependent trafficking of Rabin8 to the centrosome**. *Proc Natl Acad Sci U S A* 2011, **108**(7):2759-2764.

33. Mukhopadhyay S, Wen X, Chih B, Nelson CD, Lane WS, Scales SJ, Jackson PK: **TULP3 bridges the IFT-A complex and membrane phosphoinositides to promote trafficking of G protein-coupled receptors into primary cilia**. *Genes Dev* 2010, **24**(19):2180-2193.

34. Miyamoto T, Hosoba K, Ochiai H, Royba E, Izumi H, Sakuma T, Yamamoto T, Dynlacht BD, Matsuura S: **The Microtubule-Depolymerizing Activity of a Mitotic Kinesin Protein KIF2A Drives Primary Cilia Disassembly Coupled with Cell Proliferation**. *Cell Rep* 2015, **10**(5):664-673.

35. Verhey KJ, Dishinger J, Kee HL: **Kinesin motors and primary cilia**. *Biochem Soc Trans* 2011, **39**(5):1120-1125.

36. Kathem SH, Mohieldin AM, Nauli SM: **The Roles of Primary cilia in Polycystic Kidney Disease**. *AIMS Mol Sci* 2014, **1**(1):27-46.

37. Sun C, Zhou J, Meng X: **Primary cilia in retinal pigment epithelium development and diseases**. *J Cell Mol Med* 2021, **25**(19):9084-9088.

38. Smith CEL, Lake AVR, Johnson CA: **Primary Cilia, Ciliogenesis and the Actin Cytoskeleton: A Little Less Resorption, A Little More Actin Please**. *Front Cell Dev Biol* 2020, **8**:622822.

39. Han YG, Spassky N, Romaguera-Ros M, Garcia-Verdugo JM, Aguilar A, Schneider-Maunoury S, Alvarez-Buylla A: **Hedgehog signaling and primary cilia are required for the formation of adult neural stem cells**. *Nat Neurosci* 2008, **11**(3):277-284.

40. Cano DA, Sekine S, Hebrok M: **Primary cilia deletion in pancreatic epithelial cells results in cyst formation and pancreatitis**. *Gastroenterology* 2006, **131**(6):1856-1869.

41. Oishi I, Kawakami Y, Raya A, Callol-Massot C, Izpisua Belmonte JC: **Regulation of primary cilia formation and left-right patterning in zebrafish by a noncanonical Wnt signaling mediator, duboraya**. *Nat Genet* 2006, **38**(11):1316-1322.

42. Esteban MA, Harten SK, Tran MG, Maxwell PH: **Formation of primary cilia in the renal epithelium is regulated by the von Hippel-Lindau tumor suppressor protein**. *J Am Soc Nephrol* 2006, **17**(7):1801-1806.

43. Karalis V, Donovan KE, Sahin M: **Primary Cilia Dysfunction in Neurodevelopmental Disorders beyond Ciliopathies**. *J Dev Biol* 2022, **10**(4).

44. Horani A, Ferkol TW: **Primary ciliary dyskinesia and associated sensory ciliopathies**. *Expert Rev Respir Med* 2016, **10**(5):569-576.

45. Devlin LA, Sayer JA: **Renal ciliopathies**. *Curr Opin Genet Dev* 2019, **56**:49-60.

46. Guo J, Higginbotham H, Li J, Nichols J, Hirt J, Ghukasyan V, Anton ES: **Developmental disruptions underlying brain abnormalities in ciliopathies**. *Nat Commun* 2015, **6**:7857.

47. Gudis DA, Cohen NA: **Cilia dysfunction**. *Otolaryngol Clin North Am* 2010, **43**(3):461-472, vii.

48. Lechtreck KF: **IFT-Cargo Interactions and Protein Transport in Cilia**. *Trends Biochem Sci* 2015, **40**(12):765-778.

49. Shi L, Shi X, Shen Y: **Intraflagellar transport 46 (IFT46) is essential for trafficking IFT proteins between cilia and cytoplasm in Paramecium**. *Sci Rep* 2018, **8**(1):9259.

50. Krock BL, Perkins BD: **The intraflagellar transport protein IFT57 is required for cilia maintenance and regulates IFT-particle-kinesin-II dissociation in vertebrate photoreceptors**. *J Cell Sci* 2008, **121**(11):1907-1915.

51. Scholey JM: **Kinesin-2 motors transport IFT-particles, dyneins and tubulin subunits to the tips of Caenorhabditis elegans sensory cilia: relevance to vision research?** *Vision Res* 2012, **75**:44-52.

52. Brewer KM, Brewer KK, Richardson NC, Berbari NF: **Neuronal cilia in energy homeostasis**. *Front Cell Dev Biol* 2022, **10**:1082141.

53. Berbari NF, Bishop GA, Askwith CC, Lewis JS, Mykytyn K: **Hippocampal neurons possess primary cilia in culture**. *J Neurosci Res* 2007, **85**(5):1095-1100.

54. Khan SS, Sobu Y, Dhekne HS, Tonelli F, Berndsen K, Alessi DR, Pfeffer SR: **Pathogenic LRRK2 control of primary cilia and Hedgehog signaling in neurons and astrocytes of mouse brain**. *Elife* 2021, **10**.

55. Armato U, Chakravarthy B, Pacchiana R, Whitfield JF: **Alzheimer's disease: an update of the roles of receptors, astrocytes and primary cilia (review)**. *Int J Mol Med* 2013, **31**(1):3-10.

56. Ki SM, Jeong HS, Lee JE: **Primary Cilia in Glial Cells: An Oasis in the Journey to Overcoming Neurodegenerative Diseases**. *Front Neurosci* 2021, **15**:736888.

57. Munoz-Estrada J, Lora-Castellanos A, Meza I, Alarcon Elizalde S, Benitez-King G: **Primary cilia formation is diminished in schizophrenia and bipolar disorder: A possible marker for these psychiatric diseases**. *Schizophr Res* 2018, **195**:412-420.

58. Bisgrove BW, Yost HJ: **The roles of cilia in developmental disorders and disease**. *Development* 2006, **133**(21):4131-4143.

59. Alhassen W, Chen S, Vawter M, Robbins BK, Nguyen H, Myint TN, Saito Y, Schulmann A, Nauli SM, Civelli O *et al*: **Patterns of cilia gene dysregulations in major psychiatric disorders**. *Prog Neuropsychopharmacol Biol Psychiatry* 2021, **109**:110255.

60. Andreu-Cervera A, Catala M, Schneider-Maunoury S: **Cilia, ciliopathies and hedgehog-related forebrain developmental disorders**. *Neurobiol Dis* 2021, **150**:105236.

61. Pruski M, Lang B: **Primary Cilia-An Underexplored Topic in Major Mental Illness**. *Front Psychiatry* 2019, **10**:104.

62. Migliavacca E, Golzio C, Mannik K, Blumenthal I, Oh EC, Harewood L, Kosmicki JA, Loviglio MN, Giannuzzi G, Hippolyte L *et al*: **A Potential Contributory Role for Ciliary Dysfunction in the 16p11.2 600 kb BP4-BP5 Pathology**. *Am J Hum Genet* 2015, **96**(5):784-796.

63. Marchisella F, Coffey ET, Hollos P: **Microtubule and microtubule associated protein anomalies in psychiatric disease**. *Cytoskeleton (Hoboken)* 2016, **73**(10):596-611.

64. Toropova K, Zalyte R, Mukhopadhyay AG, Mladenov M, Carter AP, Roberts AJ: **Structure of the dynein-2 complex and its assembly with intraflagellar transport trains**. *Nat Struct Mol Biol* 2019, **26**(9):823-829.

65. Asante D, Stevenson NL, Stephens DJ: **Subunit composition of the human cytoplasmic dynein-2 complex**. *J Cell Sci* 2014, **127**(Pt 21):4774-4787.

66. Harrison PJ: **Recent genetic findings in schizophrenia and their therapeutic relevance**. *J Psychopharmacol* 2015, **29**(2):85-96.

67. Yuan S, Sun Z: **Expanding horizons: ciliary proteins reach beyond cilia**. *Annu Rev Genet* 2013, **47**:353-376.

68. Trulioff A, Ermakov A, Malashichev Y: **Primary Cilia as a Possible Link between Left-Right Asymmetry and Neurodevelopmental Diseases**. *Genes (Basel)* 2017, **8**(2).

69. Berbari NF, O'Connor AK, Haycraft CJ, Yoder BK: **The primary cilium as a complex signaling center**. *Curr Biol* 2009, **19**(13):R526-535.

70. Schmidt S, Luecken MD, Trumbach D, Hembach S, Niedermeier KM, Wenck N, Pflugler K, Stautner C, Bottcher A, Lickert H *et al*: **Primary cilia and SHH signaling impairments in human and mouse models of Parkinson's disease**. *Nat Commun* 2022, **13**(1):4819.

71. Bae JE, Kang GM, Min SH, Jo DS, Jung YK, Kim K, Kim MS, Cho DH: **Primary cilia mediate mitochondrial stress responses to promote dopamine neuron survival in a Parkinson's disease model**. *Cell Death Dis* 2019, **10**(12):952.

72. Dhekne HS, Yanatori I, Gomez RC, Tonelli F, Diez F, Schule B, Steger M, Alessi DR, Pfeffer SR: **A pathway for Parkinson's Disease LRRK2 kinase to block primary cilia and Sonic hedgehog signaling in the brain**. *Elife* 2018, **7**.

73. Nguyen VTT, Brucker L, Volz AK, Baumgartner JC, Dos Santos Guilherme M, Valeri F, May-Simera H, Endres K: **Primary Cilia Structure Is Prolonged in Enteric Neurons of 5xFAD Alzheimer's Disease Model Mice**. *Int J Mol Sci* 2021, **22**(24).

74. Karunakaran KB, Chaparala S, Lo CW, Ganapathiraju MK: **Cilia interactome with predicted protein-protein interactions reveals connections to Alzheimer's disease, aging and other neuropsychiatric processes**. *Sci Rep* 2020, **10**(1):15629.

75. Hu L, Wang B, Zhang Y: **Serotonin 5-HT6 receptors affect cognition in a mouse model of Alzheimer's disease by regulating cilia function**. *Alzheimers Res Ther* 2017, **9**(1):76.

76. Ma R, Kutchy NA, Chen L, Meigs DD, Hu G: **Primary cilia and ciliary signaling pathways in aging and age-related brain disorders**. *Neurobiol Dis* 2022, **163**:105607.

77. Rondanino C, Poland PA, Kinlough CL, Li H, Rbaibi Y, Myerburg MM, Al-bataineh MM, Kashlan OB, Pastor-Soler NM, Hallows KR *et al*: **Galectin-7 modulates the length of the primary cilia and wound repair in polarized kidney epithelial cells**. *Am J Physiol Renal Physiol* 2011, **301**(3):F622-633.

78. Chen HY, Kelley RA, Li T, Swaroop A: **Primary cilia biogenesis and associated retinal ciliopathies**. *Semin Cell Dev Biol* 2021, **110**:70-88.

79. Mustafa R, Rawas C, Mannal N, Kreiner G, Spittau B, Kaminska K, Yilmaz R, Potschke C, Kirsch J, Liss B *et al*: **Targeted Ablation of Primary Cilia in Differentiated Dopaminergic Neurons Reduces Striatal Dopamine and Responsiveness to Metabolic Stress**. *Antioxidants (Basel)* 2021, **10**(8).

80. Chen S, Alhassen W, Vakil Monfared R, Vachirakorntong B, Nauli SM, Baldi P, Alachkar A: **Dynamic Changes of Brain Cilia Transcriptomes across the Human Lifespan**. *Int J Mol Sci* 2021, **22**(19).

81. Mosko SS, Moore RY: **Neonatal suprachiasmatic nucleus lesions: effects on the development of circadian rhythms in the rat**. *Brain Res* 1979, **164**:17-38.

82. Nunez AA, Casati MJ: **The role of efferent connections of the suprachiasmatic nucleus in the control of circadian rhythms**. *Behav Neural Biol* 1979, **25**(2):263-267.

83. Van den Pol AN, Powley T: **A fine-grained anatomical analysis of the role of the rat suprachiasmatic nucleus in circadian rhythms of feeding and drinking**. *Brain Res* 1979, **160**(2):307-326.

84. Ibuka N, Kawamura H: **Loss of circadian rhythm in sleep-wakefulness cycle in the rat by suprachiasmatic nucleus lesions**. *Brain Res* 1975, **96**(1):76-81.

85. Kim M, de la Pena JB, Cheong JH, Kim HJ: **Neurobiological Functions of the Period Circadian Clock 2 Gene, Per2**. *Biomol Ther (Seoul)* 2018, **26**(4):358-367.

86. Lipton JO, Yuan ED, Boyle LM, Ebrahimi-Fakhari D, Kwiatkowski E, Nathan A, Guttler T, Davis F, Asara JM, Sahin M: **The Circadian Protein BMAL1 Regulates Translation in Response to S6K1-Mediated Phosphorylation**. *Cell* 2015, **161**(5):1138-1151.

87. Richards J, Gumz ML: **Advances in understanding the peripheral circadian clocks**. *FASEB J* 2012, **26**(9):3602-3613.

88. Noguchi T, Wang CW, Pan H, Welsh DK: **Fibroblast circadian rhythms of PER2 expression depend on membrane potential and intracellular calcium**. *Chronobiol Int* 2012, **29**(6):653-664.

89. Vallarino M, Bruzzone F, Vaudry H: **Neuroanatomical distribution of MCH in the brain and pituitary of submammalian vertebrates**. *Peptides* 2009, **30**(11):1973-1978.

90. Kawauchi H, Kawazoe I, Tsubokawa M, Kishida M, Baker BI: **Characterization of melanin-concentrating hormone in chum salmon pituitaries**. *Nature* 1983, **305**(5932):321-323.

91. Chambers J, Ames RS, Bergsma D, Muir A, Fitzgerald LR, Hervieu G, Dytko GM, Foley JJ, Martin J, Liu WS *et al*: **Melanin-concentrating hormone is the cognate ligand for the orphan G-protein-coupled receptor SLC-1**. *Nature* 1999, **400**(6741):261-265.

92. Bittencourt JC, Elias CF: **Melanin-concentrating hormone and neuropeptide EI projections from the lateral hypothalamic area and zona incerta to the medial septal nucleus and spinal cord: a study using multiple neuronal tracers**. *Brain Res* 1998, **805**(1-2):1-19.

93. Zhang Q, Yuan CF, Wu MJ, Wang YG, Qin Q, Shi YY, Liu GL, Song FZ: **Comparative proteomic analysis of proteins influenced by melanin-concentrating hormone and melanin-concentrating hormone receptor 2 interaction**. *Horm Metab Res* 2010, **42**(7):521-527.

94. Mizusawa K, Saito Y, Wang Z, Kobayashi Y, Matsuda K, Takahashi A: **Molecular cloning and expression of two melanin-concentrating hormone receptors in goldfish**. *Peptides* 2009, **30**(11):1990-1996.

95. Bittencourt JC, Presse F, Arias C, Peto C, Vaughan J, Nahon JL, Vale W, Sawchenko PE: **The melanin-concentrating hormone system of the rat brain: an immuno- and hybridization histochemical characterization**. *J Comp Neurol* 1992, **319**(2):218-245.

96. Torterolo P, Scorza C, Lagos P, Urbanavicius J, Benedetto L, Pascovich C, Lopez-Hill X, Chase MH, Monti JM: **Melanin-Concentrating Hormone (MCH): Role in REM Sleep and Depression**. *Front Neurosci* 2015, **9**:475.

97. Qu D, Ludwig DS, Gammeltoft S, Piper M, Pelleymounter MA, Cullen MJ, Mathes WF, Przypek R, Kanarek R, Maratos-Flier E: **A role for melanin-concentrating hormone in the central regulation of feeding behaviour**. *Nature* 1996, **380**(6571):243-247.

98. Rossi M, Choi SJ, O'Shea D, Miyoshi T, Ghatei MA, Bloom SR: **Melanin-concentrating hormone acutely stimulates feeding, but chronic administration has no effect on body weight**. *Endocrinology* 1997, **138**(1):351-355.

99. Lord MN, Subramanian K, Kanoski SE, Noble EE: **Melanin-concentrating hormone and food intake control: Sites of action, peptide interactions, and appetition**. *Peptides* 2021, **137**:170476.

100. Miyamoto-Matsubara M, Chung S, Saito Y: **Functional interaction of regulator of G protein signaling-2 with melanin-concentrating hormone receptor 1**. *Ann N Y Acad Sci* 2010, **1200**:112-119.

101. Verret L, Goutagny R, Fort P, Cagnon L, Salvert D, Leger L, Boissard R, Salin P, Peyron C, Luppi PH: **A role of melanin-concentrating hormone producing neurons in the central regulation of paradoxical sleep**. *BMC Neurosci* 2003, **4**:19.

102. Modirrousta M, Mainville L, Jones BE: **Orexin and MCH neurons express c-Fos differently after sleep deprivation vs. recovery and bear different adrenergic receptors**. *Eur J Neurosci* 2005, **21**(10):2807-2816.

103. Mieda M, Willie JT, Hara J, Sinton CM, Sakurai T, Yanagisawa M: **Orexin peptides prevent cataplexy and improve wakefulness in an orexin neuron-ablated model of narcolepsy in mice**. *Proc Natl Acad Sci U S A* 2004, **101**(13):4649-4654.

104. Sherwood A, Wosiski-Kuhn M, Nguyen T, Holland PC, Lakaye B, Adamantidis A, Johnson AW: **The role of melanin-concentrating hormone in conditioned reward learning**. *Eur J Neurosci* 2012, **36**(8):3126-3133.

105. Georgescu D, Sears RM, Hommel JD, Barrot M, Bolanos CA, Marsh DJ, Bednarek MA, Bibb JA, Maratos-Flier E, Nestler EJ *et al*: **The hypothalamic neuropeptide melanin-concentrating hormone acts in the nucleus accumbens to modulate feeding behavior and forced-swim performance**. *J Neurosci* 2005, **25**(11):2933-2940.

106. Chung S, Hopf FW, Nagasaki H, Li CY, Belluzzi JD, Bonci A, Civelli O: **The melanin-concentrating hormone system modulates cocaine reward**. *Proc Natl Acad Sci U S A* 2009, **106**(16):6772-6777.

107. Ruiz-Viroga V, de Ceglia M, Morelli L, Castano EM, Calvo EB, Suarez J, Rodriguez de Fonseca F, Galeano P, Lagos P: **Acute intrahippocampal administration of melanin-concentrating hormone impairs memory consolidation and decreases the expression of MCHR-1 and TrkB receptors**. *Prog Neuropsychopharmacol Biol Psychiatry* 2023, **123**:110703.

108. Vawter MP, Schulmann A, Alhassen L, Alhassen W, Hamzeh AR, Sakr J, Pauluk L, Yoshimura R, Wang X, Dai Q *et al*: **Melanin Concentrating Hormone Signaling Deficits in Schizophrenia: Association With Memory and Social Impairments and Abnormal Sensorimotor Gating**. *Int J Neuropsychopharmacol* 2020, **23**(1):53-65.

109. Oh ST, Liu QF, Jeong HJ, Lee S, Samidurai M, Jo J, Pak SC, Park HJ, Kim J, Jeon S: **Nasal Cavity Administration of Melanin-Concentrating Hormone Improves Memory Impairment in Memory-Impaired and Alzheimer's Disease Mouse Models**. *Mol Neurobiol* 2019, **56**(12):8076-8086.

110. Le Barillier L, Leger L, Luppi PH, Fort P, Malleret G, Salin PA: **Genetic deletion of melanin-concentrating hormone neurons impairs hippocampal short-term synaptic plasticity and hippocampal-dependent forms of short-term memory**. *Hippocampus* 2015, **25**(11):1361-1373.

111. Adamantidis A, de Lecea L: **A role for Melanin-Concentrating Hormone in learning and memory**. *Peptides* 2009, **30**(11):2066-2070.

112. Varas M, Perez M, Monzon ME, de Barioglio SR: **Melanin-concentrating hormone, hippocampal nitric oxide levels and memory retention**. *Peptides* 2002, **23**(12):2213-2221.

113. Monzon ME, de Souza MM, Izquierdo LA, Izquierdo I, Barros DM, de Barioglio SR: **Melanin-concentrating hormone (MCH) modifies memory retention in rats**. *Peptides* 1999, **20**(12):1517-1519.

114. Bittencourt JC, Frigo L, Rissman RA, Casatti CA, Nahon JL, Bauer JA: **The distribution of melanin-concentrating hormone in the monkey brain (Cebus apella)**. *Brain Res* 1998, **804**(1):140-143.

115. Borowsky B, Durkin MM, Ogozalek K, Marzabadi MR, DeLeon J, Lagu B, Heurich R, Lichtblau H, Shaposhnik Z, Daniewska I *et al*: **Antidepressant, anxiolytic and anorectic effects of a melanin-concentrating hormone-1 receptor antagonist**. *Nat Med* 2002, **8**(8):825-830.

116. Smith DG, Davis RJ, Rorick-Kehn L, Morin M, Witkin JM, McKinzie DL, Nomikos GG, Gehlert DR: **Melanin-concentrating hormone-1 receptor modulates neuroendocrine, behavioral,**

and corticolimbic neurochemical stress responses in mice. *Neuropsychopharmacology* 2006, **31**(6):1135-1145.

117. Reinecke A, Hoyer J, Rinck M, Becker ES: **Cognitive-behavioural therapy reduces unwanted thought intrusions in generalized anxiety disorder**. *J Behav Ther Exp Psychiatry* 2013, **44**(1):1-6.

118. Elias CF, Sita LV, Zambon BK, Oliveira ER, Vasconcelos LA, Bittencourt JC: **Melanin-concentrating hormone projections to areas involved in somatomotor responses**. *J Chem Neuroanat* 2008, **35**(2):188-201.

119. Conductier G, Martin AO, Risold PY, Jego S, Lavoie R, Lafont C, Mollard P, Adamantidis A, Nahon JL: **Control of ventricular ciliary beating by the melanin concentrating hormone-expressing neurons of the lateral hypothalamus: a functional imaging survey**. *Front Endocrinol (Lausanne)* 2013, **4**:182.

120. Berbari NF, Johnson AD, Lewis JS, Askwith CC, Mykytyn K: **Identification of ciliary localization sequences within the third intracellular loop of G protein-coupled receptors**. *Mol Biol Cell* 2008, **19**(4):1540-1547.

121. Sun X, Haley J, Bulgakov OV, Cai X, McGinnis J, Li T: **Tubby is required for trafficking G protein-coupled receptors to neuronal cilia**. *Cilia* 2012, **1**(1):21.

122. Tomoshige S, Kobayashi Y, Hosoba K, Hamamoto A, Miyamoto T, Saito Y: **Cytoskeleton-related regulation of primary cilia shortening mediated by melanin-concentrating hormone receptor 1**. *General and comparative endocrinology* 2017, **253**:44-52.

123. Hamamoto A, Yamato S, Katoh Y, Nakayama K, Yoshimura K, Takeda S, Kobayashi Y, Saito Y: **Modulation of primary cilia length by melanin-concentrating hormone receptor 1**. *Cellular signalling* 2016, **28**(6):572-584.

124. Domire JS, Green JA, Lee KG, Johnson AD, Askwith CC, Mykytyn K: **Dopamine receptor 1 localizes to neuronal cilia in a dynamic process that requires the Bardet-Biedl syndrome proteins**. *Cell Mol Life Sci* 2011, **68**(17):2951-2960.

125. Berbari NF, Pasek RC, Malarkey EB, Yazdi SM, McNair AD, Lewis WR, Nagy TR, Kesterson RA, Yoder BK: **Leptin resistance is a secondary consequence of the obesity in ciliopathy mutant mice**. *Proc Natl Acad Sci U S A* 2013, **110**(19):7796-7801.

Chapter 2 References

1. Fuchs, J.L. and H.D. Schwark, **Neuronal primary cilia: a review**. *Cell Biol Int*, 2004. **28**(2): p. 111-8.

2. Baudoin, J.P., et al., **Tangentially migrating neurons assemble a primary cilium that promotes their reorientation to the cortical plate**. *Neuron,* 2012. **76**(6): p. 1108-22.

3. Gerdes, J.M., E.E. Davis, and N. Katsanis, **The vertebrate primary cilium in development, homeostasis, and disease.** *Cell*, 2009. **137**(1): p. 32-45.

4. Louvi, A. and E.A. Grove, **Cilia in the CNS: the quiet organelle claims center stage**. *Neuron*, 2011. **69**(6): p. 1046-60.

5.Trulioff, A., A. Ermakov, and Y. Malashichev, **Primary Cilia as a Possible Link between Left-Right Asymmetry and Neurodevelopmental Diseases**. *Genes* (Basel), 2017. **8**(2).

6. Omori, Y., et al., **Identification of G Protein-Coupled Receptors (GPCRs) in Primary Cilia and Their Possible Involvement in Body Weight Control.** *PLoS One*, 2015. **10**(6): p. e0128422.

7. Hilgendorf, K.I., C.T. Johnson, and P.K. Jackson, *T***he primary cilium as a cellular receiver: organizing ciliary GPCR signaling.** *Curr Opin Cell Biol*, 2016. **39**: p. 84-92.

8. Lancaster, M.A. and J.G. Gleeson, **The primary cilium as a cellular signaling center: lessons from disease**. *Curr Opin Genet Dev,* 2009. **19**(3): p. 220-9.

9. Christensen, S.T., et al., **Primary Cilia and Coordination of Receptor Tyrosine Kinase (RTK) and Transforming Growth Factor beta (TGF-beta) Signaling**. *Cold Spring Harb Perspect Biol*, 2017. **9**(6).

10. Valencia-Gattas, M., G.E. Conner, and N.L. Fregien, **Gefitinib, an EGFR Tyrosine Kinase inhibitor, Prevents Smoke-Mediated Ciliated Airway Epithelial Cell Loss and Promotes Their Recovery.** *PLoS One*, 2016. **11**(8): p. e0160216.

11. Evans, M.J., et al., **Fibroblast growth factor-2 during postnatal development of the tracheal basement membrane zone.** *Am J Physiol Lung Cell Mol Physiol*, 2002. **283**(6): p. L1263-70.

12. Nauli, S.M., R. Pala, and S.J. Kleene, **Calcium channels in primary cilia.** *Curr Opin Nephrol Hypertens*, 2016. **25**(5): p. 452-8.

13. Nachury, M.V., ***T*he molecular machines that traffic signaling receptors into and out of cilia.** *Curr Opin Cell Biol*, 2018. **51**: p. 124-131.

14. Liu, B., et al., ***Primary cilia integrate hedgehog and Wnt signaling during tooth development.*** *J Dent Res*, 2014. **93**(5): p. 475-82.

15. May-Simera, H.L. and M.W. Kelley, **Cilia, Wnt signaling, and the cytoskeleton.** *Cilia*, 2012. **1**(1): p. 7.

16. Brailov, I., et al., **Localization of 5-HT(6) receptors at the plasma membrane of neuronal cilia in the rat brain.** *Brain Res*, 2000. **872**(1-2): p. 271-5.

17. Berbari, N.F., et al., **Bardet-Biedl syndrome proteins are required for the localization of G protein-coupled receptors to primary cilia.** *Proc Natl Acad Sci U S A*, 2008. **105**(11): p. 4242-6.

18. Domire, J.S., et al., **Dopamine receptor 1 localizes to neuronal cilia in a dynamic process that requires the Bardet-Biedl syndrome proteins.** *Cell Mol Life Sci*, 2011. **68**(17): p. 2951-60.

19. Handel, M., et al., **Selective targeting of somatostatin receptor 3 to neuronal cilia.** *Neuroscience*, 1999. **89**(3): p. 909-26.

20. Varela, L. and T.L. Horvath, **Neuronal Cilia: Another Player in the Melanocortin System**. *Trends Mol Med*, 2018. **24**(4): p. 333-334.

21. Hartwig, C., et al., **Neurodevelopmental disease mechanisms, primary cilia, and endosomes converge on the BLOC-1 and BORC complexes.** *Dev Neurobiol*, 2018. **78**(3): p. 311-330.

22. Valente, E.M., et al., **Primary cilia in neurodevelopmental disorders.** *Nat Rev Neurol*, 2014. **10**(1): p. 27-36.

23. Reiter, J.F. and M.R. Leroux, **Genes and molecular pathways underpinning ciliopathies.** *Nat Rev Mol Cell Biol*, 2017. **18**(9): p. 533-547.

24. Leung, C.C.Y. and Y.H. Wong, **Role of G Protein-Coupled Receptors in the Regulation of Structural Plasticity and Cognitive Function.** *Molecules,* 2017. **22**(7).

25. Roberts, A.J. and P.B. Hedlund, **The 5-HT(7) receptor in learning and memory.** *Hippocampus*, 2012. **22**(4): p. 762-71.

26. Bassilana, F., M. Nash, and M.G. Ludwig, **Adhesion G protein-coupled receptors: opportunities for drug discovery.** *Nat Rev Drug Discov*, 2019. **18**(11): p. 869-884.

27. Huang, Y. and A. Thathiah, **Regulation of neuronal communication by G protein-coupled receptors.** *FEBS Lett*, 2015. **589**(14): p. 1607-19.

28. Catapano, L.A. and H.K. Manji, **G protein-coupled receptors in major psychiatric disorders.** *Biochim Biophys Acta*, 2007. **1768**(4): p. 976-93.

29. Civelli, O., et al., **G protein-coupled receptor deorphanizations.** *Annu Rev Pharmacol Toxicol*, 2013. **53**: p. 127-46.

30. Hsiao, Y.C., et al., **Ahi1, whose human ortholog is mutated in Joubert syndrome, is required for Rab8a localization, ciliogenesis and vesicle trafficking.** *Hum Mol Genet*, 2009. **18**(20): p. 3926-41.

31. Alvarez Retuerto, A.I., et al., **Association of common variants in the Joubert syndrome gene (AHI1) with autism.** *Hum Mol Genet*, 2008. **17**(24): p. 3887-96.

32. Ren, Z., et al., **A cis-eQTL in AHI1 confers risk to schizophrenia in European populations**. *Neurosci Lett,* 2016. **632**: p. 130-5.

33. Ingason, A., et al., **A large replication study and meta-analysis in European samples provides further support for association of AHI1 markers with schizophrenia.** *Hum Mol Genet*, 2010. **19**(7): p. 1379-86.

34. Ingason, A., et al., **Support for involvement of the AHI1 locus in schizophrenia.** *Eur J Hum Genet,* 2007. **15**(9): p. 988-91.

35. Datta, S.R., et al., **A threonine to isoleucine missense mutation in the pericentriolar material 1 gene is strongly associated with schizophrenia.** *Mol Psychiatry*, 2010. **15**(6): p. 615-28.

36. Gurling, H.M., et al., **Genetic association and brain morphology studies and the chromosome 8p22 pericentriolar material 1 (PCM1) gene in susceptibility to schizophrenia.** *Arch Gen Psychiatry,* 2006. **63**(8): p. 844-54.

37. Schneider, E., et al., **Methylation and expression analyses of the 7q autism susceptibility locus genes MEST , COPG2, and TSGA14 in human and anthropoid primate cortices.** *Cytogenet Genome Res*, 2012. **136**(4): p. 278-87.

38. Korvatska, O., et al., **Mutations in the TSGA14 gene in families with autism spectrum disorders.** *Am J Med Genet B Neuropsychiatr Genet*, 2011. **156B**(3): p. 303-11.

39. Munoz-Estrada, J., et al., **Primary cilia formation is diminished in schizophrenia and bipolar disorder: A possible marker for these psychiatric diseases.** *Schizophr Res*, 2018. **195**: p. 412-420.

40. van Dam, T.J., et al., **Evolution of modular intraflagellar transport from a coatomer-like progenitor.** *Proc Natl Acad Sci* U S A, 2013. **110**(17): p. 6943-8.

41. Arnaiz, O., et al., ***Remodeling Cildb, a popular database for cilia and links for ciliopathies.*** *Cilia*, 2014. **3**: p. 9.

42. Arnaiz, O., et al., **Cildb: a knowledgebase for centrosomes and cilia.** Database (Oxford), 2009. **2009**: p. bap022.

43. Schou, K.B., L.B. Pedersen, and S.T. Christensen, ***I*ns and outs of GPCR signaling in primary cilia.** *EMBO Rep*, 2015. **16**(9): p. 1099-113.

44. Gandal, M.J., et al., **Transcriptome-wide isoform-level dysregulation in ASD, schizophrenia, and bipolar disorder.** *Science*, 2018. **362**(6420).

45. Fromer, M., et al., **Gene expression elucidates functional impact of polygenic risk for schizophrenia.** *Nat Neurosci,* 2016. **19**(11): p. 1442-1453.

46. Parikshak, N.N., et al., **Genome-wide changes in lncRNA, splicing, and regional gene expression patterns in autism.** *Nature*, 2016. **540**(7633): p. 423-427.

47. Kang, H.J., et al., **Spatio-temporal transcriptome of the human brain.** *Nature*, 2011. **478**(7370): p. 483-9.

48. Gandal, M.J., et al., **Shared molecular neuropathology across major psychiatric disorders parallels polygenic overlap.** *Science*, 2018. **359**(6376): p. 693-697.

49. Chang, L.C., et al., **A conserved BDNF, glutamate- and GABA-enriched gene module related to human depression identified by coexpression meta-analysis and DNA variant genome-wide association studies.** *PLoS One*, 2014. **9**(3): p. e90980.

50. Mukhopadhyay, S., et al., **TULP3 bridges the IFT-A complex and membrane phosphoinositides to promote trafficking of G protein-coupled receptors into primary cilia.** *Genes Dev,* 2010. **24**(19): p. 2180-93.

51. Beales, P.L., et al., **IFT80, which encodes a conserved intraflagellar transport protein, is mutated in Jeune asphyxiating thoracic dystrophy.** *Nat Genet,* 2007. **39**(6): p. 727-9.

52. Brazelton, W.J., et al., **The bld1 mutation identifies the Chlamydomonas osm-6 homolog as a gene required for flagellar assembly.** *Curr Biol,* 2001. **11**(20): p. 1591-4.

53. Follit, J.A., et al., **The intraflagellar transport protein IFT20 is associated with the Golgi complex and is required for cilia assembly.** *Mol Biol Cell,* 2006. **17**(9): p. 3781-92.

54. Haycraft, C.J., et al., **The C. elegans homolog of the murine cystic kidney disease gene Tg737 functions in a ciliogenic pathway and is disrupted in osm-5 mutant worms.** *Development*, 2001. **128**(9): p. 1493-505.

55. Houde, C., et al., **Hippi is essential for node cilia assembly and Sonic hedgehog signaling.** *Dev Biol,* 2006. **300**(2): p. 523-33.

56. Huangfu, D., et al., **Hedgehog signalling in the mouse requires intraflagellar transport proteins.** *Nature*, 2003. **426**(6962): p. 83-7.

57. Pazour, G.J., et al., **Chlamydomonas IFT88 and its mouse homologue, polycystic kidney disease gene tg737, are required for assembly of cilia and flagella.** *J Cell Biol*, 2000. **151**(3): p. 709-18.

58. Qin, H., J.L. Rosenbaum, and M.M. Barr, **An autosomal recessive polycystic kidney disease gene homolog is involved in intraflagellar transport in C. elegans ciliated sensory neurons.** *Curr Biol*, 2001. **11**(6): p. 457-61.

59. Tsujikawa, M. and J. Malicki, **Intraflagellar transport genes are essential for differentiation and survival of vertebrate sensory neurons.** *Neuron*, 2004. **42**(5): p. 703-16.

60. Nakayama, K. and Y. Katoh, **Ciliary protein trafficking mediated by IFT and BBSome complexes with the aid of kinesin-2 and dynein-2 motors.** *J Biochem*, 2018. **163**(3): p. 155-164.

61. Piperno, G., et al., **Distinct mutants of retrograde intraflagellar transport (IFT) share similar morphological and molecular defects.** *J Cell Biol,* 1998. **143**(6): p. 1591-601.

62. Iomini, C., et al., **Retrograde intraflagellar transport mutants identify complex A proteins with multiple genetic interactions in Chlamydomonas reinhardtii.** *Genetics*, 2009. **183**(3): p. 885-96.

63. Iomini, C., et al., **Protein particles in Chlamydomonas flagella undergo a transport cycle consisting of four phases.** *J Cell Biol,* 2001. **153**(1): p. 13-24.

64. Legue, E. and K.F. Liem, Jr., **Mutations in Ciliary Trafficking Genes affect Sonic Hedgehog-dependent Neural Tube Patterning Differentially along the Anterior-Posterior Axis.** *Neuroscience*, 2020. **450**: p. 3-14.

65. Norman, R.X., et al., **Tubby-like protein 3 (TULP3) regulates patterning in the mouse embryo through inhibition of Hedgehog signaling.** *Hum Mol Genet,* 2009. **18**(10): p. 1740-54.

66. Guan, J., et al., **Commonality in dysregulated expression of gene sets in cortical brains of individuals with autism, schizophrenia, and bipolar disorder.** *Transl Psychiatry,* 2019. **9**(1): p. 152.

67. Hansell, N.K., et al., **Genetic co-morbidity between neuroticism, anxiety/depression and somatic distress in a population sample of adolescent and young adult twins.** *Psychol Med,* 2012. **42**(6): p. 1249-60.

68. Wray, N.R., et al., **Genome-wide association study of major depressive disorder: new results, meta-analysis, and lessons learned.** *Mol Psychiatry,* 2012. **17**(1): p. 36-48.

69. Hines, L.M., et al., **Platelet adenylyl cyclase activity: a biological marker for major depression and recent drug use.** *Biol Psychiatry,* 2005. **58**(12): p. 955-62.

70. Chen, X., et al., **Ablation of Type III Adenylyl Cyclase in Mice Causes Reduced Neuronal Activity, Altered Sleep Pattern, and Depression-like Phenotypes.** *Biol Psychiatry*, 2016. **80**(11): p. 836-848.

71. Keays, D.A., et al., **Mutations in alpha-tubulin cause abnormal neuronal migration in mice and lissencephaly in humans.** *Cell*, 2007. **128**(1): p. 45-57.

72. Jaglin, X.H., et al., **Mutations in the beta-tubulin gene TUBB2B result in asymmetrical polymicrogyria.** *Nat Genet*, 2009. **41**(6): p. 746-52.

73. Tischfield, M.A., et al., **Human TUBB3 mutations perturb microtubule dynamics, kinesin interactions, and axon guidance.** *Cell*, 2010. **140**(1): p. 74-87.

74. Breuss, M., et al., **Mutations in the beta-tubulin gene TUBB5 cause microcephaly with structural brain abnormalities**. *Cell Rep,* 2012. **2**(6): p. 1554-62.

75. Cushion, T.D., et al., **De novo mutations in the beta-tubulin gene TUBB2A cause simplified gyral patterning and infantile-onset epilepsy.** *Am J Hum Genet*, 2014. **94**(4): p. 634-41.

76. Romaniello, R., et al., **Tubulin genes and malformations of cortical development.** *Eur J Med Genet,* 2018. **61**(12): p. 744-754.

77. Jaglin, X.H. and J. Chelly, **Tubulin-related cortical dysgeneses: microtubule dysfunction underlying neuronal migration defects.** *Trends Genet*, 2009. **25**(12): p. 555-66.

78. Zhao, H. and D.R. Nyholt, **Gene-based analyses reveal novel genetic overlap and allelic heterogeneity across five major psychiatric disorders.** *Hum Genet,* 2017. **136**(2): p. 263-274.

79. Monroe, T.O., et al., **PCM1 is necessary for focal ciliary integrity and is a candidate for severe schizophrenia**. *Nat Commun,* 2020. **11**(1): p. 5903.

80. Moens, L.N., et al., **PCM1 and schizophrenia: a replication study in the Northern Swedish population.** *Am J Med Genet B Neuropsychiatr Genet*, 2010. **153B**(6): p. 1240-3.

81. Eastwood, S.L., C.A. Hodgkinson, and P.J. Harrison, **DISC-1 Leu607Phe alleles differentially affect centrosomal PCM1 localization and neurotransmitter release.** *Mol Psychiatry,* 2009. **14**(6): p. 556-7.

82. Kamiya, A., et al., **Recruitment of PCM1 to the centrosome by the cooperative action of DISC1 and BBS4: a candidate for psychiatric illnesses.** *Arch Gen Psychiatry,* 2008. **65**(9): p. 996-1006.

83. Rampino, A., et al., **Expression of DISC1-interactome members correlates with cognitive phenotypes related to schizophrenia.** *PLoS One,* 2014. **9**(6): p. e99892.

84. Zoubovsky, S., et al., **Neuroanatomical and behavioral deficits in mice haploinsufficient for Pericentriolar material 1 (Pcm1).** *Neurosci Res,* 2015. **98**: p. 45-9.

85. Verleyen, D., F.P. Luyten, and P. Tylzanowski, **Orphan G-protein coupled receptor 22 (Gpr22) regulates cilia length and structure in the zebrafish Kupffer's vesicle.** *PLoS One,* 2014. **9**(10): p. e110484.

86. Pala, R., et al., **Personalized Nanotherapy by Specifically Targeting Cell Organelles To Improve Vascular Hypertension.** *Nano Lett,* 2019. **19**(2): p. 904-914.

87. Pala, R., et al., **Ciliotherapy: Remote Control of Primary Cilia Movement and Function by Magnetic Nanoparticles**. *ACS Nano*, 2019. **13**(3): p. 3555-3572.

Chapter 3 References

1. Liu Z, Tu H, Kang Y, Xue Y, Ma D, Zhao C, Li H, Wang L, Liu F: **Primary cilia regulate hematopoietic stem and progenitor cell specification through Notch signaling in zebrafish**. *Nature communications* 2019, **10**(1):1839.

2. Guo J, Otis JM, Higginbotham H, Monckton C, Cheng J, Asokan A, Mykytyn K, Caspary T, Stuber GD, Anton ES: **Primary Cilia Signaling Shapes the Development of Interneuronal Connectivity**. *Developmental cell* 2017, **42**(3):286-300 e284.

3. Nechipurenko IV, Doroquez DB, Sengupta P: **Primary cilia and dendritic spines: different but similar signaling compartments**. *Molecules and cells* 2013, **36**(4):288-303.

4. Breunig JJ, Sarkisian MR, Arellano JI, Morozov YM, Ayoub AE, Sojitra S, Wang B, Flavell RA, Rakic P, Town T: **Primary cilia regulate hippocampal neurogenesis by mediating sonic hedgehog signaling**. *Proceedings of the National Academy of Sciences of the United States of America* 2008, **105**(35):13127-13132.

5. Han YG, Spassky N, Romaguera-Ros M, Garcia-Verdugo JM, Aguilar A, Schneider-Maunoury S, Alvarez-Buylla A: **Hedgehog signaling and primary cilia are required for the formation of adult neural stem cells**. *Nature neuroscience* 2008, **11**(3):277-284.

6. Oishi I, Kawakami Y, Raya A, Callol-Massot C, Izpisua Belmonte JC: **Regulation of primary cilia formation and left-right patterning in zebrafish by a noncanonical Wnt signaling mediator, duboraya**. *Nature genetics* 2006, **38**(11):1316-1322.

7. Nachury MV, Mick DU: **Establishing and regulating the composition of cilia for signal transduction**. *Nature reviews Molecular cell biology* 2019, **20**(7):389-405.

8. Berbari NF, O'Connor AK, Haycraft CJ, Yoder BK: **The primary cilium as a complex signaling center**. *Current biology : CB* 2009, **19**(13):R526-535.

9. Wheatley DN: **Nanobiology of the primary cilium--paradigm of a multifunctional nanomachine complex**. *Methods in cell biology* 2008, **90**:139-156.

10. Insinna C, Besharse JC: **Intraflagellar transport and the sensory outer segment of vertebrate photoreceptors**. *Developmental dynamics : an official publication of the American Association of Anatomists* 2008, **237**(8):1982-1992.

11. Kang N, Ro H, Park Y, Kim HT, Huh TL, Rhee M: **Seson, a novel zinc finger protein, controls cilia integrity for the LR patterning during zebrafish embryogenesis**. *Biochemical and biophysical research communications* 2010, **401**(2):169-174.

12. Nonaka S, Tanaka Y, Okada Y, Takeda S, Harada A, Kanai Y, Kido M, Hirokawa N: **Randomization of left-right asymmetry due to loss of nodal cilia generating leftward flow of extraembryonic fluid in mice lacking KIF3B motor protein**. *Cell* 1998, **95**(6):829-837.

13. Yoshiba S, Shiratori H, Kuo IY, Kawasumi A, Shinohara K, Nonaka S, Asai Y, Sasaki G, Belo JA, Sasaki H *et al*: **Cilia at the node of mouse embryos sense fluid flow for left-right determination via Pkd2**. *Science* 2012, **338**(6104):226-231.

14. Nauli SM, Jin X, AbouAlaiwi WA, El-Jouni W, Su X, Zhou J: **Non-motile primary cilia as fluid shear stress mechanosensors**. *Methods in enzymology* 2013, **525**:1-20.

15. Bargmann CI: **Chemosensation in C. elegans**. *WormBook : the online review of C elegans biology* 2006:1-29.

16. Atkinson KF, Sherpa RT, Nauli SM: **The Role of the Primary Cilium in Sensing Extracellular pH**. *Cells* 2019, **8**(7).

17. Choi H, Madhu V, Shapiro IM, Risbud MV: **Nucleus pulposus primary cilia alter their length in response to changes in extracellular osmolarity but do not control TonEBP-mediated osmoregulation**. *Scientific reports* 2019, **9**(1):15469.

18. Christensen ST, Voss JW, Teilmann SC, Lambert IH: **High expression of the taurine transporter TauT in primary cilia of NIH3T3 fibroblasts**. *Cell biology international* 2005, **29**(5):347-351.

19. Kuhara A, Okumura M, Kimata T, Tanizawa Y, Takano R, Kimura KD, Inada H, Matsumoto K, Mori I: **Temperature sensing by an olfactory neuron in a circuit controlling behavior of C. elegans**. *Science* 2008, **320**(5877):803-807.

20. Moorman SJ, Shorr AZ: **The primary cilium as a gravitational force transducer and a regulator of transcriptional noise**. *Developmental dynamics : an official publication of the American Association of Anatomists* 2008, **237**(8):1955-1959.

21. O'Hagan R, Silva M, Nguyen KCQ, Zhang W, Bellotti S, Ramadan YH, Hall DH, Barr MM: **Glutamylation Regulates Transport, Specializes Function, and Sculpts the Structure of Cilia**. *Current biology : CB* 2017, **27**(22):3430-3441 e3436.

22. Wang J, Kaletsky R, Silva M, Williams A, Haas LA, Androwski RJ, Landis JN, Patrick C, Rashid A, Santiago-Martinez D *et al*: **Cell-Specific Transcriptional Profiling of Ciliated Sensory Neurons Reveals Regulators of Behavior and Extracellular Vesicle Biogenesis**. *Current biology : CB* 2015, **25**(24):3232-3238.

23. Brailov I, Bancila M, Brisorgueil MJ, Miquel MC, Hamon M, Verge D: **Localization of 5-HT(6) receptors at the plasma membrane of neuronal cilia in the rat brain**. *Brain Res* 2000, **872**(1-2):271-275.

24. Berbari NF, Lewis JS, Bishop GA, Askwith CC, Mykytyn K: **Bardet-Biedl syndrome proteins are required for the localization of G protein-coupled receptors to primary cilia**. *Proceedings of the National Academy of Sciences of the United States of America* 2008, **105**(11):4242-4246.

25. Domire JS, Green JA, Lee KG, Johnson AD, Askwith CC, Mykytyn K: **Dopamine receptor 1 localizes to neuronal cilia in a dynamic process that requires the Bardet-Biedl syndrome proteins**. *Cellular and molecular life sciences : CMLS* 2011, **68**(17):2951-2960.

26. Handel M, Schulz S, Stanarius A, Schreff M, Erdtmann-Vourliotis M, Schmidt H, Wolf G, Hollt V: **Selective targeting of somatostatin receptor 3 to neuronal cilia**. *Neuroscience* 1999, **89**(3):909-926.

27. Omori Y, Chaya T, Yoshida S, Irie S, Tsujii T, Furukawa T: **Identification of G Protein-Coupled Receptors (GPCRs) in Primary Cilia and Their Possible Involvement in Body Weight Control**. *PLoS One* 2015, **10**(6):e0128422.

28. Varela L, Horvath TL: **Neuronal Cilia: Another Player in the Melanocortin System**. *Trends in molecular medicine* 2018, **24**(4):333-334.

29. Orbach R, Howard J: **The dynamic and structural properties of axonemal tubulins support the high length stability of cilia**. *Nature communications* 2019, **10**(1):1838.

30. Phua SC, Chiba S, Suzuki M, Su E, Roberson EC, Pusapati GV, Schurmans S, Setou M, Rohatgi R, Reiter JF *et al*: **Dynamic Remodeling of Membrane Composition Drives Cell Cycle through Primary Cilia Excision**. *Cell* 2017, **168**(1-2):264-279 e215.

31. Silverman MA, Leroux MR: **Intraflagellar transport and the generation of dynamic, structurally and functionally diverse cilia**. *Trends in cell biology* 2009, **19**(7):306-316.

32. Dewan K, Benloucif S, Reid K, Wolfe LF, Zee PC: **Light-induced changes of the circadian clock of humans: increasing duration is more effective than increasing light intensity**. *Sleep* 2011, **34**(5):593-599.

33. Wright KP, Jr., McHill AW, Birks BR, Griffin BR, Rusterholz T, Chinoy ED: **Entrainment of the human circadian clock to the natural light-dark cycle**. *Current biology : CB* 2013, **23**(16):1554-1558.

34. Buhr ED, Yoo SH, Takahashi JS: **Temperature as a universal resetting cue for mammalian circadian oscillators**. *Science* 2010, **330**(6002):379-385.

35. Damiola F, Le Minh N, Preitner N, Kornmann B, Fleury-Olela F, Schibler U: **Restricted feeding uncouples circadian oscillators in peripheral tissues from the central pacemaker in the suprachiasmatic nucleus**. *Genes & development* 2000, **14**(23):2950-2961.

36. Casey T, Patel OV, Plaut K: **Transcriptomes reveal alterations in gravity impact circadian clocks and activate mechanotransduction pathways with adaptation through epigenetic change**. *Physiological genomics* 2015, **47**(4):113-128.

37. Robinson EL, Fuller CA: **Gravity and thermoregulation: metabolic changes and circadian rhythms**. *Pflugers Archiv : European journal of physiology* 2000, **441**(2-3 Suppl):R32-38.

38. Fuller CA: **The effects of gravity on the circadian timing system**. *Journal of gravitational physiology : a journal of the International Society for Gravitational Physiology* 1994, **1**(1):P1-4.

39. Gu W, Geddes BJ, Zhang C, Foley KP, Stricker-Krongrad A: **The prolactin-releasing peptide receptor (GPR10) regulates body weight homeostasis in mice**. *Journal of molecular neuroscience : MN* 2004, **22**(1-2):93-103.

40. Nagata A, Hamamoto A, Horikawa M, Yoshimura K, Takeda S, Saito Y: **Characterization of ciliary targeting sequence of rat melanin-concentrating hormone receptor 1**. *General and comparative endocrinology* 2013, **188**:159-165.

41. Hughes JW, Cho JH, Conway HE, DiGruccio MR, Ng XW, Roseman HF, Abreu D, Urano F, Piston DW: **Primary cilia control glucose homeostasis via islet paracrine interactions**. *Proceedings of the National Academy of Sciences of the United States of America* 2020, **117**(16):8912-8923.

42. Lee H, Song J, Jung JH, Ko HW: **Primary cilia in energy balance signaling and metabolic disorder**. *BMB reports* 2015, **48**(12):647-654.

43. Berbari NF, Pasek RC, Malarkey EB, Yazdi SM, McNair AD, Lewis WR, Nagy TR, Kesterson RA, Yoder BK: **Leptin resistance is a secondary consequence of the obesity in**

ciliopathy mutant mice. *Proceedings of the National Academy of Sciences of the United States of America* 2013, **110**(19):7796-7801.

44. Koemeter-Cox AI, Sherwood TW, Green JA, Steiner RA, Berbari NF, Yoder BK, Kauffman AS, Monsma PC, Brown A, Askwith CC *et al*: **Primary cilia enhance kisspeptin receptor signaling on gonadotropin-releasing hormone neurons**. *Proceedings of the National Academy of Sciences of the United States of America* 2014, **111**(28):10335-10340.

45. Diniz GB, Battagello DS, Klein MO, Bono BSM, Ferreira JGP, Motta-Teixeira LC, Duarte JCG, Presse F, Nahon JL, Adamantidis A *et al*: **Ciliary melanin-concentrating hormone receptor 1 (MCHR1) is widely distributed in the murine CNS in a sex-independent manner**. *Journal of neuroscience research* 2020, **98**(10):2045-2071.

46. Wang Z, Phan T, Storm DR: **The type 3 adenylyl cyclase is required for novel object learning and extinction of contextual memory: role of cAMP signaling in primary cilia**. *The Journal of neuroscience : the official journal of the Society for Neuroscience* 2011, **31**(15):5557-5561.

47. Bae YK, Barr MM: **Sensory roles of neuronal cilia: cilia development, morphogenesis, and function in C. elegans**. *Frontiers in bioscience : a journal and virtual library* 2008, **13**:5959-5974.

48. Benton R, Vannice KS, Vosshall LB: **An essential role for a CD36-related receptor in pheromone detection in Drosophila**. *Nature* 2007, **450**(7167):289-293.

49. Mure LS, Le HD, Benegiamo G, Chang MW, Rios L, Jillani N, Ngotho M, Kariuki T, Dkhissi-Benyahya O, Cooper HM *et al*: **Diurnal transcriptome atlas of a primate across major neural and peripheral tissues**. *Science* 2018, **359**(6381).

50. van Dam TJP, Townsend MJ, Turk M, Schlessinger A, Sali A, Field MC, Huynen MA: **Evolution of modular intraflagellar transport from a coatomer-like progenitor**. *P Natl Acad Sci USA* 2013, **110**(17):6943-6948.

51. Arnaiz O, Cohen J, Tassin AM, Koll F: **Remodeling Cildb, a popular database for cilia and links for ciliopathies**. *Cilia* 2014, **3**:9.

52. Arnaiz O, Malinowska A, Klotz C, Sperling L, Dadlez M, Koll F, Cohen J: **Cildb: a knowledgebase for centrosomes and cilia**. *Database : the journal of biological databases and curation* 2009, **2009**:bap022.

53. Alhassen W, Chen S, Vawter M, Robbins BK, Nguyen H, Myint TN, Saito Y, Schulmann A, Nauli SM, Civelli O *et al*: **Patterns of cilia gene dysregulations in major psychiatric disorders**. *Progress in Neuro-Psychopharmacology and Biological Psychiatry* 2021:110255.

54. Ceglia N, Liu Y, Chen S, Agostinelli F, Eckel-Mahan K, Sassone-Corsi P, Baldi P: **CircadiOmics: circadian omic web portal**. *Nucleic acids research* 2018, **46**(W1):W157-W162.

55. Patel VR, Eckel-Mahan K, Sassone-Corsi P, Baldi P: **CircadiOmics: integrating circadian genomics, transcriptomics, proteomics and metabolomics**. *Nature methods* 2012, **9**(8):772-773.

56. Agostinelli F, Ceglia N, Shahbaba B, Sassone-Corsi P, Baldi P: **What time is it? Deep learning approaches for circadian rhythms**. *Bioinformatics* 2016, **32**(19):3051.

57. Mikula S, Trotts I, Stone JM, Jones EG: **Internet-enabled high-resolution brain mapping and virtual microscopy**. *NeuroImage* 2007, **35**(1):9-15.

58. Christensen ST, Pedersen LB, Schneider L, Satir P: **Sensory cilia and integration of signal transduction in human health and disease**. *Traffic* 2007, **8**(2):97-109.

59. Satir P, Christensen ST: **Overview of structure and function of mammalian cilia**. *Annual review of physiology* 2007, **69**:377-400.

60. Thomas J, Morle L, Soulavie F, Laurencon A, Sagnol S, Durand B: **Transcriptional control of genes involved in ciliogenesis: a first step in making cilia**. *Biology of the cell* 2010, **102**(9):499-513.

61. Garcia G, 3rd, Reiter JF: **A primer on the mouse basal body**. *Cilia* 2016, **5**:17.

62. Pedersen LB, Rosenbaum JL: **Intraflagellar transport (IFT) role in ciliary assembly, resorption and signalling**. *Current topics in developmental biology* 2008, **85**:23-61.

63. Mourao A, Christensen ST, Lorentzen E: **The intraflagellar transport machinery in ciliary signaling**. *Current opinion in structural biology* 2016, **41**:98-108.

64. Taschner M, Lorentzen E: **The Intraflagellar Transport Machinery**. *Cold Spring Harbor perspectives in biology* 2016, **8**(10).

65. Nakayama K, Katoh Y: **Ciliary protein trafficking mediated by IFT and BBSome complexes with the aid of kinesin-2 and dynein-2 motors**. *J Biochem* 2018, **163**(3):155-164.

66. Mykytyn K, Askwith C: **G-Protein-Coupled Receptor Signaling in Cilia**. *Cold Spring Harbor perspectives in biology* 2017, **9**(9).

67. Hirano T, Katoh Y, Nakayama K: **Intraflagellar transport-A complex mediates ciliary entry and retrograde trafficking of ciliary G protein-coupled receptors**. *Molecular biology of the cell* 2017, **28**(3):429-439.

68. Schou KB, Pedersen LB, Christensen ST: **Ins and outs of GPCR signaling in primary cilia**. *EMBO Rep* 2015, **16**(9):1099-1113.

69. Green JA, Gu C, Mykytyn K: **Heteromerization of ciliary G protein-coupled receptors in the mouse brain**. *PloS one* 2012, **7**(9):e46304.

70. Engle SE, Bansal R, Antonellis PJ, Berbari NF: **Cilia signaling and obesity**. *Seminars in cell & developmental biology* 2020.

71. Berbari NF, Malarkey EB, Yazdi SM, McNair AD, Kippe JM, Croyle MJ, Kraft TW, Yoder BK: **Hippocampal and cortical primary cilia are required for aversive memory in mice**. *PloS one* 2014, **9**(9):e106576.

72. Kobayashi T, Ishida Y, Hirano T, Katoh Y, Nakayama K: **Cooperation of the IFT-A complex with the IFT-B complex is required for ciliary retrograde protein trafficking and GPCR import**. *Molecular biology of the cell* 2020:mbcE20080556.

73. McIntyre JC, Hege MM, Berbari NF: **Trafficking of ciliary G protein-coupled receptors**. *Methods in cell biology* 2016, **132**:35-54.

74. Kobayashi T, Ishida Y, Hirano T, Katoh Y, Nakayama K: **Cooperation of the IFT-A complex with the IFT-B complex is required for ciliary retrograde protein trafficking and GPCR import**. *Mol Biol Cell* 2021, **32**(1):45-56.

75. Siljee JE, Wang Y, Bernard AA, Ersoy BA, Zhang S, Marley A, Von Zastrow M, Reiter JF, Vaisse C: **Subcellular localization of MC4R with ADCY3 at neuronal primary cilia underlies a common pathway for genetic predisposition to obesity**. *Nat Genet* 2018, **50**(2):180-185.

76. Hamamoto A, Yamato S, Katoh Y, Nakayama K, Yoshimura K, Takeda S, Kobayashi Y, Saito Y: **Modulation of primary cilia length by melanin-concentrating hormone receptor 1**. *Cell Signal* 2016, **28**(6):572-584.

77. Kobayashi Y, Okada T, Miki D, Sekino Y, Koganezawa N, Shirao T, Diniz GB, Saito Y: **Properties of primary cilia in melanin-concentrating hormone receptor 1-bearing hippocampal neurons in vivo and in vitro**. *Neurochem Int* 2021, **142**:104902.

78. Graybiel AM, Aosaki T, Flaherty AW, Kimura M: **The basal ganglia and adaptive motor control**. *Science* 1994, **265**(5180):1826-1831.

79. Bednark JG, Campbell ME, Cunnington R: **Basal ganglia and cortical networks for sequential ordering and rhythm of complex movements**. *Frontiers in human neuroscience* 2015, **9**:421.

80. Talakoub O, Neagu B, Udupa K, Tsang E, Chen R, Popovic MR, Wong W: **Time-course of coherence in the human basal ganglia during voluntary movements**. *Scientific reports* 2016, **6**:34930.

81. Li X, Luo F, Shi L, Woodward DJ, Chang J: **Ensemble neural activity of the frontal cortical basal ganglia system predicts reaction time task performance in rats**. *Neuroscience research* 2011, **71**(2):149-160.

82. Jin DZ, Fujii N, Graybiel AM: **Neural representation of time in cortico-basal ganglia circuits**. *Proceedings of the National Academy of Sciences of the United States of America* 2009, **106**(45):19156-19161.

83. Morita M, Hikida T: **[Distinct roles of the direct and indirect pathways in the basal ganglia circuit mechanism]**. *Nihon shinkei seishin yakurigaku zasshi = Japanese journal of psychopharmacology* 2015, **35**(5-6):107-111.

84. Ikemoto S, Yang C, Tan A: **Basal ganglia circuit loops, dopamine and motivation: A review and enquiry**. *Behavioural brain research* 2015, **290**:17-31.

85. Kreitzer AC, Malenka RC: **Striatal plasticity and basal ganglia circuit function**. *Neuron* 2008, **60**(4):543-554.

86. Foley P, Riederer P: **The motor circuit of the human basal ganglia reconsidered**. *Journal of neural transmission Supplementum* 2000(58):97-110.

87. Avasthi P, Marley A, Lin H, Gregori-Puigjane E, Shoichet BK, von Zastrow M, Marshall WF: **A chemical screen identifies class a g-protein coupled receptors as regulators of cilia**. *ACS chemical biology* 2012, **7**(5):911-919.

88. Haber SN: **The place of dopamine in the cortico-basal ganglia circuit**. *Neuroscience* 2014, **282**:248-257.

89. Macar F, Coull J, Vidal F: **The supplementary motor area in motor and perceptual time processing: fMRI studies**. *Cognitive processing* 2006, **7**(2):89-94.

90. Wiener M, Turkeltaub P, Coslett HB: **The image of time: a voxel-wise meta-analysis**. *NeuroImage* 2010, **49**(2):1728-1740.

91. Matell MS, Meck WH: **Cortico-striatal circuits and interval timing: coincidence detection of oscillatory processes**. *Brain research Cognitive brain research* 2004, **21**(2):139-170.

92. Bussi IL, Levin G, Golombek DA, Agostino PV: **Involvement of dopamine signaling in the circadian modulation of interval timing**. *The European journal of neuroscience* 2014, **40**(1):2299-2310.

93. Jones CR, Malone TJ, Dirnberger G, Edwards M, Jahanshahi M: **Basal ganglia, dopamine and temporal processing: performance on three timing tasks on and off medication in Parkinson's disease**. *Brain and cognition* 2008, **68**(1):30-41.

94. Yang YK, Yeh TL, Chiu NT, Lee IH, Chen PS, Lee LC, Jeffries KJ: **Association between cognitive performance and striatal dopamine binding is higher in timing and motor tasks in patients with schizophrenia**. *Psychiatry research* 2004, **131**(3):209-216.

95. Avanzino L, Pelosin E, Vicario CM, Lagravinese G, Abbruzzese G, Martino D: **Time Processing and Motor Control in Movement Disorders**. *Frontiers in human neuroscience* 2016, **10**:631.

96. Boyd LA, Edwards JD, Siengsukon CS, Vidoni ED, Wessel BD, Linsdell MA: **Motor sequence chunking is impaired by basal ganglia stroke**. *Neurobiology of learning and memory* 2009, **92**(1):35-44.

97. Nagasaki H, Nakamura R, Taniguchi R: **Disturbances of rhythm formation in patients with Parkinson's disease: part II. a forced oscillation model.** *Perceptual and motor skills* 1978, **46**(1):79-87.

Chapter 4 References

1. Alachkar A, Alhassen L, Wang Z, Wang L, Onouye K, Sanathara N, Civelli O (2016) **Inactivation of the melanin concentrating hormone system impairs maternal behavior.** *European neuropsychopharmacology: the journal of the European College of Neuropsychopharmacology,* 26:1826–1835
2. Alhassen L, Phan A, Alhassen W, Nguyen P, Lo A, Shaharuddin H, Sanathara N, Civelli O, Alachkar A (2019) **The role of olfaction in MCH-regulated spontaneous maternal responses.** *Brain Res,* 1719:71–76

3. Alhassen W, Chen S, Vawter M, Robbins BK, Nguyen H, Myint TN, Saito Y, Schulmann A, Nauli SM, Civelli O et al (2021) **Patterns of cilia gene dysregulations in major psychiatric disorders.** *Prog Neuropsychopharmacol Biol Psychiatry,* 109:110255
4. Arletti R, Benelli A, Bertolini A (1992) **Oxytocin involvement in male and female sexual behavior.** *Ann N Y Acad Sci,* 652:180–193
5. Atkinson, K.F., Sherpa, R.T., and Nauli, S.M. (2019). **The role of the primary cilium in sensing extracellular pH.** *Cells, 8*.
6. Bansal R, Engle SE, Antonellis PJ, Whitehouse LS, Baucum AJ 2nd, Cummins TR, Reiter JF, Berbari NF (2019) **Hedgehog pathway activation alters ciliary signaling in primary hypothalamic cultures.** *Front Cell Neurosci,* 13:266
7. Bargmann, C.I. (2006). **Chemosensation in C. elegans.** *Worm- Book: the online review of C. elegans biology,* 1–29.
8. Berbari NF, Johnson AD, Lewis JS, Askwith CC, Mykytyn K (2008) **Identification of ciliary localization sequences within the third intracellular loop of G protein-coupled receptors.** *Mol Biol Cell,* 19:1540–1547
9. Berbari NF, Lewis JS, Bishop GA, Askwith CC, Mykytyn K (2008) **Bardet-Biedl syndrome proteins are required for the localization of G protein-coupled receptors to primary cilia.** *Proc Natl Acad Sci USA,* 105:4242–4246
10. Berbari NF, O'Connor AK, Haycraft CJ, Yoder BK (2009) **The primary cilium as a complex signaling center.** *Current biology: CB,* 19:R526-535
11. Bishop GA, Berbari NF, Lewis J, Mykytyn K (2007) **Type III adenylyl cyclase localizes to primary cilia throughout the adult mouse brain.** *J Comp Neurol,* 505:562–571
12. Blanco-Centurion C, Liu M, Konadhode RP, Zhang X, Pelluru D, van den Pol AN, Shiromani PJ (2016) **Optogenetic activation of melanin-concentrating hormone neurons increases non-rapid eye movement and rapid eye movement sleep during the night in rats.** *Eur J Neurosci,* 44:2846–2857

13. Blouin AM, Fried I, Wilson CL, Staba RJ, Behnke EJ, Lam HA, Maidment NT, Karlsson KAE, Lapierre JL, Siegel JM (2013) **Human hypocretin and melanin-concentrating hormone lev- els are linked to emotion and social interaction.** *Nat Commun,* 4:1547
14. Borowsky B, Durkin MM, Ogozalek K, Marzabadi MR, DeLeon J, Lagu B, Heurich R, Lichtblau H, Shaposhnik Z, Daniewska I et al (2002) **Antidepressant, anxiolytic and anorectic effects of a melanin-concentrating hormone-1 receptor antagonist.** *Nat Med,* 8:825–830
15. Brailov I, Bancila M, Brisorgueil MJ, Miquel MC, Hamon M, Verge D (2000) **Localization of 5-HT(6) receptors at the plasma membrane of neuronal cilia in the rat brain.** *Brain Res,* 872:271–275
16. Brodsky M, Lesiak AJ, Croicu A, Cohenca N, Sullivan JM, Neumaier JF (2017) **5-HT6 receptor blockade regulates primary cilia morphology in striatal neurons.** *Brain Res,* 1660:10–19
17. Buch T, Heppner FL, Tertilt C, Heinen TJ, Kremer M, Wunderlich FT, Jung S, Waisman A (2005) **A Cre-inducible diphtheria toxin receptor mediates cell lineage ablation after toxin administration.** *Nat Methods,* 2:419–426
18. Chaki S, Funakoshi T, Hirota-Okuno S, Nishiguchi M, Shimazaki T, Iijima M, Grottick AJ, Kanuma K, Onodera K, Sekiguchi Y et al (2005) A**nxiolytic- and antidepressant-like profile of ATC0065 and ATC0175: nonpeptidic and orally active melanin-concentrating hormone receptor 1 antagonists.** *J Pharmacol Exp Ther,* 313:831–839
19. Chung S, Hopf FW, Nagasaki H, Li CY, Belluzzi JD, Bonci A, Civelli O (2009) **The melanin-concentrating hormone system modulates cocaine reward.** *Proc Natl Acad Sci USA,* 106:6772–6777
20. Chung S, Verheij MM, Hesseling P, van Vugt RW, Buell M, Belluzzi JD, Geyer MA, Martens GJ, Civelli O (2011) **The melanin-concentrating hormone MCH system modulates behaviors associated with psychiatric disorders.** *PloS ONE,* 6:e19286

21. Clary-Meinesz CF, Cosson J, Huitorel P, Blaive B (1992) **Temperature effect on the ciliary beat frequency of human nasal and tracheal ciliated cells.** *Biol Cell,* 76:335–338

22. Cohen H, Liberzon I, Matar MA (2014) **Translational implications of oxytocin-mediated social buffering following immobilization stress in female prairie voles.** *Biol Psychiat,* 76:268–269

23. Della-Zuana O, Presse F, Ortola C, Duhault J, Nahon JL, Levens N (2002) **Acute and chronic administration of melanin- concentrating hormone enhances food intake and body weight in Wistar and Sprague-Dawley rats.** *International journal of obesity and related metabolic disorders: journal of the International Association for the Study of Obesity,* 26:1289–1295

24. Devera A, Pascovich C, Lagos P, Falconi A, Sampogna S, Chase MH, Torterolo P (2015) **Melanin-concentrating hormone (MCH) modulates the activity of dorsal raphe neurons.** *Brain Res,* 1598:114–128

25. Dilsiz P, Aklan I, Sayar Atasoy N, Yavuz Y, Filiz G, Koksallar F, Ates T, Oncul M, Coban I, Ates Oz E et al (2020) **MCH neuron activity is sufficient for reward and reinforces feeding.** *Neuroendocrinol,* 110:258–270

26. Diniz GB, Battagello DS, Klein MO, Bono BSM, Ferreira JGP, Motta-Teixeira LC, Duarte JCG, Presse F, Nahon JL, Adamantidis A et al (2020) **Ciliary melanin-concentrating hormone receptor 1 (MCHR1) is widely distributed in the murine CNS in a sex-independent manner.** *J Neurosci Res,* 98:2045–2071

27. Domire JS, Green JA, Lee KG, Johnson AD, Askwith CC, Mykytyn K (2011) **Dopamine receptor 1 localizes to neuronal cilia in a dynamic process that requires the Bardet-Biedl syndrome proteins.** *Cell Mol life Sci: CMLS,* 68:2951–2960

28. Engle SE, Bansal R, Antonellis PJ, Berbari NF (2021) **Cilia signaling and obesity.** *Semin Cell Dev Biol,* 110:43–50

29. G. Paxinos, K.F. (2001). **The mouse brain in stereotaxic coordinates.** (Academic Press).

30. Garcia-Fuster MJ, Parks GS, Clinton SM, Watson SJ, Akil H, Civelli O (2012) **The melanin-concentrating hormone (MCH) system in an animal model of depression-like behavior.** *Eur Neuropsychopharmacology: the journal of the European College of Neuropsychopharmacology,* 22:607–613
31. Gehlert DR, Rasmussen K, Shaw J, Li X, Ardayfio P, Craft L, Coskun T, Zhang HY, Chen Y, Witkin JM (2009) **Preclinical evaluation of melanin-concentrating hormone receptor 1 antagonism for the treatment of obesity and depression.** *J Pharmacol Exp Ther,* 329:429–438
32. Gomori A, Ishihara A, Ito M, Mashiko S, Matsushita H, Yumoto M, Ito M, Tanaka T, Tokita S, Moriya M et al (2003) **Chronic intracerebroventricular infusion of MCH causes obesity in mice. Melanin-concentrating hormone.** *American journal of physiology. Endocrinol Metab,* 284:E583-588
33. Gonzalez JA, Iordanidou P, Strom M, Adamantidis A, Burdakov D (2016) **Awake dynamics and brain-wide direct inputs of hypothalamic MCH and orexin networks.** *Nat Commun,* 7:11395
34. Gonzalez MI, Baker BI, Wilson CA (1997) **Stimulatory effect of melanin-concentrating hormone on luteinising hormone release.** *Neuroendocrinology,* 66:254–262
35. Gonzalez MI, Vaziri S, Wilson CA (1996) **Behavioral effects of alpha-MSH and MCH after central administration in the female rat.** *Peptides,* 17:171–177
36. Hamamoto A, Yamato S, Katoh Y, Nakayama K, Yoshimura K, Takeda S, Kobayashi Y, Saito Y (2016) **Modulation of primary cilia length by melanin-concentrating hormone receptor 1.** *Cell Signal,* 28:572–584
37. Handel M, Schulz S, Stanarius A, Schreff M, Erdtmann-Vourliotis M, Schmidt H, Wolf G, Holly V (1999) **Selective targeting of somatostatin receptor 3 to neuronal cilia.** *Neuroscience,* 89:909–926

38. Hartwig C, Monis WJ, Chen X, Dickman DK, Pazour GJ, Faundez V (2018) **Neurodevelopmental disease mechanisms, primary cilia, and endosomes converge on the BLOC-1 and BORC complexes.** *Dev Neurobiol,* 78:311–330

39. Hassani OK, Lee MG, Jones BE (2009) **Melanin-concentrating hormone neurons discharge in a reciprocal manner to orexin neurons across the sleep-wake cycle.** *Proc Natl Acad Sci U S A,* 106:2418–2422

40. Hervieu GJ, Cluderay JE, Harrison D, Meakin J, Maycox P, Nasir S, Leslie RA (2000) **The distribution of the mRNA and protein products of the melanin-concentrating hormone (MCH) receptor gene, slc-1, in the central nervous system of the rat.** *Eur J Neurosci,* 12:1194–1216

41. Hu L, Wang B, Zhang Y (2017) **Serotonin 5-HT6 receptors affect cognition in a mouse model of Alzheimer's disease by regulating cilia function.** *Alzheimer's Res Ther,* 9:76

42. Humphries S (2013) **A physical explanation of the temperature dependence of physiological processes mediated by cilia and flagella.** *Proc Natl Acad Sci USA,* 110:14693–14698

43. Kobayashi Y, Okada T, Miki D, Sekino Y, Koganezawa N, Shirao T, Diniz GB, Saito Y (2021) **Properties of primary cilia in melanin-concentrating hormone receptor 1-bearing hippocampal neurons in vivo and in vitro.** *Neurochemistry international,* 142:104902

44. Kobayashi, Y., Tomoshige, S., Imakado, K., Sekino, Y., Kogan- ezawa, N., Shirao, T., Diniz, G.B., Miyamoto, T., and Saito, Y. **Ciliary GPCR-based transcriptome as a key regulator of cilia length control.** FASEB BioAdvances *n/a*.

45. Kong D, Vong L, Parton LE, Ye C, Tong Q, Hu X, Choi B, Bruning JC, Lowell BB (2010) **Glucose stimulation of hypothalamic MCH neurons involves K(ATP) channels, is modulated by UCP2, and regulates peripheral glucose homeostasis.** *Cell Metab,* 12:545–552

46. Krashes MJ, Koda S, Ye C, Rogan SC, Adams AC, Cusher DS, Maratos-Flier E, Roth BL, Lowell BB (2011) **Rapid, reversible activation of AgRP neurons drives feeding behavior in mice.** *J Clin Invest,* 121:1424–1428

47. Kuhara A, Okumura M, Kimata T, Tanizawa Y, Takano R, Kimura KD, Inada H, Matsumoto K, Mori I (2008) **Temperature sensing by an olfactory neuron in a circuit controlling behavior of C. elegans.** *Sci,* 320:803–807

48. Lopez Hill X, Pascovich C, Urbonavicius J, Torterolo P, Scorza MC (2013) **The median raphe nucleus participates in the depressive-like behavior induced by MCH: differences with the dorsal raphe nucleus.** *Peptides,* 50:96–99

49. Marsh DJ, Weingarth DT, Novi DE, Chen HY, Trumbauer ME, Chen AS, Guan XM, Jiang MM, Feng Y, Camacho RE et al (2002) **Melanin-concentrating hormone 1 receptor-deficient mice are lean, hyperactive, and hyperphagic and have altered metabolism.** *Proc Natl Acad Sci USA,* 99:3240–3245

50. Mattis J, Tye KM, Ferenczi EA, Ramakrishnan C, O'Shea DJ, Prakash R, Gunaydin LA, Hyun M, Fenno LE, Gradinaru V et al (2011) **Principles for applying optogenetic tools derived from direct comparative analysis of microbial opsins**. *Nat Methods,* 9:159–172

51. Miyoshi K, Kasahara K, Miyazaki I, Asanuma M (2009) **Lithium treatment elongates primary cilia in the mouse brain and in cultured cells.** *Biochem Biophys Res Commun,* 388:757–762

52. Naganuma F, Bandaru SS, Absi G, Mahoney CE, Scammell TE, Vetrivelan R (2018) **Melanin-concentrating hormone neurons contribute to dysregulation of rapid eye movement sleep in narcolepsy.** *Neurobiol Dis,* 120:12–20

53. Nahon JL, Presse F, Bittencourt JC, Sawchenko PE, Vale W (1989) T**he rat melanin-concentrating hormone messenger ribonucleic acid encodes multiple putative neuropeptides coexpressed in the dorsolateral hypothalamus.** *Endocrinology,* 125:2056–2065

54. Nauli SM, Jin X, AbouAlaiwi WA, El-Jouni W, Su X, Zhou J (2013) **Non-motile primary cilia as fluid shear stress mechanosensors.** *Methods Enzymol,* 525:1–20

55. Noble EE, Hahn JD, Konanur VR, Hsu TM, Page SJ, Cortella AM, Liu CM, Song MY, Suarez AN, Szujewski CC et al (2018) **Control of feeding behavior by cerebral ventricular volume transmission of melanin concentrating hormone.** *Cell metabolism,* 28(55):68-e57

56. Nonaka S, Tanaka Y, Okada Y, Takeda S, Harada A, Kanai Y, Kido M, Hirokawa N (1998) **Randomization of left-right asymmetry due to loss of nodal cilia generating leftward flow of extraembryonic fluid in mice lacking KIF3B motor protein.** *Cell,* 95:829–837

57. O'Callaghan C, Achaval M, Forsythe I, Barry PW (1995) **Brain and respiratory cilia: the effect of temperature.** *Biol Neonate,* 68:394–397

58. Oh ST, Liu QF, Jeong HJ, Lee S, Samidurai M, Jo J, Pak SC, Park HJ, Kim J, Jeon S (2019) **Nasal cavity administration of melanin-concentrating hormone improves memory impairment in memory-impaired and Alzheimer's disease mouse models.** *Mol Neurobiol,* 56:8076–8086

59. Omori Y, Chaya T, Yoshida S, Irie S, Tsujii T, Furukawa T (2015) **Identification of G protein-coupled receptors GPCRs in primary cilia and their possible involvement in body weight control.** *PloS one,* 10:e0128422

60. Onaka T, Takayanagi Y, Yoshida M (2012) **Roles of oxytocin neurons in the control of stress, energy metabolism, and social behaviour.** *J Neuroendocrinol,* 24:587–598

61. Parkes D, Vale W (1992) **Secretion of melanin-concentrating hormone and neuropeptide-EI from cultured rat hypothalamic cells.** *Endocrinology,* 131:1826–1831

62. Paxinos, G.W., Charles. (2007). **The rat brain in stereotaxic coordinates.**

63. Pedersen CA, Caldwell JD, Walker C, Ayers G, Mason GA (1994) **Oxytocin activates the postpartum onset of rat maternal behavior in the ventral tegmental and medial preoptic areas.** *Behav Neurosci,* 108:1163–1171

64. Pedersen CA, Prange AJ Jr (1979) **Induction of maternal behavior in virgin rats after intracerebroventricular administration of oxytocin.** *Proc Natl Acad Sci USA,* 76:6661–6665

65. Phan, J., Alhassen, L., Argelagos, A., Alhassen, W., Vachirakorntong, B., Lin, Z.T., Sanathara, N., and Alachkar, A. (2020). **Mating and parenting experiences sculpture mood-modulating effects of oxytocin-MCH signaling.** *Sci Rep-Uk 10*.

66. Reiter JF, Leroux MR (2017) **Genes and molecular pathways underpinning ciliopathies.** *Nat Rev Mol Cell Biol,* 18:533–547

67. Rondini TA, Donato J Jr, Rodrigues Bde C, Bittencourt JC, Elias CF (2010) **Chemical identity and connections of medial preoptic area neurons expressing melanin-concentrating hormone during lactation.** *J Chem Neuroanat,* 39:51–62

68. Saito Y, Cheng M, Leslie FM, Civelli O (2001) **Expression of the melanin-concentrating hormone (MCH) receptor mRNA in the rat brain.** *J Comp Neurol,* 435:26–40

69. Saito Y, Nothacker HP, Wang Z, Lin SH, Leslie F, Civelli O (1999) **Molecular characterization of the melanin-concentrating- hormone receptor.** *Nature,* 400:265–269

70. Sanathara NM, Garau C, Alachkar A, Wang L, Wang Z, Nishi- mori K, Xu X, Civelli O (2018) **Melanin concentrating hormone modulates oxytocin-mediated marble burying.** *Neuropharmacology,* 128:22–32

71. Schneider CA, Rasband WS, Eliceiri KW (2012) **NIH image to ImageJ: 25 years of image analysis.** *Nat Methods,* 9:671–675

72. Shearman LP, Camacho RE, Sloan Stribling D, Zhou D, Bednarek MA, Hreniuk DL, Feighner SD, Tan CP, Howard AD, Van der Ploeg LH et al (2003) **Chronic MCH-1 receptor modulation alters appetite, body weight and adiposity in rats.** *Eur J Pharmacol,* 475:37–47

73. Shimazaki T, Yoshimizu T, Chaki S (2006) **Melanin-concentrating hormone MCH1 receptor antagonists: a potential new approach to the treatment of depression and anxiety disorders.** *CNS Drugs,* 20:801–811

74. Stanic D, Malmgren H, He H, Scott L, Aperia A, Hokfelt T (2009) **Developmental changes in frequency of the ciliary somatostatin receptor 3 protein.** *Brain Res,* 1249:101–112

75. Tomoshige S, Kobayashi Y, Hosoba K, Hamamoto A, Miyamoto T, Saito Y (2017) **Cytoskeleton-related regulation of primary cilia shortening mediated by melanin-concentrating hormone receptor 1.** *Gen Comp Endocrinol,* 253:44–52

76. Torterolo P, Lagos P, Sampogna S, Chase MH (2008) **Melanin- concentrating hormone (MCH) immunoreactivity in non-neuronal cells within the raphe nuclei and subventricular region of the brainstem of the cat.** *Brain Res,* 1210:163–178

77. Tsang SH, Aycinena ARP, Sharma T (2018) **Ciliopathy: Bardet- Biedl syndrome**. *Adv Exp Med Biol,* 1085:171–174

78. Urbanavicius J, Lagos P, Torterolo P, Abin-Carriquiry JA, Scorza C (2016) **Melanin-concentrating hormone projections to the dorsal raphe nucleus: an immunofluorescence and in vivo microdialysis study.** *J Chem Neuroanat,* 72:16–24

79. Urbanavicius J, Lagos P, Torterolo P, Scorza C (2014) **Prodepressive effect induced by microinjections of MCH into the dorsal raphe: time course, dose dependence, effects on anxiety-related behaviors, and reversion by nortriptyline.** *Behav Pharmacol,* 25:316–324

80. Valente EM, Rosti RO, Gibbs E, Gleeson JG (2014) **Primary cilia in neurodevelopmental disorders.** *Nat Rev Neurol,* 10:27–36

81. Varela L, Horvath TL (2018) **Neuronal cilia: another player in the melanocortin system.** *Trends Mol Med,* 24:333–334

82. Vawter MP, Schulmann A, Alhassen L, Alhassen W, Hamzeh AR, Sakr J, Pauluk L, Yoshimura R, Wang X, Dai Q et al (2020) **Melanin concentrating hormone signaling**

deficits in schizophrenia: association with memory and social impairments and abnormal sensorimotor gating. *Int J Neuropsychopharmacol,* 23:53–65

83. Wheatley DN (2008) **Nanobiology of the primary cilium–paradigm of a multifunctional nanomachine complex.** *Methods Cell Biol,* 90:139–156
84. Yoshiba S, Shiratori H, Kuo IY, Kawasumi A, Shinohara K, Nonaka S, Asai Y, Sasaki G, Belo JA, Sasaki H et al (2012) **Cilia at the node of mouse embryos sense fluid flow for left-right determination via Pkd2.** *Science,* 338:226–231
85. Zhang Q, Nishimura D, Seo S, Vogel T, Morgan DA, Searby C, Bugge K, Stone EM, Rahmouni K, Sheffield VC (2011) **Bardet- Biedl syndrome 3 (Bbs3) knockout mouse model reveals common BBS-associated phenotypes and Bbs3 unique phenotypes.** *Proc Natl Acad Sci USA,* 108:20678–20683

Chapter 5 References

1. Fuchs JL, Schwark HD (2004) **Neuronal primary cilia: a review.** *Cell Biol Int,* 28(2):111–118
2. Baudoin JP et al (2012) **Tangentially migrating neurons assemble a primary cilium that promotes their reorientation to the cortical plate.** *Neuron* 76(6):1108–1122
3. Gerdes JM, Davis EE, Katsanis N (2009) **The vertebrate primary cilium in development, homeostasis, and disease.** *Cell,* 137(1):32–45
4. Abou Alaiwi WA, Lo ST, Nauli SM (2009) **Primary cilia: highly sophisticated biological sensors.** *Sensors,* 9(9):7003–7020
5. Brailov I et al (2000) **Localization of 5-HT(6) receptors at the plasma membrane of neuronal cilia in the rat brain.** *Brain Res,* 872(1–2):271–275
6. Berbari NF, Lewis JS, Bishop GA, Askwith CC, Mykytyn K (2008) **Bardet-Biedl syndrome proteins are required for the local- ization of G protein-coupled receptors to primary cilia.** *Proc Natl Acad Sci USA,* 105(11):4242–4246

7. Domire JS et al (2011) **Dopamine receptor 1 localizes to neuronal cilia in a dynamic process that requires the Bardet-Biedl syndrome proteins.** *Cell Mol Life Sci : CMLS,* 68(17):2951–2960
8. Handel M et al (1999) **Selective targeting of somatostatin receptor 3 to neuronal cilia.** *Neuroscience,* 89(3):909–926
9. Omori Y et al (2015) **Identification of G protein-coupled recep- tors (GPCRs) in primary cilia and their possible involvement in body weight control.** *PLoS ONE,* 10(6):e0128422
10. Varela L, Horvath TL (2018) **Neuronal cilia: another player in the melanocortin system.** *Trends Mol Med,* 24(4):333–334
11. Louvi A, Grove EA (2011) **Cilia in the CNS: the quiet organelle claims center stage.** *Neuron,* 69(6):1046–1060
12. Trulioff A, Ermakov A, Malashichev Y (2017) **Primary cilia as a possible link between left-right asymmetry and neurodevelopmental diseases.** *Genes,* 8(2):48
13. Nauli SM et al (2013) **Non-motile primary cilia as fluid shear stress mechanosensors.** *Methods Enzymol,* 525:1–20
14. Atkinson KF, Sherpa RT, Nauli SM (2019) **The role of the primary cilium in sensing extracellular pH.** *Cells,* 8(7):704
15. Christensen ST, Voss JW, Teilmann SC, Lambert IH (2005) **High expression of the taurine transporter TauT in primary cilia of NIH3T3 fibroblasts.** *Cell Biol Int,* 29(5):347–351
16. Bargmann CI (2006) **Chemosensation in C. elegans.** *WormBook* 1–29
17. Alhassen W et al (2022) **Regulation of brain primary cilia length by MCH signaling: evidence from pharmacological, genetic, optogenetic, and chemogenic manipulations.** *Mol Neurobiol,* 59(1):245–265
18. Baldi P et al (2021) **Large-scale analysis reveals spatiotemporal circadian patterns of cilia transcriptomes in the primate brain.** *J Neurosci Res,* 99(10):2610–2624

19. Chen S et al (2021) **Dynamic changes of brain cilia transcrip- tomes across the human lifespan.** *Int J Mol Sci,* 22(19):10387
20. Hartwig C et al (2018) **Neurodevelopmental disease mechanisms, primary cilia, and endosomes converge on the BLOC-1 and BORC complexes.** *Dev Neurobiol,* 78(3):311–330
21. Valente EM, Rosti RO, Gibbs E, Gleeson JG (2014) **Primary cilia in neurodevelopmental disorders.** *Nat Rev Neurol,* 10(1):27–36
22. Reiter JF, Leroux MR (2017) **Genes and molecular pathways underpinning ciliopathies.** *Nat Rev Mol Cell Biol,* 18(9):533–547
23. Berbari NF et al (2014) **Hippocampal and cortical primary cilia are required for aversive memory in mice.** *PLoS ONE,* 9(9):e106576
24. Bowie E and Goetz SC (2020) **TTBK2 and primary cilia are essential for the connectivity and survival of cerebellar Purkinje neurons**. *eLife* 9
25. Ramos C et al (2021) **Neuron-specific cilia loss differentially alters locomotor responses to amphetamine in mice.** *J Neurosci Res,* 99(3):827–842
26. Alhassen W et al (2021) **Patterns of cilia gene dysregulations in major psychiatric disorders.** *Prog Neuropsychopharmacol Biol Psychiatry,* 109:110255
27. Reig R, Silberberg G (2014) **Multisensory integration in the mouse striatum.** *Neuron,* 83(5):1200–1212
28. Pan WX, Mao T, Dudman JT (2010) **Inputs to the dorsal striatum of the mouse reflect the parallel circuit architecture of the forebrain.** *Front Neuroanat,* 4:147
29. Voorn P, Vanderschuren LJ, Groenewegen HJ, Robbins TW, Pennartz CM (2004) **Putting a spin on the dorsal-ventral divide of the striatum.** *Trends Neurosci,* 27(8):468–474
30. Gerfen CR (1992) **The neostriatal mosaic: multiple levels of compartmental organization in the basal ganglia.** *Annu Rev Neurosci,* 15:285–320

31. Gerfen CR (1984) **The neostriatal mosaic: compartmentalization of corticostriatal input and striatonigral output systems.** *Nature,* 311(5985):461–464
32. Morita M, Hikida T (2015) **Distinct roles of the direct and indirect pathways in the basal ganglia circuit mechanism.** *J Psychopharmacol,* 35(5–6):107–111
33. Ikemoto S, Yang C, Tan A (2015) **Basal ganglia circuit loops, dopamine and motivation: a review and enquiry.** *Behav Brain Res,* 290:17–31
34. Kreitzer AC, Malenka RC (2008) **Striatal plasticity and basal ganglia circuit function.** *Neuron,* 60(4):543–554
35. Foley P, Riederer P (2000) **The motor circuit of the human basal ganglia reconsidered.** *J Neural Transm Suppl,* 58:97–110
34. Trujillo CM, Yanes CM, Marrero A, Monzon M (1986) **Neuronal cilia in the embryonic thalamus and striatum of Gallotia galloti (Reptilia, Lacertidae)**. *J Hirnforsch* 27(6):691–694
35. Milhaud M, Pappas GD (1968) **Cilia formation in the adult cat brain after pargyline treatment.** *J Cell Biol*, 37(3):599–609
36. Hilgendorf KI, Johnson CT, Jackson PK (2016) **The primary cilium as a cellular receiver: organizing ciliary GPCR signaling.** *Curr Opin Cell Biol,* 39:84–92
37. Lancaster MA, Gleeson JG (2009) **The primary cilium as a cellular signaling center: lessons from disease.** *Curr Opin Genet Dev* 19(3):220–229
38. Christensen ST, Morthorst SK, Mogensen JB, Pedersen LB (2017) **Primary cilia and coordination of receptor tyrosine kinase (RTK) and transforming growth factor beta (TGF-beta) signaling.** *Cold Spring Harbor Perspect Biol* 9(6):a028167
39. Valencia-Gattas M, Conner GE, Fregien NL (2016) **Gefitinib, an EGFR tyrosine kinase inhibitor, prevents smoke-mediated ciliated airway epithelial cell loss and promotes their recovery.** *PLoS ONE,* 11(8):e0160216

40. Evans MJ et al (2002) **Fibroblast growth factor-2 during postnatal development of the tracheal basement membrane zone.** *Am J Physiol Lung Cell Mol Physiol,* 283(6):L263-1270

43. Nauli SM, Pala R, Kleene SJ (2016) **Calcium channels in primary cilia.** *Curr Opin Nephrol Hypertens,* 25(5):452–458

44. Nachury MV (2018) **The molecular machines that traffic signaling receptors into and out of cilia.** *Curr Opin Cell Biol,* 51:124–131

45. Liu B, Chen S, Cheng D, Jing W, Helms JA (2014) **Primary cilia integrate hedgehog and Wnt signaling during tooth development.** *J Dent Res,* 93(5):475–482

46. May-Simera HL, Kelley MW (2012) **Cilia, Wnt signaling, and the cytoskeleton.** *Cilia,* 1(1):7

47. Hirst WD et al (2003) **Differences in the central nervous system distribution and pharmacology of the mouse 5-hydroxy- tryptamine-6 receptor compared with rat and human receptors investigated by radioligand binding, site-directed mutagenesis, and molecular modeling.** *Mol Pharmacol*, 64(6):1295–1308

48. Graybiel AM (1990) **Neurotransmitters and neuromodulators in the basal ganglia.** *Trends Neurosci,* 13(7):244–254

49. Mizushima K et al (2000) **A novel G-protein-coupled receptor gene expressed in striatum.** *Genomics,* 69(3):314–321

50. Kumar JS et al (2016) **Radiosynthesis and in vivo evaluation of neuropeptide Y5 receptor (NPY5R) PET Tracers.** *ACS Chem Neurosci,* 7(5):540–545

51. Gerfen CR et al (1990) **D1 and D2 dopamine receptor-regu- lated gene expression of striatonigral and striatopallidal neurons.** *Science,* 250(4986):1429–1432

52. Kobayashi Y et al (2021) **Properties of primary cilia in melanin-concentrating hormone receptor 1-bearing hippocampal neurons in vivo and in vitro.** *Neurochem Int,* 142:104902

53. Ehrlich AT et al (2018) **Mapping GPR88-Venus illuminates a novel role for GPR88 in sensory processing.** *Brain Struct Funct,* 223(3):1275–1296

54. Miyoshi K et al (2014) **Lack of dopaminergic inputs elongates the primary cilia of striatal neurons.** *PLoS ONE,* 9(5):e97918

55. Brodsky M et al (2017) **5-HT6 receptor blockade regulates primary cilia morphology in striatal neurons.** *Brain Res,* 1660:10–19

56. Jasso KR et al (2021) **An N-terminal fusion allele to study mela- nin concentrating hormone receptor 1.** *Genesis,* 59(7–8):e23438

57. Middleton FA, Strick PL (2000) **Basal ganglia output and cogni- tion: evidence from anatomical, behavioral, and clinical studies.** *Brain Cogn,* 42(2):183–200

58. Chudasama Y, Robbins TW (2006) **Functions of frontostriatal systems in cognition: comparative neuropsychopharmacological studies in rats, monkeys and humans.** *Biol Psychol,* 73(1):19–38

59. Hikosaka O, Ghazizadeh A, Griggs W, Amita H (2018) **Parallel basal ganglia circuits for decision making.** *J Neural Transm,* 125(3):515–529

60. McDonald RJ, Hong NS (2013) **How does a specific learning and memory system in the mammalian brain gain control of behavior?** *Hippocampus,* 23(11):1084–1102

61. Haynes WIA et al (2018) **Altered anatomical connections of associative and limbic cortico-basal-ganglia circuits in obsessive- compulsive disorder.** *Eur Psychiatry: J Assoc Eur Psychiatrists,* 51:1–8

62. Maia TV, Cooney RE, Peterson BS (2008) T**he neural bases of obsessive-compulsive disorder in children and adults.** *Dev Psychopathol,* 20(4):1251–1283

63. Caligiore D, Mannella F, Arbib MA, Baldassarre G (2017) **Dysfunctions of the basal ganglia-cerebellar-thalamo-cortical system produce motor tics in Tourette syndrome.** *PLoS Comput Biol,* 13(3):e1005395

64. Ramkiran S, Heidemeyer L, Gaebler A, Shah NJ, Neuner I (2019) **Alterations in basal ganglia-cerebello-thalamo-cortical connectivity and whole brain functional network topology in Tourette's syndrome.** *NeuroImage Clin,* 24:101998

65. Vicente AM, Martins GJ, Costa RM (2020) **Cortico-basal ganglia circuits underlying dysfunctional control of motor behaviors in neuropsychiatric disorders.** *Curr Opin Genet Dev,* 65:151–159

66. Mills KL et al (2012) **Altered cortico-striatal-thalamic connectivity in relation to spatial working memory capacity in children with ADHD.** *Front Psych,* 3:2

67. Kwak Y et al (2010) **Altered resting state cortico-striatal connectivity in mild to moderate stage Parkinson's disease.** *Front Syst Neurosci,* 4:143

68. Perez-Costas E, Melendez-Ferro M, Roberts RC (2010) **Basal ganglia pathology in schizophrenia: dopamine connections and anomalies.** *J Neurochem,* 113(2):287–302

69. Bogerts B, Meertz E, Schonfeldt-Bausch R (1985) **Basal ganglia and limbic system pathology in schizophrenia. A morphometric study of brain volume and shrinkage.** *Arch Gen Psychiatry,* 42(8):784–791

70. Avram M, Brandl F, Bauml J, Sorg C (2018) **Cortico-thalamic hypo- and hyperconnectivity extend consistently to basal ganglia in schizophrenia. Neuropsychopharmacology :** *Off Publ Am Coll Neuropsychopharmacol,* 43(11):2239–2248

71. Fuccillo MV (2016) **Striatal circuits as a common node for autism pathophysiology.** *Front Neurosci,* 10:27

72. Schuetze M et al (2016) **Morphological alterations in the thala- mus, striatum, and pallidum in autism spectrum disorder.** *Neuropsychopharmacology : Off Publ Am Coll Neuropsychopharmacol,* 41(11):2627–2637

73. Chiken S, Takada M, Nambu A (2021) **Altered dynamic information flow through the cortico-basal ganglia pathways mediates Parkinson's disease symptoms.** *Cereb Cortex,* 31(12):5363–5380
74. Martinu K, Monchi O (2013) **Cortico-basal ganglia and cortico- cerebellar circuits in Parkinson's disease: pathophysiology or compensation?** *Behav Neurosci,* 127(2):222–236
75. Braak H, Del Tredici K (2008) **Cortico-basal ganglia-cortical circuitry in Parkinson's disease reconsidered.** *Exp Neurol,* 212(1):226–229
76. Blumenstock S, Dudanova I (2020) **Cortical and striatal circuits in Huntington's disease.** *Front Neurosci,* 14:82
77. Paylor R, Spencer CM, Yuva-Paylor LA, Pieke-Dahl S (2006) **The use of behavioral test batteries, II: effect of test interval.** *Physiol Behav,* 87(1):95–102
78. Alachkar A et al (2018) **Prenatal one-carbon metabolism dysregulation programs schizophrenia-like deficits.** *Mol Psychiatry,* 23(2):282–294
79. Alhassen S et al (2021) **Intergenerational trauma transmission is associated with brain metabotranscriptome remodeling and mitochondrial dysfunction.** *Commun Biol,* 4(1):783
80. Deacon RM, Rawlins JN (2006) **T-maze alternation in the rodent.** *Nat Protoc,* 1(1):7–12
81. Kaidanovich-Beilin O, Lipina T, Vukobradovic I, Roder J, Woodgett JR (2011) **Assessment of social interaction behaviors.** *J Vis Exp,* (48):2473
82. McGaugh JL (2000) **Memory–a century of consolidation**. *Science,* 287(5451):248–251
83. Eryilmaz H et al (2017) **Neural determinants of human goal- directed vs. habitual action control and their relation to trait motivation.** *Sci Rep,* 7(1):6002
84. Balleine BW, O'Doherty JP (2010) **Human and rodent homologies in action control: corticostriatal determinants of goal- directed and habitual action.** *Neuropsychopharmacology : Off Publ Am Coll Neuropsychopharmacol,* 35(1):48–69

85. Thorn CA, Atallah H, Howe M, Graybiel AM (2010) **Differential dynamics of activity changes in dorsolateral and dorso- medial striatal loops during learning.** *Neuron,* 66(5):781–795

86. Dezfouli A, Balleine BW (2013) **Actions, action sequences and habits: evidence that goal-directed and habitual action control are hierarchically organized.** *PLoS Comput Biol,* 9(12):e1003364

87. Gremel CM, Costa RM (2013) **Orbitofrontal and striatal circuits dynamically encode the shift between goal-directed and habitual actions.** *Nat Commun,* 4:2264

88. Floresco SB (2015) **The nucleus accumbens: an interface between cognition, emotion, and action.** *Annu Rev Psychol,* 66:25–52

89. Shiotsuki H et al (2010) **A rotarod test for evaluation of motor skill learning.** *J Neurosci Methods,* 189(2):180–185

90. Deacon RM (2013) **Measuring motor coordination in mice.** *J Vis Exp : JoVE,* 75:e2609

91. Graybiel AM, Aosaki T, Flaherty AW, Kimura M (1994) **The basal ganglia and adaptive motor control.** *Science,* 265(5180):1826–1831

92. Geddes CE, Li H, Jin X (2018) **Optogenetic editing reveals the hierarchical organization of learned action sequences.** *Cell* 174(1):32-43 e15

93. Geyer MA, Braff DL (1987) **Startle habituation and sensorimotor gating in schizophrenia and related animal models.** *Schizophr Bull,* 13(4):643–668

94. Fobbs WC et al (2020) **Continuous representations of speed by striatal medium spiny neurons.** *J Neurosci: Off J Soc Neurosc,* 40(8):1679–1688

95. Yttri EA, Dudman JT (2016) **Opponent and bidirectional control of movement velocity in the basal ganglia.** *Nature,* 533(7603):402–406

96. Rueda-Orozco PE, Robbe D (2015) **The striatum multiplexes contextual and kinematic information to constrain motor habits execution.** *Nat Neurosci,* 18(3):453–460

97. Lipton DM, Gonzales BJ, Citri A (2019) **Dorsal striatal circuits for habits, compulsions and addictions.** *Front Syst Neurosci,* 13:28

98. Banca P et al (2015) **Imbalance in habitual versus goal directed neural systems during symptom provocation in obsessive-compulsive disorder.** *Brain : J Neurol,* 138(Pt 3):798–811

99. Smith KS, Graybiel AM (2013) **A dual operator view of habit- ual behavior reflecting cortical and striatal dynamics.** *Neuron*, 79(2):361–374

100. Gu BM, van Rijn H, Meck WH (2015) **Oscillatory multiplexing of neural population codes for interval timing and working memory.** *Neurosci Biobehav Rev,* 48:160–185

101. Brodziak A, Brewczynski A, Bajor G (2013) **Clinical significance of knowledge about the structure, function, and impairments of working memory.** *Med Sci Monitor : Int Med J Exp Clin Res,* 19:327–338

102. Nyberg L, Eriksson J (2015) **Working memory: maintenance, updating, and the realization of intentions.** *Cold Spring Harb Perspect Biol,* 8(2):a021816

103. Cools R, Gibbs SE, Miyakawa A, Jagust W, D'Esposito M (2008) **Working memory capacity predicts dopamine synthesis capacity in the human striatum.** *J neurosci: Off J Soc Neurosci,* 28(5):1208–1212

104. Akhlaghpour H, Wiskerke J, Choi JY, Taliaferro JP, Au J, Witten IB (2016) **Dissociated sequential activity and stimulus encoding in the dorsomedial striatum during spatial working memory.** *eLife,* 5:e19507

105. Haeger A, Lee H, Fell J, Axmacher N (2015) **Selective processing of buildings and faces during working memory: the role of the ventral striatum.** *Eur J Neurosci,* 41(4):505–513

106. van den Bos R (2015) **The dorsal striatum and ventral striatum play different roles in the programming of social behaviour: a tribute to Lex Cools.** *Behav Pharmacol*, 26(1–2):6–17

107. Goodin P, Lamp G, Hughes ME, Rossell SL, Ciorciari J (2019) **Decreased response to positive facial affect in a depressed cohort in the dorsal striatum during a working memory task-a preliminary fMRI study.** *Front Psych,* 10:60

108. Rhee S, Kirschen GW, Gu Y, Ge S (2016) **Depletion of primary cilia from mature dentate granule cells impairs hippocampus- dependent contextual memory.** *Sci Rep,* 6:34370

109. Joel D, Weiner I (2000) **The connections of the dopaminergic system with the striatum in rats and primates: an analysis with respect to the functional and compartmental organization of the striatum.** *Neuroscience,* 96(3):451–474

110. Groenewegen HJ, Trimble M (2007) **The ventral striatum as an interface between the limbic and motor systems.** *CNS Spectr,* 12(12):887–892

111. Lopes da Silva FH, Arnolds DE, Neijt HC (1984) **A functional link between the limbic cortex and ventral striatum: physiology of the subiculum accumbens pathway.** *Exp Brain Res,* 55(2):205–214

112. Kelley AE, Domesick VB, Nauta WJ (1982) **The amygdalostriatal projection in the rat–an anatomical study by anterograde and retrograde tracing methods**. *Neuroscience,* 7(3):615–630

113. Haber SN, Calzavara R (2009) **The cortico-basal ganglia integrative network: the role of the thalamus.** *Brain Res Bull* 78(2–3):69–74

114. Baladron J, Hamker FH (2015) **A spiking neural network based on the basal ganglia functional anatomy.** *Neural Netw : off J Int Neural Netw Soc,* 67:1–13

115. Garcia-Munoz M, Carrillo-Reid L, Arbuthnott GW (2010) **Functional anatomy: dynamic states in basal ganglia circuits.** *Front Neuroanat,* 4:144

116. Herrero MT, Barcia C, Navarro JM (2002) **Functional anatomy of thalamus and basal ganglia. Child's Nerv Syst: ChNS :** *Off J Int Soc Pediatr Neurosurg,* 18(8):386–404

117. Ishihara H, Yoshida K, Nemoto K, Tsuneoka K, Shikita M (1993) **Constitutive overexpression of the c-fos gene in radi- ation-induced granulocytic leukemia in mice.** *Radiat Res,* 135(3):394–399

118. Reiss M, Radin AI, Weisberg TF (1990) **Constitutive expression of the c-fos protooncogene in murine keratinocytes: potentiation of the mitogenic response to insulin-like growth factor 1.** *Can Res,* 50(20):6641–6648

119. Allman MJ, Teki S, Griffiths TD, Meck WH (2014) **Properties of the internal clock: first- and second-order principles of subjective time.** *Annu Rev Psychol,* 65:743–771

120. Mathias B, Tillmann B, Palmer C (2016) **Sensory, cognitive, and sensorimotor learning effects in recognition memory for music.** *J Cogn Neurosci,* 28(8):1111–1126

121. Hidalgo-Balbuena AE, Luma AY, Pimentel-Farfan AK, Pena- Rangel T, Rueda-Orozco PE (2019) **Sensory representations in the striatum provide a temporal reference for learning and executing motor habits.** *Nat Commun,* 10(1):4074

122. Howley SA, Prasad SE, Pender NP, Murphy KC (2012) **Relationship between reaction time, fine motor control, and visual-spatial perception on vigilance and visual-motor tasks in 22q11.2 Deletion Syndrome.** *Res Dev Disabil,* 33(5):1495–1502

123. Terry P, Doumas M, Desai RI, Wing AM (2009) **Dissociations between motor timing, motor coordination, and time perception after the administration of alcohol or caffeine**. *Psychopharmacology,* 202(4):719–729

124. Schubotz RI, Friederici AD, von Cramon DY (2000) **Time perception and motor timing: a common cortical and subcortical basis revealed by fMRI.** *Neuroimage,* 11(1):1–12

125. Treisman M, Faulkner A, Naish PL (1992) **On the relation between time perception and the timing of motor action: evidence for a temporal oscillator controlling the timing of move- ment.** *Q J Exp Psych. A, Human Exp Psychol,* 45(2):235–263

126. Gu H, Schulz KP, Fan J, Yang Y (2021) **Temporal dynamics of functional brain states underlie cognitive performance.** *Cereb Cortex,* 31(4):2125–2138

127. Barrouillet P, Bernardin S, Portrat S, Vergauwe E, Camos V (2007) **Time and cognitive load in working memory.** *J Exp Psychol. Lear, Mem, Cogn,* 33(3):570–585

128. Zhang G, Li Y, Zhang J (2019) **Tracking the dynamic functional network interactions during goal-directed auditory tasks by brain state clustering.** *Front Neurosci,* 13:1220

129. Huberle E, Brugger P (2018) **Altered time judgements highlight common mechanisms of time and space perception.** *Cogn Neuropsychol,* 35(8):458–470

130. Fontes R et al (2016) **Time perception mechanisms at central nervous system.** *Neurol Int,* 8(1):5939

131. Pouthas V, Perbal S (2004) **Time perception depends on accurate clock mechanisms as well as unimpaired attention and memory processes.** *Acta Neurobiol Exp,* 64(3):367–385

132. Gallistel CR, Gibbon J (2000) **Time, rate, and conditioning.** *Psychol Rev,* 107(2):289–344

133. Meck WH, Doyere V, Gruart A (2012) **Interval timing and time- based decision making.** *Front Integr Neurosci,* 6:13

134. Bonnefond M, Jensen O (2012) **Alpha oscillations serve to protect working memory maintenance against anticipated distracters.** *Current biology : CB,* 22(20):1969–1974

135. Brody CD, Hernandez A, Zainos A, Romo R (2003) **Timing and neural encoding of somatosensory parametric working memory in macaque prefrontal cortex.** *Cereb Cortex,* 13(11):1196–1207

136. Fortin C, Breton R (1995) **Temporal interval production and pro- cessing in working memory.** *Percept Psychophys,* 57(2):203–215

137. Macar F, Coull J, Vidal F (2006) **The supplementary motor area in motor and perceptual time processing: fMRI studies.** *Cogn Process,* 7(2):89–94

138. Wiener M, Turkeltaub P, Coslett HB (2010) **The image of time: a voxel-wise meta-analysis.** *Neuroimage,* 49(2):1728–1740

139. Magalhaes F et al (2018) **Neurochemical changes in basal ganglia affect time perception in parkinsonians.** *J Biomed Sci,* 25(1):26

140. Talakoub O et al (2016) **Time-course of coherence in the human basal ganglia during voluntary movements.** *Sci Rep,* 6:34930

141. Yin HH (2014) **Action, time and the basal ganglia.** *Philos Trans R Soc Lond Ser B, Biol Sci,* 369(1637):20120473

142. Gershman SJ, Moustafa AA, Ludvig EA (2014) **Time representa- tion in reinforcement learning models of the basal ganglia.** *Front Comput Neurosci,* 7:194

143. Li X, Luo F, Shi L, Woodward DJ, Chang J (2011) **Ensemble neural activity of the frontal cortical basal ganglia system predicts reaction time task performance in rats.** *Neurosci Res,* 71(2):149–160

144. Jin DZ, Fujii N, Graybiel AM (2009) **Neural representation of time in cortico-basal ganglia circuits.** *Proc Natl Acad Sci USA,* 106(45):19156–19161

145. Lo CC, Wang XJ (2006) **Cortico-basal ganglia circuit mechanism for a decision threshold in reaction time tasks.** *Nat Neurosci,* 9(7):956–963

146. Vakil E, Kahan S, Huberman M, Osimani A (2000) **Motor and non-motor sequence learning in patients with basal ganglia lesions: the case of serial reaction time (SRT).** *Neuropsychologia,* 38(1):1–10

147. Bussi IL, Levin G, Golombek DA, Agostino PV (2014) **Involvement of dopamine signaling in the circadian modulation of interval timing.** *Eur J Neurosci,* 40(1):2299–2310

148. Jones CR, Malone TJ, Dirnberger G, Edwards M, Jahanshahi M (2008) **Basal ganglia, dopamine and temporal processing: performance on three timing tasks on and off medication in Parkinson's disease.** *Brain Cogn,* 68(1):30–41

149. Yang YK et al (2004) **Association between cognitive performance and striatal dopamine binding is higher in timing and motor tasks in patients with schizophrenia.** *Psychiatry Res,* 131(3):209–216

150. Coslett HB, Wiener M, Chatterjee A (2010) **Dissociable neural systems for timing: evidence from subjects with basal ganglia lesions.** *PLoS ONE,* 5(4):e10324

151. Mello GB, Soares S, Paton JJ (2015) **A scalable population code for time in the striatum.** *Current biology : CB,* 25(9):1113–1122 152.

152. Gouvea TS, Monteiro T, Motiwala A, Soares S, Machens C, Paton JJ (2015) **Striatal dynamics explain duration judgments.** *eLife,* 4:e11386

153. Asai Y, Nomura T, Abe K, Matsuo Y, Sato S (2003) **Classification of dynamics of a model of motor coordination and comparison with Parkinson's disease data.** *Biosystems,* 71(1–2):11–21

154. Verschueren SM, Swinnen SP, Dom R, De Weerdt W (1997) **Interlimb coordination in patients with Parkinson's disease: motor learning deficits and the importance of augmented information feedback.** *Exp Brain Res,* 113(3):497–508

155. Yaguez L, Canavan AG, Lange HW, Homberg V (1999) **Motor learning by imagery is differentially affected in Parkinson's and Huntington's diseases.** *Behav Brain Res,* 102(1–2):115–127

156. Heindel WC, Butters N, Salmon DP (1988) **Impaired learning of a motor skill in patients with Huntington's disease.** *Behav Neurosci,* 102(1):141–147

157. Bloch MH et al (2011) **Poor fine-motor and visuospatial skills predict persistence of pediatric-onset obsessive-compulsive disorder into adulthood.** *J Child Psychol Psychiatry,* 52(9):974–983 158. Bedard

158. MJ, Joyal CC, Godbout L, Chantal S (2009) **Executive functions and the obsessive-compulsive disorder: on the importance of subclinical symptoms and other**

concomitant factors. *Arch Clin Neuropsychol : Off J Natl Acad Neuropsychol,* 24(6):585–598

159. Fenollar-Cortes J, Gallego-Martinez A, Fuentes LJ (2017) **The role of inattention and hyperactivity/impulsivity in the fine motor coordination in children with ADHD.** *Res Dev Disabil,* 69:77–84

160. Fliers EA et al (2012) **Genome-wide association study of motor coordination problems in ADHD identifies genes for brain and muscle function.** *World J Biol Psychiatry : Off J World Fed Soc Biol Psychiatry,* 13(3):211–222

161. Schiffman J et al (2009) **Childhood motor coordination and adult schizophrenia spectrum disorders.** *Am J Psychiatry,* 166(9):1041–1047

162. Martino D et al (2019) **Motor timing in Tourette syndrome: the effect of movement lateralization and bimanual coordination.** *Front Neurol,* 10:385

163. Eapen V et al (2019) **Social communication deficits and restricted repetitive behavior symptoms in Tourette syndrome.** *Neuropsychiatr Dis Treat,* 15:2151–2160

164. Leckman JF, King RA, Bloch MH (2014) **Clinical features of Tourette syndrome and tic disorders.** *J Obs-compuls Relat Disord,* 3(4):372–379

165. South M, Ozonoff S, McMahon WM (2005) **Repetitive behavior profiles in Asperger syndrome and high-functioning autism.** *J Autism Dev Disord,* 35(2):145–158

166. Bodfish JW, Symons FJ, Parker DE, Lewis MH (2000) **Varieties of repetitive behavior in autism: comparisons to mental retardation.** *J Autism Dev Disord,* 30(3):237–243

167. Morrens M, Hulstijn W, Lewi PJ, De Hert M, Sabbe BG (2006) **Stereotypy in schizophrenia.** *Schizophr Res,* 84(2–3):397–404

168. Tracy JI et al (1996) **Repetitive behaviors in schizophrenia: a single disturbance or discrete symptoms?** *Schizophr Res,* 20(1–2):221–229

169. Selles RR et al (2018) I**nitial psychometrics, outcomes, and correlates of the Repetitive Body Focused Behavior Scale: examina- tion in a sample of youth with anxiety and/or obsessive-compulsive disorder.** *Compr Psychiatry,* 81:10–17

170. McDougle CJ et al (1995) **A case-controlled study of repetitive thoughts and behavior in adults with autistic disorder and obsessive-compulsive disorder.** *Am J Psychiatry,* 152(5):772–777

171. Kurlan R (2004) **Disabling repetitive behaviors in Parkinson's disease.** *Mov Disord : Off J Mov Disord Soc,* 19(4):433–437

172. O'Boyle DJ, Freeman JS, Cody FW (1996) **The accuracy and precision of timing of self-paced, repetitive movements in subjects with Parkinson's disease.** *Brain : J Neurol,* 119(Pt 1):51–70

173. Pastor MA, Jahanshahi M, Artieda J, Obeso JA (1992) **Performance of repetitive wrist movements in Parkinson's disease.** *Brain : a J Neurol,* 115(Pt 3):875–891

174. Koyama T, Tachimori H, Osada H, Kurita H (2006) **Cognitive and symptom profiles in high-functioning pervasive developmental disorder not otherwise specified and attention-deficit/ hyperactivity disorder.** *J Autism Dev Disord,* 36(3):373–380

175. Cheng CH, Chan PS, Hsu SC, Liu CY (2018) **Meta-analysis of sensorimotor gating in patients with autism spectrum disorders.** *Psychiatry Res,* 262:413–419

176. Oranje B, Lahuis B, van Engeland H, Jan van der Gaag R, Kemner C (2013) **Sensory and sensorimotor gating in children with multiple complex developmental disorders (MCDD) and autism.** *Psychiatry Res,* 206(2–3):287–292

177. San-Martin R et al (2020) **Meta-analysis of sensorimotor gating deficits in patients with schizophrenia evaluated by prepulse inhibition test.** *Schizophr Bull,* 46(6):1482–1497

178. Hazlett EA, Buchsbaum MS (2001) **Sensorimotor gating deficits and hypofrontality in schizophrenia.** *Front Biosci,* 6:D1069-1072

179. Braff DL, Geyer MA (1990) **Sensorimotor gating and schizophrenia. Human and animal model studies.** *Arch Gen psychiatry,* 47(2):181–188

180. Pittenger C et al (2016) **OCD is associated with an altered association between sensorimotor gating and cortical and subcortical 5-HT1b receptor binding.** *J Affect Disord,* 196:87–96

181. Schleyken S et al (2020) **Deep brain stimulation and sensorimotor gating in tourette syndrome and obsessive-compulsive disorder.** *J Psychiatr Res,* 129:272–280

182. Ahmari SE, Risbrough VB, Geyer MA, Simpson HB (2012) **Impaired sensorimotor gating in unmedicated adults with obsessive-compulsive disorder.** *Neuropsychopharmacology : Off Publ Am Coll Neuropsychopharmacol,* 37(5):1216–1223

183. Buse J, Beste C, Herrmann E, Roessner V (2016) **Neural correlates of altered sensorimotor gating in boys with Tourette syndrome: a combined EMG/fMRI study.** *World J Biol Psychiatry : Off J World Feder Soc Biol Psychiatry,* 17(3):187–197

184. Zoetmulder M, Biernat HB, Nikolic M, Korbo L, Jennum PJ (2014) **Sensorimotor gating deficits in multiple system atrophy: comparison with Parkinson's disease and idiopathic REM sleep behavior disorder.** *Parkinsonism Relat Disord,* 20(3):297–302

185. Holstein DH et al (2013) **Sensory and sensorimotor gating in adult attention-deficit/hyperactivity disorder (ADHD)**. *Psychiatry Res,* 205(1–2):117–126

186. Valls-Sole J, Munoz JE, Valldeoriola F (2004) **Abnormalities of prepulse inhibition do not depend on blink reflex excitability: a study in Parkinson's disease and Huntington's disease.** *Clin Neurophysiol : Off J Int Feder Clin Neurophysiol,* 115(7):1527–1536

187. Swerdlow NR et al (1995) **Impaired prepulse inhibition of acoustic and tactile startle response in patients with Huntington's disease.** *J Neurol Neurosurg Psychiatry,* 58(2):192–200

188. Tao K et al (2022) **Disrupted social memory ensembles in the ventral hippocampus underlie social amnesia in autism-associated Shank3 mutant mice.** *Mol Psychiatry,* 9:7

189. Henderson HA et al (2009) **Self-referenced memory, social cognition, and symptom presentation in autism**. *J Child Psychol Psychiatry,* 50(7):853–861

190. Harvey PO, Lepage M (2014) **Neural correlates of recognition memory of social information in people with schizophrenia.** *J Psychiatry Neurosci : JPN,* 39(2):97–109

191. Takahashi H et al (2005) **Spatial working memory deficit correlates with disorganization symptoms and social functioning in schizophrenia.** *Psychiatry Clin Neurosci,* 59(4):453–460

192. Mavrogiorgou P et al (2016) **Social cognition and metacognition in obsessive-compulsive disorder: an explorative pilot study.** *Eur Arch Psychiatry Clin Neurosci,* 266(3):209–216

193. Sowerby P, Seal S, Tripp G (2011) **Working memory deficits in ADHD: the contribution of age, learning/language difficulties, and task parameters.** *J Atten Disord,* 15(6):461–472

194. Demeter G et al (2013) **Intact short-term memory and impaired executive functions in obsessive compulsive disorder.** 66(1–2):35–41

195. Dittrich WH, Johansen T (2013) **Cognitive deficits of executive functions and decision-making in obsessive-compulsive disorder.** *Scand J Psychol,* 54(5):393–400

196. Dutschke LL et al (2018) **Gesture impairments in schizophrenia are linked to increased movement and prolonged motor planning and execution.** *Schizophr Res,* 200:42–49

197. Carnahan H, Aguilar O, Malla A, Norman R (1997) **An investigation into movement planning and execution deficits in individuals with schizophrenia.** *Schizophr Res,* 23(3):213–221

198. Shafer RL, Lewis MH, Newell KM, Bodfish JW (2021) **Atypical neural processing during the execution of complex sensorimotor behavior in autism.** *Behav Brain Res,* 409:113337

199. Stoit AM, van Schie HT, Slaats-Willemse DI, Buitelaar JK (2013) **Grasping motor impairments in autism: not action planning but movement execution is deficient.** *J Autism Dev Disord,* 43(12):2793–2806

200. Chey J, Lee J, Kim YS, Kwon SM, Shin YM (2002) **Spatial working memory span, delayed response and executive function in schizophrenia.** *Psychiatry Res* 110(3):259–271

201. van der Wee NJ et al (2003) **Spatial working memory deficits in obsessive compulsive disorder are associated with excessive engagement of the medial frontal cortex.** *Neuroimage,* 20(4):2271–2280

202. Steele SD, Minshew NJ, Luna B, Sweeney JA (2007) **Spatial working memory deficits in autism.** *J Autism Dev Disord,* 37(4):605–612

203. Possin KL, Filoteo JV, Song DD, Salmon DP (2008) **Spatial and object working memory deficits in Parkinson's disease are due to impairment in different underlying processes.** *Neuropsychology,* 22(5):585–595

204. Possin KL et al (2017) **Egocentric and allocentric visuospatial working memory in premotor Huntington's disease: a double dissociation with caudate and hippocampal volumes.** *Neuropsychologia,* 101:57–64

205. Avanzino L et al (2016) T**ime processing and motor control in movement disorders.** *Front Hum Neurosci,* 10:631

206. Boyd LA et al (2009) **Motor sequence chunking is impaired by basal ganglia stroke.** *Neurobiol Learn Mem,* 92(1):35–44

207. Nagasaki H, Nakamura R, Taniguchi R (1978) **Disturbances of rhythm formation in patients with Parkinson's disease: part II. a forced oscillation model.** *Perceptual Mot Skills,* 46(1):79–87

208. Lemoine L et al (2021) **The specific role of the striatum in inter- val timing: the Huntington's disease model.** *NeuroImage Clinical,* 32:102865

209. Churchyard AJ et al (2001) **Gait dysfunction in Huntington's disease: parkinsonism and a disorder of timing. Implications for movement rehabilitation.** *Adv Neurol,* 87:375–385

210. Freeman JS et al (1996) **Abnormalities of motor timing in Huntington's disease.** *Parkinsonism Relat Disord,* 2(2):81–93

211. Snowden AW, Buhusi CV (2019) **Neural correlates of interval timing deficits in schizophrenia.** *Front Hum Neurosci,* 13:9

212. Ward RD, Kellendonk C, Kandel ER, Balsam PD (2012) **Timing as a window on cognition in schizophrenia.** *Neuropharmacology,* 62(3):1175–1181

213. Carroll CA, O'Donnell BF, Shekhar A, Hetrick WP (2009) **Timing dysfunctions in schizophrenia span from millisecond to several-second durations.** *Brain Cogn,* 70(2):181–190

214. Shapiro Z, Huang-Pollock C (2019) **A diffusion-model analysis of timing deficits among children with ADHD.** *Neuropsychology,* 33(6):883–892

215. Slater JL, Tate MC (2018) **Timing deficits in ADHD: insights from the neuroscience of musical rhythm.** *Front Comput Neurosci,* 12:51

216. Noreika V, Falter CM, Rubia K (2013) **Timing deficits in atten- tion-deficit/hyperactivity disorder (ADHD): evidence from neurocognitive and neuroimaging studies**. *Neuropsychologia,* 51(2):235–266

217. Falter CM, Noreika V, Wearden JH, Bailey AJ (2012) **More consistent, yet less sensitive: interval timing in autism spectrum disorders.** *Q J Exp Psychol,* 65(11):2093–2107

218. D'Cruz AM et al (2009) **Lateralized response timing deficits in autism.** *Biol Psychiat,* 66(4):393–397

219. Allman MJ, Meck WH (2012) **Pathophysiological distortions in time perception and timed performance.** *Brain : a J Neurol,* 135(Pt 3):656–677

220. Vicario CM et al (2010) **Time processing in children with Tourette's syndrome.** *Brain Cogn,* 73(1):28–34

Chapter 6 References

1. Vallarino M, Andersen AC, Delbende C, Ottonello I, Eberle AN, Vaudry H: **Melanin-concentrating hormone (MCH) immunoreactivity in the brain and pituitary of the dogfish Scyliorhinus canicula. Colocalization with alpha-melanocyte-stimulating hormone (alpha-MSH) in hypothalamic neurons**. *Peptides* 1989, **10**(2):375-382.

2. Saito Y, Cheng M, Leslie FM, Civelli O: **Expression of the melanin-concentrating hormone (MCH) receptor mRNA in the rat brain**. *J Comp Neurol* 2001, **435**(1):26-40.

3. Wang T, Yuan D, Zhou C, Lin F, Wei R, Chen H, Wu H, Xin Z, Liu J, Gao Y *et al*: **Molecular characterization of melanin-concentrating hormone (MCH) in Schizothorax prenanti: cloning, tissue distribution and role in food intake regulation**. *Fish Physiol Biochem* 2016, **42**(3):883-893.

4. Matsuda K, Shimakura S, Maruyama K, Miura T, Uchiyama M, Kawauchi H, Shioda S, Takahashi A: **Central administration of melanin-concentrating hormone (MCH) suppresses food intake, but not locomotor activity, in the goldfish, Carassius auratus**. *Neurosci Lett* 2006, **399**(3):259-263.

5. Morens C, Norregaard P, Receveur JM, van Dijk G, Scheurink AJ: **Effects of MCH and a MCH1-receptor antagonist on (palatable) food and water intake**. *Brain Res* 2005, **1062**(1-2):32-38.

6. Sahu A: **Leptin decreases food intake induced by melanin-concentrating hormone (MCH), galanin (GAL) and neuropeptide Y (NPY) in the rat**. *Endocrinology* 1998, **139**(11):4739-4742.

7. Bachner D, Kreienkamp H, Weise C, Buck F, Richter D: **Identification of melanin concentrating hormone (MCH) as the natural ligand for the orphan somatostatin-like receptor 1 (SLC-1)**. *FEBS Lett* 1999, **457**(3):522-524.

8. Hung CJ, Ono D, Kilduff TS, Yamanaka A: **Dual orexin and MCH neuron-ablated mice display severe sleep attacks and cataplexy**. *Elife* 2020, **9**.

9. Boutin JA, Jullian M, Frankiewicz L, Galibert M, Gloanec P, Le Diguarher T, Dupuis P, Ko A, Ripoll L, Bertrand M *et al*: **MCH-R1 Antagonist GPS18169, a Pseudopeptide, Is a Peripheral Anti-Obesity Agent in Mice**. *Molecules* 2021, **26**(5).

10. Kokkotou E, Jeon JY, Wang X, Marino FE, Carlson M, Trombly DJ, Maratos-Flier E: **Mice with MCH ablation resist diet-induced obesity through strain-specific mechanisms**. *Am J Physiol Regul Integr Comp Physiol* 2005, **289**(1):R117-124.

11. Ito M, Gomori A, Ishihara A, Oda Z, Mashiko S, Matsushita H, Yumoto M, Ito M, Sano H, Tokita S *et al*: **Characterization of MCH-mediated obesity in mice**. *Am J Physiol Endocrinol Metab* 2003, **284**(5):E940-945.

12. Gomori A, Ishihara A, Ito M, Mashiko S, Matsushita H, Yumoto M, Ito M, Tanaka T, Tokita S, Moriya M *et al*: **Chronic intracerebroventricular infusion of MCH causes obesity in mice. Melanin-concentrating hormone**. *Am J Physiol Endocrinol Metab* 2003, **284**(3):E583-588.

13. Saito Y: **[Role of MCH-MCH receptor system in feeding and depression]**. *Nihon Yakurigaku Zasshi* 2007, **130**(1):34-38.

14. Garcia-Fuster MJ, Parks GS, Clinton SM, Watson SJ, Akil H, Civelli O: **The melanin-concentrating hormone (MCH) system in an animal model of depression-like behavior**. *Eur Neuropsychopharmacol* 2012, **22**(8):607-613.

15. Torterolo P, Scorza C, Lagos P, Urbanavicius J, Benedetto L, Pascovich C, Lopez-Hill X, Chase MH, Monti JM: **Melanin-Concentrating Hormone (MCH): Role in REM Sleep and Depression**. *Front Neurosci* 2015, **9**:475.

16. Mutlu-Burnaz O, Yulug B, Oncul M, Celik E, Atasoy NS, Cankaya S, Hanoglu L, Velioglu HA: **Chemogenetic inhibition of MCH neurons does not alter memory performance in mice**. *Biomed Pharmacother* 2022, **155**:113771.

17. Sanathara N, Alhassen L, Marmouzi I, Khoudari M, Phan J, Alhassen W, Civelli O, Alachkar A: **Oxytocin-MCH circuit regulates monosynaptic inputs to MCH neurons and modulates social recognition memory**. *Neuropharmacology* 2021, **184**:108423.

18. Monzon ME, de Souza MM, Izquierdo LA, Izquierdo I, Barros DM, de Barioglio SR: **Melanin-concentrating hormone (MCH) modifies memory retention in rats**. *Peptides* 1999, **20**(12):1517-1519.

19. Bittencourt JC, Presse F, Arias C, Peto C, Vaughan J, Nahon JL, Vale W, Sawchenko PE: **The melanin-concentrating hormone system of the rat brain: an immuno- and hybridization histochemical characterization**. *J Comp Neurol* 1992, **319**(2):218-245.

20. Concetti C, Burdakov D: **Orexin/Hypocretin and MCH Neurons: Cognitive and Motor Roles Beyond Arousal**. *Front Neurosci* 2021, **15**:639313.

21. Lalonde R, Qian S: **Exploratory activity, motor coordination, and spatial learning in Mchr1 knockout mice**. *Behav Brain Res* 2007, **178**(2):293-304.

22. Smith DG, Davis RJ, Rorick-Kehn L, Morin M, Witkin JM, McKinzie DL, Nomikos GG, Gehlert DR: **Melanin-concentrating hormone-1 receptor modulates neuroendocrine, behavioral, and corticolimbic neurochemical stress responses in mice**. *Neuropsychopharmacology* 2006, **31**(6):1135-1145.

23. Vawter MP, Schulmann A, Alhassen L, Alhassen W, Hamzeh AR, Sakr J, Pauluk L, Yoshimura R, Wang X, Dai Q *et al*: **Melanin Concentrating Hormone Signaling Deficits in Schizophrenia: Association With Memory and Social Impairments and Abnormal Sensorimotor Gating**. *Int J Neuropsychopharmacol* 2020, **23**(1):53-65.

24. Fernando AB, Economidou D, Theobald DE, Zou MF, Newman AH, Spoelder M, Caprioli D, Moreno M, Hipolito L, Aspinall AT *et al*: **Modulation of high impulsivity and attentional performance in rats by selective direct and indirect dopaminergic and noradrenergic receptor agonists**. *Psychopharmacology (Berl)* 2012, **219**(2):341-352.

25. Ramanzini GC, Volpato GL, Visconti MA: **Does MCH play a role on establishment or maintenance of social hierarchy in Nile tilapia?** *Physiol Behav* 2018, **183**:33-38.

26. Gonzalez MI, Vaziri S, Wilson CA: **Behavioral effects of alpha-MSH and MCH after central administration in the female rat**. *Peptides* 1996, **17**(1):171-177.

27. Blouin AM, Fried I, Wilson CL, Staba RJ, Behnke EJ, Lam HA, Maidment NT, Karlsson KAE, Lapierre JL, Siegel JM: **Human hypocretin and melanin-concentrating hormone levels are linked to emotion and social interaction**. *Nat Commun* 2013, **4**:1547.

28. Calvez J, Fromentin G, Nadkarni N, Darcel N, Even P, Tome D, Ballet N, Chaumontet C: **Inhibition of food intake induced by acute stress in rats is due to satiation effects**. *Physiol Behav* 2011, **104**(5):675-683.

29. Whiddon BB, Palmiter RD: **Ablation of neurons expressing melanin-concentrating hormone (MCH) in adult mice improves glucose tolerance independent of MCH signaling**. *The Journal of neuroscience : the official journal of the Society for Neuroscience* 2013, **33**(5):2009-2016.

30. Macneil DJ: **The role of melanin-concentrating hormone and its receptors in energy homeostasis**. *Front Endocrinol (Lausanne)* 2013, **4**:49.

31. Hsiao YC, Munoz-Estrada J, Tuz K, Ferland RJ: **The Transition Zone Protein AHI1 Regulates Neuronal Ciliary Trafficking of MCHR1 and Its Downstream Signaling Pathway**. *J Neurosci* 2021, **41**(17):3932-3943.

32. Diniz GB, Battagello DS, Klein MO, Bono BSM, Ferreira JGP, Motta-Teixeira LC, Duarte JCG, Presse F, Nahon JL, Adamantidis A *et al*: **Ciliary melanin-concentrating hormone receptor 1 (MCHR1) is widely distributed in the murine CNS in a sex-independent manner**. *J Neurosci Res* 2020, **98**(10):2045-2071.

33. Pottorf TS, Fagan MP, Burkey BF, Cho DJ, Vath JE, Tran PV: **MetAP2 inhibition reduces food intake and body weight in a ciliopathy mouse model of obesity**. *JCI Insight* 2020, **5**(2).

34. Ritter A, Louwen F, Yuan J: **Deficient primary cilia in obese adipose-derived mesenchymal stem cells: obesity, a secondary ciliopathy?** *Obes Rev* 2018, **19**(10):1317-1328.

35. Szmigielska A, Krzemien G, Roszkowska-Blaim M, Obersztyn E: **Polydactyly and obesity - the clinical manifestation of ciliopathy: a boy with Bardet-Biedl syndrome**. *Dev Period Med* 2016, **20**(2):105-109.

36. Acs P, Bauer PO, Mayer B, Bera T, Macallister R, Mezey E, Pastan I: **A novel form of ciliopathy underlies hyperphagia and obesity in Ankrd26 knockout mice**. *Brain Struct Funct* 2015, **220**(3):1511-1528.

37. Berbari NF, Pasek RC, Malarkey EB, Yazdi SM, McNair AD, Lewis WR, Nagy TR, Kesterson RA, Yoder BK: **Leptin resistance is a secondary consequence of the obesity in ciliopathy mutant mice**. *Proc Natl Acad Sci U S A* 2013, **110**(19):7796-7801.

38. Munoz-Estrada J, Lora-Castellanos A, Meza I, Alarcon Elizalde S, Benitez-King G: **Primary cilia formation is diminished in schizophrenia and bipolar disorder: A possible marker for these psychiatric diseases**. *Schizophr Res* 2018, **195**:412-420.

39. Guemez-Gamboa A, Coufal NG, Gleeson JG: **Primary cilia in the developing and mature brain**. *Neuron* 2014, **82**(3):511-521.

40. Schou KB, Pedersen LB, Christensen ST: **Ins and outs of GPCR signaling in primary cilia**. *EMBO Rep* 2015, **16**(9):1099-1113.

41. Kobayashi Y, Saito Y: **Evaluation of ciliary-GPCR dynamics using a validated organotypic brain slice culture method**. *Methods Cell Biol* 2023, **175**:69-83.

42. Brewer KM, Engle SE, Bansal R, Brewer KK, Jasso KR, McIntyre JC, Vaisse C, Reiter JF, Berbari NF: **Physiological Condition-Dependent Changes in Ciliary GPCR Localization in the Brain**. *eNeuro* 2023, **10**(3).

43. Engle SE, Antonellis PJ, Whitehouse LS, Bansal R, Emond MR, Jontes JD, Kesterson RA, Mykytyn K, Berbari NF: **A CreER mouse to study melanin concentrating hormone signaling in the developing brain**. *Genesis* 2018, **56**(8):e23217.

44. Alhassen W, Alhassen S, Chen J, Monfared RV, Alachkar A: **Cilia in the Striatum Mediate Timing-Dependent Functions**. *Mol Neurobiol* 2023, **60**(2):545-565.

45. Alhassen S, Chen S, Alhassen L, Phan A, Khoudari M, De Silva A, Barhoosh H, Wang Z, Parrocha C, Shapiro E *et al*: **Intergenerational trauma transmission is associated with brain metabotranscriptome remodeling and mitochondrial dysfunction**. *Commun Biol* 2021, **4**(1):783.

46. Alhassen L, Phan A, Alhassen W, Nguyen P, Lo A, Shaharuddin H, Sanathara N, Civelli O, Alachkar A: **The role of Olfaction in MCH-regulated spontaneous maternal responses**. *Brain Res* 2019, **1719**:71-76.

47. Azizi-Malekabadi H, Pourganji M, Zabihi H, Saeedjalali M, Hosseini M: **Tamoxifen antagonizes the effects of ovarian hormones to induce anxiety and depression-like behavior in rats**. *Arq Neuropsiquiatr* 2015, **73**(2):132-139.

48. Kazakova SB, Fedotova Iu O, Sapronov NS: **[Effect of tamoxifen on anxiety in ovariectomized and intact female rats]**. *Eksp Klin Farmakol* 2007, **70**(5):3-8.

49. Galvano E, Pandit H, Sepulveda J, Ng CAS, Becher MK, Mandelblatt JS, Van Dyk K, Rebeck GW: **Behavioral and transcriptomic effects of the cancer treatment tamoxifen in mice**. *Front Neurosci* 2023, **17**:1068334.

50. Li X, Du ZJ, Chen MQ, Chen JJ, Liang ZM, Ding XT, Zhou M, Li SJ, Li XW, Yang JM *et al*: **The effects of tamoxifen on mouse behavior**. *Genes Brain Behav* 2020, **19**(4):e12620.

51. Mueser KT, McGurk SR: **Schizophrenia**. *Lancet* 2004, **363**(9426):2063-2072.

52. Kokkinidis L, Anisman H: **Amphetamine models of paranoid schizophrenia: an overview and elaboration of animal experimentation**. *Psychological bulletin* 1980, **88**(3):551-579.

53. Manahan-Vaughan D, von Haebler D, Winter C, Juckel G, Heinemann U: **A single application of MK801 causes symptoms of acute psychosis, deficits in spatial memory, and impairment of synaptic plasticity in rats**. *Hippocampus* 2008, **18**(2):125-134.

54. Lipska BK, Weinberger DR: **Subchronic treatment with haloperidol and clozapine in rats with neonatal excitotoxic hippocampal damage**. *Neuropsychopharmacology : official publication of the American College of Neuropsychopharmacology* 1994, **10**(3):199-205.

55. Hoffman DC: **Typical and atypical neuroleptics antagonize MK-801-induced locomotion and stereotypy in rats**. *Journal of neural transmission General section* 1992, **89**(1-2):1-10.

56. Wilson CA, Koenig JI: **Social interaction and social withdrawal in rodents as readouts for investigating the negative symptoms of schizophrenia**. *European neuropsychopharmacology : the journal of the European College of Neuropsychopharmacology* 2014, **24**(5):759-773.

57. Neill JC, Harte MK, Haddad PM, Lydall ES, Dwyer DM: **Acute and chronic effects of NMDA receptor antagonists in rodents, relevance to negative symptoms of schizophrenia: a translational link to humans**. *European neuropsychopharmacology : the journal of the European College of Neuropsychopharmacology* 2014, **24**(5):822-835.

58. Ellenbroek BA, Cools AR: **Animal models for the negative symptoms of schizophrenia**. *Behavioural pharmacology* 2000, **11**(3-4):223-233.

59. Alachkar A, Wang L, Yoshimura R, Hamzeh AR, Wang Z, Sanathara N, Lee SM, Xu X, Abbott GW, Civelli O: **Prenatal one-carbon metabolism dysregulation programs schizophrenia-like deficits**. *Mol Psychiatry* 2018, **23**(2):282-294.

60. Kelly MP, Stein JM, Vecsey CG, Favilla C, Yang X, Bizily SF, Esposito MF, Wand G, Kanes SJ, Abel T: **Developmental etiology for neuroanatomical and cognitive deficits in mice overexpressing Galphas, a G-protein subunit genetically linked to schizophrenia**. *Molecular psychiatry* 2009, **14**(4):398-415, 347.

61. Brzozka MM, Radyushkin K, Wichert SP, Ehrenreich H, Rossner MJ: **Cognitive and sensorimotor gating impairments in transgenic mice overexpressing the schizophrenia susceptibility gene Tcf4 in the brain**. *Biological psychiatry* 2010, **68**(1):33-40.

62. Ozawa K, Hashimoto K, Kishimoto T, Shimizu E, Ishikura H, Iyo M: **Immune activation during pregnancy in mice leads to dopaminergic hyperfunction and cognitive impairment in the offspring: a neurodevelopmental animal model of schizophrenia**. *Biological psychiatry* 2006, **59**(6):546-554.

63. O'Tuathaigh CM, Babovic D, O'Sullivan GJ, Clifford JJ, Tighe O, Croke DT, Harvey R, Waddington JL: **Phenotypic characterization of spatial cognition and social behavior in mice with 'knockout' of the schizophrenia risk gene neuregulin 1**. *Neuroscience* 2007, **147**(1):18-27.

64. Swerdlow NR, Light GA, Cadenhead KS, Sprock J, Hsieh MH, Braff DL: **Startle gating deficits in a large cohort of patients with schizophrenia: relationship to medications, symptoms, neurocognition, and level of function**. *Archives of general psychiatry* 2006, **63**(12):1325-1335.

65. Borowsky B, Durkin MM, Ogozalek K, Marzabadi MR, DeLeon J, Lagu B, Heurich R, Lichtblau H, Shaposhnik Z, Daniewska I *et al*: **Antidepressant, anxiolytic and anorectic effects of a melanin-concentrating hormone-1 receptor antagonist**. *Nat Med* 2002, **8**(8):825-830.

66. Roy M, David NK, Danao JV, Baribault H, Tian H, Giorgetti M: **Genetic inactivation of melanin-concentrating hormone receptor subtype 1 (MCHR1) in mice exerts anxiolytic-like behavioral effects**. *Neuropsychopharmacology* 2006, **31**(1):112-120.

67. Marsh DJ, Weingarth DT, Novi DE, Chen HY, Trumbauer ME, Chen AS, Guan XM, Jiang MM, Feng Y, Camacho RE *et al*: **Melanin-concentrating hormone 1 receptor-deficient mice are lean, hyperactive, and hyperphagic and have altered metabolism**. *Proc Natl Acad Sci U S A* 2002, **99**(5):3240-3245.

68. Monfared RV, Alhassen W, Truong TM, Gonzales MAM, Vachirakorntong V, Chen S, Baldi P, Civelli O, Alachkar A: **Transcriptome Profiling of Dysregulated GPCRs Reveals Overlapping Patterns across Psychiatric Disorders and Age-Disease Interactions**. *Cells* 2021, **10**(11).

69. Smith DG, Tzavara ET, Shaw J, Luecke S, Wade M, Davis R, Salhoff C, Nomikos GG, Gehlert DR: **Mesolimbic dopamine super-sensitivity in melanin-concentrating hormone-1 receptor-deficient mice**. *J Neurosci* 2005, **25**(4):914-922.

70. Stubbs T, Koemeter-Cox A, Bingman JI, Zhao F, Kalyanasundaram A, Rowland LA, Periasamy M, Carter CS, Sheffield VC, Askwith CC *et al*: **Disruption of dopamine receptor 1 localization to primary cilia impairs signaling in striatal neurons**. *J Neurosci* 2022, **42**(35):6692-6705.

71. Mustafa R, Rawas C, Mannal N, Kreiner G, Spittau B, Kaminska K, Yilmaz R, Potschke C, Kirsch J, Liss B *et al*: **Targeted Ablation of Primary Cilia in Differentiated Dopaminergic Neurons Reduces Striatal Dopamine and Responsiveness to Metabolic Stress**. *Antioxidants (Basel)* 2021, **10**(8).

72. Bae JE, Kang GM, Min SH, Jo DS, Jung YK, Kim K, Kim MS, Cho DH: **Primary cilia mediate mitochondrial stress responses to promote dopamine neuron survival in a Parkinson's disease model**. *Cell Death Dis* 2019, **10**(12):952.

73. Leaf A, Von Zastrow M: **Dopamine receptors reveal an essential role of IFT-B, KIF17, and Rab23 in delivering specific receptors to primary cilia**. *Elife* 2015, **4**.

74. Upadhyay VS, Muntean BS, Kathem SH, Hwang JJ, Aboualaiwi WA, Nauli SM: **Roles of dopamine receptor on chemosensory and mechanosensory primary cilia in renal epithelial cells**. *Front Physiol* 2014, **5**:72.

75. Abdul-Majeed S, Nauli SM: **Dopamine receptor type 5 in the primary cilia has dual chemo- and mechano-sensory roles**. *Hypertension* 2011, **58**(2):325-331.

76. Iwanaga T, Hozumi Y, Takahashi-Iwanaga H: **Immunohistochemical demonstration of dopamine receptor D2R in the primary cilia of the mouse pituitary gland**. *Biomed Res* 2011, **32**(3):225-235.

77. Marley A, von Zastrow M: **DISC1 regulates primary cilia that display specific dopamine receptors**. *PLoS One* 2010, **5**(5):e10902.

78. Barbeito P, Garcia-Gonzalo FR: **HTR6 and SSTR3 targeting to primary cilia**. *Biochem Soc Trans* 2021, **49**(1):79-91.

79. Mustafa R, Kreiner G, Kaminska K, Wood AJ, Kirsch J, Tucker KL, Parlato R: **Targeted Depletion of Primary Cilia in Dopaminoceptive Neurons in a Preclinical Mouse Model of Huntington's Disease**. *Front Cell Neurosci* 2019, **13**:565.

80. Miyoshi K, Kasahara K, Murakami S, Takeshima M, Kumamoto N, Sato A, Miyazaki I, Matsuzaki S, Sasaoka T, Katayama T *et al*: **Lack of dopaminergic inputs elongates the primary cilia of striatal neurons**. *PLoS One* 2014, **9**(5):e97918.

81. Kiser D, Steemers B, Branchi I, Homberg JR: **The reciprocal interaction between serotonin and social behaviour**. *Neurosci Biobehav Rev* 2012, **36**(2):786-798.

82. Alhassen W, Kobayashi Y, Su J, Robbins B, Nguyen H, Myint T, Yu M, Nauli SM, Saito Y, Alachkar A: **Regulation of Brain Primary Cilia Length by MCH Signaling: Evidence from Pharmacological, Genetic, Optogenetic, and Chemogenic Manipulations**. *Mol Neurobiol* 2022, **59**(1):245-265.

83. Adamantidis A, Thomas E, Foidart A, Tyhon A, Coumans B, Minet A, Tirelli E, Seutin V, Grisar T, Lakaye B: **Disrupting the melanin-concentrating hormone receptor 1 in mice leads to cognitive deficits and alterations of NMDA receptor function**. *Eur J Neurosci* 2005, **21**(10):2837-2844.

84. Jovasevic V, Zhang H, Sananbenesi F, Guedea AL, Soman KV, Wiktorowicz JE, Fischer A, Radulovic J: **Primary cilia are required for the persistence of memory and stabilization of perineuronal nets**. *iScience* 2021, **24**(6):102617.

85. Amador-Arjona A, Elliott J, Miller A, Ginbey A, Pazour GJ, Enikolopov G, Roberts AJ, Terskikh AV: **Primary cilia regulate proliferation of amplifying progenitors in adult hippocampus: implications for learning and memory**. *J Neurosci* 2011, **31**(27):9933-9944.

86. Berbari NF, Malarkey EB, Yazdi SM, McNair AD, Kippe JM, Croyle MJ, Kraft TW, Yoder BK: **Hippocampal and cortical primary cilia are required for aversive memory in mice**. *PLoS One* 2014, **9**(9):e106576.

87. Rhee S, Kirschen GW, Gu Y, Ge S: **Depletion of primary cilia from mature dentate granule cells impairs hippocampus-dependent contextual memory**. *Sci Rep* 2016, **6**:34370.

88. Wang Z, Phan T, Storm DR: **The type 3 adenylyl cyclase is required for novel object learning and extinction of contextual memory: role of cAMP signaling in primary cilia**. *J Neurosci* 2011, **31**(15):5557-5561.

89. Swerdlow NR, Shoemaker JM, Kuczenski R, Bongiovanni MJ, Neary AC, Tochen LS, Saint Marie RL: **Forebrain D1 function and sensorimotor gating in rats: effects of D1 blockade, frontal lesions and dopamine denervation**. *Neurosci Lett* 2006, **402**(1-2):40-45.

90. Geyer MA, Krebs-Thomson K, Braff DL, Swerdlow NR: **Pharmacological studies of prepulse inhibition models of sensorimotor gating deficits in schizophrenia: a decade in review**. *Psychopharmacology (Berl)* 2001, **156**(2-3):117-154.

91. van den Pol AN, Acuna-Goycolea C, Clark KR, Ghosh PK: **Physiological properties of hypothalamic MCH neurons identified with selective expression of reporter gene after recombinant virus infection**. *Neuron* 2004, **42**(4):635-652.

92. Chee MJ, Pissios P, Maratos-Flier E: **Neurochemical characterization of neurons expressing melanin-concentrating hormone receptor 1 in the mouse hypothalamus**. *J Comp Neurol* 2013, **521**(10):2208-2234.

93. Chung S, Verheij MM, Hesseling P, van Vugt RW, Buell M, Belluzzi JD, Geyer MA, Martens GJ, Civelli O: **The melanin-concentrating hormone (MCH) system modulates behaviors associated with psychiatric disorders**. *PLoS One* 2011, **6**(7):e19286.

94. Hintermann E, Erb C, Talke-Messerer C, Liu R, Tanner H, Flammer J, Eberle AN: **Expression of the melanin-concentrating hormone receptor in porcine and human ciliary epithelial cells**. *Invest Ophthalmol Vis Sci* 2001, **42**(1):206-209.

95. Nagata A, Hamamoto A, Horikawa M, Yoshimura K, Takeda S, Saito Y: **Characterization of ciliary targeting sequence of rat melanin-concentrating hormone receptor 1**. *Gen Comp Endocrinol* 2013, **188**:159-165.

96. Saito Y, Hamamoto A, Kobayashi Y: **[Selective signaling pathway via feeding-related ciliary GPCR, melanin-concentrating hormone receptor 1]**. *Nihon Yakurigaku Zasshi* 2019, **154**(4):179-185.

Chapter 7 References

1. Nahon JL, Presse F, Bittencourt JC, Sawchenko PE, Vale W: **The rat melanin-concentrating hormone messenger ribonucleic acid encodes multiple putative neuropeptides coexpressed in the dorsolateral hypothalamus**. *Endocrinology* 1989, **125**(4):2056-2065.

2. Bachner D, Kreienkamp H, Weise C, Buck F, Richter D: **Identification of melanin concentrating hormone (MCH) as the natural ligand for the orphan somatostatin-like receptor 1 (SLC-1)**. *FEBS Lett* 1999, **457**(3):522-524.

3. Saito Y, Nothacker HP, Wang Z, Lin SH, Leslie F, Civelli O: **Molecular characterization of the melanin-concentrating-hormone receptor**. *Nature* 1999, **400**(6741):265-269.

4. Macdonald D, Murgolo N, Zhang R, Durkin JP, Yao X, Strader CD, Graziano MP: **Molecular characterization of the melanin-concentrating hormone/receptor complex: identification of critical residues involved in binding and activation**. *Mol Pharmacol* 2000, **58**(1):217-225.

5. Rodriguez M, Beauverger P, Naime I, Rique H, Ouvry C, Souchaud S, Dromaint S, Nagel N, Suply T, Audinot V *et al*: **Cloning and molecular characterization of the novel human melanin-concentrating hormone receptor MCH2**. *Mol Pharmacol* 2001, **60**(4):632-639.

6. Sankhe AS, Bordeleau D, Alfonso DIM, Wittman G, Chee MJ: **Loss of glutamatergic signalling from MCH neurons reduced anxiety-like behaviours in novel environments**. *J Neuroendocrinol* 2023, **35**(1):e13222.

7. Urbanavicius J, Lagos P, Torterolo P, Scorza C: **Prodepressive effect induced by microinjections of MCH into the dorsal raphe: time course, dose dependence, effects on anxiety-related behaviors, and reversion by nortriptyline**. *Behav Pharmacol* 2014, **25**(4):316-324.

8. Galiano S, Ceras J, Cirauqui N, Perez S, Juanenea L, Rivera G, Aldana I, Monge A: **Novel series of substituted biphenylmethyl urea derivatives as MCH-R1 antagonists for the treatment of obesity**. *Bioorg Med Chem* 2007, **15**(11):3896-3911.

9. Kim N, Meyers KM, Mendez-Andino JL, Warshakoon NC, Ji W, Wos JA, Colson A, Mitchell MC, Davis JR, Pinney BB *et al*: **Identification of substituted 4-aminopiperidines and 3-aminopyrrolidines as potent MCH-R1 antagonists for the treatment of obesity**. *Bioorg Med Chem Lett* 2006, **16**(20):5445-5450.

10. Kokkotou E, Jeon JY, Wang X, Marino FE, Carlson M, Trombly DJ, Maratos-Flier E: **Mice with MCH ablation resist diet-induced obesity through strain-specific mechanisms**. *Am J Physiol Regul Integr Comp Physiol* 2005, **289**(1):R117-124.

11. Collins CA, Kym PR: **Prospects for obesity treatment: MCH receptor antagonists**. *Curr Opin Investig Drugs* 2003, **4**(4):386-394.

12. Ito M, Gomori A, Ishihara A, Oda Z, Mashiko S, Matsushita H, Yumoto M, Ito M, Sano H, Tokita S *et al*: **Characterization of MCH-mediated obesity in mice**. *Am J Physiol Endocrinol Metab* 2003, **284**(5):E940-945.

13. Gomori A, Ishihara A, Ito M, Mashiko S, Matsushita H, Yumoto M, Ito M, Tanaka T, Tokita S, Moriya M *et al*: **Chronic intracerebroventricular infusion of MCH causes obesity in mice. Melanin-concentrating hormone**. *Am J Physiol Endocrinol Metab* 2003, **284**(3):E583-588.

14. Le Thuc O, Cansell C, Bourourou M, Denis RG, Stobbe K, Devaux N, Guyon A, Cazareth J, Heurteaux C, Rostene W *et al*: **Central CCL2 signaling onto MCH neurons mediates metabolic and behavioral adaptation to inflammation**. *EMBO Rep* 2016, **17**(12):1738-1752.

15. Sasikumar TK, Qiang L, Burnett DA, Greenlee WJ, Hawes BE, Kowalski TJ, O'Neill K, Spar BD, Weig B: **Novel aminobenzimidazoles as selective MCH-R1 antagonists for the treatment of metabolic diseases**. *Bioorg Med Chem Lett* 2006, **16**(20):5427-5431.

16. Torterolo P, Scorza C, Lagos P, Urbanavicius J, Benedetto L, Pascovich C, Lopez-Hill X, Chase MH, Monti JM: **Melanin-Concentrating Hormone (MCH): Role in REM Sleep and Depression**. *Front Neurosci* 2015, **9**:475.

17. Price SK, Masho SW: **What does it mean when we screen? A closer examination of perinatal depression and psychosocial risk screening within one MCH home visiting program**. *Matern Child Health J* 2014, **18**(4):765-771.

18. Garcia-Fuster MJ, Parks GS, Clinton SM, Watson SJ, Akil H, Civelli O: **The melanin-concentrating hormone (MCH) system in an animal model of depression-like behavior**. *Eur Neuropsychopharmacol* 2012, **22**(8):607-613.

19. Saito Y: **[Role of MCH-MCH receptor system in feeding and depression]**. *Nihon Yakurigaku Zasshi* 2007, **130**(1):34-38.

20. Diniz GB, Battagello DS, Klein MO, Bono BSM, Ferreira JGP, Motta-Teixeira LC, Duarte JCG, Presse F, Nahon JL, Adamantidis A *et al*: **Ciliary melanin-concentrating hormone receptor 1 (MCHR1) is widely distributed in the murine CNS in a sex-independent manner**. *J Neurosci Res* 2020, **98**(10):2045-2071.

21. Alhassen W, Kobayashi Y, Su J, Robbins B, Nguyen H, Myint T, Yu M, Nauli SM, Saito Y, Alachkar A: **Regulation of Brain Primary Cilia Length by MCH Signaling: Evidence from Pharmacological, Genetic, Optogenetic, and Chemogenic Manipulations**. *Mol Neurobiol* 2022, **59**(1):245-265.

22. Kobayashi Y, Tomoshige S, Imakado K, Sekino Y, Koganezawa N, Shirao T, Diniz GB, Miyamoto T, Saito Y: **Ciliary GPCR-based transcriptome as a key regulator of cilia length control**. *FASEB Bioadv* 2021, **3**(9):744-767.

23. Nino-Rivero S, Torterolo P, Lagos P: **Melanin-concentrating hormone receptor-1 is located in primary cilia of the dorsal raphe neurons**. *J Chem Neuroanat* 2019, **98**:55-62.

24. Hamamoto A, Yamato S, Katoh Y, Nakayama K, Yoshimura K, Takeda S, Kobayashi Y, Saito Y: **Modulation of primary cilia length by melanin-concentrating hormone receptor 1**. *Cell Signal* 2016, **28**(6):572-584.

25. Kobayashi Y, Okada T, Miki D, Sekino Y, Koganezawa N, Shirao T, Diniz GB, Saito Y: **Properties of primary cilia in melanin-concentrating hormone receptor 1-bearing hippocampal neurons in vivo and in vitro**. *Neurochem Int* 2021, **142**:104902.

26. Shearman LP, Camacho RE, Sloan Stribling D, Zhou D, Bednarek MA, Hreniuk DL, Feighner SD, Tan CP, Howard AD, Van der Ploeg LH *et al*: **Chronic MCH-1 receptor modulation alters appetite, body weight and adiposity in rats**. *Eur J Pharmacol* 2003, **475**(1-3):37-47.

27. Heifetz A, Barker O, Verquin G, Wimmer N, Meutermans W, Pal S, Law RJ, Whittaker M: **Fighting obesity with a sugar-based library: discovery of novel MCH-1R antagonists by a**

new computational-VAST approach for exploration of GPCR binding sites. *J Chem Inf Model* 2013, **53**(5):1084-1099.

28. Hausen AC, Ruud J, Jiang H, Hess S, Varbanov H, Kloppenburg P, Bruning JC: **Insulin-Dependent Activation of MCH Neurons Impairs Locomotor Activity and Insulin Sensitivity in Obesity**. *Cell Rep* 2016, **17**(10):2512-2521.

29. Jeon JY, Bradley RL, Kokkotou EG, Marino FE, Wang X, Pissios P, Maratos-Flier E: **MCH-/- mice are resistant to aging-associated increases in body weight and insulin resistance**. *Diabetes* 2006, **55**(2):428-434.

30. Boutin JA, Jullian M, Frankiewicz L, Galibert M, Gloanec P, Le Diguarher T, Dupuis P, Ko A, Ripoll L, Bertrand M *et al*: **MCH-R1 Antagonist GPS18169, a Pseudopeptide, Is a Peripheral Anti-Obesity Agent in Mice**. *Molecules* 2021, **26**(5).

31. Sakurai T, Ogawa K, Ishihara Y, Kasai S, Nakayama M: **The MCH(1) receptor, an anti-obesity target, is allosterically inhibited by 8-methylquinoline derivatives possessing subnanomolar binding and long residence times**. *Br J Pharmacol* 2014, **171**(5):1287-1298.

32. Jeon MK, Cheon HG: **Promising strategies for obesity pharmacotherapy: melanocortin-4 (MC-4) receptor agonists and melanin concentrating hormone (MCH) receptor-1 antagonists**. *Curr Top Med Chem* 2009, **9**(6):504-538.

33. Hadden M, Deering DM, Henderson AJ, Surman MD, Luche M, Khmelnitsky Y, Vickers S, Viggers J, Cheetham S, Guzzo PR: **Synthesis and SAR of 4-aryl-1-(indazol-5-yl)pyridin-2(1H)ones as MCH-1 antagonists for the treatment of obesity**. *Bioorg Med Chem Lett* 2010, **20**(23):7020-7023.

34. Vaughan JM, Fischer WH, Hoeger C, Rivier J, Vale W: **Characterization of melanin-concentrating hormone from rat hypothalamus**. *Endocrinology* 1989, **125**(3):1660-1665.

35. Naito N, Kawazoe I, Nakai Y, Kawauchi H: **Melanin-concentrating hormone-like immunoreactive material in the rat hypothalamus; characterization and subcellular localization**. *Cell Tissue Res* 1988, **253**(2):291-295.

36. Kawauchi H: **Melanin concentrating hormone. II. Structure and biosynthesis of melanin-concentrating hormone**. *Life Sci* 1989, **45**(13):1133-1140.

37. Jezova D, Bartanusz V, Westergren I, Johansson BB, Rivier J, Vale W, Rivier C: **Rat melanin-concentrating hormone stimulates adrenocorticotropin secretion: evidence for a site of action in brain regions protected by the blood-brain barrier**. *Endocrinology* 1992, **130**(2):1024-1029.

38. Guyon A, Conductier G, Rovere C, Enfissi A, Nahon JL: **Melanin-concentrating hormone producing neurons: Activities and modulations**. *Peptides* 2009, **30**(11):2031-2039.

39. Noble EE, Hahn JD, Konanur VR, Hsu TM, Page SJ, Cortella AM, Liu CM, Song MY, Suarez AN, Szujewski CC *et al*: **Control of Feeding Behavior by Cerebral Ventricular Volume Transmission of Melanin-Concentrating Hormone**. *Cell Metab* 2018, **28**(1):55-68 e57.

40. Eric Hu X, Wos JA, Dowty ME, Suchanek PM, Ji W, Chambers JB, Benoit SC, Clegg DJ, Reizes O: **Small-molecule melanin-concentrating hormone-1 receptor antagonists require brain penetration for inhibition of food intake and reduction in body weight**. *J Pharmacol Exp Ther* 2008, **324**(1):206-213.

41. Schinkel AH: **P-Glycoprotein, a gatekeeper in the blood-brain barrier**. *Adv Drug Deliv Rev* 1999, **36**(2-3):179-194.

42. Witty DR, Bateson J, Hervieu GJ, Al-Barazanji K, Jeffrey P, Hamprecht D, Haynes A, Johnson CN, Muir AI, O'Hanlon PJ *et al*: **Discovery of potent and stable conformationally constrained analogues of the MCH R1 antagonist SB-568849**. *Bioorg Med Chem Lett* 2006, **16**(18):4872-4878.

43. Castrucci AM, Visconti MA, Matsunaga TO, Hadley ME, Hruby VJ: **Enzymological studies of melanin concentrating hormone (MCH) and related analogues**. *Comp Biochem Physiol B* 1992, **103**(2):317-320.

44. Matsunaga TO, Castrucci AM, Hadley ME, Hruby VJ: **Melanin concentrating hormone (MCH): synthesis and bioactivity studies of MCH fragment analogues**. *Peptides* 1989, **10**(2):349-354.

45. Audinot V, Beauverger P, Lahaye C, Suply T, Rodriguez M, Ouvry C, Lamamy V, Imbert J, Rique H, Nahon JL *et al*: **Structure-activity relationship studies of melanin-concentrating hormone (MCH)-related peptide ligands at SLC-1, the human MCH receptor**. *J Biol Chem* 2001, **276**(17):13554-13562.

46. Kokkotou E, Mastaitis JW, Qu D, Hoersch D, Slieker L, Bonter K, Tritos NA, Maratos-Flier E: **Characterization of [Phe(13), Tyr(19)]-MCH analog binding activity to the MCH receptor**. *Neuropeptides* 2000, **34**(3-4):240-247.

47. Glick M, Segal-Lieberman G, Cohen R, Kronfeld-Schor N: **Chronic MCH infusion causes a decrease in energy expenditure and body temperature, and an increase in serum IGF-1 levels in mice**. *Endocrine* 2009, **36**(3):479-485.

48. Smith DG, Davis RJ, Rorick-Kehn L, Morin M, Witkin JM, McKinzie DL, Nomikos GG, Gehlert DR: **Melanin-concentrating hormone-1 receptor modulates neuroendocrine, behavioral, and corticolimbic neurochemical stress responses in mice**. *Neuropsychopharmacology* 2006, **31**(6):1135-1145.

49. Brewer KM, Engle SE, Bansal R, Brewer KK, Jasso KR, McIntyre JC, Vaisse C, Reiter JF, Berbari NF: **Physiological Condition-Dependent Changes in Ciliary GPCR Localization in the Brain**. *eNeuro* 2023, **10**(3).

50. Hartwig C, Monis WJ, Chen X, Dickman DK, Pazour GJ, Faundez V: **Neurodevelopmental disease mechanisms, primary cilia, and endosomes converge on the BLOC-1 and BORC complexes**. *Dev Neurobiol* 2018, **78**(3):311-330.

51. Reiter JF, Leroux MR: **Genes and molecular pathways underpinning ciliopathies**. *Nat Rev Mol Cell Biol* 2017, **18**(9):533-547.

52. Karalis V, Donovan KE, Sahin M: **Primary Cilia Dysfunction in Neurodevelopmental Disorders beyond Ciliopathies**. *J Dev Biol* 2022, **10**(4).

53. Holtz AM, VanCoillie R, Vansickle EA, Carere DA, Withrow K, Torti E, Juusola J, Millan F, Person R, Guillen Sacoto MJ *et al*: **Heterozygous variants in MYH10 associated with neurodevelopmental disorders and congenital anomalies with evidence for primary cilia-dependent defects in Hedgehog signaling**. *Genet Med* 2022, **24**(10):2065-2078.

54. Valente EM, Rosti RO, Gibbs E, Gleeson JG: **Primary cilia in neurodevelopmental disorders**. *Nat Rev Neurol* 2014, **10**(1):27-36.

55. Monfared RV, Alhassen W, Truong TM, Gonzales MAM, Vachirakorntong V, Chen S, Baldi P, Civelli O, Alachkar A: **Transcriptome Profiling of Dysregulated GPCRs Reveals Overlapping Patterns across Psychiatric Disorders and Age-Disease Interactions**. *Cells* 2021, **10**(11).

56. Baldi P, Alhassen W, Chen S, Nguyen H, Khoudari M, Alachkar A: **Large-scale analysis reveals spatiotemporal circadian patterns of cilia transcriptomes in the primate brain**. *J Neurosci Res* 2021, **99**(10):2610-2624.

57. Alhassen W, Chen S, Vawter M, Robbins BK, Nguyen H, Myint TN, Saito Y, Schulmann A, Nauli SM, Civelli O *et al*: **Patterns of cilia gene dysregulations in major psychiatric disorders**. *Prog Neuropsychopharmacol Biol Psychiatry* 2021, **109**:110255.

58. Vawter MP, Schulmann A, Alhassen L, Alhassen W, Hamzeh AR, Sakr J, Pauluk L, Yoshimura R, Wang X, Dai Q *et al*: **Melanin Concentrating Hormone Signaling Deficits in Schizophrenia: Association With Memory and Social Impairments and Abnormal Sensorimotor Gating**. *Int J Neuropsychopharmacol* 2020, **23**(1):53-65.

59. Miyoshi K, Kasahara K, Miyazaki I, Asanuma M: **Lithium treatment elongates primary cilia in the mouse brain and in cultured cells**. *Biochem Biophys Res Commun* 2009, **388**(4):757-762.

60. Sriram K, Insel PA: **G Protein-Coupled Receptors as Targets for Approved Drugs: How Many Targets and How Many Drugs?** *Mol Pharmacol* 2018, **93**(4):251-258.

61. Luthin DR: **Anti-obesity effects of small molecule melanin-concentrating hormone Receptor 1 (MCHR1) antagonists**. *Life Sci* 2007, **81**(6):423-440.

62. Johansson A: **Evolution of physicochemical properties of melanin concentrating hormone receptor 1 (MCHr1) antagonists**. *Bioorganic & medicinal chemistry letters* 2016, **26**(19):4559-4564.

63. Omran Z: **Obesity: Current Treatment and Future Horizons**. *Mini reviews in medicinal chemistry* 2017, **17**(1):51-61.

64. MooreA, Sargent BJ, Guzzo PR, Surman MD: **From preclinical to clinical development: the example of a novel treatment for obesity**. *Neurobiology of disease* 2014, **61**:47-54.

65. Sanathara NM, Garau C, Alachkar A, Wang L, Wang Z, Nishimori K, Xu X, Civelli O: **Melanin concentrating hormone modulates oxytocin-mediated marble burying**. *Neuropharmacology* 2018, **128**:22-32.

66. Oh ST, Liu QF, Jeong HJ, Lee S, Samidurai M, Jo J, Pak SC, Park HJ, Kim J, Jeon S: **Nasal Cavity Administration of Melanin-Concentrating Hormone Improves Memory Impairment in Memory-Impaired and Alzheimer's Disease Mouse Models**. *Molecular neurobiology* 2019.